

# A preliminary analysis of the sediment budget across the Swartvlei estuary mouth

Adriaan Roets

*Thesis presented in fulfilment of the requirements for the degree  
Master of Science in the Faculty of Engineering  
at Stellenbosch University*



Supervisor: Mr. Geoff Toms  
Department of Civil Engineering

December 2014

## **DECLARATION**

By submitting this thesis electronically, I declare that the entirety of the work contained therein is my own, original work, that I am the sole author thereof (save to the extent explicitly otherwise stated), that reproduction and publication thereof by Stellenbosch University will not infringe any third party rights and that I have not previously in its entirety or in part submitted it for obtaining any qualification.

December 2014

Copyright © 2014 Stellenbosch University

All rights reserved

## ABSTRACT

The Swartvlei estuary and lake system is situated on the southern coast of the Western Cape Province of South Africa and forms part of the core conservation area of the Wilderness National Park. The Swartvlei system comprises two interlinked water bodies, namely Swartvlei Lake and Swartvlei estuary. SANParks have been monitoring this estuary closely over the past two decades, due to its importance to the ecology and to tourism. There are also low-lying properties on the perimeter of the Swartvlei estuary which run the risk of occasional flooding. Two of the major monitoring issues in this estuary system are the water level required for successful mouth breaching, and the influence of the water level on the low-lying properties.

This study presents a preliminary analysis of the sediment budget across the Swartvlei estuary mouth. The objective of this study was to identify the various sediment contributory factors and to estimate the quantities that each individually contributed towards the defined sediment budget.

The contributors identified were as follows:

- Longshore transport, consisting of contributors such as
  - Slumping and erosion of the sandy cliffs at Gericke Point
  - Accumulated beach sand from dunes and beach material along the Swartvlei coastline
- Aeolian transport
- Estuary contributions such as
  - Slumping and erosion along the dunes and the low-lying western sandbank
  - Sediment pulses from tidal variations, as well as riverine sediment flushing.

By combining extensive literature from similarly shaped bay beaches, relevant case studies and on site surveys with SANPark records, on-site photography and historical imagery, a hypothesis was formed. This hypothesis was focused on the assumed theoretical sediment transport regime along the Swartvlei coastline and, in particular, on the estuary mouth region. Furthermore, from available information gathered from a desktop study and on-site investigations, a MIKE 21 SW numerical model was combined with a Kamphuis bulk long-shore transport formula to produce the following results (Kamphuis, 2010):

- Longshore transport of 180 000-200 000 m<sup>3</sup>/yr entering the budget area (west to east).
- Longshore transport of 200 000–230 000 m<sup>3</sup>/yr exiting the budget boundary (west to east).

A Preliminary Analysis of the Sediment Budget Across the Swartvlei Estuary Mouth

- Estuary inputs, originating from dune slumping and erosion along the western sandbank, were defined and calculated to be in the range of 20 000–25 000 m<sup>3</sup>/yr.
- Aeolian transport of 7 000-9 000 m<sup>3</sup>/yr, with marine and estuarine inputs balancing the budget.

Agricultural extraction and human intervention has reduced the flooding potential of the Swartvlei estuary, which in turn leads to reduced scour potential. The lack of flooding potential which drives sediment out of the river into the longshore transport system, combined with the now dominant marine processes, has resulted in the accumulation of marine sediment in the estuary mouth until a mouth opening is initiated. This scenario has resulted in the estuary mouth behaving as a sink, rather than a source. Beaches to the east of the estuary mouth have responded by retreating, due to the lack of supplementary sediment. To define and quantify the sediment transport regime occurring at the Swartvlei estuary mouth, it is recommended that additional studies into bathymetry, wave and wind climate, current, sediment transport as well as numerical modelling be conducted supplementary to this study.

## OPSOMMING

Die Swartvlei meer en see monding is geleë aan die kaapse suidkus van Suid- Afrika. Dit vorm deel van die kern bewarings area van die Wilderness Nationale Park. Die Swartvlei sisteem bestaan uit twee verbinde, kern dele nl: Swartvlei meer en estuarium.

Vir die afgelope twee dekades is hierdie area onder die noue toesig van SANParke as gevolg van die belangrikheid van die area met betrekking tot toerisme en ekologie. Daar is ook menigde laag liggende eiendomme aan die oewers, wat baie sensitief is vir watervlak stygings. Die optimum water vlakke benodig vir die uitskuring van die gety monding het ook implikasies vir die laag liggende eiendome en vereis noukeurige monitering.

'n Voorlopige analise van die sediment begroting rondom die gety monding word deur hierdie studie voorgelê.

Die doel van hierdie ondersoek was om die verskillende primêre bydraers tot die sediment begroting te identifiseer en te kwantifiseer. Die bydraers is geïdentifiseer as volg:

- Langstrandse vervoer wat potensieel gevoed word deur:
  - Erosie en ineenstorting van die sand-krans naby Gericke Punt
  - Sediment afkomstig van die duine en strande geleë aan die Swartvlei kuslyn
- Eoliese vervoer
- Potensiele gety monding bydrae naamlik:
  - Ineenstorting en erosie van sand duine en sand bank aan die westelike oewer
  - Sediment bydraes deur gety ossillasies asook sediment uitspoeling deur rivier vloede.

Deur relevante literatuur rakende soortgelyke baai-vorme, gevalle studies en tipiese prosesse in die tipe omgewings met SANPark rekords, opmetings, terrein fotos en historiese fotografie te vergelyk, was 'n hipotese gekonstrueer. Die hipotese het gefokus op die teoretiese sediment vervoer situasie aan die Swartvlei kuslyn en meer spesifiek om die gety monding te beskryf. Die beskikbare data, verkry vanuit ondersoek en opmetings was gebruik om 'n MIKE 21 SW numeriese model op te stel. Die model resultate was toe gekombineer met langstrand vervoer formules van Kamphuis in 'n poging om die hipotese te bevestig. Die resultate was as volg:

- Langstrandse vervoer van 180 000- 200 000 m<sup>3</sup>/jr. oor die westelike grens van die sediment begroting

A Preliminary Analysis of the Sediment Budget Across the Swartvlei Estuary Mouth

- Langstrandse vervoer van 200 000 – 230 000 m<sup>3</sup>/jr. oor die oostelike grens van die begroting.
- Die bydrae van die gety monding is bereken om in die omgewing van 20 000 – 25 000 m<sup>3</sup>/jr. te wees.
- Eoliese vervoer van 7000-9000 m<sup>3</sup>/jr. met mariene - en monding insette wat die sediment begroting balanseer.

Deur verdere studie in die historiese fotografie vir die area, is daar bevind dat die gety monding meer sediment absorbeer as wat dit weer uitlaat. Dit is verder toegeskryf aan 'n tekort aan uitskuurings vermoë as gevolg van gety monding manipulasie asook lanbou en munisipale onttrekkings vanuit die waterbronne wat die estuarium voed. Sediment bou dus op in die mond area en word verhoed om die strande aan die oostelike kant van die gety monding te voed. Die resultaat hiervan is die erosie van hierdie strande. Daar word dienooreenkomstig aangeraai dat bykomende studies in die velde van bodem topografie, golf - en wind klimaat, strome, numeriese modellering, rivier vloede en sediment vervoer uitgevoer word. Dit sal verseker dat daar ingeligte besluite geneem kan word rakende die suksesvolle bestuur van hierdie kosbare gety monding.

**TABLE OF CONTENTS**

<b>DECLARATION</b>	<b>ii</b>
<b>ABSTRACT</b>	<b>iii</b>
<b>OPSOMMING</b>	<b>v</b>
<b>TABLE OF CONTENTS</b>	<b>vii</b>
<b>TABLE OF FIGURES</b>	<b>x</b>
<b>TABLE OF TABLES</b>	<b>xvi</b>
<b>DEFINITIONS AND ABBREVEATIONS</b>	<b>xviii</b>
<b>1. INTRODUCTION AND BACKGROUND</b>	<b>1</b>
1.1 INTRODUCTION	1
1.2 OBJECTIVE	2
1.3 CHAPTER OVERVIEW	3
<b>2. LITERATURE STUDY</b>	<b>5</b>
2.1 INTRODUCTION	5
2.2 ESTUARIES	5
2.2.1 Estuaries in general	5
2.2.2 Estuaries in South Africa	5
2.2.3 Basic hydrodynamics and sediment transport	6
2.2.4 Tides	7
2.2.5 Estuary channels	8
2.2.6 Effects of dominant flows on sedimentation	8
2.2.7 Sedimentation in estuaries	9
2.2.8 Sandbar formation	10
2.2.9 Estuary mouth dynamics	10
2.3 BAY SHAPE AND ORIENTATION	11
2.4 MARINE SEDIMENT TRANSPORT	19
2.4.1 Introduction	19
2.4.2 Cross-shore transport	22
2.4.3 Longshore transport	27
2.4.4 Aeolian transport	29
2.5 A SEDIMENT BUDGET ANALYSIS	32
2.5.1 Introduction	32
2.5.2 Data commonly used in a sediment budget	33
2.5.3 Building a sediment budget	34
2.6 RELEVANT CASE STUDIES AROUND THE WORLD	35
2.6.1 Moore River estuary, Western Australia	35

2.6.2	Zandvlei estuary, Western Cape, South Africa	39
<b>3.</b>	<b>SWARTVLEI</b>	<b>42</b>
3.1	BACKGROUND	42
3.2	RIVER CATCHMENTS	44
3.3	GEOLOGY	46
3.4	CLIMATE	47
3.5	RAINFALL	52
3.6	ESTUARY CONDITIONS	53
3.7	PHYSIO-CHEMICAL CHARACTERISTICS	55
3.8	MOUTH DYNAMICS	56
3.9	SWARTVLEI COASTLINE	59
<b>4.</b>	<b>METHODOLOGY</b>	<b>67</b>
4.1	MODELLING APPROACH	69
4.2	DESKTOP STUDY	71
4.2.1	Desktop study description	71
4.3	ON-SITE INVESTIGATION	75
<b>5.</b>	<b>DATA COLLECTION</b>	<b>78</b>
5.1	ON SITE INVESTIGATION	78
5.1.1	Beach Survey	78
5.1.2	Sand Grain analysis	84
5.2	ESTUARY PROFILE DATA	91
<b>6.</b>	<b>NUMERICAL MODELLING</b>	<b>98</b>
6.1	AVAILABLE DATA	98
6.1.1	Hind cast data	98
6.2	MODEL SET-UP	104
6.2.1	Study area	104
<b>7.</b>	<b>HYPOTHESIS</b>	<b>119</b>
<b>8.</b>	<b>RESULTS</b>	<b>138</b>
8.1	MIKE 21 SW OUTPUT	138
8.3	SWARTVLEI ESTUARY MOUTH SEDIMENT BUDGET	145
<b>9.</b>	<b>CONCLUSIONS AND RECOMMENDATIONS</b>	<b>150</b>
	<b>REFERENCES</b>	<b>154</b>
	<b>APPENDIX 1: AVERAGE YEARLY RAINFALL FOR THE SEDGEFIELD REGION (2002-2010)</b>	<b>160</b>
	<b>APPENDIX 2: GANTT CHART</b>	<b>162</b>
	<b>APPENDIX 3: TRIMBLE GPS TECHNICAL INFORMATION</b>	<b>163</b>
	<b>APPENDIX 4: CONTOUR PLAN OF THE ESTUARY REGION</b>	<b>164</b>

<b>APPENDIX 5: MIKE 21 SW DESCRIPTION</b>	<b>165</b>
<b>APPENDIX 6: PHOTO REPORT</b>	<b>166</b>
<b>APPENDIX 7: BEACH SURVEY</b>	<b>167</b>
7.1 PROFILE ONE	168
7.2 PROFILE TWO	172
7.3 PROFILE THREE	174
7.4 PROFILE FOUR	177
7.5 PROFILE FIVE	179
7.6 PROFILE SIX	182
7.7 PROFILE - LEFT BANK OF THE RIVER	184
7.8 PROFILE BERM-LONG PROFILE	187
7.9 PROFILE BERM - CROSS PROFILE	191
7.10 PROFILE RIVER-RIGHT BANK	193
7.11 PROFILE SEVEN	196
7.12 PROFILE EIGHT	198
7.13 PROFILE NINE	200
7.14 PROFILE TEN	203
<b>APPENDIX 8: KAMPHUIS BULK SEDIMENT TRANSPORT CALCULATION</b>	<b>205</b>
<b>APPENDIX 9: LAYOUT OF INCIDENT WAVE ANGLE</b>	<b>206</b>
<b>APPENDIX 10: MIKE OUTPUT LOCATIONS</b>	<b>207</b>

## TABLE OF FIGURES

Figure 1: The position of Swartvlei relative to the surrounding estuaries .....	6
Figure 2: Estuary types based on flood types (Ranasinghe, 1999).....	9
Figure 3: The process of estuary mouth closure (Ranasinghe, 1999).....	11
Figure 4: : (a) <i>Headland-bay beaches are present along the South African coast; (b) Headland-bay beach on the West coast; (c) Algoa bay in the Eastern Cape; (d) Mossel bay on the southern Cape coast (Malan, 2012).</i> .....	13
Figure 5: The bay at Swartvlei fitting the headland bay beach trend (Google Earth).....	14
Figure 6: Definition sketch of the logarithmic spiral model (Hsu, 2010) .....	15
Figure 7: Comparison of log-spiral models to actual bays (Hsu & Evans, 1989).....	16
Figure 8: Definition sketch of the parabolic bay shape equation (Hsu & Evans, 1989) .....	17
Figure 9: Predicted parabolic and natural planforms of Keppel Island, Queensland, Australia (Hsu & Evans, 1989).....	18
Figure 10: Definition sketch of the hyperbolic tangent shape model (Moreno & Kraus, 1999) .....	19
Figure 11: Typical net longshore transport rates in Southern Africa in m <sup>3</sup> /yr (Schoonees, 2012) .....	20
Figure 12: Example of longshore transport (Theron, 2004) .....	21
Figure 13: Example of cross-shore transport (Theron, 2004) .....	21
Figure 14: Typical winter and summer beach profiles (FEMA, 2007).....	23
Figure 15: Illustration of the beach profile change due to cross shore transport (Schoonees, 2012) .....	24
Figure 16: Winter and summer bluff profiles (FEMA, 2007) .....	25
Figure 17: Accuracy of the CERC/SPM formula (Schoonees & Theron, 1994).....	28
Figure 18: Accuracy of computed longshore transport with Kamphuis bulk longshore transport formula (Schoonees & Theron, 1996) .....	29
Figure 19: Four mechanism initiating Aeolian transport (Sloss, C. R., Hesp, P. & Shepherd, M., 2012).....	31

Figure 20: Schematic of the net sediment budget model for the Humber Estuary, UK (Townend & Whitehead, 2003) ..... 33

Figure 21: Schematic of the net sediment budget model for Southampton Water, UK (Townend & Whitehead, 2003) ..... 33

Figure 22: Moore river estuary, Western Australia (Anderson, 2004) ..... 36

Figure 23: Hydrology of Moore River Estuary and surrounds, 1 January 1999 to 1 December 2002. Displays the bar status (open, intermittent or closed), water level in the estuary and riverine flow from Gingin Brook and Moore River (Anderson, 2004). ..... 37

Figure 24: Hydrology of Moore River Estuary and surrounds, 1 December 2001 to 1 December 2002. Displays the bar status (open, intermittent or closed), water level in the estuary and riverine flow from Gingin Brook and Moore River (Anderson, 2004). ..... 38

Figure 25: Zandvlei estuary (note the close proximity of residential properties to the estuary, similar to the case of Swartvlei) (City of Cape Town Municipality, 2008) ..... 40

Figure 26: Mechanical opening of Zandvlei estuary mouth (City of Cape Town Municipality, 2008) ..... 41

Figure 27: The Swartvlei system showing the extent of the three river catchment areas (Whitfield et al., 1983) ..... 43

Figure 28: Railway crossing over Swartvlei ..... 44

Figure 29: Flow patterns of two inflowing rivers to Swartvlei, showing the lack of seasonal peaks (CSIR, 1983). ..... 45

Figure 30: Wind patterns for Cape St. Blaize-Mossel Bay, 1970-1980 (CSIR, 1983) ..... 49

Figure 31: VOS data for the construction of wave roses (CSIR, 1983) ..... 50

Figure 32: Historical wave climate for the Sedgefield coast (CSIR, 1983). ..... 51

Figure 33: Mean monthly rainfall and stream flow for the Karatara River (DWA, 2009) ..... 53

Figure 34: Positions A, B and C indicate where current measurements were taken (Whitfield, 1986) ..... 55

Figure 35: Sectional representation of current velocities measurements in m/s (Whitfield, 1986)) ..... 55

Figure 36: Mouth condition after the artificial opening of the estuary mouth ..... 57

Figure 37: Eleven year record illustrating, between red lines, the peak closure periods (EWISA, 2003) ..... 58

Figure 38: Layout of The Swartvlei bay area ..... 59

Figure 39: Mathematical representation of spiral bay shape geometry of Swartvlei Bay..... 60

Figure 40: Site specific presentation of PBSE ..... 61

Figure 41: Western edge of Swartvlei bay, Gericke point with steep sandstone bluffs..... 62

Figure 42: High dunes with wider beaches east of Gericke point..... 63

Figure 43: Dune system with buffer dunes present ..... 64

Figure 44: Swartvlei estuary mouth ..... 65

Figure 45: Erosion east of estuary mouth..... 66

Figure 46: Defined study area ..... 68

Figure 47: On-site imagery of a typical calm Sedgefield surf zone immediately east of the Gericke Point parking area..... 70

Figure 48: Illustration of the peak transport zone (Longuet-Higgins, 1970)..... 73

Figure 49: Beach profiles locations and pathways..... 79

Figure 50: Operation of Trimble GPS ..... 79

Figure 51: Summary of beach profile survey ..... 81

Figure 52: Left (western) bank of the estuary ..... 82

Figure 53: Dune rock formation on the eastern bank of the estuary ..... 83

Figure 54: Steep and narrow beach profile, east of estuary mouth..... 83

Figure 55: Wentworth and ASTM classification table (CEM, 2006)..... 85

Figure 56: Locations of sediment sampling points (Google) ..... 86

Figure 57: Grain size distribution: Gericke Point..... 88

Figure 58: Grain size distribution: Estuary Mouth ..... 89

Figure 59: Grain size distribution: Sand Spit ..... 90

Figure 60: Grain size distribution: River..... 90

Figure 61: Locations of historical river profiles..... 91

Figure 62: Location of NCEP hind cast modelling (Google)..... 98

Figure 63: Hs versus Tp for 2009 .....	99
Figure 64: Maximum monthly Hs for 2009.....	100
Figure 65: Maximum daily Hs for 2009 .....	100
Figure 66: Relevant Cartesian coordinate system .....	104
Figure 67: Study area.....	105
Figure 68: Model boundaries and mesh with numbered areas with finer mesh indicated ..	106
Figure 69: Mesh set-up for Swartvlei bay .....	106
Figure 70: MIKE bathymetric scatter data in bay area .....	107
Figure 71: MIKE bathymetric scatter data with a more sensitive depth scale.....	108
Figure 72: Interpolated bathymetric chart.....	109
Figure 73: Bathymetric chart of total model area .....	109
Figure 74: Close up bathymetric chart of Sedgefield Bay .....	110
Figure 75: SANHO 123 bathymetric chart .....	111
Figure 76: Insertion of domain bathymetry file.....	112
Figure 77: Model time definition .....	112
Figure 78: Hypothetical equilibrium shoreline profile (Green) of a typical headland bay coastline under soft sediment conditions (Mather, 2008).....	119
Figure 79: Orientation map for the Swartvlei bay.....	120
Figure 80: Rocky shoreline immediately east of Gericke Point.....	121
Figure 81: Current beach profile compared with a mathematical PBSE of Gericke Point ..	122
Figure 82: Erosion of sand cliffs at Gericke Point.....	123
Figure 83: Tapering of the cliffs into steep dunes .....	123
Figure 84: Swartvlei Estuary in 1936, showing two historical sediment sources (CSIR, 1983) .....	125
Figure 85: Dunes and beach profile leading up to the estuary mouth .....	126
Figure 86: Deep channel near west bank of estuary.....	127
Figure 87: Western bank of estuary with slumping present .....	128
Figure 88: Historical vegetation lines with defined area for contribution from the estuary ..	129

A Preliminary Analysis of the Sediment Budget Across the Swartvlei Estuary Mouth

Figure 89: Historical mouth imagery and sand bank growth ..... 131

Figure 90: Dune rock present on the eastern bank of the estuary mouth..... 132

Figure 91: Initial definition of sediment budget boundary..... 134

Figure 92: Illustration of theoretical sediment contributors along the Swartvlei coastline ... 134

Figure 93: Preliminary sediment budget across the Swartvlei estuary mouth ..... 136

Figure 94: Illustration of MIKE 21 SW output locations, the orange numbered transport profiles comprising the individual output points which are also indicated ..... 139

Figure 95: Individual MIKE 21 SW output points ..... 139

Figure 96: Gentler beach slopes east of Gericke Point..... 143

Figure 97: Calculated sediment transport vectors (orange) ..... 145

Figure 98: Net sediment budget across the Swartvlei estuary mouth ..... 146

Figure 99: Trimble profiles..... 167

Figure 100: Location of position one ..... 168

Figure 101: Profile one..... 169

Figure 102: Profile one with sheer sandstone cliffs ..... 170

Figure 103: Beach near profile one ..... 171

Figure 104: Erosion of the sandstone cliffs near profile one ..... 171

Figure 105: Location of profile two ..... 172

Figure 106: Profile two ..... 173

Figure 107: Profile two ..... 174

Figure 108: Position of profile three..... 175

Figure 109: Profile three..... 176

Figure 110: Profile three: On site photo..... 177

Figure 111: Position of profile four..... 178

Figure 112: Profile four..... 179

Figure 113: Location of profile five ..... 180

Figure 114: Profile Five ..... 181

Figure 115: On site photo of profile five..... 181

## A Preliminary Analysis of the Sediment Budget Across the Swartvlei Estuary Mouth

Figure 116: Position of profile six .....	182
Figure 117: Profile six .....	183
Figure 118: On-site profile photo of profile six .....	183
Figure 119: Position of profile LB .....	184
Figure 120: Illustration of profile LB.....	185
Figure 121: On-site photo of profile LB.....	186
Figure 122: On-site photo of profile LB and profile pathway in red .....	187
Figure 123: Location of Berm longitudinal profile.....	188
Figure 124: Illustration of Longitudinal profile of sand berm.....	190
Figure 125: On-site photo of longitudinal profile of the sand berm.....	190
Figure 126: Location of cross profile of the sand berm .....	191
Figure 127: Cross profile of sand berm .....	192
Figure 128: On-Site photo of sand berm cross profile .....	193
Figure 129: Location of profile RB.....	194
Figure 130: Profile of right bank of the river.....	195
Figure 131: On-site photo of the right bank of Swartvlei estuary .....	195
Figure 132: Location of profile seven .....	196
Figure 133: Illustration of profile seven.....	197
Figure 134: On-site photo of profile seven.....	197
Figure 135: Erosion at profile seven.....	198
Figure 136: Location of profile 8.....	199
Figure 137: Survey of profile 8 .....	200
Figure 138: Location of profile nine .....	201
Figure 139: Illustration of profile nine .....	202
Figure 140: On-site photo of profile nine .....	202
Figure 141: Location of profile 10 .....	203
Figure 142: Illustration of profile ten .....	204

## TABLE OF TABLES

Table 1: Run-off contributions of feeder rivers (CSIR, 1983) .....	44
Table 2: Summary of water availability (Fijen & Kapp, 1995).....	46
Table 3: Mean wave direction for incident waves for 2009 (NCEP, 2011). .....	52
Table 4: Table showing the percentage of open mouth conditions during certain months (EWISA, 2003).....	58
Table 5: Benchmark details.....	78
Table 6: Various levels relative to MSL (SANHO, 2013).....	80
Table 7: Sieve analysis .....	87
Table 8: Wave height bins.....	101
Table 9: Wave period bins.....	101
Table 10: Number of occurrences when comparing significant wave height (in meters) with accompanying peak periods (in seconds) for 2009 .....	102
Table 11: Percentage occurrence of wave height with its corresponding period for 2009..	102
Table 12: Average incident wave directions (in degrees) for significant wave heights and wave periods.....	103
Table 13: Theoretical height of breaking wave to corresponding depths .....	141
Table 14: Bulk sediment transport rates for the area studied estimated using Kamphuis (2010) .....	144
Table 15: Preliminary sediment budget across the Swartvlei estuary mouth .....	148
Table 16: Profile one .....	168
Table 17: Profile two .....	172
Table 18: Profile three.....	175
Table 19: Position four .....	178
Table 20: Profile five .....	180
Table 21: Profile six.....	182
Table 22: Profile LB.....	185
Table 23: Longitudinal profile of berm .....	189

A Preliminary Analysis of the Sediment Budget Across the Swartvlei Estuary Mouth

Table 24: Cross Profile of sand berm .....	192
Table 25: River right bank profile.....	194
Table 26: Profile seven data.....	196
Table 27: Profile eight data .....	199
Table 28: Profile nine data .....	201
Table 29: Profile ten data .....	203

**DEFINITIONS AND ABBREVEATIONS**

m <sup>3</sup> /yr	Cubic meters per year
m	meters
Sink	Refers to the ability to store sediment
Source	Refers to the ability to provide sediment
Overwash	The flow of water and sediment over the crest of the beach/berm that does not directly return to the sea
Fluvial	Refers to processes associated with rivers or streams. Relating or inhabiting a river
SANHO	South African Hydrographic Office
SANPARKS	South African National Parks
HAT	Highest Astronomical Tide
LAT	Lowest Astronomical Tide
MLWS	Mean Low Water Springs
MHWS	Mean High Water Springs
MHWN	Mean High Water Neap
MLWN	Mean Low Water Neap
MSL	Mean Sea Level
ML	Mean Level
CD	Chart Datum
Shoaling	A bottom effect which influences the height of waves moving from deep to shallow water.
Ebb Tide	Movement of the tide out to sea
Flood Tide	Incoming or rising tide
DHI	Danish Hydraulic Institute
Orographic	Resulting from the effects of mountains forcing moist air to rise
PBSE	Parabolic Bay Shape Equation

# 1. INTRODUCTION AND BACKGROUND

## 1.1 INTRODUCTION

The Swartvlei estuary and lake system is situated on the Cape South Coast and forms part of the core conservation area of the Wilderness National Park. The Swartvlei system comprises two connected bodies of water: Swartvlei Lake and Swartvlei estuary. To understand the current sediment transport regime at the Swartvlei estuary mouth, an understanding of the Swartvlei system, geology and metocean conditions is needed. The maximum depth in the estuary has been measured at 4 m; there is a narrow central channel bordered by intertidal sand flats of varying depths (Kok & Whitfield, 1986). The Swartvlei Lake itself has a mean depth of 5.5 m and a maximum depth of 16.7 m, as stated from studies done by Fijen & Kapp (1995).

The Swartvlei system is situated in a dynamic climate which ranges from moderate to wet conditions, with a monthly rainfall (total mm) ranging between 11 mm and 244 mm (Fijen & Kapp, 1995). Average temperatures in the area vary from 25 °C in the summer to 19 °C in the winter (CSIR, 1983). The Swartvlei catchment is fed by three main rivers, namely the Hoëkraal, Wolwedraai and Karatara rivers. These rivers contribute relatively equal amounts of annual run-off to supplement the Swartvlei system, with a total average freshwater input of  $66 \times 10^6 \text{ m}^3$  each year (Fijen & Kapp, 1995).

During high flood periods these rivers in the catchment areas of the Swartvlei system contribute to the sediment flowing into the lake. The lake, however, is a vast system with various deep sections. Swartvlei Lake, as a result, absorbs significant amounts of the sediment due to it settling in these deep sections. This, in turn, leads to an initial estimate that the sediment entering the system originating from the catchment areas, possibly never reaches the estuary mouth area in large enough quantities to have any significant effect on the sediment budget.

The Swartvlei system is situated behind a Holocene coastal dune belt, 2 km long and between 30 meters and 75 meters high (CSIR, 1983). The estuary forms a 7.2 km long channel that connects the lake to the sea. The geology of Swartvlei and its surroundings has been described in depth by Martin (1962) and Birch & Du Plessis (1977). Swartvlei is situated on a system of quaternary sand which lies along the coast in an area known as the Wilderness-Knysna embayment. The Swartvlei system is bordered to the west by the Gericke Point dune rock formation and to the east by similar formations. According to the CSIR, dune sand frequents the estuary (CSIR, 1983).

During the dryer summer months, wave climates accompanied by dominant marine processes combined with a lack of flushing potential originating from lower run off percentages and increased agricultural and domestic abstractions from the inland side of the Swartvlei system, initiates onshore sand bar migration, as well as berm build up at the mouth of the estuary (Fijen & Kapp, 1995). This leads to predominantly closed mouth conditions towards the end of the summer period as well as throughout the winter months (EWISA, 2003). However, during the above-mentioned closed mouth conditions the ingress of sand into the estuary can still occur as a result of incident dynamic wave climates, resulting in the overtopping of the sand bar. Overtopping is especially evident during the early stages of mouth closure, when the level of this sand bar is relatively low.

When the mouth is closed the river inflows and, especially, floods from the delayed effects of the winter rainfall, result in increased water levels throughout the interlinked estuary system. Residential properties are common around the banks of the Swartvlei estuary and the rising water levels pose a threat to these properties which results in a management strategy being required to mitigate potential flooding (Fijen & Kapp, 1995).

According to records from SANParks, the estuary inlet is open approximately 50% of the time (Fijen & Kapp, 1995). The mouth is closed during winters (97%). The Swartvlei mouth is mechanically opened when the water level in the lake exceed +2.0 m above Mean Sea Level. In cases where a higher run-off has been present, the mouth has stayed open for longer, leading to a greater scouring of the mouth area. (Fijen & Kapp, 1995)

Following the identification of the various sediment contributors, a preliminary sediment budget will be calculated to establish an estimate of the sediment transport regime occurring at the Swartvlei estuary mouth. The direction of transport will also be estimated, to establish whether the direction from west to east is, in fact, the correct dominant direction. An estimate of the sediment contribution along the half-heart embayment is necessary, as well as the contribution from the estuary itself.

## **1.2 OBJECTIVE**

The aim of the study will be to identify and preliminarily quantify the various contributors of sediment towards the Swartvlei estuary mouth. This will be necessary in order to reach the objective set by this thesis of establishing a preliminary sediment budget for the Swartvlei estuary mouth.

### 1.3 CHAPTER OVERVIEW

The study itself will commence after this introduction with a review of literature aimed at identifying the physical processes affecting estuaries in general. The literature study will focus on various scenarios and processes linked to estuarine environments. Aspects of relevant case studies and bulk sediment transport models will be included. The literature review is presented in Chapter 2.

In Chapter 3 the literature study will be used as a foundation to describe the Swartvlei focus area in detail. The various processes and scenarios linked to estuaries that were defined in general will be narrowed down to site-specific processes and scenarios affecting only the Swartvlei study area. This chapter will focus mainly on describing the study area.

In Chapter 4 the methodology is set out with regard to identifying the processes, formulae and parameters needed for successful data collection and numerical modelling. The strategy for the MIKE 21 SW model set-up and the selection of a bulk longshore transport formula is discussed.

Chapter 5 describes the data collection with reference to the on-site investigations e.g. historical records, on-site photography and sand grain analysis. The results of a sand grain analysis are also presented in this chapter, together with historical estuary profile data.

Chapter 6 describes the MIKE 21 SW numerical model. Emphasis is placed on the available data, the input parameters used, and mesh and bathymetry outputs for use in a MIKE 21 SW model. The limitations, which are due to a lack of available data, are also discussed.

In Chapter 7 the methodology set out in Chapter 4 and relevant academic literature are combined with the information resulting from the data collection reported in Chapter 5 to form a hypothesis. This hypothesis describes the sediment transport regime that theoretically exists along the Swartvlei coastline. The aim of this chapter is to theoretically define the sediment transport regime occurring at the Swartvlei estuary mouth using the data that is available. Emphasis will be put on describing the form of the headland bay, the bulk longshore transport along the coastline and the various sediment-contributing factors in and around the estuary mouth.

In Chapter 8 the results of an on-site GPS survey is combined with the output from a numerical model and the Kamphuis formula for bulk longshore transport (Kamphuis, 2010). This chapter focuses on verifying the theoretical transport scenario at the Swartvlei estuary mouth with calculated quantities. The end result is the presentation of a preliminary sediment budget for the Swartvlei estuary mouth calculated from the available data. A discussion on the accuracy of the data follows, with recommendations on possible further studies.

The conclusion of this study is set out in Chapter 9, as well as recommendations derived from the findings.

## 2. LITERATURE STUDY

### 2.1 INTRODUCTION

The literature study will focus on presenting various scenarios and processes affecting estuarine environments in general. Included will be aspects of relevant case studies, as well as sediment transport models.

### 2.2 ESTUARIES

#### 2.2.1 Estuaries in general

Estuaries are partly closed bodies of water in a coastal environment with one or more rivers or streams flowing into them. One end of an estuary is generally open to the sea.

*'Estuaries form a transition zone between river and ocean environments and are subject to both marine influences, such as tides, waves, and the influx of saline water; and riverine influences, such as flows of fresh water and sediment. The inflow of both seawater and freshwater provides high levels of nutrients in both the water column and sediment, making estuaries among the most productive natural habitats in the world. The location of estuaries on the boundary between coastal and catchment environments, makes them not only vulnerable to changes in the catchment area, but to developments within the estuary itself as well. Changes in river catchments have resulted in sediment transport imbalances leading to problems within the delicate sediment balances of South African estuaries. Floods that were used to flush out estuaries and maintain sediment balances throughout the estuaries have now been interrupted for agricultural or development use' - (Ranasinghe, 1999).*

As described by Ranasinghe (1999), the dynamic nature of an estuary is influenced by various riverine and marine processes. A sediment budget defined around an estuary mouth will thus also be influenced by these dynamic processes. Furthermore, emphasis must be placed on initially identifying these key contributors for the successful calculation of a sediment budget across an estuary mouth.

#### 2.2.2 Estuaries in South Africa

The South African coastline extends approximately 3 000 km from the Orange (Gariep) River (28°38'S; 16°28'E) on the west (Atlantic Ocean) coast to Kosi Bay (26°54'S; 32°53'E) on the east (Indian Ocean) coast. Some 300 estuarine systems have been identified along the coast of South Africa (Whitfield, 2000). Estuaries are the meeting places of freshwater from rivers and saltwater from the sea and, as such, are dynamic environments characterised by large fluctuations in their environmental condition. The distribution of these estuaries is shown in Figure 1, with Swartvlei highlighted in red.

## A Preliminary Analysis of the Sediment Budget Across the Swartvlei Estuary Mouth

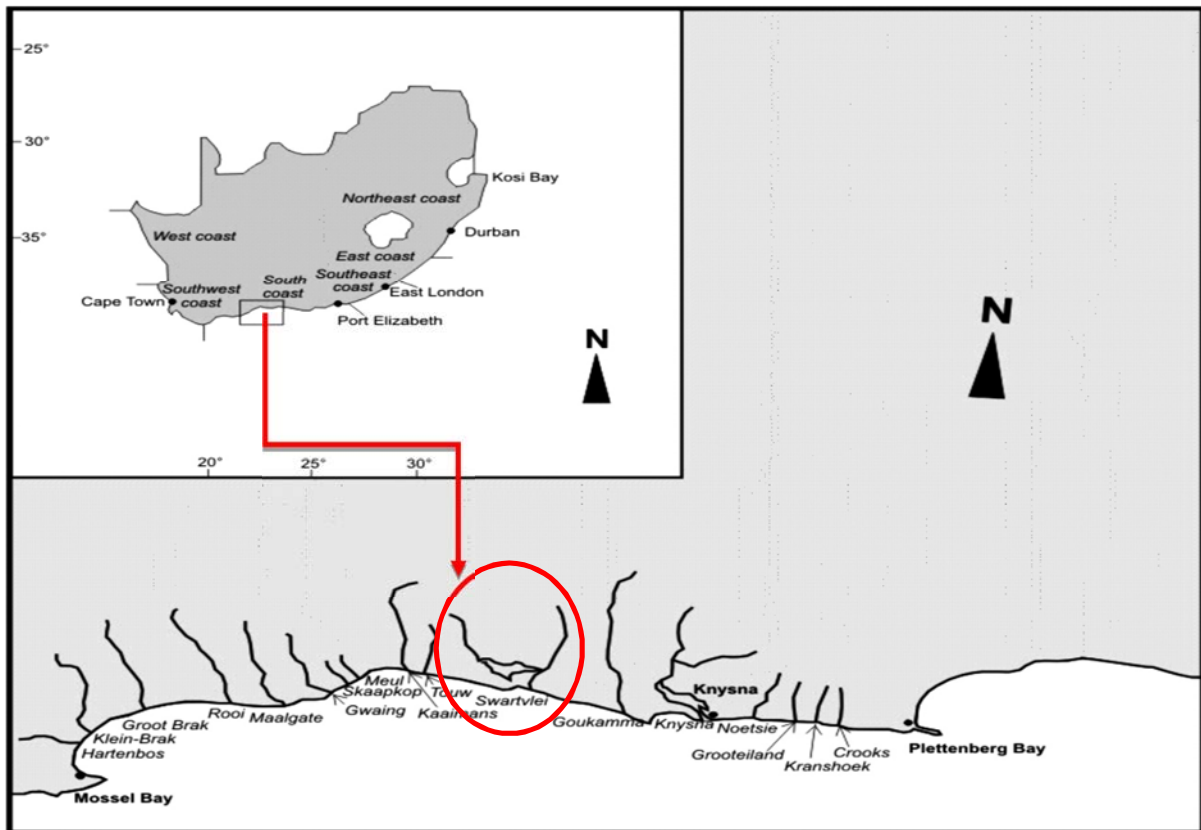


Figure 1: The position of Swartvlei relative to the surrounding estuaries

### 2.2.3 Basic hydrodynamics and sediment transport

In an academic study by Beck (2005) adapted from the work of Ranasinghe (1999), three factors are identified as influencing the hydrodynamic - and sediment transport processes in South African estuaries. The inflow of water into an estuary system is identified as the first factor. Studies have shown that a reduced riverine flooding potential can lead to a build-up of sediment in the mouth area. This refers to the fact that incoming waves transport vast quantities of sediment in and around the estuary mouth. Suspended sediment is transported by high energy incident waves and, as the waves lose energy due to bottom friction and depth restrictions, is stored on the sand bar situated in front of the river mouth. If the estuary is in an open mouth state the balance is kept by the out-flowing water transporting settled sediment back out to sea, thus flattening the top of the sand bar (Ranasinghe, 1999).

The second factor is tidal flow. During a normal tidal action sediment moves in and out of the estuary mouth and, depending on whether the estuary is ebb or flood dominated, results in a net movement of sediment in or out of the estuary. Local wave conditions also contribute significantly to the stirring up and movement of sediment in the estuary mouth area. Wave action is, however, dampened within an estuary and tidal flows combined with freshwater or

river flows are therefore partly responsible for the transportation of sediment within an estuary (Ranasinghe, 1999).

It is therefore important to incorporate these factors into the process of defining the sediment budget boundary. If the boundaries are defined too narrowly and close together, a large range of estuary and marine processes will have significant effects on the sediment budget, making it very difficult to accurately predict the contributors towards the budget.

The third and final factor is dependent on the conditions of the mouth. Estuaries in South Africa are generally small in both size and flow capacities. However, the study area is characterized with an above average bi-modal yearly rainfall but, due to the increasing pressure of municipal and agricultural abstraction, a state of low flow throughout the catchment areas results in periods where the scour potential of the interlinked estuary system is reduced. A decrease in the flooding potential leads to the onshore migration of the sand bar, due to the dominance of pertinent marine processes at the estuary mouth. The end result of this phenomenon is the closure of the estuary mouth due to a build-up of marine sediment. Elevated water levels or significant floods are once again required to initiate open mouth conditions and to restart the cycle.

The general low rainfall climate of South Africa, combined with the agricultural and domestic water abstraction occurring along most South African rivers, leads to a scenario where estuaries tend to close during low water supply conditions. Estuary mouths are influenced by a number of factors; mainly, but not limited to, marine processes e.g. wave climates, currents and sediment transport regimes, as well as riverine influences e.g. tidal influences and flushing by floods, thus making them truly dynamic.

#### **2.2.4 Tides**

Tides occur as a result of the gravitational pull of the sun, moon and earth. The paths of the moon around the earth and the earth around the sun are both elliptical, thus resulting in a maximum and a minimum gravitational pull during each cycle. In addition, the axis of the earth is inclined towards its orbit around the sun. Therefore, the gravitational tide-producing force at a given point varies in a complex but predictable way. South African tides occur twice a day and such a tide event is called a semi-diurnal tide (Beck, 2005).

The tide producing forces are responsible not only for ebb and flow patterns, but for neap and spring tides as well. Spring tides occur at full moon and new moon, when the alignment of the sun and the moon causes tides to be at their greatest. Neap tides are a result of the sun and the moon's forces opposing each other (Schumann, 2003).

Tidal amplitudes around the world vary considerably, with tides in South Africa being classed as microtidal (a tidal range of 0-2 m). Further in-depth information on tidal influences and terminology can be found in the work of Schumann (2003).

### **2.2.5 Estuary channels**

A special characteristic of estuaries is their channels. These channels can be divided into two main parts, the flood channels and the ebb channels. According to a study done by Deyr (1997), the ebb channel forms when the tidal flats become exposed and the flow then tends to follow a natural meandering action over the tidal flats. Flood flows can cut across these banks and secondary channels can be formed. In this way the main channel can be divided into two branches, one dominated by ebb currents and one dominated by flood currents.

A regular feature of estuaries is the crossing of these two currents, with the presence of shoaling as a result of this action. Sand is deposited in the flood-dominated channel during ebb tide and deposited in the ebb-dominated channel during the flood tide. Deposition of sediment is a frequent occurrence, as the ebb and flood channels may cross several times. A misperception is thus created that estuaries are undergoing sedimentation when, in fact, the channels are dynamic and moving, thus causing shoaling in different places (Ranasinghe, 1999).

### **2.2.6 Effects of dominant flows on sedimentation**

Depending on the relative strength of the tidal flow, river flow and wave actions, estuaries can be classified as tidal, river or wave dominated. In tide dominated estuaries the river flows are insignificant in comparison to the tidal flows, except when higher flood periods occur. The opposite is true in river flow dominated estuaries. Sedimentation is closely linked to the type of flow dominating an estuary and is illustrated in Figure 2 (Ranasinghe, 1999).

Tide dominated estuaries can be sub-divided into flow or ebb-dominated estuaries. The type of current dominance will be determined by whether the estuary is ebb- or flow-dominated. The mouth characteristics and tidal flats will, in turn, be determined by the dominant currents in the estuary channels.

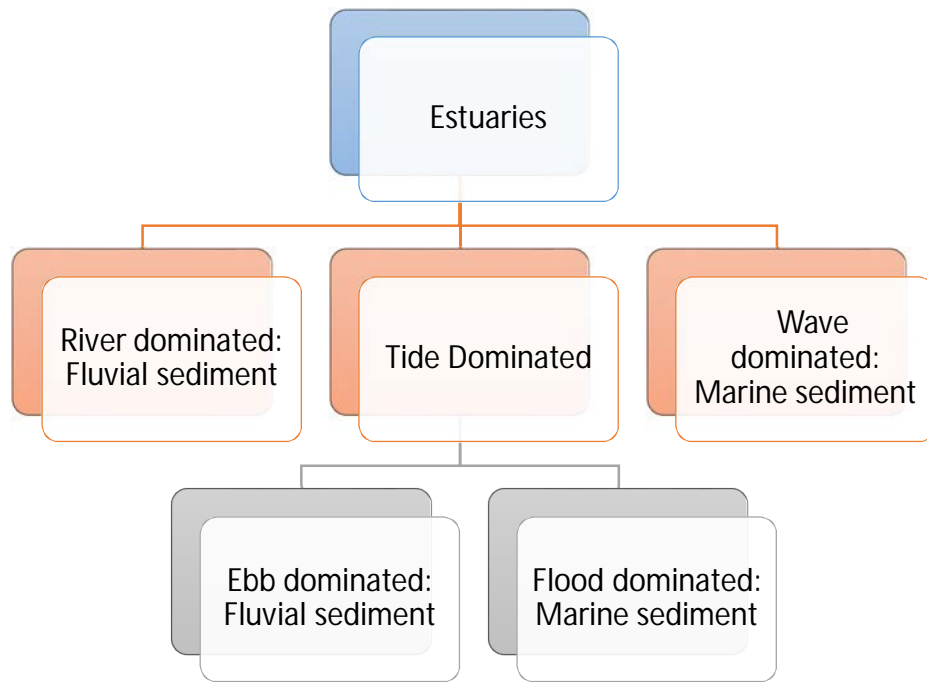


Figure 2: Estuary types based on flood types (Ranasinghe, 1999)

### 2.2.7 Sedimentation in estuaries

Sediments in estuaries can be fluvial, i.e. catchment derived, or of marine origin. Tide-dominated estuaries can be either flood- or ebb-dominated, depending on the relative strength of the ebb and flood currents. In flood-dominated estuaries the flood currents are stronger than the ebb currents and as such, the marine sediments entering the mouths during flood tides cannot all be removed during ebb tides. Flood-tide dominated estuaries are, therefore, mainly characterised by sediments of marine origin. Many South African estuaries are flood-tide dominated and even under natural conditions marine sediments tend to accumulate in the estuaries, especially near the mouth. Ebb-dominated estuaries are less likely to be dominated by marine sediments. This is as a result of the ebb floods being stronger than the tidal flood flows. The sediment from the marine environment is then flushed out by the stronger ebb currents (Schumann, 2003).

Sedimentation usually takes place in three different regions in an estuary. At the tidal head, sediment accumulates because of the change in bed slope from the steeper river to the estuary. This accumulated sediment is mainly of fluvial origin. At the mouth of the estuary marine sediment, diverted from the littoral drift, accumulates on the flood tidal delta inside the estuary because of the decrease in strength of tidal currents as they emerge from the narrow inlet into the wider estuary.

In between the sedimentation at the head and at the mouth, sediment accumulation also occurs where tidal mixing between the fresh water from the catchment and the sea water takes place. The fine material carried by the fresh water flocculates and settles in the mixing zone, due to the difference in density of the two water bodies (Schumann, 2003).

### 2.2.8 Sandbar formation

The formation and migration of sandbars are commonly observed in the surf zone. Recent studies indicate that sandbars are not stable, but are in continuous migration during storms (Hoefel & Elgar, 2003). Therefore, the understanding and prediction of sandbar formation and migration is one of the major problems in coastal morphodynamic research and is essential for developing effective soft engineering measures to prevent beach erosion.

Sandbars are defined as submerged, partly exposed ridges of sand or coarse materials that have been built up by nearshore wave action. One of the main drivers of sand bar formation is the swirling turbulence of waves breaking off a beach, resulting in the excavation of a trough in the sandy bottom. Some of the sand is then carried onto the beach and the rest is deposited on the offshore flank of the trough. The sandbar builds up due to this backwash and the rip-currents running along the flanks of the bar. The top of the sandbar is kept under the still water line due to the plunging action of the waves breaking on top of the sandbar. These troughs and bars are most prolific during high storm periods with heavy surf, as during calm sea states the bar migrates shoreward (Britannica, 2000).

Through recent morphological research, coupled with observations of alongshore uniform equilibrium profiles worldwide, it is now generally accepted that *barred profiles* are generated by large storms, while *planar beach* profiles are caused by shoreward sediment transport in the milder wave conditions in between the storm events (Dean, 1977) (Elgar, *et al.*, 2001) (Plant, *et al.*, 2001).

On the mechanisms of sandbar formation, there currently exist two types of theory. One is the forced response mechanism (Yu & Mei, 2000), which states that the formation of sandbars is a passive response to the hydrodynamic forcing, and thus the beach profile has the same length scale as that of the hydrodynamic forcing when the profile reaches equilibrium. The other theory is the self-organisation mechanism of Falques *et al.* (2000), which does not consider the beach profile as a stable profile, but a continually evolving one (Dean, 1977).

### 2.2.9 Estuary mouth dynamics

The size of a system inlet depends largely on the size of the system. The inlet size is also partially linked to the tidal prism. The inlet has to be able to accommodate large tidal inflows;

if it cannot, scouring will take place and a larger inlet will be formed. If the size of the tidal influx decreases, for example due to sedimentation, the reduced tidal currents will not be able to flush out the estuary inlet entirely and this will result in the inlet becoming smaller (Ranasinghe, 1999). This process is illustrated in Figure 3.

Usually an inlet is maintained in a state of dynamic equilibrium through the interaction of several processes. Estuaries are seen as dynamic entities, because floods and storms can have a significant impact on the estuarine morphology, but under normal circumstances the estuary will return to its equilibrium state. The governing influences are defined as, but not limited to, the following: wave climates, tidal ranges, flooding potential, sediment supply from longshore transport, to name but a few. Higher waves tend to be responsible for mouth closure, especially during storms. As a result, estuaries on wave-sheltered coasts tend to have permanently open mouths. A higher tidal range, with flood and ebb tidal ranges in balance, on the other hand, also tends to keep the mouth open (Ranasinghe, 1999).

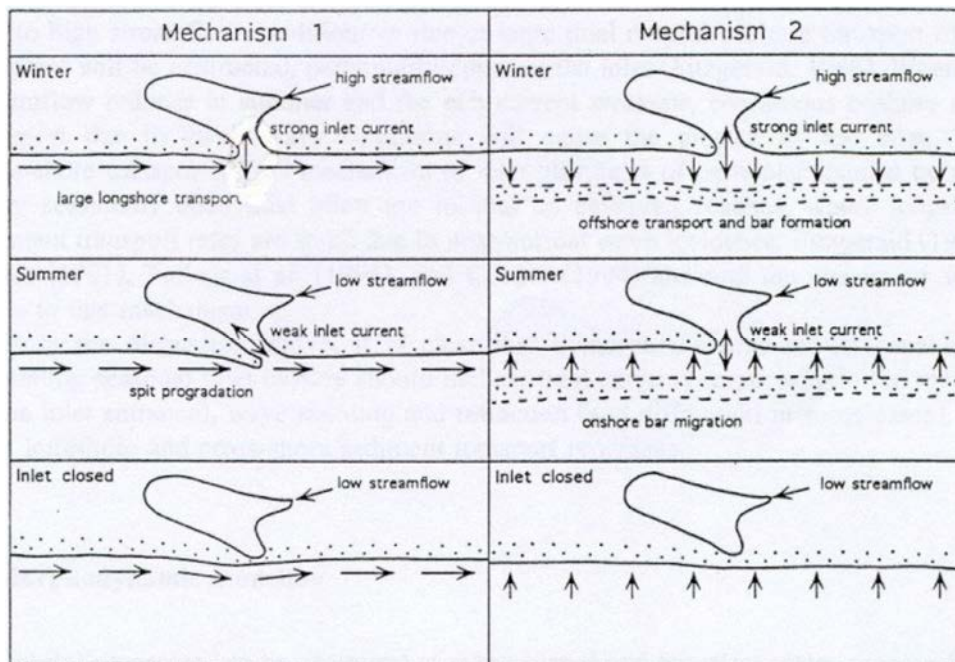


Figure 3: The process of estuary mouth closure (Ranasinghe, 1999)

### 2.3 BAY SHAPE AND ORIENTATION

The shape and orientation of soft coastlines are primarily dependent on the redistribution of sediment through coastal processes. When a net loss of sediment is present, erosion occurs. Conversely, a net import of sediment leads to accretion. A state of equilibrium is said to be reached when there is no further net movement of sediment (Dronkers, 2005; (Komar, 1998).

*Static equilibrium* exists where there is almost no littoral drift. This is typical of bays where the incident waves are breaking simultaneously and parallel to the shoreline. The *planform*, often described as the perimeter or shape of a bay that is in static equilibrium, is governed by the wave state and bathymetry. A bay that is in a state of *dynamic equilibrium* is in need of a constant sediment source to maintain the stability of the coastline in the long term. If the sediment supply is interrupted, the planform of the bay will revert to that of the *static equilibrium* state. It is important to note that dynamic equilibrium can also apply to coastlines where the direction and magnitude of longshore transport oscillates with the seasons. A coastline may also be in the unstable state of natural reshaping, where changes in the sediment supply, wave state, bathymetry or sheltering may lead to erosion or accretion of the beach (Hsu, 2010).

As a result of the dynamic attributes of coastlines constantly adapting to the dominant processes, headland-bay beaches may be formed as these coastlines tend to adapt in order to reach equilibrium. The ideal scenario is the case where a wave set approaches an infinitely long straight coastline. This coastline is a soft coastline and the wave incident angle is oblique. As a result of the waves breaking at an angle to the coastline, a longshore current is created. For the described ideal case there is no variance in longshore transport, the coast will enter a state of dynamic equilibrium with zero net transport. Specific to headland bays and the South African south coast is the case where there is a section of less erodible coastline present on a predominately soft coastline. This less erodible section acts similar to a groyne, in the sense of interrupting the longshore transport.

Furthermore, on the lee side of this rocky outcrop or headland, erosion will occur due to the lack of supplementing sediment. If incident waves approach the headland at an angle, refraction and diffraction of wave energy around the structure will be present. Smaller waves will enter the lee side of the structure into the sheltered area. This results in a wave height or wave set-up difference between the sheltered section and the immediate 'open coastline' in the bay. This phenomenon leads to a longshore variation in wave set-up and, in turn, generates a longshore current towards the sheltered area. The ideal scenario will be the accretion of the sheltered area until the waves are breaking normally against the entire shoreline and the coastline can enter a state of dynamic equilibrium (Malan, 2012).

This is, however, an idealised case, with waves and wind direction varying with climate patterns and changes dependent on the orientation of the bay. The ability of a coastline to adapt to a state of equilibrium is therefore seen as seasonal.

## A Preliminary Analysis of the Sediment Budget Across the Swartvlei Estuary Mouth

From Figure 4 it is seen that headland bay beaches are common on the South African coastline, and especially on the South Coast. These bays are characterised by a spiral shaped coastline present in the lee of a predominant headland. In Figure 4 three general bays are presented – one on the western coast and two on the southern coast of South Africa. Following these typical headland bay scenarios on the South African coast, Figure 5 depicts how the bay from Gericke Point towards the Swartvlei estuary mouth fits the general trend of headland bay beaches. One characteristic of these typical headland bay beaches is the long coastline present. This is a major attraction for residential development and tourists. The development often occurs within the dynamic coastal process zone, without consideration for the assigned setback lines. It is therefore a matter of great importance to monitor erosion on the coastlines, estuary mouth behaviour and also to monitor water levels in these areas.



Figure 4: : (a) Headland-bay beaches are present along the South African coast; (b) Headland-bay beach on the West coast; (c) Algoa bay in the Eastern Cape; (d) Mossel bay on the southern Cape coast (Malan, 2012).

## A Preliminary Analysis of the Sediment Budget Across the Swartvlei Estuary Mouth

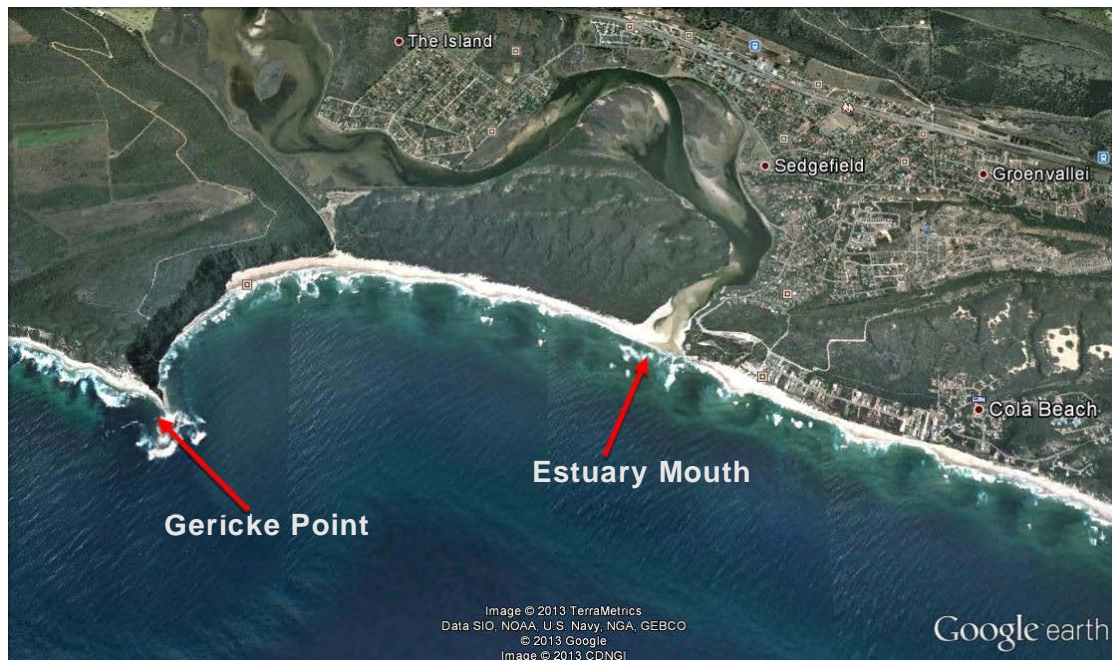


Figure 5: The bay at Swartvlei fitting the headland bay beach trend (Google Earth)

A characteristic of these headland bays is the variation in metocean processes influencing them at any given time. Furthermore, in-depth numerical simulation of these bays and the pertinent marine processes, with the various available numerical modelling packages, is technically difficult. Common practice has therefore evolved into the empirical prediction of the planform of the bay in static equilibrium, based on the direction of the primary wave condition. This planform is then compared to the current shape of the bay to determine whether the bay is in a state of static equilibrium and, if not, the possible amount of erosion that might occur should the bay become unstable (Hsu, 2010). Much work has also been done on the stabilisation of bays through the use of these static shapes ((Silvester, *et al.*, 1972); (Silvester & Ho, 1980)). By predicting the stable shape of a bay, small scale bays can be designed in order to reach static equilibrium.

Many mathematical expressions have been developed to describe the static equilibrium planform. The three primary models are (1) the logarithmic spiral model by Krumbein (1944), as cited by Yasso (1965), (2) the parabolic model by Hsu & Evans (1989) and (3) the hyperbolic tangent model by Moreno & Kraus (1999).

The first model to be fitted to headland-bay beaches was that of the logarithmic spiral (henceforth log-spiral) by Krumbein (1944) and later Yasso (1965). In this first model the logarithmic equation was selected in an attempt to simulate the appearance of seaward-

concave shaped bays in which the radius increases with the distance from the headland (Yasso, 1965).

Bays in the U.S.A. were fitted with the logarithmic expression given by the following expression:

$$R_2 = R_1 e^{\theta \cot \alpha}$$

In this equation the length of consecutive radii is separated by an angle,  $\theta$ . Refer to Figure 6 for a definition sketch. The angle  $\alpha$  is the angle between the radius and the tangent to the curve, which remains constant.

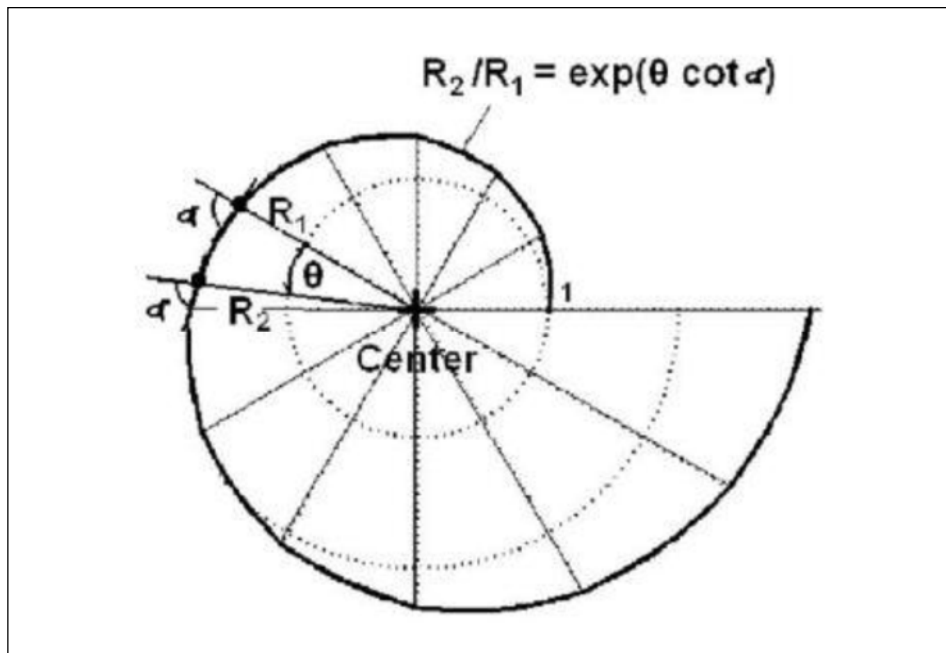


Figure 6: Definition sketch of the logarithmic spiral model (Hsu, 2010)

According to Hsu (2010), the log-spiral model was severely limited in the sense that the centre of the spiral often did not match the point where the incident waves started diffracting. Hsu (2010) also noted that the model did, however, resemble the up-drift end of the bay with reasonable accuracy, but that it failed to simulate the straighter section on the down drift side of the headland bay coastline. This concept is illustrated in Figure 7 by Hsu & Evans (1989).

As a result of these noted limitations of the log-spiral model, a Parabolic Bay Shape Equation (PBSE) was proposed by Hsu & Evans (1989). The PBSE was derived empirically by fitting it to the planform of 27 bays (including prototypes and models) in the static equilibrium state (Hsu, 2010). The objective of this model was to simulate the theoretical static bay shape as a result of the influence of an oblique wave incidence angle, the point of diffraction and a reference point located at the down coast limit of the coastline (Hsu & Evans, 1989). Further

down drift from the reference point, the beach is assumed to be straight and parallel to the dominant wave crests. The definition sketch is shown in Figure 8.

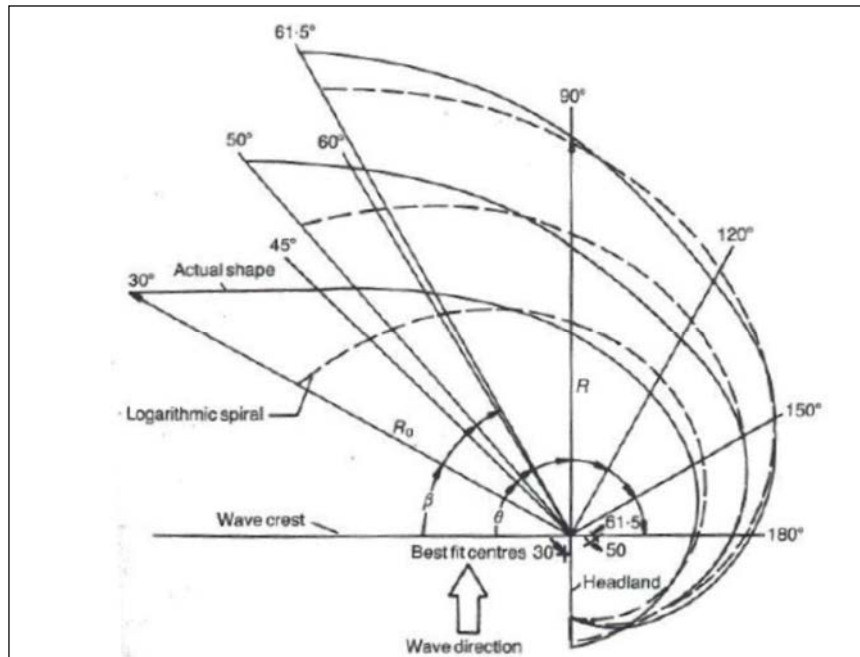


Figure 7: Comparison of log-spiral models to actual bays (Hsu & Evans, 1989)

Radii ( $R_i$ ) are drawn from the diffraction point to points along the beach at arc angles  $\theta_i$  to the wave crest line. The radius drawn to the down coast limit of the beach is called the control line ( $R_0$ ), which makes an angle  $\beta$  to the wave crest line. The ratio of each  $R_i$  to the control line is given by the following equation as:

$$\frac{R}{R_0} = C_0 + C_1 \left(\frac{\beta}{\theta}\right) + C_2 \left(\frac{\beta}{\theta}\right)^2$$

The constants are dependent only on the angle of obliquity,  $\beta$ , and can be linearly interpolated from tables and figures presented in Hsu & Evans (1989).

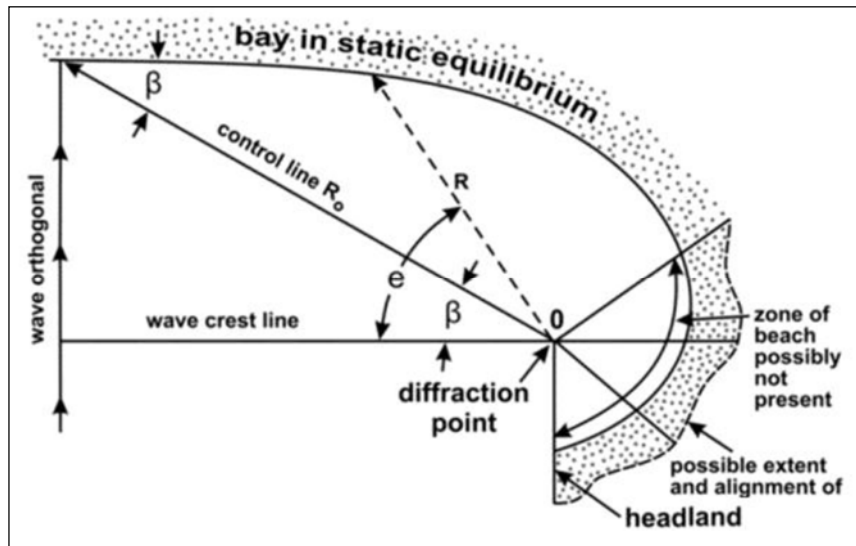


Figure 8: Definition sketch of the parabolic bay shape equation (Hsu & Evans, 1989)

In the work done by Hsu & Evans (1989), the parabolic model was compared to two natural beaches in an attempt to assess the accuracy of fit of the PBSE. One beach was in static equilibrium and the other a model or ideal beach. A comparison of the natural bay shape and that predicted by the parabolic model is shown in Figure 9. Something to note is the relative accuracy with which the model predicts the planform of the bay, especially on the down drift side of the beach (Hsu & Evans, 1989).

Aerial imagery or nautical charts are used as input parameters to derive the positions of the three control points, (1) being the diffraction point, (2) the down drift end of the beach and (3) the start of the tangential section of the beach. These three points determine the final bay shape predicted by the model. The PBSE model is thus a very useful prediction model, in the sense that the input parameters needed for the set-up of the model are readily available (Malan, 2012).

## A Preliminary Analysis of the Sediment Budget Across the Swartvlei Estuary Mouth

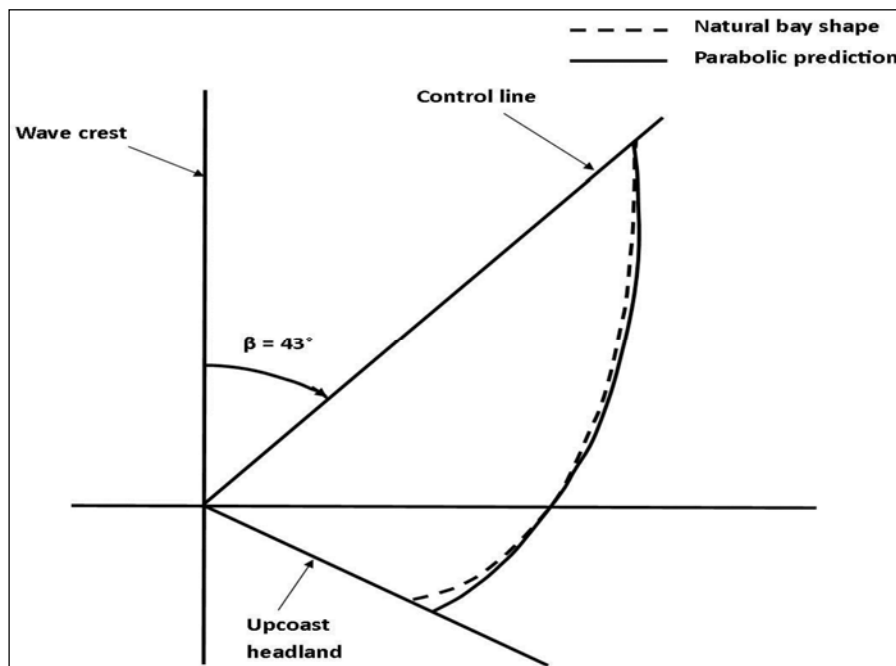


Figure 9: Predicted parabolic and natural planforms of Keppel Island, Queensland, Australia (Hsu & Evans, 1989)

In an effort to gauge the uncertainty caused by subjectivity in the choice of the control points, Lausman *et al.* (2010) generated a database of the chosen positions of the control points. Expert volunteers were asked to choose the control points of a stable bay. It was found that the PBSE was a robust method when the user could see the effect of the choice of the control points on the predicted planform.

According to a study performed by Moreno & Kraus (1999), it was found that the parabolic model was too insensitive to the parameters determining the parabolic shape. Furthermore, this study concluded that the control point was not well defined and therefore the selection of the parameters had little influence on the final predicted *planform*. Moreno & Kraus (1999) went on to propose a hyperbolic tangent shape (presented in Figure 10) as a method that is simpler to apply and will fit bays with a single headland as well. The shape is described by:

$$y = \pm a \tanh^m(bx)$$

where  $y$  is the cross-shore distance,  $x$  is the alongshore distance and  $a$ ,  $b$  and  $m$  are coefficients which are empirically determined. The asymptote at  $y = a$  indicates the general shoreline trend.

The  $x$ -axis is drawn parallel to the asymptote and the  $y$ -axis normal to that in the landward direction. The origin should be placed at a point where the tangent to the shoreline is normal to the asymptote as shown in Figure 10 (Moreno & Kraus, 1999). According to the study this

model is therefore a relatively simple and well defined process. Another useful property of the hyperbolic tangent equation is the fact that the asymptote at  $y = a$  defines the down drift edge of the beach, thereby eliminating the confusion of the PBSE (Moreno & Kraus, 1999).

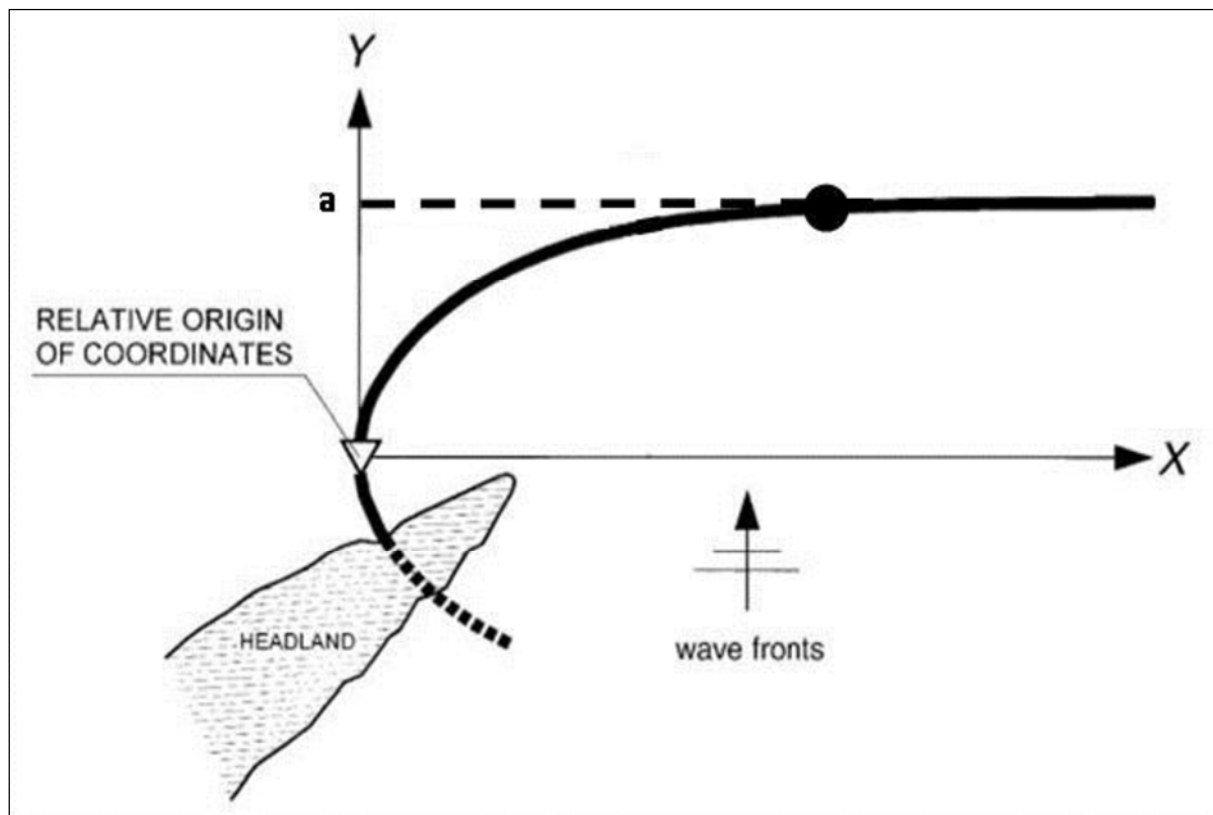


Figure 10: Definition sketch of the hyperbolic tangent shape model (Moreno & Kraus, 1999)

Although easily applicable, the hyperbolic tangent model (like the log-spiral model) fails to place its origin at the diffraction point and to relate the bay shape to the angle of incident wave energy (Hsu, 2010). It is therefore not able to be used as a test for the stability of a headland-bay beach, or predict the effects of changes such as varying diffraction points, e.g. the extension of a breakwater (Hsu, 2010).

## 2.4 MARINE SEDIMENT TRANSPORT

### 2.4.1 Introduction

Literature from a study done by Theron (2004) on the sediment regime encountered along the southern coast of South Africa, with special emphasis on the East London area, suggested that net sediment transport along the South African coast is usually south to north. Furthermore, Theron indicated the longshore sediment transport encountered along the South African coastline would be in the region of 400 000-1 200 000 m<sup>3</sup> per annum on average. This estimation is stated to be valid for the exposed, open South African coast, while the potential

transport due to wave energy is sometimes even higher. This concept is illustrated in Figure 11. Along rocky shorelines or sheltered areas, Theron estimates a net average longshore transport rate between 10 000 m<sup>3</sup> and 400 000 m<sup>3</sup> per annum.

Within the coastal zone, there are a number of processes that can transport varying amounts of marine sediments along a coastline. Longshore transport has been identified as one of the main processes involved in transporting marine sediments. These sediments, in turn, are then potentially available to be transported into the estuary itself, mainly by means of tidal flow through the mouth, sometimes in conjunction with wave action.



Figure 11: Typical net longshore transport rates in Southern Africa in m<sup>3</sup>/yr (Schoonees, 2012)

Cross shore transport is also identified as a significant contributor towards individual sediment transport events. For individual events that lead to severe cross-shore transport, rates are estimated to be as high as 150 000 m<sup>3</sup> measured over a period of 2 days for very large sea storms and a shoreline length of 500 m (Theron, 2004). More typical shorter-term storm net cross-shore rates would be in the order of a few m<sup>3</sup>/m per hour for 24 hours. Most Southern African sea storms have a duration of a few hours to a few days (Theron, 2004).

Aeolian transport has been identified as a sediment transport mechanism above the high-water line. A study by Theron (2004) stated that sediment is rarely transported by individual processes, but rather by combinations of, for example, longshore, cross-shore and Aeolian transport. The quantification within the surf zone is also a combination of transport modes including circulation patterns such as rip-currents, which makes the quantification of amounts transported very difficult (Theron, 2004).

A Preliminary Analysis of the Sediment Budget Across the Swartvlei Estuary Mouth

There are also a few processes, such as wind action and wave *overwash*, which can transport marine sediment directly into the estuary, i.e. tidal flow through the mouth is not necessarily required to facilitate these sediment inputs. Sediment transport in the near shore region is usually categorised as being between the longshore (parallel to the shoreline, Figure 12) and cross-shore (perpendicular to the shoreline, Figure 13) (Theron, 2004).

Furthermore, marine sediment transport is dependent on wave and tide conditions, with the result that it changes continually, not only in direction and rate, but also in the location where it takes place in the near shore zone. The sediment movements near estuary mouths are therefore a dynamic response to these complex wave and current systems.

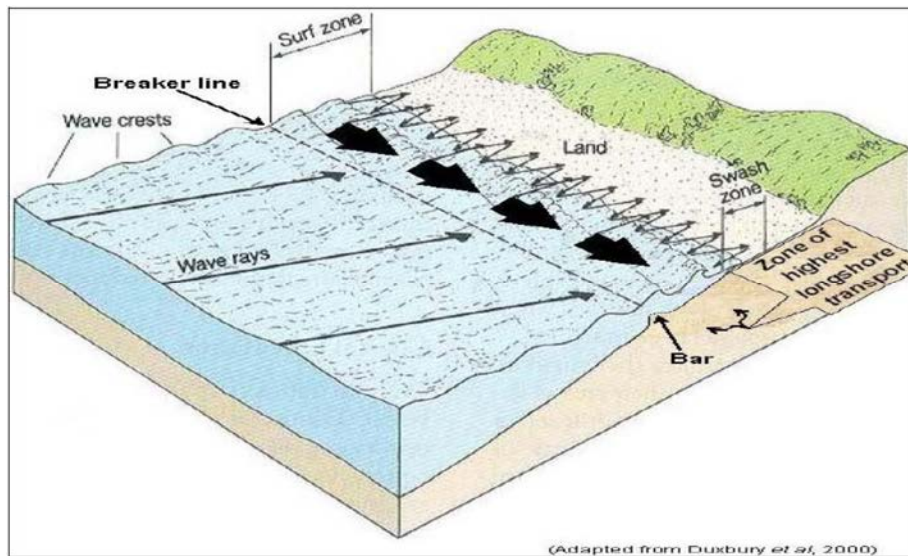


Figure 12: Example of longshore transport (Theron, 2004)

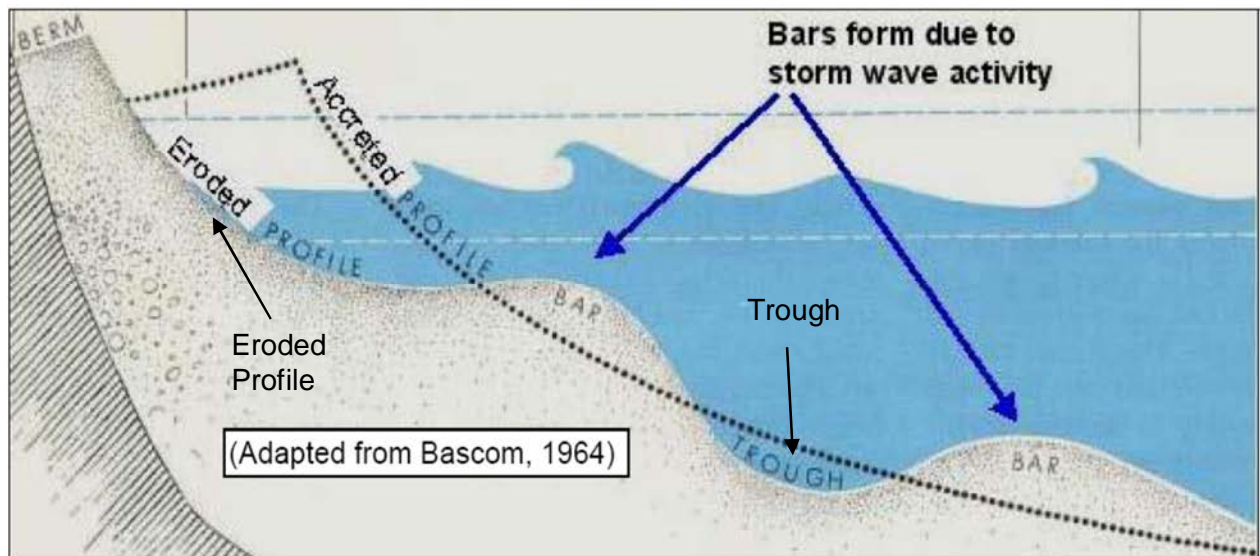


Figure 13: Example of cross-shore transport (Theron, 2004)

### 2.4.2 Cross-shore transport

Cross-shore transport takes place perpendicular to the shore and is a direct result of wave conditions. When there is a storm event, the initial beach cross profile is impacted by recurring wave actions, which cause the beach to erode on the landward side and accrete in the surf zone to a maximum depth (the 'close out depth') (Schoonees & Theron, 1994). In cases where a narrow beach zone is followed by a steep dune or bluff system on the landward side, the run-up due to these storm effects can lead to dune toe erosion.

Defining the manner in which these dunes and bluffs contribute to the sediment budget will guide the preliminary process of estimating quantities from these contributors. Combining the expected seasonal beach profiles, illustrated in Figure 14, with the known prevailing wind and wave climates in this area, erosion was identified as playing a major role in depositing sediment in the transport regime along the Swartvlei coastline. In a journal published by FEMA (Federal Emergency Management Agency - a division of the U.S. Department of Homeland Security) on Guidelines and Specification for Flood Hazard Mapping Partners (February 2007) - the process of erosion was defined as follows:

*Erosion processes and consequences can either be 'episodic' or 'chronic'. These two descriptions are very important temporal components of erosion processes and their results. Episodic erosion is the shore and backshore adjustment that results from short duration, high intensity meteorologic and oceanic storm events. This type of event response results in shore adjustment and occurs during a single storm event or during a series of closely spaced storm events within a storm (FEMA, 2007).*

Chronic erosion is associated with slow, long term processes such as gradual shoreline adjustment associated with:

1. Sea level rise
2. Land subsidence
3. Changes in sediment supply due to watershed modifications or dam building
4. Adjustments in rainfall, run-off and wave climate associated with global warming

A Preliminary Analysis of the Sediment Budget Across the Swartvlei Estuary Mouth

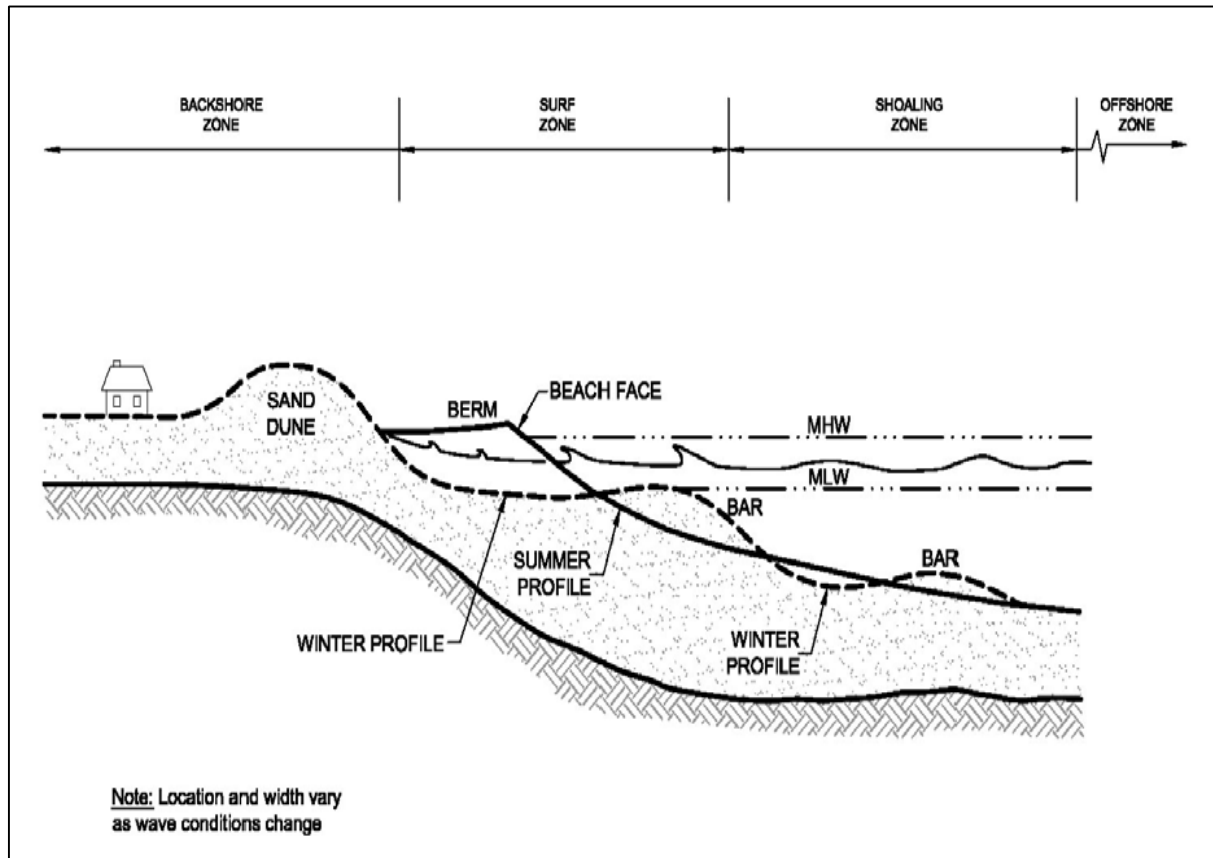


Figure 14: Typical winter and summer beach profiles (FEMA, 2007)

The concept of erosion during winter storm periods is illustrated in Figures 15 and 16. It is noted that, although the beach profile dramatically reduces during winter periods, a similar but less intense consistent wave climate during the summer periods should restore the dune equilibrium profile to acceptable levels.

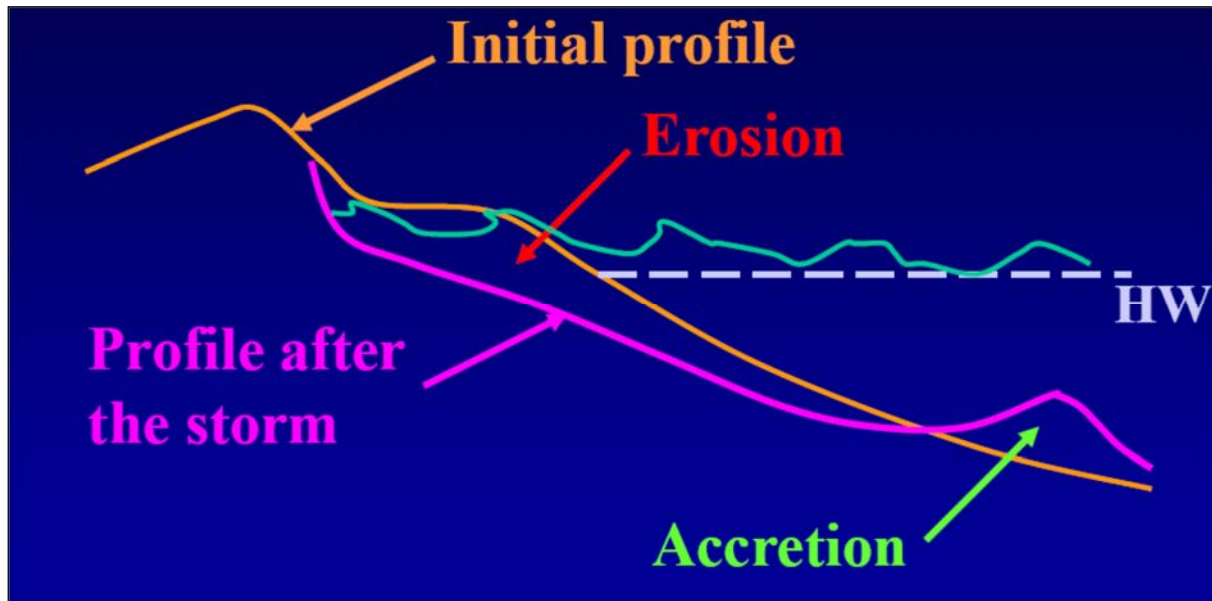


Figure 15: Illustration of the beach profile change due to cross shore transport (Schoonees, 2012)

If storm water levels reach sufficient elevations to intersect the toe of the bluff, storm waves can directly impinge on the bluff face, causing bluff toe erosion (FEMA, 2007). If enough material is eroded from the toe during a storm, the upper portion of the bluff can fail, resulting in bluff retreat or bluff slumping. This phenomenon of slumping has been identified as a process possibly leading to sediment contributions from certain main areas along the Swartvlei coastline. It should be noted that significant bluff failure may not occur during all storm events. However, if the bluff materials are erodible, similar to the sand stone cliffs at Gericke Point, toe erosion and bluff failures are possible during individual storm events. Illustrated in Figure 16 are the phenomena of bluff erosion and slumping during winter and summer periods.

## ERODIBLE BLUFFS

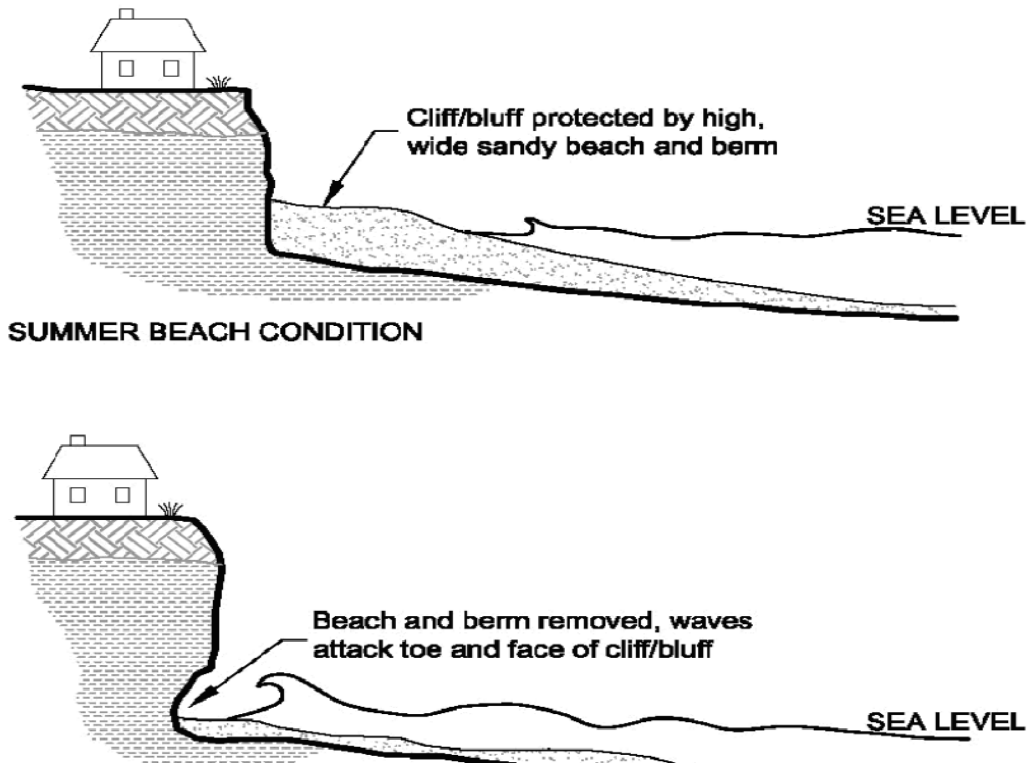


Figure 16: Winter and summer bluff profiles (FEMA, 2007)

To estimate these beach profile changes, two types of modelling are used:

1. Physical modelling
2. Mathematical modelling

The mathematical models include:

- Swart(1974)
- Larson and Krauss(SBeach, 1989)
- Kriebel and Dean(1993)
- UNIBEST(Deltares, 2011)
- MIKE LITPACK( DHI, 2012)
- Xbeach (Deltares, 2014)

In the execution of these models there does, however, exist some limitation. These limitations include the following:

## A Preliminary Analysis of the Sediment Budget Across the Swartvlei Estuary Mouth

- Two dimensional modelling limitations
- calibration for accretion is limited
- Lack of accurate simulation for the following processes:
  - Overwash
  - Dune Slumping
  - Effects of seawalls and revetments again
- Physical sediment modelling is difficult and often results in inaccurate values

For the empirical prediction approach, beach slopes and profiles can be estimated by means of the Bruune rule and Dean profiling (CEM, 2006).

$$y = Ax^{0.67}$$

where

$$A = f(\text{fall velocity})$$

According to Theron (2004), maximum transport occurs at a depth less than 10 m (MSL), with smaller quantities being transported to a depth of roughly 15 m (MSL).

The Kriebel & Dean (1993) method was introduced as a simplified analytical model for predicting dynamic profile response during storms. This method is based on the observation that beaches tend to respond exponentially towards a new equilibrium profile over time. For laboratory conditions, where a beach is suddenly subjected to steady wave action, the time-dependent shoreline response  $R(t)$  may be approximated by the form:

$$R(t) = R_{\infty} \left(1 - e^{-\frac{t}{T_s}}\right)$$

where  $R_{\infty}$  is the equilibrium beach response and  $T_s$  is the characteristic time-scale of the system.

An exponential response of this kind has been observed in wave tank experiments by Swart (1974), Dette & Uliczka (1987) and Larson & Kraus (1989).

According to studies done by Dr Andrew Mather of the University of KwaZulu-Natal and a University presentation by Dr Schoonees of WSP Consulting Engineers, typical cross-shore erosion distances for the South-African coast vary from 10 m 80 m. This relates to a cross-shore transport rate of 20 m<sup>3</sup>/m–120 m<sup>3</sup>/m (Mather, 2008) (Schoonees, 2012).

Due to the complex nature of cross-shore sediment transport, its contribution towards the bulk sediment transport along the coastline defined in this study will not be considered. Erosion of

the Sedgefield bay coastline will, however, be considered and the impacts discussed in detail in Chapter 3.

### 2.4.3 Longshore transport

The basis of a bulk longshore transport analysis is an accurate knowledge of the details of the particulates involved (sand, gravel, cobbles, cohesive materials etc.).

The main driver of longshore transport include:

1. Wave generated currents, as a result of:
  - Oblique incident waves
  - Longshore variation in wave height

The CERC formula (CEM, 2006) for longshore transport is represented as follows:

Longshore transport rate:

$$S = K * P_{ls} * f$$

Energy flux factor ( $P_{ls}$ ):

$$P_{ls} = (EC_g)_b * \cos \theta_b * \sin \theta_b$$

Wave energy density:

$$E_b = \frac{1}{8} * \rho g H_{bs}^2$$

where:

K = 1289

$H_{bs}$  = significant breaker height

$(EC_g)_b$  = wave energy flux in the breaker zone

$\Theta_b$  = wave incidence angle at breaker line

$f$  = frequency of wave condition occurrence

Some issues regarding the sensitivity of this equation have, however, been raised and this has led to the formulation of new equations to describe the dynamic phenomenon of longshore transport, which take into account more parameters (Schoonees & Theron, 1994).

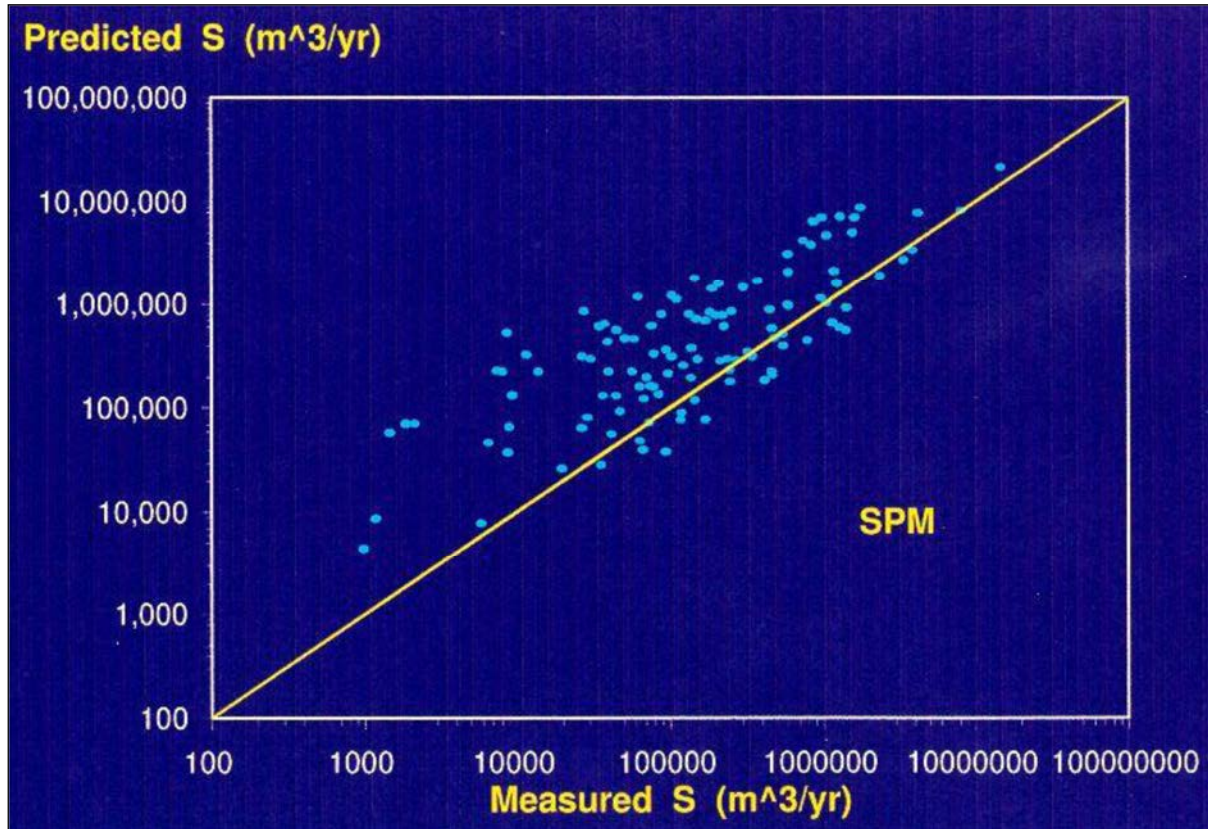


Figure 17: Accuracy of the CERC/SPM formula (Schoonees & Theron, 1994)

As a result of these multiple studies into longshore transport, updated and more accurate transport formulae have been formulated. One of these is the Kamphuis formula for bulk transport (Kamphuis, 2010). Kamphuis has taken the original CERC formula and recalibrated it to include more parameters.

Longshore transport rate according to the modified Kamphuis formula (Schoonees, 2001):

$$S = 38900 * z$$

$$z = \frac{1}{(1 - p)(\rho - \rho_s)} * \frac{\rho}{T_p} * L_0^{1.25} * H_{bs}^2 (\tan \alpha)^{0.75} * \left(\frac{1}{D_{50}}\right)^{0.25} * (\sin 2\theta_b)^{0.6}$$

where z is a function of:

- Significant wave height at breaker line ( $H_{bs}$ )
- Peak wave period ( $T_p$ )
- Wave incidence angle at the breaker line ( $\theta_b$ )
- Beach slope ( $\tan \alpha$ )
- Median grain size ( $D_{50}$ )

Density of the sediment grains ( $\rho_s$ )

Offshore wavelength( $L_0$ )

Density of seawater ( $\rho$ )

Porosity ( $p$ )

Frequency of occurrence of the wave condition ( $f$ ;  $0 < f \leq 1$ )

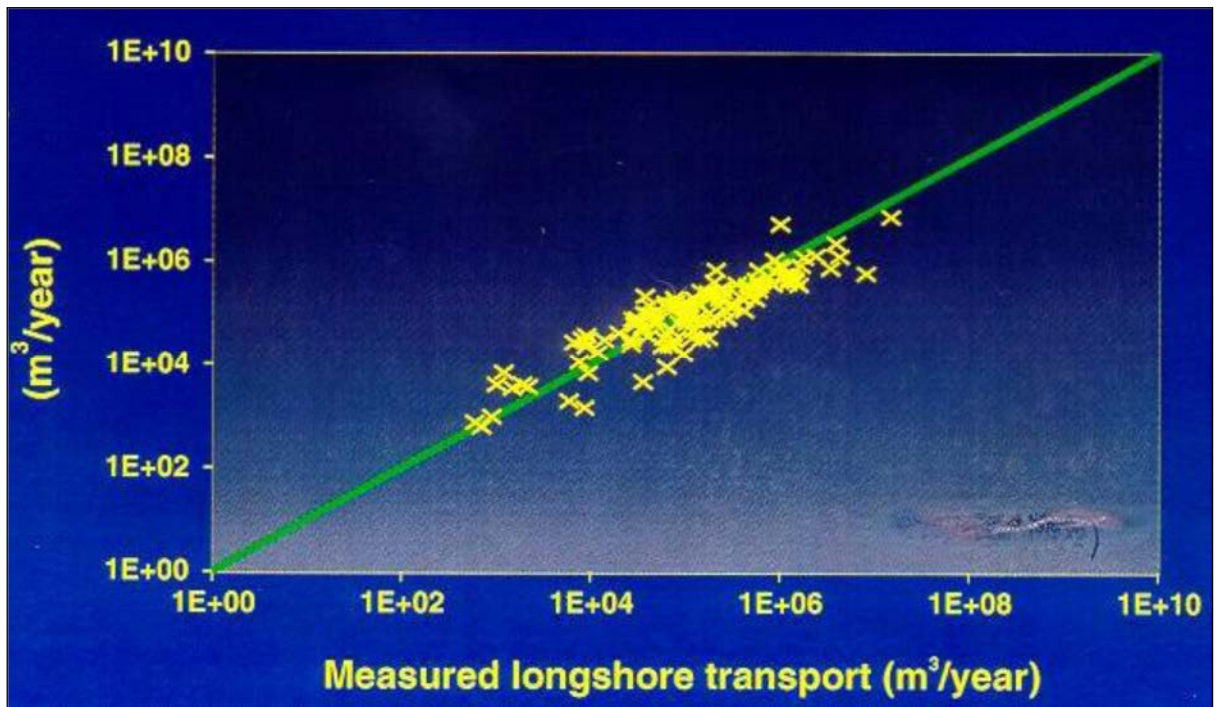


Figure 18: Accuracy of computed longshore transport with Kamphuis bulk longshore transport formula (Schoonees & Theron, 1996)

The studies of (Schoonees & Theron, 1996) illustrate the accuracy of the Kamphuis formula. See Figure 18.

#### 2.4.4 Aeolian transport

According to a research article published by Sloss, C.R., Hesp, P. & Shepherd, M. (2012), coastal dunes are an interlinked dynamic system of ridges that form landward of the foreshore. L.Barwell (2011), regards coastal dune systems as comprising of three dominant zones

1. Fore dune
2. Central dune
3. Back dune

These dune systems differ from other coastal landforms in the sense that they are fundamentally shaped by the movement of air (aeolian transport), rather than by tidal, wave or current action.

Initiation of aeolian transportation is controlled by wind velocity, the characteristics of sediments, beach morphology, moisture content, and the degree of roughness elements that may be present (e.g. driftwood and vegetation). The movement of sediment into the buffer dune environment often initiates coastal dune formation.

Beach sediment transport initiated by wind occurs primarily within 0.5 m above the beach surface, with nearly 90% of movement within a zone of 0.3 m above the beach surface (Bagnold 1941). Once the sediment particle is lifted, it is transported within the dominant wind column along a parabolic trajectory. The speed and distance that the grain will be transported is determined by grain's size, shape and density in relationship to the drag component. The characteristics of the sediment present on a beach, combined with the wind patterns present, result in a certain threshold condition that initiates Aeolian transport.

Once the threshold value is exceeded, sediment can be transported by four interchanging possibilities: traction or creep, saltation, reptation and/or suspension (Figure 19).

1. *Traction (creep) load*: The traction load refers to particles that are too large and/or dense to be entrained by the lift component, or are just pushed along by other grains colliding with the surface grains, and are rolled along the surface due to the traction of the drag force.
2. *Saltation*: Saltation refers to the process in which the sand grains are lifted up into the air and suspended for a short distance before falling back to the surface with a parabolic trajectory. The height and time that the grains remain suspended is determined by grain size, shape, density-lift relationship, drag force, turbulence and velocity of the wind flow.
3. *Reptation*: During saltation, grains in motion may collide with particles on the ground and set them in motion at wind velocities lower than those required to move them by wind alone (i.e., the impact force reduces the lift force required to entrain sediment). When this occurs the process is termed *reptation*.
4. *Suspension*: A very small amount of dust (clay and silt sized particles) and the finest sand particles may be carried in the air for some distance within the dominant wind column without following the typical bouncing motion of saltating or reptating grains. Silt and clay particles may be carried to much greater heights, but this sediment, if present, is usually transported beyond the area of sand dunes.

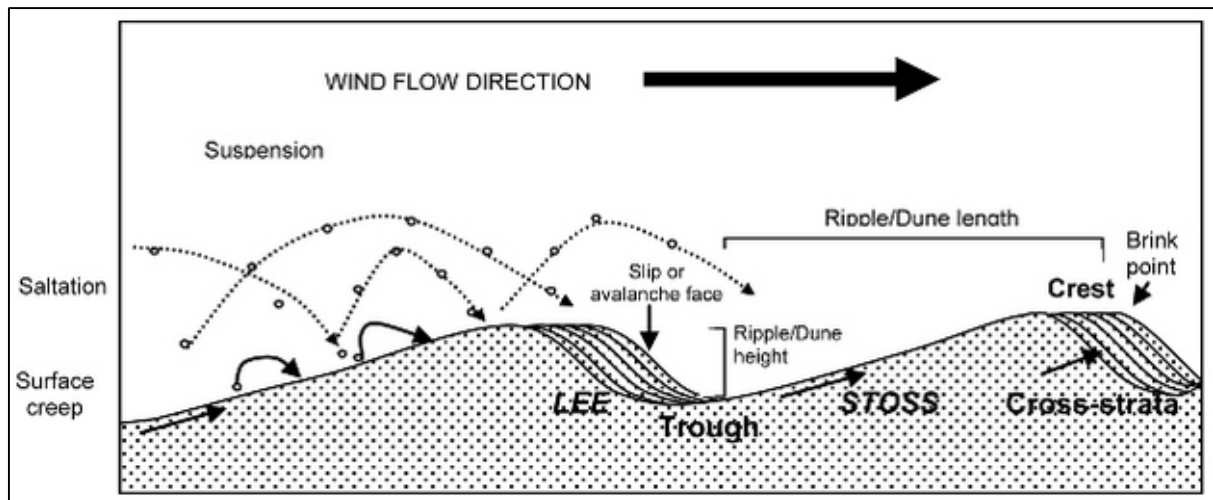


Figure 19: Four mechanism initiating Aeolian transport (Sloss, C. R., Hesp, P. & Shepherd, M., 2012)

Using the methodology described by the CEM (2006) the threshold wind speed ( $U_{*t}$ ) can be calculated using Bagnold (1941):

$$U_{*t} = A_t \sqrt{\frac{(\rho_s - \rho_a)gD}{\rho_a}}$$

In which  $\rho_s$  the mass density of the sediment,  $\rho_a$  the mass density of the air, and  $A_t = 0.118$ . The mean sand grain diameter ( $D$ ) can be obtained from on-site geotechnical sampling investigations or from available, published data. Specific gravity for these calculations were defined as 9.81 m/s<sup>2</sup>.

Combining the pertinent wind characteristics with equation 4-16, CEM (2006) Part III, chapter 4, the amount of sediment being transported ( $q$ ) by the calculated wind speed occurring at that time at a design level ( $u_*$ ) can be estimated by;

$$q = K \left( \frac{u_*}{\sqrt{gD}} \right)^3$$

The empirical coefficient ( $K$ ) is defined by:

$$K = e^{-9.63+4.91D}$$

## 2.5 A SEDIMENT BUDGET ANALYSIS

### 2.5.1 Introduction

Literature published by ABPMer (2008) describes a sediment budget as a balance of the sediment volume entering and exiting a particular section of the coast or an estuary. Sediment budget analysis consists of the evaluation of sediment fluxes, sources and sinks from different processes that give rise to additions and subtractions within a control volume (e.g. a section of coast or an estuary) in order to gain a better understanding of the sediment dynamics of the estuary system.

According to this study a control volume or area is selected and boundaries are then defined on the desired perimeter. The sediment budget, in turn, analyses the sediment entering and exiting over these predefined boundaries. A source increases the quantity of material within the control volume and a sink reduces it. Within the cell there may be point sources and sinks, such as tidal inlets, and line sources and sinks, such as movements on and off the beach (ABPMer, 2008).

An estuary provides a readily defined control volume, where point sources and sinks exist in the form of rivers, other terrestrial outfalls and the open sea. Line sources and sinks may be defined in terms of erosion from cliffs and transfers to or from salt marshes, wetlands or other intertidal areas. The sub-tidal beds also need consideration as important sources or sinks. Material stored in suspension within the volume of water that moves back and forth under tidal action within the estuary also needs to be considered (ABPMer, 2008).

There are two ways in which the budget can be constructed:

- Definition of changes in surface volume within the control volume to give a balance. This is applicable to non-cohesive shores, where suspended sediment concentrations are low, and with similar material types.
- Definition of exchanges in mass to and from the water column to give a mass balance.

Sediment budgets are a means of synthesising the outputs from numerous available analyses and modelling techniques. A budget can also be calculated from historical data and an analysis of change, enabling comparisons between similar budgets which have been derived using the output from computational models. Model outputs can be used to predict the likely budget resulting from some change or development in the system and are usually presented as a tabulation of sources and sinks or a schematic to illustrate the exchanges occurring (ABPMer, 2008). Two different illustrations are shown in the figures below. Figure 20 focuses on the tide volumes while Figure 21 is an illustration of the annual sediment movement.

A Preliminary Analysis of the Sediment Budget Across the Swartvlei Estuary Mouth

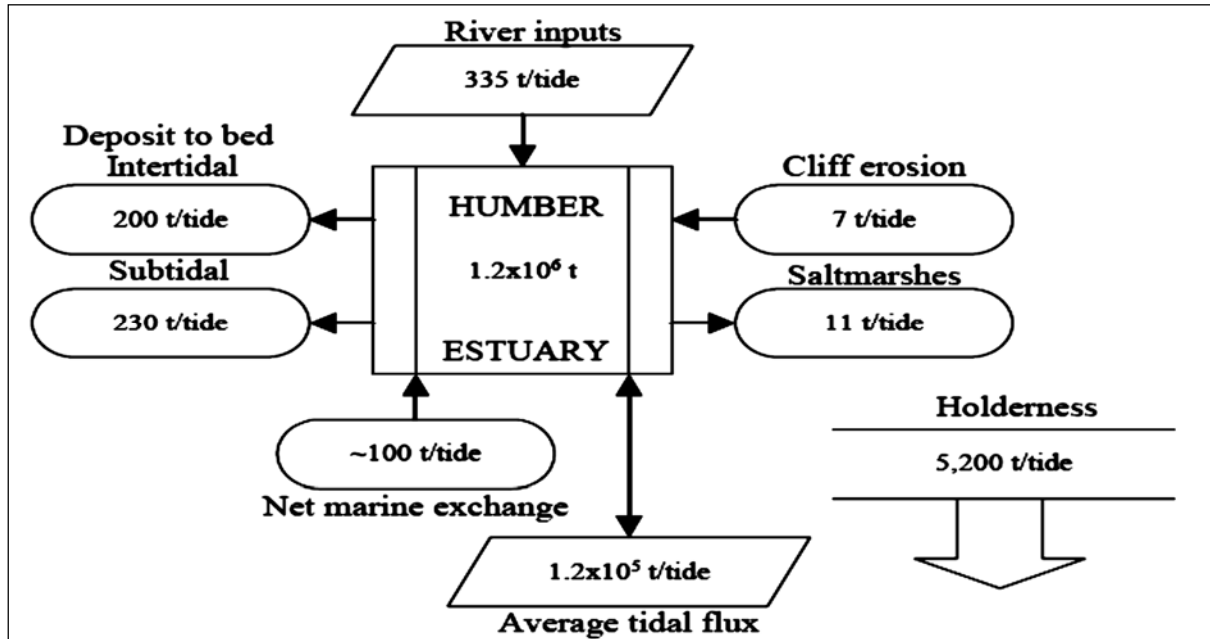


Figure 20: Schematic of the net sediment budget model for the Humber Estuary, UK (Townend & Whitehead, 2003)

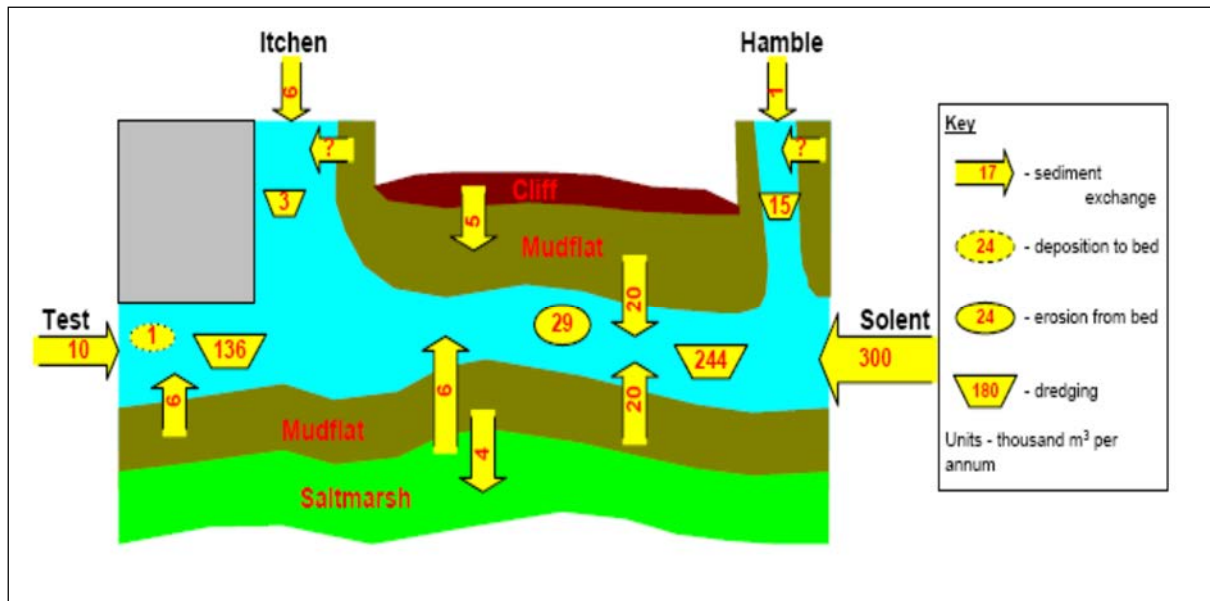


Figure 21: Schematic of the net sediment budget model for Southampton Water, UK (Townend & Whitehead, 2003)

2.5.2 Data commonly used in a sediment budget

Sediment budgets are developed from a variety of available information. Regarding an estuary system, the more common sources of data providing input to the method include (ABPMer, 2008):

- Bathymetric data sets
- Suspended sediment concentration measurements
- Sea bed density
- Fluvial discharge
- Discharge measurements at the mouth of the estuary
- Estimates of littoral drift from standard equations or numerical models and wave data
- Estimates of sediment transport made by numerical models

### **2.5.3 Building a sediment budget**

The steps required to produce a typical sediment budget were summarised by ABPMer (2008) as follows:

1. Schematise the estuary system into a simple flow chart. Try to devise a schematisation which states the focus of the analysis simply and succinctly.
2. Gather available information.
3. Choose the units of the sediment budget:  $\text{m}^3/\text{year}$  is preferred.
4. Choose whether the budget is to be in terms of cohesive and/or non-cohesive sediment. In practice the cohesive sediment and the non-cohesive sediment budgets may be developed independently, though it may not be necessary to complete both for the sediment budget, depending on the identified requirements of the analysis.
5. Evaluate the most straightforward inputs to the sediment budget first. These are often:
  - a. Sediment volume within the system (which can be derived from suspended sediment concentration measurements and the volume of the estuary from charts).
  - b. The fluvial input to the system (which can be derived from fluvial discharge and concentration).
  - c. The morphological trend (derived from comparison of bathymetric data)
6. Evaluate the more difficult inputs. Some sediment budget inputs can be difficult to derive from observations, e.g. net flux from or to the sea in wide estuaries and the extent of erosion of intertidal areas resulting from wave action. Furthermore, it may be best to derive these values by balancing the budget and providing data for all the other budget contributions. If this is not possible, then the derivation of these contributions

may require in-depth analysis, numerical modelling of sediment transport and/or further data collection to determine the sediment contributions.

7. Build iteratively; start on the basis of the available data and gradually improve the sediment budget as knowledge of the system and better data becomes available.
8. Undertake a thorough search for any available historical and anecdotal data (including geological data if relevant). Use this historical data to improve the data in the sediment budget and to aid the understanding of the sediment budget result.
9. Once numbers are available to complete the sediment budget, an uncertainty assessment for all the contributions towards the sediment budget should be executed.

## **2.6 RELEVANT CASE STUDIES AROUND THE WORLD**

### **2.6.1 Moore River estuary, Western Australia**

The Moore River Estuary (Figure 22) is similar to Swartvlei in the sense that it is intermittently open to the ocean. This means that riverine input is able to interact with seawater in the estuary at irregular stages of varying duration throughout the year. Through a modelling analysis of the sand bar at the estuary inlet, researchers suggested that when the bar is open the estuary is dominated by riverine input from the catchment. When the bar is closed, seawater becomes trapped and stratification develops throughout the estuary (Anderson, 2004).



*Figure 22: Moore river estuary, Western Australia (Anderson, 2004)*

Other studies have shown that estuary closure in the south west of Australia is due to a number of factors that reduce flow in the bar channel (Hodgkin & Clark, 1988). A combination of reduced river discharge, the build-up of an oceanic bar as a result of onshore sediment transported by long-period swell wave action during summer, weakened estuary current, longshore sediment transport processes and growth of a sub-tidal estuary sill can cause the mouth of an estuary to become blocked ((Ranasinghe, 1999); (Hodgkin & Clark, 1988); (Marshall, 1993); (Todd, 1995)). Other factors contributing to estuary mouth closure are evaporation and the deposit of sand on the coast following the scouring effect of winter storms (Hodgkin & Clark, 1988).

In the south west of Australia, an estuary is usually isolated from the ocean during the dry summer and early autumn period by an extensive sandy barrier known as a wave-built berm (Potter & Hyndes, 1999). When water levels rise in late winter or early spring as a result of an increase in freshwater river discharge from increased rainfall, a channel is scoured through the sand bar and allows water exchange between the estuary and ocean (Potter & Hyndes,

## A Preliminary Analysis of the Sediment Budget Across the Swartvlei Estuary Mouth

1999) (Griffiths, 2001)). This breaching of the sand bar results in a significant decrease of the water levels within the estuary (Froneman, 2004). The oceanic sediment transport then builds the bar and, as the dry summer approaches, the bar isolates the estuary, once again completing the natural cycle. Therefore, the closure of the mouth of an estuary by the presence of a sand bar occurs when the stream flow is low and/or when the onshore or longshore sediment transport is high (Ranasinghe, 1999).

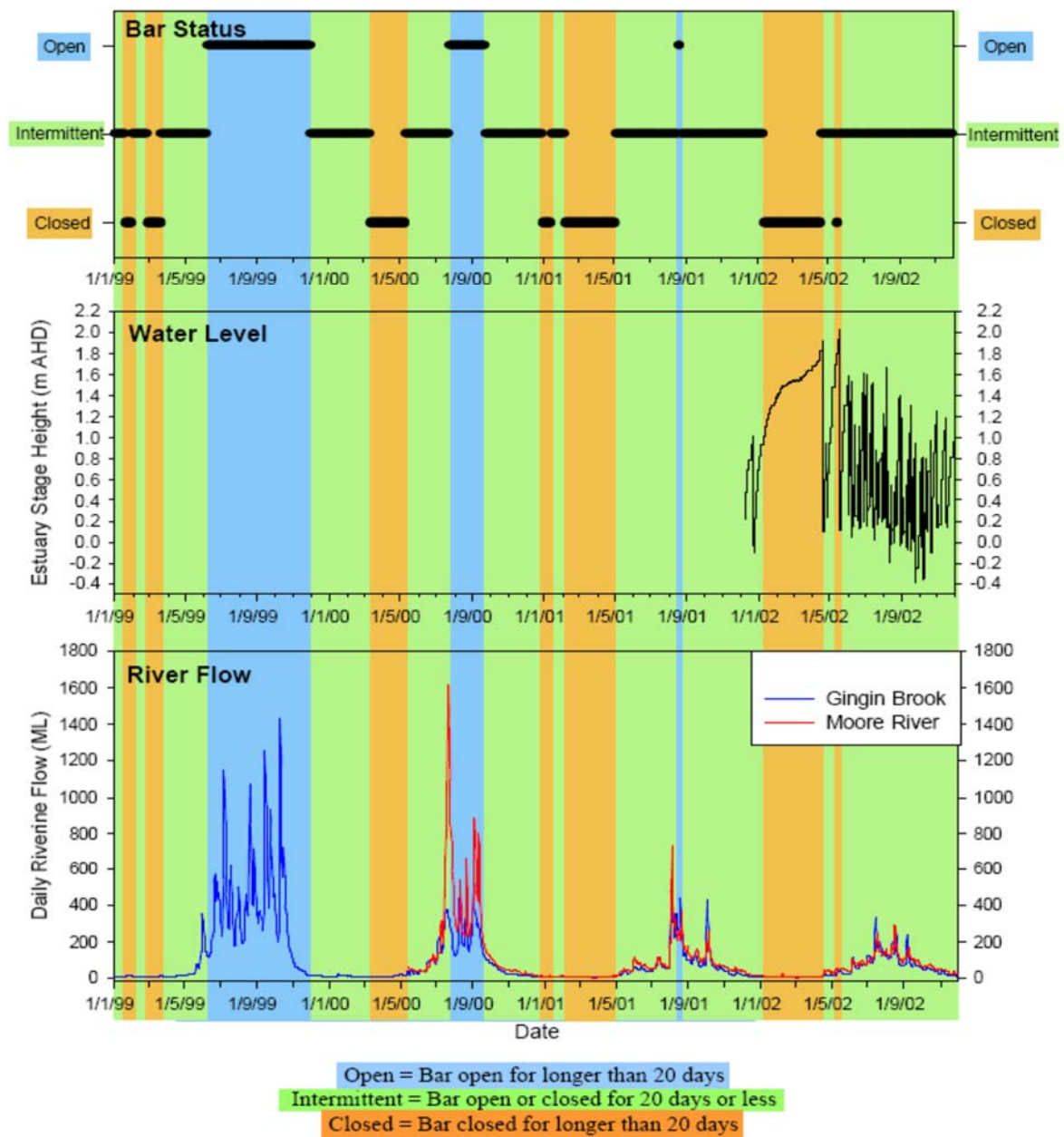


Figure 23: Hydrology of Moore River Estuary and surrounds, 1 January 1999 to 1 December 2002. Displays the bar status (open, intermittent or closed), water level in the estuary and riverine flow from Gingin Brook and Moore River (Anderson, 2004).

## A Preliminary Analysis of the Sediment Budget Across the Swartvlei Estuary Mouth

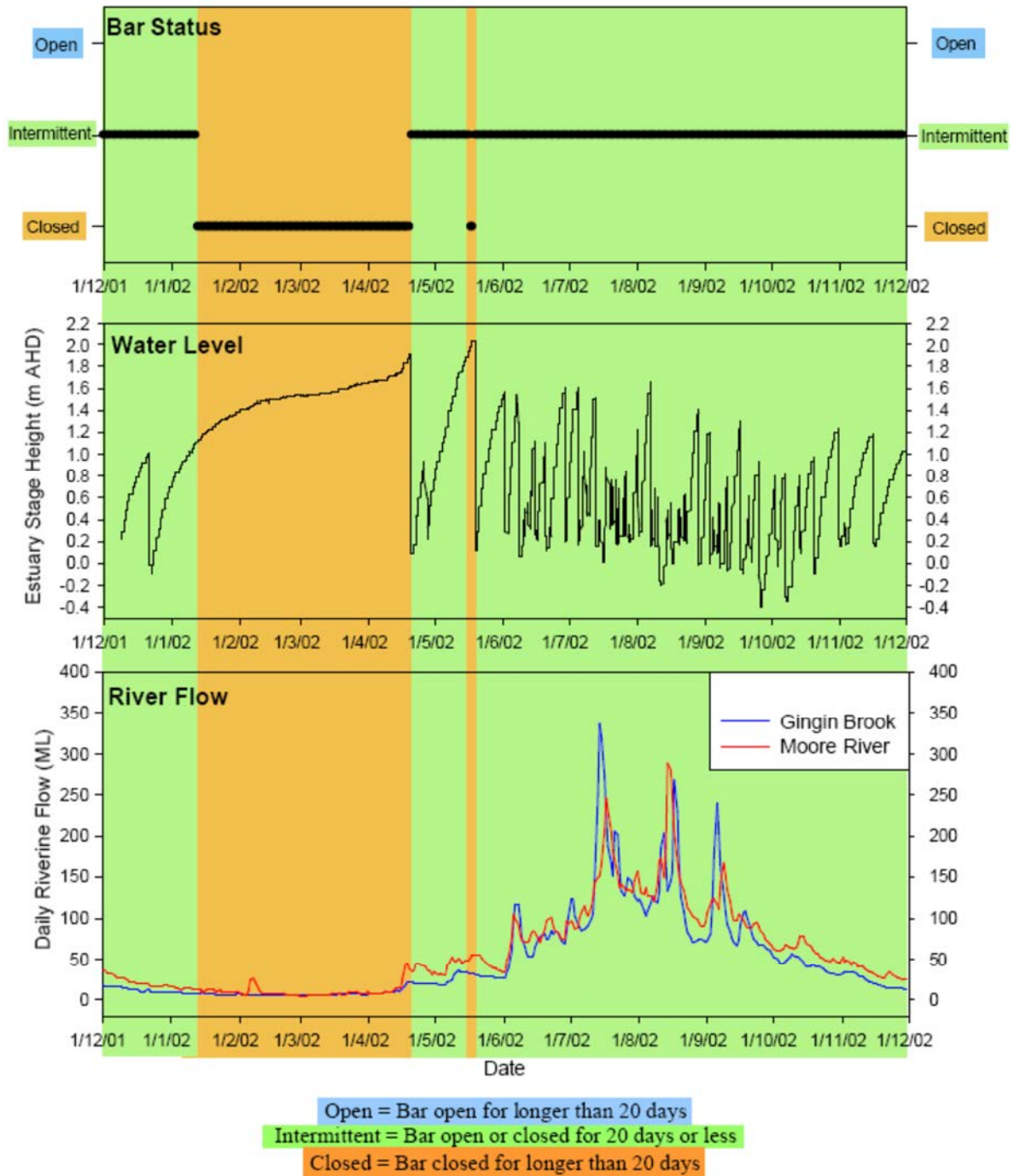


Figure 24: Hydrology of Moore River Estuary and surrounds, 1 December 2001 to 1 December 2002. Displays the bar status (open, intermittent or closed), water level in the estuary and riverine flow from Gingin Brook and Moore River (Anderson, 2004).

From Figure 23 and Figure 24 it is seen that for instances of high flow and raised water levels the bar is scoured away, resulting in an open state for the estuary. The pattern of opening and closing of the sand bar at the mouth of the estuary, changes with time. The bar is open or closed from a few days to a number of months, as it fluctuates between being breached and

blocked. In the analysis of this model, the bar is termed 'intermittent' if the estuary mouth is open or closed for 20 days or less as a result of the bar migration at the mouth of the estuary. While the bar is in an intermittent state, the estuary system is adjusting to the changes caused by suddenly becoming either blocked or connected to the ocean. When the bar opens, the estuary system must adjust to a large decrease in water level as the contents of the estuary are flushed out to the ocean.

The Moore River estuary system is a dynamic system and is dominated by riverine flow and fresh groundwater input. Generally groundwater is dominant when the bar is closed and riverine processes dominate the open estuary, but also interact with the ocean at the mouth (Anderson, 2004).

### **2.6.2 Zandvlei estuary, Western Cape, South Africa**

Zandvlei estuary (Figure 25) is situated near Muizenberg in the Western Cape Province of South Africa. Zandvlei is located in a winter rainfall area and preventive measures are taken during the winter months to reduce flooding. The estuary is artificially managed by the City of Cape Town Municipality, mainly by means of two mechanisms: the rubble weir and the sandbar, both situated downstream of the Royal bridge (City of Cape Town Municipality, 2008).

In 2004 consulting engineers undertook a hydraulic modelling exercise for Zandvlei, using revised inflow data from the various catchments. This revised model study showed that the rubble weir would need to be at a level of 0.6 m MSL to enable a 1 in 100 year flood to pass through the outlet, relating to a water level of 1.78 m MSL in the vlei. The rubble weir is currently situated at 0.7 m MSL, although several requests have been made to raise the level to 0.8 m and even 0.9 m MSL. If the weir were to be raised to a level of 0.9 m MSL, the result would be the flooding of properties. As a result of this foreseen damage to civil structures, the level is maintained as is during the winter months (City of Cape Town Municipality, 2008).



*Figure 25: Zandvlei estuary (note the close proximity of residential properties to the estuary, similar to the case of Swartvlei) (City of Cape Town Municipality, 2008)*

In order to avoid the vleei operating at low levels throughout the winter months, it has been decided to periodically close the sandbar when the existing vleei water levels are low, when the inflow from feeder rivers is not excessive and when there is no impending cold front. The City of Cape Town municipality has acknowledged that this strategy makes the low lying areas vulnerable to flooding, but with careful monitoring of water levels, as well as cold fronts, a suitable water level can be maintained.

During the summer months when the risk of flooding is low, the sandbar is closed to raise the water level in the vleei. No alteration is made to the rubble weir but, due to an ecological requirement, the salinity levels must be constantly maintained. This is achieved by opening the sandbar five to six times during the summer period to allow spring high tides to penetrate into the estuary (see Figure 26). Each mechanical opening is estimated to cost the municipality R20 000, so it is crucial to apply these management strategies correctly (City of Cape Town Municipality, 2008).

A Preliminary Analysis of the Sediment Budget Across the Swartvlei Estuary Mouth



*Figure 26: Mechanical opening of Zandvlei estuary mouth (City of Cape Town Municipality, 2008)*

### 3. SWARTVLEI

#### 3.1 BACKGROUND

Swartvlei estuary was formed during the last ice age (16 000-45 000 years ago). At that stage the bottom of the valley was at least 30 m below the present sea level (Martin, 1962). This meant that at the end of the ice age, when the sea level rose, the valley was flooded and formed the Swartvlei estuary.

According to studies done by Birch and Du Plessis (1977), the historical Swartvlei system was systematically filled, over the years, by windblown sand originating from the local dune system together with wave action, resulting in the portion of the drowned valley forming what is now Swartvlei. These processes formed a littoral shelf around the deeper lake section. Finer sediments originating from the feeder rivers have accumulated slowly in the central basin of the lake. The Swartvlei Lake currently has a surface area of 14.2 km<sup>2</sup>. The maximum depth in the estuary was measured at 4 m, with a narrow central channel bordered by intertidal sand flats of varying depth (Kok & Whitfield, 1986). Swartvlei itself has a mean depth of 5.5 m and a maximum depth of 16.7 m.

Three rivers drain into Swartvlei; the Karatara, the Wolwe and the Hoëkraal Rivers (see Figure 27). The total Swartvlei catchment area is approximately 340 km<sup>2</sup> with each of the three catchments contributing more or less equally to the amounts of fresh water entering Swartvlei (Whitfield *et al.* 1983).

## A Preliminary Analysis of the Sediment Budget Across the Swartvlei Estuary Mouth

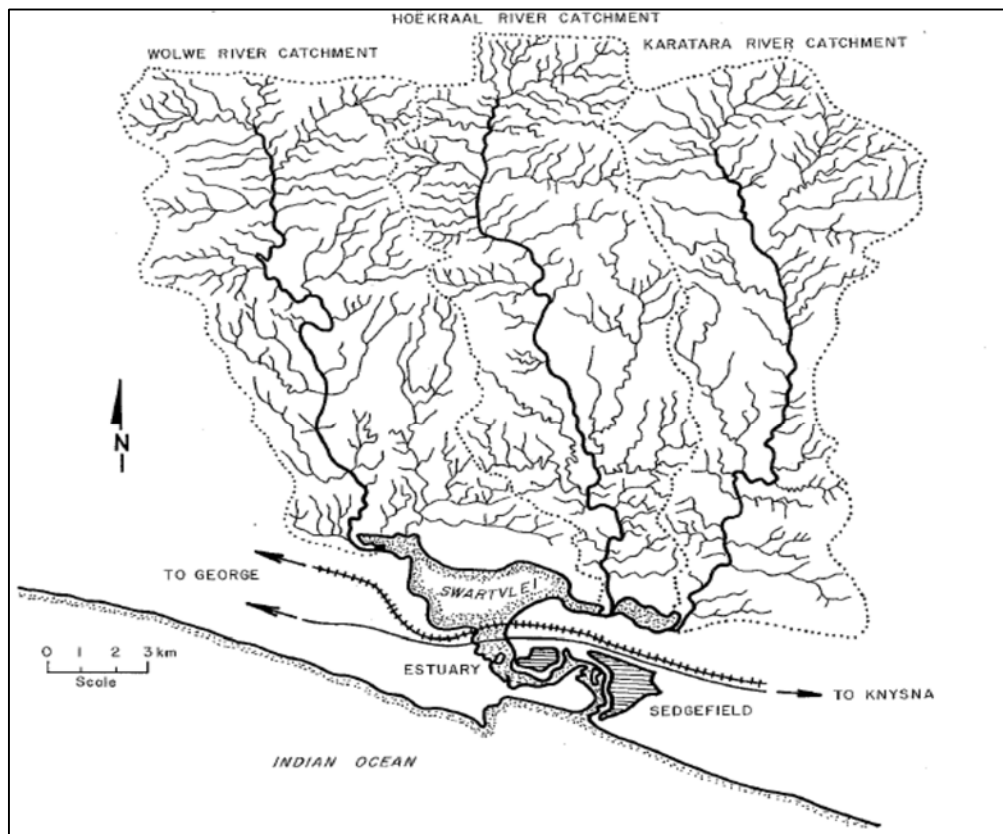


Figure 27: The Swartvlei system showing the extent of the three river catchment areas  
(Whitfield *et al.*, 1983)

A road bridge and a railway bridge have been constructed across the system, just below the point where the lake enters the estuary channel (James & Harrison 2008). According to an analysis by Whitfield, *et al.* (1983), hydrological data has shown that the road bridge has no effect on the tidal movement in the estuary and very minimal effects on the ecology of the estuary (Whitfield *et al.*, 1983).

The railway bridge, on the other hand, does interfere with the flow of water (Whitfield *et al.* 1983). It acts as an obstruction to flood flows which would otherwise scour the estuary and also limits tidal flows to some extent (DWA, 2009). However, tidal flows would not increase significantly if the bridge was removed, because of the shallowness of the estuary (DWA, 2009).

From SANParks records presented in Table 2, forestry and agricultural abstractions combined with the obstructions of the railway bridge and N2 road bridge, the absorbing capacity of the lake and the shallowness of the estuary itself are also influencing the flooding potential originating from the feeder rivers towards the lake and out of the estuary mouth (Fijen & Kapp, 1995). These floods play a vital role in the scouring of the raised sand berm in front of the estuary mouth, necessary to create a channel for open mouth conditions.

Howard & Allanson (1979), estimated a mean sedimentation rate of 2 mm per year, but this is historical data and should be investigated in more updated studies (CSIR, 1983).



Figure 28: Railway crossing over Swartvlei

### 3.2 RIVER CATCHMENTS

The total Swartvlei catchment area is 340 km<sup>2</sup> with the Wolwe river system covering 125 km<sup>2</sup>, the Hoëkraal system covering 109 km<sup>2</sup> and the Karatara River system 106 km<sup>2</sup> (CSIR, 1983). The three river catchments contribute in relatively equal amounts to Swartvlei.

Table 1: Run-off contributions of feeder rivers (CSIR, 1983)

River	Run-off (10 <sup>6</sup> m <sup>3</sup> )
Wolwe River	19.8
Karatara River	20.1
Hoëkraal River	24.8

Combining these run-off totals and adding another 1x10<sup>6</sup> m<sup>3</sup> for smaller streams gives a total freshwater input of 66 x 10<sup>6</sup> m<sup>3</sup> per year (EWISA, 2003). The climate in this region is such that there is no distinct rainfall pattern throughout the year, which leads to a constant freshwater inflow into the lake system. Floods are short lived and result in peak inflow periods. The Sedgefield municipality abstracts water out of the Karatara River every year and the amount increases dramatically close to and during the holiday season. Water abstraction for domestic and agricultural usage is increasing and this is seen as problematic for the natural functionality of the sand-berm, which is flushed out by the lagged flooding effects of the dominant rainy

period of June to August. The interference with the natural processes leading to open mouth conditions is, in turn, mitigated by artificial management of the mouth area (Fijen & Kapp, 1995).

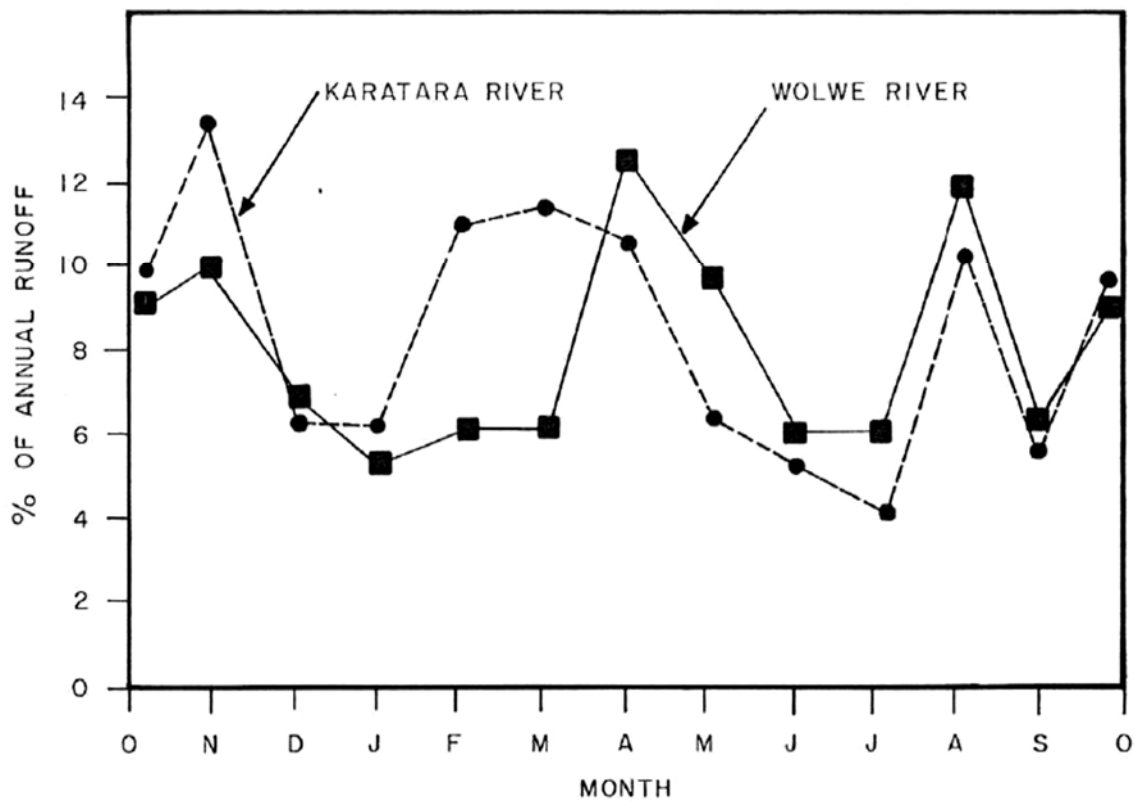


Figure 29: Flow patterns of two inflowing rivers to Swartvlei, showing the lack of seasonal peaks (CSIR, 1983)

Figure 29 illustrates the lack of seasonal run off peaks in the Swartvlei catchment area. The rivers of the Swartvlei catchment area are characteristically stained brown by humic matter from the vegetation in the area. They are low in electrolytes and can be classified as acidic (pH 4-5). The dissolved organic matter concentration of the Wolwe River is only approximately half that of the Karatara and Hoëkraal rivers (CSIR, 1983).

According to a study done by Howard-Williams and Allonson (1978) this reflects the geology of the catchment area. The Wolwe River is situated in a large area of Cape granite and the other two rivers are situated in Table Mountain sandstone. From studies done on suspended materials in the Wolwe River it was found that this system is responsible for much of the fine sediment carried into the lake. Although the rivers usually carry low silt loads (< 10 mg per litre) this can increase to 250 mg per litre during periods of flooding (CSIR, 1983).

From research done by SANParks, a summary of water availability and usage was compiled (Fijen & Kapp, 1995). This report gives insight into what amount of run-off can be expected in the estuary and at the mouth area. Auxiliary implications of the already stated water abstractions for residential and agricultural usage, is the dying off of vegetation on the banks of the lake and estuary. Vegetation plays a key role in anchoring the lake and estuary banks and losses will result in erosion and slumping.

*Table 2: Summary of water availability (Fijen & Kapp, 1995)*

		Value x 106 m <sup>3</sup> /annum
<b>Virgin runoff</b>	Average	70.6
	Minimum	22.7
	Maximum	347.0
<b>Average abstractions</b>	Forestry	18.7(17%)
	Agriculture	3.6(5%)
	Domestic	0.3(<1%)
<b>Present available runoff</b>	Average	48.0(68%)
<b>Potential extra future abstractions</b>	Agricultural	2.8
	Domestic	1.0
<b>Future available runoff</b>	Average	44.2(63%)

At present, in the Swartvlei catchment area, abstraction comprises 23%-35% of the total water resources (Fijen & Kapp, 1995). According to the SANPark records, this means that these present abstractions are consuming a significant part of the base flow of all rivers feeding the lake and estuary system. Furthermore, due to the increased water demand for residential and agricultural use, future abstractions will have to rely more on storm run-off, which would mean larger risks and influences on vital processes occurring at the estuary mouth. If the stormwater run-off is collected, the scouring of the estuary bed and sand berm will be influenced, which would potentially lead to raised water levels in the lake and estuary which could furthermore result in damage to residential areas as well as have negative impacts on estuarine ecology. A summary of the water availability scenario of Swartvlei is presented in Table 2.

### 3.3 GEOLOGY

The Swartvlei system is situated behind a Holocene coastal dune belt, 2 km long and 30 m to 75 m high (CSIR, 1983). The estuary forms a 7.2 km long channel that connects the lake to the sea. The geology of Swartvlei and its surroundings has been described by Martin (1962)

and Birch & Du Plessis (1977). Swartvlei is situated on a system of quaternary sand which lies along the coast in an area known as the Wilderness-Knysna embayment. The Swartvlei system is bordered to the west by the Gericke Point dune rock formation and to the east by similar formations. According to studies done by the CSIR (1983), dune sand frequents the estuary.

### **3.4 CLIMATE**

According to research published by the CSIR, south-westerly winds predominate throughout the year (CSIR, 1983). North and north-westerly winds dominate during the winter months, south-easterly winds during the summer months are generally secondary to the dominant south-westerly winds. Strong winds are rare in this area, with a total of 97 % below 30 km per hour (CSIR, 1983). Cloudy conditions are rather common and as a result of this the sun shines only 50 to 60 per cent of the time (CSIR, 1983).

These dominant south westerly winds, combined with the main deep sea swells originating from the south west, are main factors in wave generation and, accordingly, initiate dominant sediment transportation. The dominant offshore winds result in an incident wave climate that drives an alongshore current. This current in turn will be the transporter of the longshore sediment. The wind patterns over the South Atlantic and South Indian oceans are influenced by a number of dominant meteorological features. In order to understand the weather patterns at Swartvlei, a basic understanding of how these wind patterns form is necessary. Warm air rises in the tropics near the equator and then moves southwards to descend in the vicinity of 30°S, to form the so called Hadley cells (CSIR, 1983). This descending air causes two semi-permanent anti-cyclonic high-pressure systems to form, which are centred over the South Atlantic and Indian oceans, with air moving in an anti-clockwise rotation around the centre of the high pressure system. South of the Hadley cell, cyclonic low pressure systems are found, originating from the polar circle margin of the 'Roaring forties'. These low-pressure systems move in a clockwise rotation from West to East. The whole system is dynamic and moves between 5 and 10 degrees latitude southwards in the summer, and northwards in the winter (CSIR, 1983).

In the Southern Cape, the cyclonic coastal lows are confined to areas below the escarpment of the Outeniqua Mountains. They are characterised by sharp changes in wind direction, temperature and humidity as they move along the coast eastwards, typically bringing high intermittent rains. The wind change is normally to the north-west, which is the dominant wind in the winter months. Due to the northward shift of the 'Roaring Forties' belt, there is an increase in coastal lows and the associated cold fronts in the winter (CSIR, 1983). These

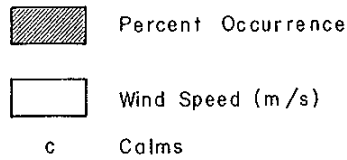
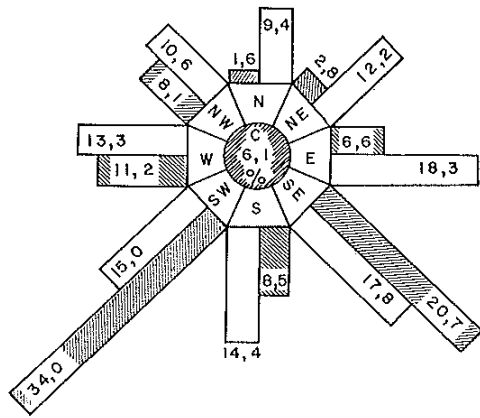
winter wave and wind conditions have major influences on the coastline, as well as the estuary mouth. Erosion rates are elevated, resulting from higher wind and wave set-up, which promote higher run-up levels. Combine these metocean processes with the dune sand geology that is found in and around the Swartvlei bay area (CSIR, 1983), and the longshore and cross shore sediment transport rates could be considerably elevated.

There is an entire reverse of conditions during the summer months. The southern Indian Ocean counter clockwise high pressure system is now present to the south of the sub-continent and causes dominant dry and cool south westerly winds along the coast. Rainfall in the area is now caused by advection of cool moist air by this high pressure system and by the influence of the mountains (CSIR, 1983).

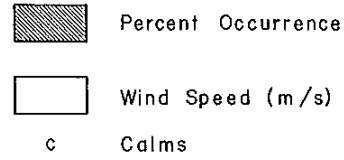
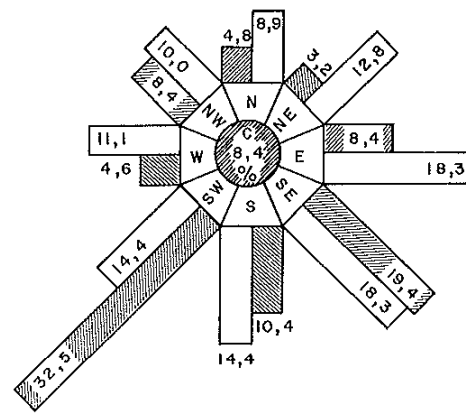
The wind climate constructed from historical data gathered by the CSIR for the years 1970-1980 is presented as wind roses in Figure 30.

A Preliminary Analysis of the Sediment Budget Across the Swartvlei Estuary Mouth

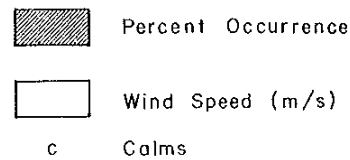
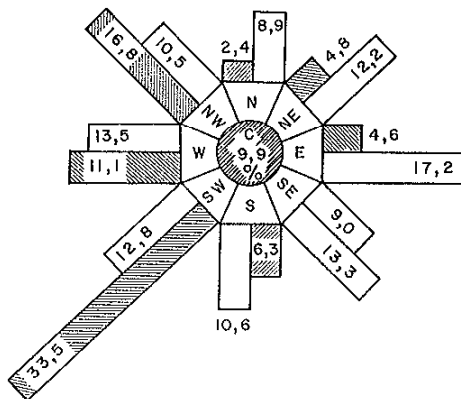
SPRING



SUMMER



AUTUMN



WINTER

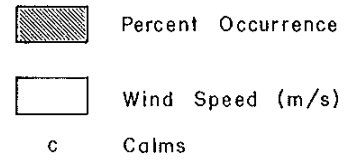
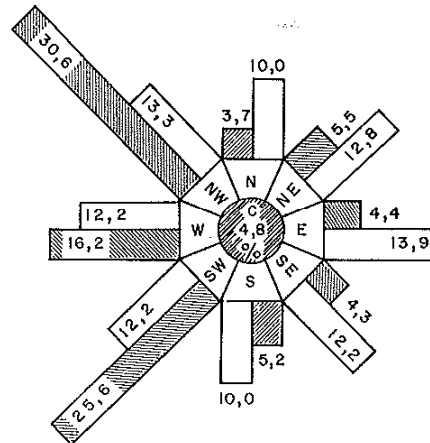


Figure 30: Wind patterns for Cape St. Blaize-Mossel Bay, 1970-1980 (CSIR, 1983)

From a 'green' report by the CSIR (1983), 'Estuaries of the Cape, No. 22', historical wave height data was obtained for the construction of the wave roses. These wave patterns were measured using a clinometer during the period 1968-1972. The measurements are presented in the wave rose in Figure 32. Using data from visually observing ships (VOS), a 20 year

## A Preliminary Analysis of the Sediment Budget Across the Swartvlei Estuary Mouth

record of deep sea waves was used to calculate the median and maximum wave heights for the Swartvlei coastline. The VOS data is presented in Figure 31.

Direction	Degrees	Occurrence (percent) of total per year			
		Spring	Summer	Autumn	Winter
E	90	3,5	3,4	3,0	1,8
ESE - SE	120	2,0	2,1	2,3	1,3
SE - SSE	150	1,3	1,4	2,0	1,2
S	180	2,1	3,0	3,0	2,2
E:E - S	90 - 180	8,9	9,9	10,3	6,5
SSW - SW	210	6,7	7,8	6,0	6,1
SW - WSW	240	7,9	5,1	5,4	8,1
W	270	2,9	1,6	2,4	4,5
E:SSW-W	210 - 270	17,5	14,5	13,8	18,7

Figure 31: VOS data for the construction of wave roses (CSIR, 1983)

A Preliminary Analysis of the Sediment Budget Across the Swartvlei Estuary Mouth

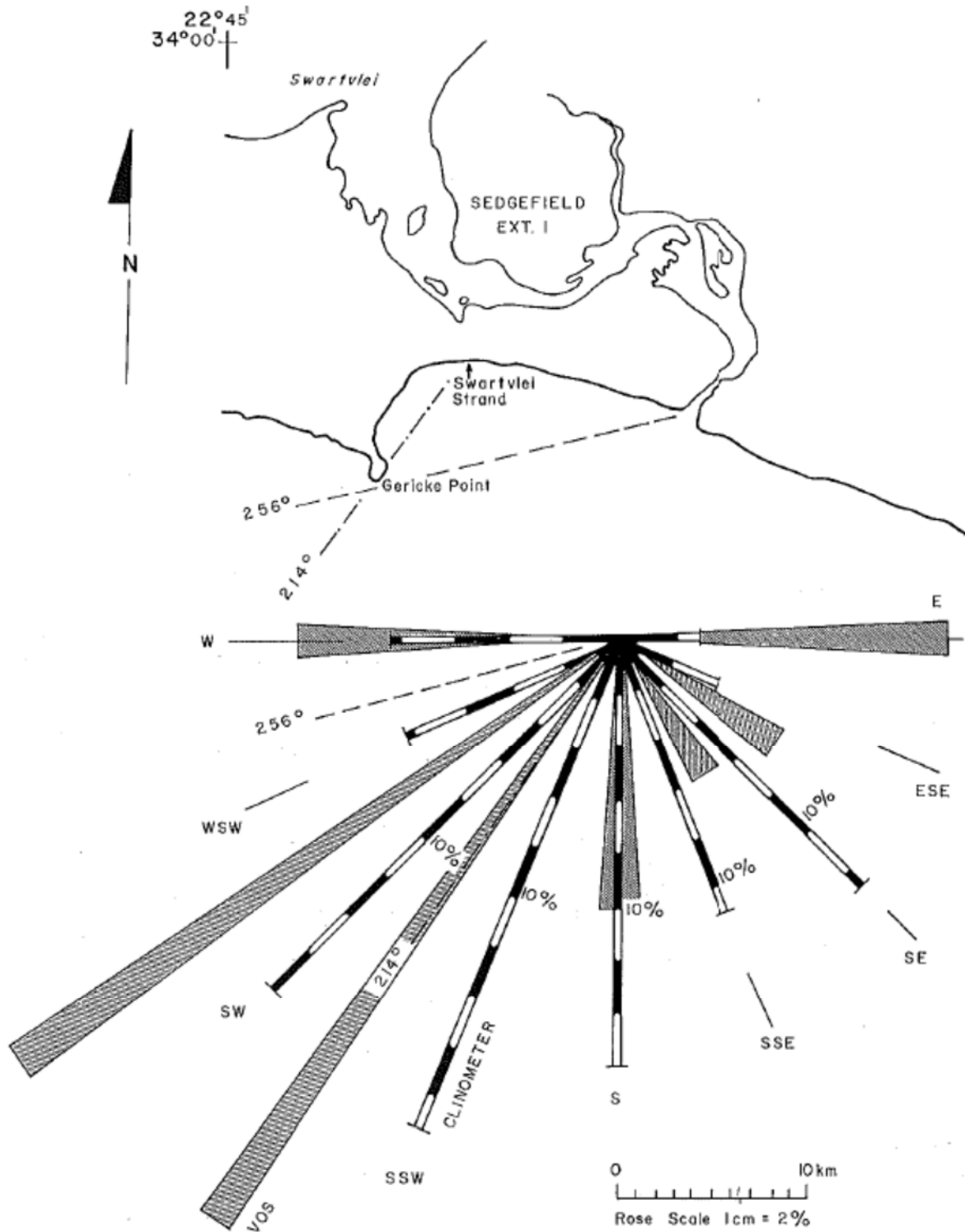


Figure 32: Historical wave climate for the Sedgefield coast (CSIR, 1983).

The VOS (visually observing ship) data is, however, very basic and subject to human interpretation on the given day. As a result of the historic nature of this data, it will not be used for any calculations but merely as a basic foundation to form an understanding of the local metocean conditions.

Also presented is NCEP hindcast data. The NCEP data will form the basis of this study and provide insight into local wave climates. An in-depth description of this type of data and calculation techniques will follow in coming chapters.

*Table 3: Mean wave direction for incident waves for 2009 (NCEP, 2011).*

$T_p / H_s$	0-2	2-4	4-6	6-8	8-10	10-12	> 12
0-1	0	0	0	0	0	0	0
1-1.5	0	0	0	110.555	155.978	223.03	0
1.5-2	0	0	0	144.45	179.57	214.39	218.6
2-2.5	0	0	200	131.14	182.86	210.6	216.24
2.5-3	0	0	118.9	140	174.8	203.4	211.5
3-3.5	0	0	98.71	132.95	167	209.5	215.6
3.5-4	0	0	0	115.3	168.5	212.2	215.5
4-4.5	0	0	0	110	156.19	216.1	212.81
4.5-5	0	0	0	93.9	190.24	210	214.9
5-5.5	0	0	0	0	221.8	213.8	218.9
> 5.5	0	0	0	0	218.7	219.2	216.1

From Table 3 it is seen that the incoming wave directions for the modelling year (2009), varied from 180 degrees to 270 degrees. This supports the VOS data findings included in the published research by the CSIR. A south westerly wave direction is seen to be the dominant wave incidence direction for this study area.

### 3.5 RAINFALL

Based on the wind patterns published by CSIR (1983), the southern coastal areas of the Garden Route are characterised by a so-called bimodal rainfall pattern (2 peaks per year) with a very strong orographic influence. Estuary mouth conditions are mainly influenced by the dominant rainfall period of June to August. This bi-modal rainfall pattern is illustrated in Figure 33. This means that moisture laden air ascends and then cools off against the Outeniqua Mountain range. Thunderstorms are relatively rare and contribute little to the rainfall. The average humidity is relatively high and is adjudged to be in the order of 88 percent (DWA, 2009). The humidity is caused by the close proximity of the warm Agulhas current (EWISA, 2003).

Most of the rainfall data is based on the Weather Bureau's daily reports from their network of rainfall stations, of which eight exist in the vicinity of Swartvlei. The annual rainfall increases from about 650 mm along the coast to about 1 100 mm in the mountain areas. The data in the mountain area is important for the sediment budget, because it causes the river water levels to rise in response to the rainfall. This in turn raises the water levels in the lake, causing an

outflow of water along the estuary and through the mouth, initiating a flushing effect at the estuary mouth. Monthly rainfalls vary erratically between 11 mm and 244 mm (EWISA, 2003).

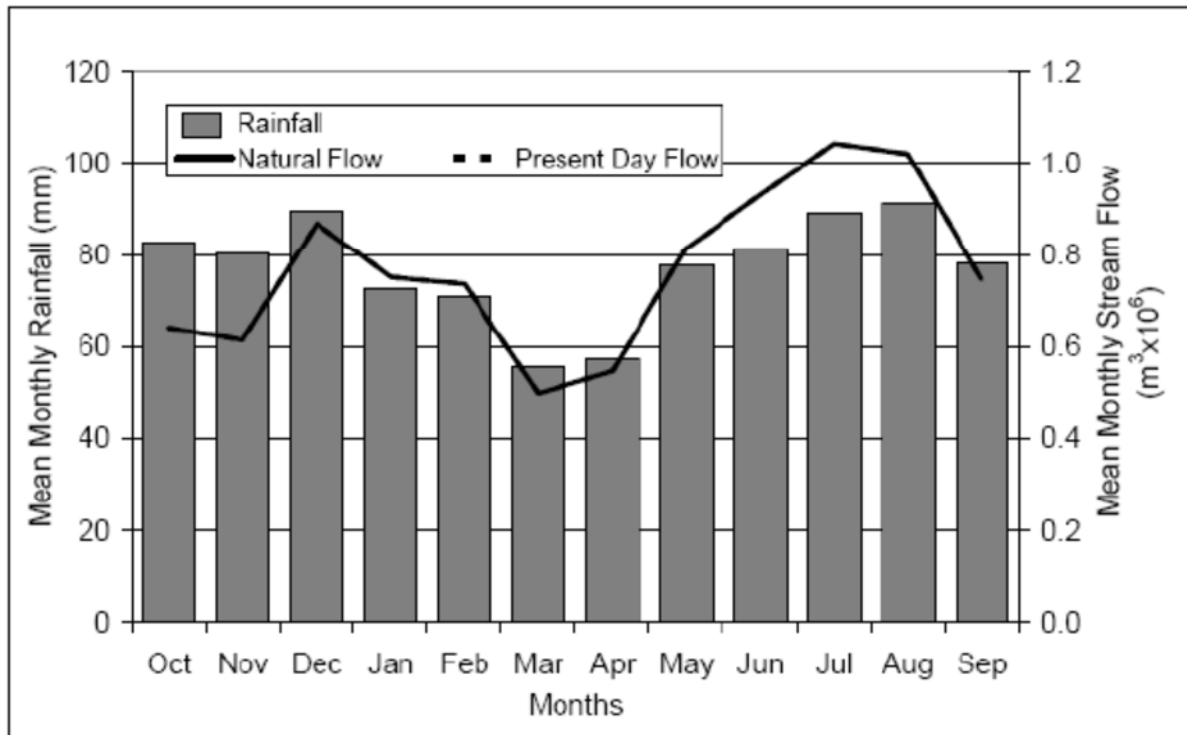


Figure 33: Mean monthly rainfall and stream flow for the Karatara River (DWA, 2009)

Figure 33 illustrates the average monthly rainfall in the second largest river catchment, the Karatara River. It demonstrates the irregularity of the mean monthly rainfall in the region. In Appendix 1 the average monthly rainfall in the Sedgefield region from 2002-2010 is attached (Mynhart, 2012). According to this report by Mynhart, the average yearly rainfall for the Sedgefield region is 879 mm.

### 3.6 ESTUARY CONDITIONS

From available historical Google imagery (see Figure 89) and relevant literature on sedimentation in estuaries presented in Chapter 2, it has been identified that the Swartvlei estuary has a tendency towards the seasonal absorption of marine sediment. This observation refers to the dominance of marine sediment rather than fluvial (catchment derived) sediment in the mouth area. Focusing on the available data i.e. Google imagery and a basic geotechnical sand grain analysis (presented in Chapter 5), the area in front of the estuary mouth is defined as being dominated by marine sediments.

The main reason for the presence of these marine sediments is the dominant marine processes present at the estuary mouth. These processes will be discussed in detail in

Chapter 3.8. As a result of the marine influences at the river mouth, the salinity conditions in the Swartvlei estuary are dependent on the state of the estuary mouth i.e., whether it is open or closed. Generally, salinity in the estuary decreases from the mouth to the railway bridge and also from spring to neap tides (Whitfield, *et al.*, 1983). Vertical mixing of the water column is greatest during spring tides. During neap tides, the salinity of water draining out of the estuary varies from 10-34 ppt (parts per thousand) which results in some stratification in the deeper portions of the estuary. As more sea water enters the estuary towards spring tide, this stratification is broken down (Whitfield, *et al.*, 1983). During a tidal cycle a substantial amount of water is retained in the estuary, which means that over a period of several tides the water in the middle section of the estuary moves back and forth, with the seawater front acting as a piston. Studies have shown that the incoming tide moves faster than the outgoing tide exits, and because of this phenomenon the estuary tends to fill with water (to a maximum of 1.3 m above MSL) during the days approaching the spring tide and vice-versa during neap tide. The lowest recorded levels during neap tide have been in the order of 0.3 m above MSL (Kluger, 1975). Salinities in the estuary are low when the estuary becomes closed off, or when the rivers are in flood.

Figure 34, shows the location of current measurements taken during a spring tide. The measurements were taken during a study conducted by Whitfield (1986). The apparatus used was a NBA current meter which was attached to a calibrated winch on board a small boat. A rope was connected by its end to points A and C respectively, parallel to the water surface, see Figure 34. During the spring tide cycle the current velocities were measured at a depth of 30 cm below the surface and at 5 m intervals along the rope. The results of this study are shown in Figure 35.

A Preliminary Analysis of the Sediment Budget Across the Swartvlei Estuary Mouth

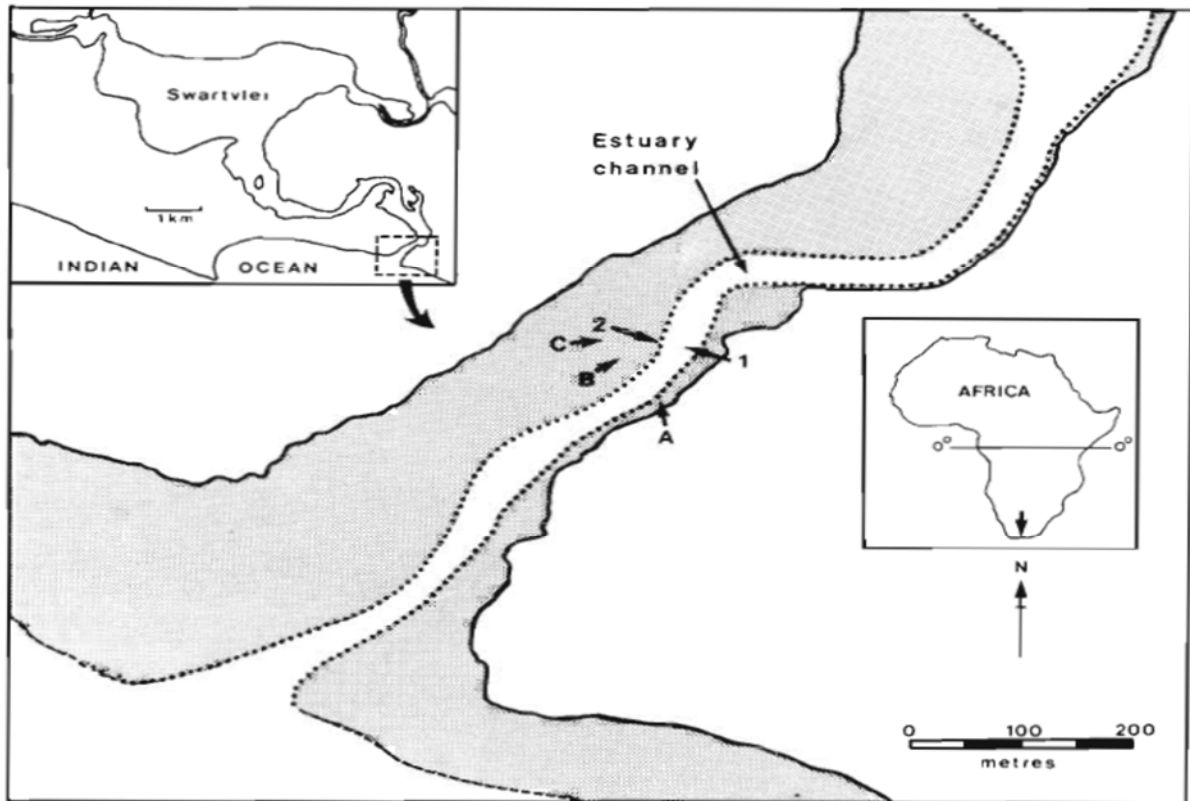


Figure 34: Positions A, B and C indicate where current measurements were taken (Whitfield, 1986)

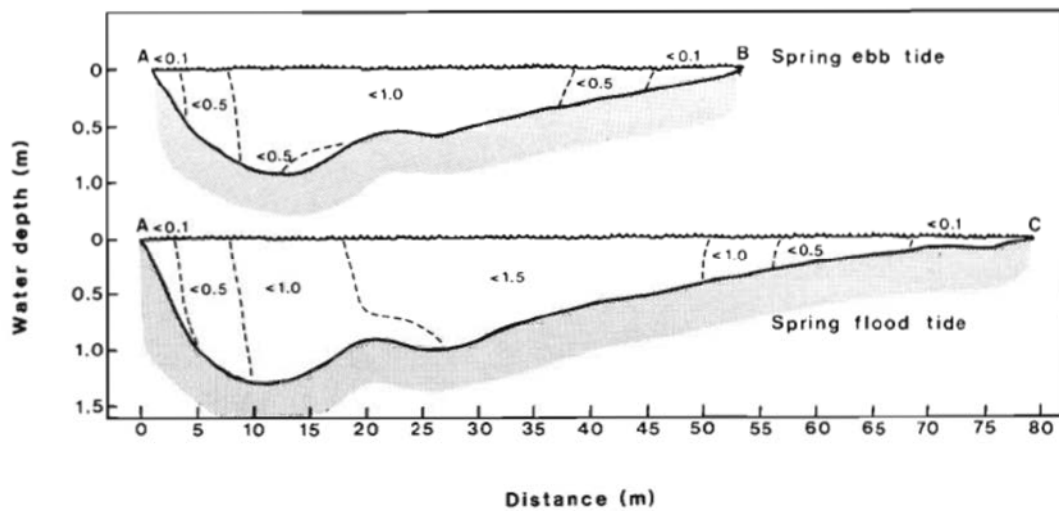


Figure 35: Sectional representation of current velocities measurements in m/s (Whitfield, 1986))

### 3.7 PHYSIO-CHEMICAL CHARACTERISTICS

During the tidal phase, when water enters from the estuary mouth, the salinity of the estuary water is generally higher than that of the surface water of the lake. This tidal flow of dense

estuarine water runs down the sandy slope near the vicinity of the railway bridge and accumulates in the Swartvlei basin to form an estimated 5 m thick layer (DWA, 2009). If a surge of water with higher salinity enters Swartvlei, the previously formed layer will be displaced upwards and a new, now more saline, water layer will form across the bottom. The result of this stratification phenomenon is that the surface salinity varies between 1 and 12 parts per thousand and the bottom salinities rise to 20 parts per thousand (DWA, 2009).

The closing of the estuary mouth has a marked effect on the maintenance of stratification, because it prevents the inflow of fresh saline water via the mouth area into the estuary. When this closure of the estuary mouth takes place, the lake, and more specifically the estuary region, enters a 'lagoon' state and the water becomes stagnant. This allows wind mixing to take effect and the disturbance of the surface water, combined with a viscous drag effect, gradually mixes the different salinity layers. The longer the mouth stays closed the more likely it becomes that the stratification will break down and oxygenation of the bottom layer will occur. The level to which the lake rises has minimal influence on the chemical attributes of the estuary. In this case, the length of time the mouth stays closed, as well as the wind effects, play key roles (DWA, 2009).

### **3.8 MOUTH DYNAMICS**

Referring to the literature study, Figure 3, the general process of estuary mouth closure is demonstrated by (Ranasinghe, 1999).

Site specific to the Swartvlei estuary mouth is the presence of an offshore sand bar. During the winter months the dominant wind and wave climates are dynamic and high in energy. The processes that lead to sand bar formation tend to shift offshore, resulting in the offshore migration of the sand bar. During the winter months the sand bar thus migrates offshore whilst winter rainfall feeds the catchment areas. The lagged effects of the elevated water levels and offshore migration of the sand bar during winter creates a platform for an open mouth condition during spring and early summer. The elevated water levels, combined with run-off created by winter rainfalls, leads to floods that scour an initial channel through the sand bar, resulting in open mouth conditions from October to March (Fijen & Kapp, 1995).

During these summer months the dominant wave and wind conditions change, as do the intensities. Summer wave conditions are more constant and less intense than winter wave climates, resulting in the onshore migration of the sand bar (Ranasinghe, 1999). As the summer months continue, the effects of the floods from the river and lake regions become less and the marine processes tend to dominate. The flood tide becomes more dominant than the ebb tide and sediment transported into the mouth by marine processes is not flushed out

## A Preliminary Analysis of the Sediment Budget Across the Swartvlei Estuary Mouth

effectively by estuarine processes. The result is the further onshore migration of the sand bar during the summer period and finally the tendency of closed mouth conditions during parts of autumn and early winter, as illustrated in Figure 37 and Table 4. (Fijen & Kapp, 1995).

When the mouth is closed, river inflows, and especially floods, result in an increase in water levels in the lake and estuarine areas. The level of the sand berm can increase to more than 3.7 m MSL, but when the water level at the Swartvlei lake monitoring point approaches +2.0 m MSL the mouth is artificially opened by SANParks (see Figure 36). The resulting outflow then erodes the berm, scours out the sediment, and the estuary mouth is opened to the sea, allowing the process to repeat itself.



*Figure 36: Mouth condition after the artificial opening of the estuary mouth*

A Preliminary Analysis of the Sediment Budget Across the Swartvlei Estuary Mouth

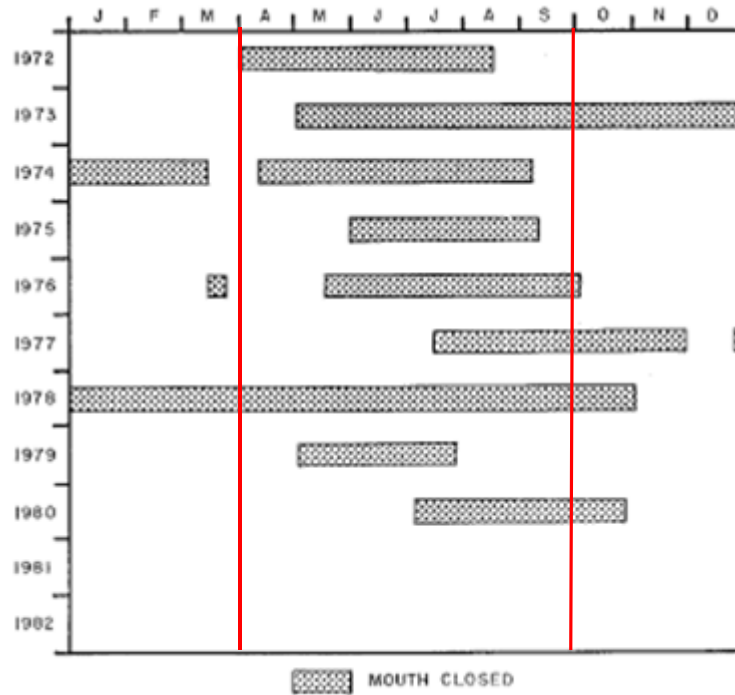


Figure 37: Eleven year record illustrating, between red lines, the peak closure periods (EWISA, 2003)

Table 4: Table showing the percentage of open mouth conditions during certain months (EWISA, 2003)

Months	J	F	M	A	M	J	J	A	S	O	N	D
Run-off percentage from rivers towards the Swartvlei system	6	5	7	7	9	10	8	11	10	11	10	5
No. of times mouth is Open	2	1	2	1	0	2	4	2	6	4	4	3
Percentage of time with open mouth conditions	66	67	63	54	36	35	32	40	47	57	78	74

Figure 37 and Table 4 illustrate the nature of open mouth conditions in the Swartvlei estuary mouth. The Swartvlei estuary mouth is open 55% of the time according to SANPark data and the delayed August floods resulting from the accumulation of winter rainfall are the major initiator of open mouth conditions during spring and summer (Fijen & Kapp, 1995).

### 3.9 SWARTVLEI COASTLINE

The Swartvlei coastline has three distinctive attributes, namely: (1) the headland (Gericke Point), (2) soft coastline with a preceding soft dune system, and (3) the Swartvlei estuary mouth. Refer to Figure 38 for the graphic illustration of the described scenario.

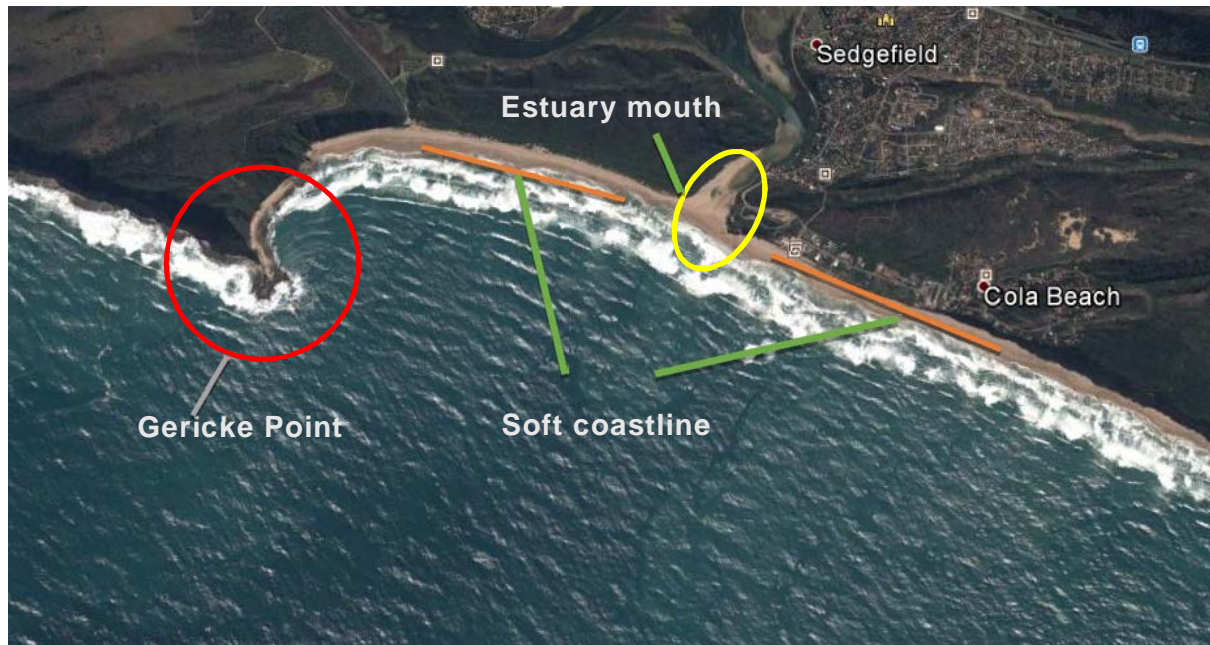


*Figure 38: Layout of The Swartvlei bay area*

Using the literature presented in Chapter 2.3, a theoretical approach was followed to mathematically predict the planform of the ideal dynamic equilibrium of the Swartvlei bay by means of an applied Parabolic Bay Shape Equation (PBSE).

Radii ( $R_i$ ) are drawn from the diffraction point to points along the beach at arc angles  $\theta_i$  to the wave crest line. The radius drawn to the down coast limit of the beach is called the control line ( $R_0$ ), which makes an angle  $\beta$  to the wave crest line. With reference to the CEM (2006), Chapter III part 2, the following equation obtained from studies done by Hsu and Evans (1989) was used:

$$\frac{R}{R_0} = C_0 + C_1 \left(\frac{\beta}{\theta}\right) + C_2 \left(\frac{\beta}{\theta}\right)^2$$

where the geometric parameters  $R$ ,  $R_0$ ,  $\beta$  and  $\theta$  are presented in Figure 8. Values for the coefficients  $C_0$ ,  $C_1$  and  $C_2$  are provided in CEM (2006).

Using NCEP hindcast data and historical Google imagery, the following parameters were defined:

## A Preliminary Analysis of the Sediment Budget Across the Swartvlei Estuary Mouth

$\beta = 42^\circ$  (relates to an incident wave of  $215^\circ$ ), this wave angle was based on the average incident wave angle from the NCEP data as well as corresponding historical Google wave angle imagery. A comparison of the typical incident wave climates are attached in Appendix 9.

Using this  $\beta$  value and the CEM (2006), the coefficients are;

$$C_0 = 0$$

$$C_1 = 1.37$$

$$C_2 = -0.38$$

Incorporating these coefficients into the Hsu and Evans (1989) PBSE equation, the following representation, Figure 39, of the planform of Swartvlei bay was calculated:

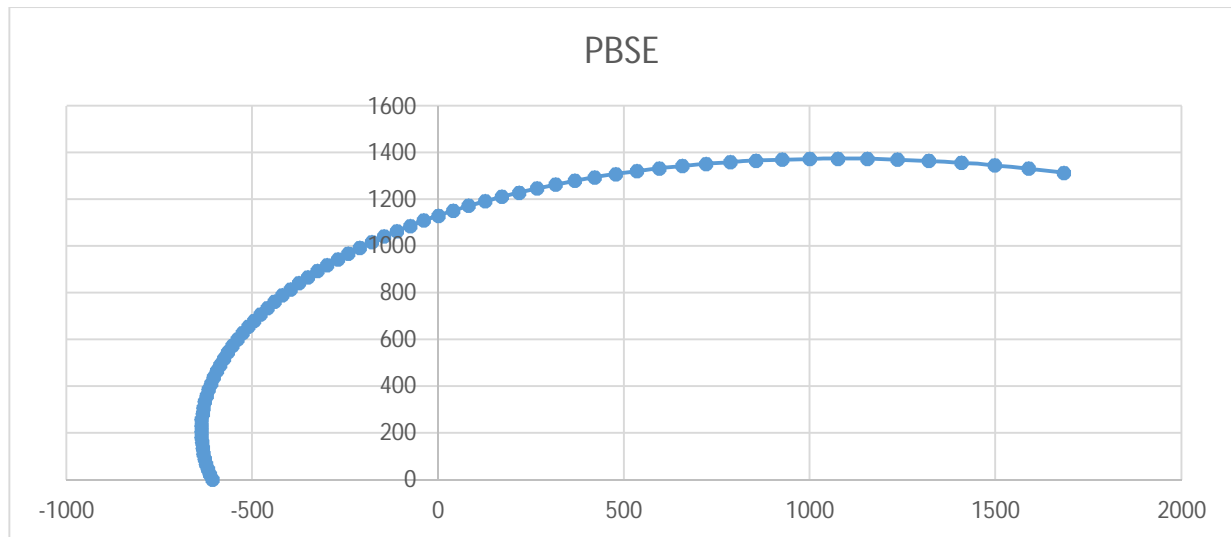


*Figure 39: Mathematical representation of spiral bay shape geometry of Swartvlei Bay*

By using the available NCEP data, historical imagery and coefficient values based on CEM literature, Figure 39 graphically illustrates the results of the applied PBSE. The origin is situated at a fixed point at the end of the headland. The x and y axes describe, respectively, the alongshore distance (m) and the cross shore distance (m).

Furthermore, using the raw calculated data with the PBSE, the values were incorporated into an AutoCAD simulation to illustrate the theoretical planform parabolic shape of Swartvlei Bay graphically. The results are illustrated in Figure 40.



Figure 40: Site specific presentation of PBSE

Referring to Chapter 2.3, as well as the results obtained from the mathematical implementation of the PBSE, Swartvlei bay is seen to fit the description of a typical headland bay beach. The interruption of longshore transport is seen in the historical imagery (see Figure 38). The headland is impeding the natural longshore transport and is preventing the bay from reaching a theoretical static equilibrium. The dominant wave angles observed from the presented NCEP and CSIR data are diffracted around Gericke Point. As a result of this diffraction phenomenon a difference in wave setup is created. This difference in wave setup and diffraction of the dominant wave climates around Gericke Point possibly creates a return current inside the sheltered bay towards Gericke Point.

The return current originating from south westerly incident waves combined with the less dominant transport of sediment from east to west during south easterly wave climates should, theoretically, also lead to sediment accretion in the lee of Gericke point. In historical Google imagery it is, however, visible that there is a lack of sediment in the lee of Gericke Point as well as the protrusion of a rocky shoreline. Further investigation suggests that this lack of sediment could be as a result of, but not limited to, the following:

- The headland, Gericke Point, is not protruding far enough seaward to block west to east and less dominant east to west transport past the point. Certain sections of the headland are also low-crested, which would lead to transport over and past the headland.

A Preliminary Analysis of the Sediment Budget Across the Swartvlei Estuary Mouth

- The bathymetry present in the lee of the headland is too steep for sufficient settlement of sediment.
- The rocky shoreline acts as a hard shoreline and limits the amount of sediment available for distribution. Furthermore, this rocky shoreline does not act as efficiently as the adjacent sandy shoreline in absorbing and dissipating the incoming wave energy.

The above-mentioned factors could all possibly contribute to the lack of visible accretion in the lee of the headland. A dynamic dissimilarity is thus created between the various sediment transport regimes, demonstrating a less dominant east to west sediment transport regime, compared to a dominant west to east regime, taking into account the geographical features encountered along the Swartvlei coastline.

The area in the lee of Gericke point is predominantly rocky with steep sandstone bluffs. Refer to Figure 41 for illustration.



*Figure 41: Western edge of Swartvlei bay, Gericke point with steep sandstone bluffs*

Although this area is on the lee side of the headland, thus in a sheltered bay, it is still influenced by metocean conditions and marine processes. From on-site investigations it was seen that

erosion is present on the sandstone bluffs lee of the headland. Combining these observations with the literature regarding erosion presented in Chapter 2.4.2, it can be seen that the processes occurring in this area is best described by Figure 16. A thin sand lens overlies a rocky beach, with a bedrock platform fronting the bluff. From on-site investigations and historical imagery, these thin deposits of sand were observed to be removed during the storm season. If storm water levels reach sufficient elevations to intersect the toe of the bluff, storm waves could directly impinge on the bluff face, causing bluff toe erosion (FEMA, 2007). If enough material is eroded from the toe during a storm, the upper portion of the bluff could fail, resulting in bluff retreat or bluff slumping. It should be noted that significant bluff failure may not occur during all storm events. However, if the bluff materials are erodible, as is the sandstone at Gericke point, toe erosion and bluff failures are possible during individual storm events.

Moving in an easterly direction away from Gericke Point, the sandstone bluffs and narrow coastline gradually give way to a high dune system and wider dune sand beaches.



*Figure 42: High dunes with wider beaches east of Gericke point*

Instantly noticeable are the wider beaches in this area (Figure 42). This could be a result of sediment from the sandstone bluffs being able to settle in this area, along with contributions from the soft dune system present along this section of coastline. At first glance, the beaches in this area consists of a mild slope with a wide beach section, possibly resulting in greater run-up absorption.

The dunes at the back of the beach are steep in nature and fronted by a natural buffer zone (see Figure 43). Although this area is a soft coastline, it still remains unspoilt by human development. Natural dune processes are occurring along the western beaches, resulting in gentler beach slopes along the dynamic coastline of the study area. According to Barwell (2011), these dune buffer zones are extremely important in stabilising beach areas with regard to erosion and marine processes. In principle these buffer dunes act in two ways (Barwell, 2011):

1. Anchor the foot of the dune
2. Trap aeolian sediment transport, thus promoting dune accretion

Although these beaches will be affected by seasonal changes in wind and wave climates, they will potentially return to a state of equilibrium as described by the literature in Chapter 2.



*Figure 43: Dune system with buffer dunes present*

Moving away from the soft coastline in an easterly direction, the Swartvlei estuary mouth is found, in the middle of the Swartvlei bay.



*Figure 44: Swartvlei estuary mouth*

This area will be the focus area of the study. Illustrated in Figure 44 is the Swartvlei estuary mouth, seen from the Sedgefield parking area, with Myoli beach to the east and Gericke point to the West. Clearly visible in this imagery is the sandbar in front of the estuary mouth. With reference to the work of Ranasinghe (1999) and literature presented in Chapter 2, this bar will migrate seasonally as a result of seasonal wave climates as well as floods originating from the Swartvlei catchment areas. Furthermore, the oscillation between the wave climates and estuarine processes, under natural conditions, will result in open and closed mouth conditions at various times. However, artificial management (opening) of the mouth interferes with the natural cycle and the berm is kept at a lower height than natural conditions would initiate. The artificial management thus restricts the volume of water stored in the estuary system, which, in turn, relates to flushing capacity. The artificial management may result in more open mouth conditions, but the duration of these open mouth periods is much less compared to open

mouth conditions initiated through natural conditions. The mouth dynamics and processes are discussed in full in sections 3.6 and 3.8, respectively.

Moving in an easterly direction, away from the river mouth, is Myoli beach. A distinct feature of this area is the short and steep beach section. Erosion is clearly visible along the entire stretch of coastline east of the estuary mouth (see Figure 45).



*Figure 45: Erosion east of estuary mouth*

## 4. METHODOLOGY

Following the literature presented in Chapter 2, and the application thereof on Swartvlei in Chapter 3 respectively, the following processes and areas were identified as possible influences on the sediment budget occurring at the Swartvlei estuary mouth:

- Bay shape and orientation
- Specific features of the Swartvlei embayment (e.g. headlands etc.)
- Estuary characteristics and contributions from slumping, erosion and flushing.
- Various marine processes
- Various possible contributors of sediment
- Dominant offshore wave and wind climates, as well as local and inshore wind and wave climates

The methodology will focus on describing the onsite investigations, data collection and modelling approaches needed to assess the effects of the influences described above. In doing so, the methodology will be subdivided into three main sections, namely:

1. Modelling Approach
2. Desktop Study
3. On-site investigation

The study area is defined in Figure 46, with Gericke point to the west, the Swartvlei estuary mouth in the middle of the Swartvlei bay area and Myoli beach to the east of the estuary mouth.

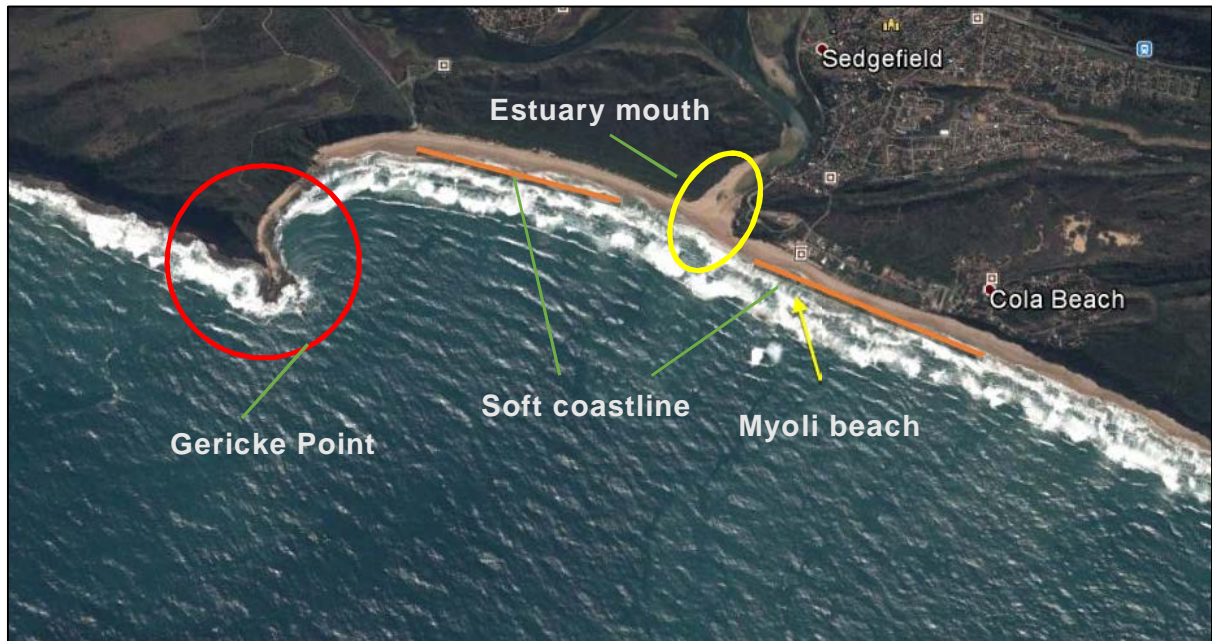


Figure 46: Defined study area

The author executed the desktop study and MIKE 21 numerical modelling at the University of Stellenbosch. For the coastal impacts, the MIKE 21 SW package was used to model the half-heart embayment. The MIKE 21 software was selected because it is a professional engineering software package designed for simulating flows, waves, sediments and ecology in rivers, lakes, bays, estuaries and coastal environments.

The modelling system is designed on an integrated modular framework with a variety of add-on modules. The add-on module that was used for the numerical modelling of the Swartvlei bay area was MIKE 21 SW (spectral wave). MIKE 21 SW is a 3<sup>rd</sup> generation spectral wind-wave model that simulates the growth, decay and transformation of wind generated waves and swells in offshore and coastal areas. The model includes wave growth by action of wind, non-linear wave-wave interaction, dissipation by white capping, dissipation by wave breaking, dissipation due to bottom friction, as well as refraction due to depth variation and wave-current interaction (DHI, 2011).

This MIKE 21 SW data was then combined with the Kamphuis formula for bulk longshore transport. Output profiles were selected along the coastline covering the entire surf zone and beyond. The output profiles consisted of individual points for which the wave height, wave period and wave direction at breaking were simulated by MIKE 21 SW (at each individual point along each profile). The transport rates were calculated along these output lines along the entire Swartvlei coastline by means of a statistical cumulative approach for each line, whereby the bulk transport between each point and the shoreline was computed and added in proportion to the number of days per year waves broke at that point or shallower. The

cumulative approach resulted in a bulk sediment transport rate across each line or profile. From these outputs, a preliminary sediment transport regime was estimated across these profiles along the entire Swartvlei bay coastline and, in turn, a preliminary sediment budget across the estuary mouth boundaries was calculated. The ranges of magnitude resulting from the longshore transport across the estuary mouth and dune slumping within the estuary were investigated. Contributions of auxiliary marine and estuarine processes, as well as aeolian transport, were estimated to balance the budget. By balancing the amount of sediment travelling in each direction, a proposed sediment budget could be estimated.

#### **4.1 MODELLING APPROACH**

##### **Short description of MIKE SW**

The MIKE 21 SW numerical model includes a new generation spectral wind wave model based on unstructured meshes. The model simulates the growth, decay and transformation of wind generated waves and swell in offshore and coastal areas (DHI, 2011).

MIKE 21 SW includes the following physical phenomena:

- Wave growth by action of wind
- Non-linear wave-wave interaction
- Dissipation due to white-capping
- Dissipation due to bottom friction
- Dissipation due to depth induced wave breaking
- Refraction and shoaling due to depth variations
- Wave current interaction
- Effect of time-varying water depth, flooding and drying.

The discretisation of the governing equation in geographical and spectral space is performed using the cell-centred finite volume method. In the geographical domain an unstructured triangular mesh technique is used. The time integration is performed using a fractional step approach where a multi-sequence explicit method is applied for the propagation of wave action. Refer to Appendix 5 for an in-depth report on the capabilities of this specific numerical model.

### Application of MIKE 21 SW

MIKE 21 SW was used for the numerical modelling of wave climates originating from the offshore NCEP location into Swartvlei bay. The NCEP hindcast data was used as input parameters. Available SANPark records on wave climates, wind directions and bathymetry were combined with other available sources in an attempt to reconstruct the metocean conditions present at Swartvlei.



*Figure 47: On-site imagery of a typical calm Sedgfield surf zone immediately east of the Gericke Point parking area.*

The outputs of the MIKE 21 SW numerical model were then used as input for the calculation of the bulk longshore sediment transport, which to a large extent is determined by wave conditions (typical calm wave climate depicted in Figure 47) and associated wave induced currents. The calculated quantities were then analysed in an attempt to replicate the hypothesis set out in this study. Limitations and sensitivities were also identified and discussed, in order to make recommendations on future studies that are needed.

## 4.2 DESKTOP STUDY

### 4.2.1 Desktop study description

The desktop study was used to gather and analyse available data from a variety of sources as input for the MIKE 21 SW numerical model as well as the bulk longshore transport equation. Following the completion of the MIKE 21 SW numerical model, the results of the wave climates driving the longshore current were combined with a bulk longshore sediment transport formula. This bulk longshore sediment regime, together with the calculated contribution from the estuary was used to verify the hypothesis set out in Chapter 7, by using the calculated quantities and direction. It is important to note that these calculations only estimate the bulk transport rates with the data available. In-depth numerical studies, in conjunction with extensive data measuring campaigns, are recommended for verification of these results.

#### 4.2.1.1 Bulk longshore transport equations

##### Close out depth:

Longshore transport is concentrated within an optimum zone of transportation, but it is often very difficult to accurately establish these zones without long term sampling and modelling techniques. A simplified way of determining this longshore transport zone may be useful. Hallermeier (1978) investigated the seaward limit of effective profile changes resulting from wave action, termed closure depth,  $h_c$ , with the intention of defining the limits of cross-shore sediment transport. While it is thus not directly related to longshore transport, it does serve as a useful parameter in defining the seaward limit of sediment movement by wave action. It is also readily related to common parameters of wave height and period.

Birkemeier (1985) improved and simplified Hallermeier's work by applying it to measurements of profile change at Duck, in the USA. Birkemeier's closure depth  $h_c$  is relative to mean low water (MLW) and is given by the following equation:

$$h_c = 1.75 * H_e - 57.9 \left( \frac{H_e^2}{gT_e^2} \right)$$

where:  $H_e$  is the effective significant wave height (the height exceeded for only 12 hours per year)

$T_e$  is the associated wave period

$g$  is the acceleration due to gravity

$H_e$  can be determined from:

$$H_e = H_s + 5.6\sigma_H$$

where:  $H_s$  is the annual mean significant wave height and  $\sigma_H$  is its standard deviation.

Birkemeier (1985) also proposed a simplified formulation for the closure depth ( $h_c$ ) that was independent of the wave period, as follows:

$$h_c = 1.57 * H_e$$

This equation provides us with a simple means of demarcating the seaward boundary, after which no notable sediment movement due to wave action occurs in the cross-shore profile. In this study, this close-out depth will be used as an indicator or guideline in defining the area of longshore transport.

Using this simplified equation by Birkemeier, together with the available NCEP hindcast data, the parameters for the study area are as follows:

- $H_{s \text{ mean}} = 2.815 \text{ m}$
- $\sigma_h = 1.061$
- $H_e = 8.12 \text{ m}$ , which corresponds to a wave height exceeded for only 12 hours per year according to the 2009 NCEP wave record.
- $h_c = 12.748 \text{ m}$

These parameters were calculated from NCEP hindcast data for 2009. Using the formulae by Birkemeier it was estimated that the close-out depth for the study area would be in the region of 13 m. Using the a theoretical representation of sediment transport in the surf zone (see Figure 48) obtained from Longuet-Higgins (1970) on the classification of peak longshore transport in relation to the surfzone, it is estimated that the maximum transport in the study area would be at 0.5-0.6 of the width of the surf zone.

## A Preliminary Analysis of the Sediment Budget Across the Swartvlei Estuary Mouth

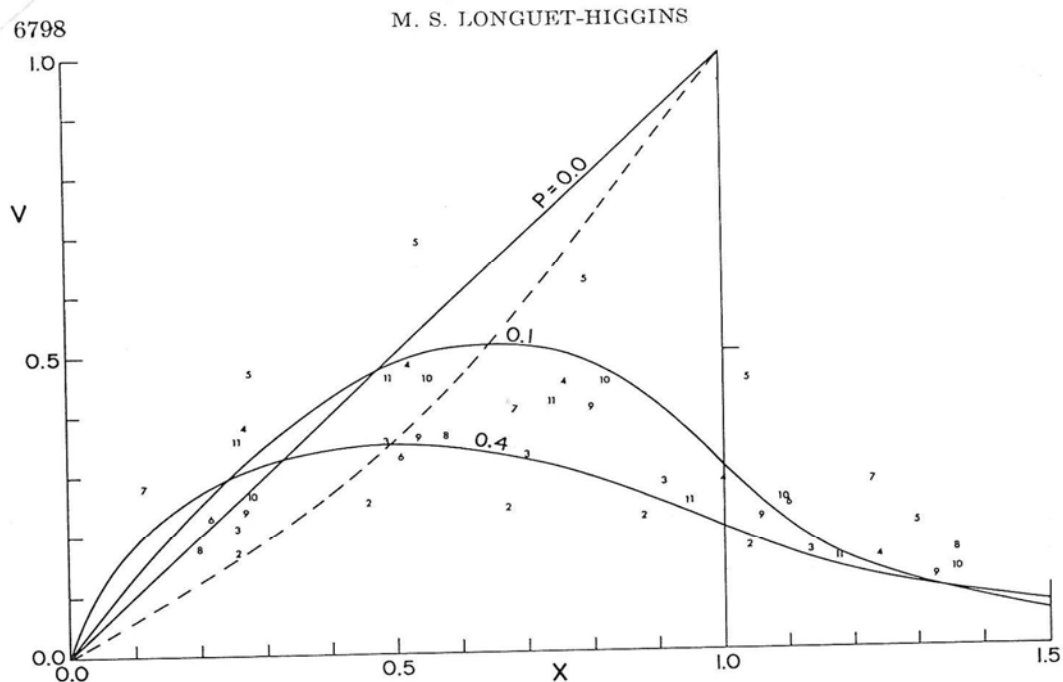


Fig. 4a. Comparison of the longshore velocities measured by Galvin and Eagleson [1965; series II] with the theoretical profiles derived in section 2 of the present paper. The plotted numbers correspond to the number of each run (Table 2).

Figure 48: Illustration of the peak transport zone (Longuet-Higgins, 1970)

Using the calculated Birkemeier close-out depth of approximately 13 m, accompanied by the conservative indication of the Longuet-Higgins (1970) principle of maximum sediment transport at 0.5-0.6 of the surf zone width, a preliminary transport zone could be identified for the sediment transport regime along the Swartvlei Bay coastline. The theoretical estimate would now be verified with the application of the Kamphuis bulk longshore transport formula with input from the MIKE 21 SW numerical data.

#### Kamphuis bulk longshore sediment transport:

According to the studies of Schoonees and Theron, presented in section 2.4.3, it was decided to use the Kamphuis formula for bulk longshore transport for the study area under consideration (Kamphuis, 2010). This formula embodies a suitable approach in order to neither over nor underestimate the final transport volume (Schoonees & Theron, 1996).

From Figure 17, it was deduced that the CERC formula was over estimating the transport volumes. As already stated, the sediment budget for the Swartvlei estuary mouth was calculated using a MIKE 21 SW model together with the Kamphuis equation for bulk longshore transport. These calculated quantities were then combined with the contribution from the estuary itself (i.e. dune slumping) to finally form a preliminary sediment budget for the Swartvlei estuary mouth.

To understand the output of Kamphuis's equation it is first and foremost important to understand the input parameters. The parameters are as follows:

- Beach slope
- Significant wave height at breaking
- Peak wave period
- Sand grain size
- Wave incidence angle at breaking

Incorporating the above mentioned parameters into the site visit and data collection campaign, an attempt could be made to assign values to these parameters from the available data.

Kamphuis (2010) derived an expression that includes the effects of three additional beach forming parameters, in addition to the CERC formula. These parameters are: wave period (wave steepness), beach slope and grain size.

$$\frac{Q_s}{\rho H_{sb}^3 / T_{op}} = 1.3 * 10^{-3} \left( \frac{H_{sb}}{L_{op}} \right)^{-1.25} m_b^{0.75} \left( \frac{H_{sb}}{D_{50}} \right)^{0.25} \sin 2\alpha_b^{0.6}$$

where,

$Q_s$  = sediment transport rate

$H_{sb}$  = significant breaking wave height

$\rho$  = density of water

$T_{op}$  = wave period

$L_{op}$  = wave length in deep water

$M_b$  = beach slope

$D_{50}$  = median grain size

$\alpha_b$  = angle of wave incidence at breaking

According to work done by Schoonees and Theron, the accuracy of the Kamphuis formula is represented in Figure 18.

This Kamphuis equation for bulk longshore transport reduces to:

$$Q_s = 2.27 H_{sb}^2 T_p^{1.5} m_b^{0.75} D^{-0.25} (\sin 2\alpha_b)^{0.6}$$

where  $Q_s$  is kg/s underwater. This may be converted to

$$Q_k = 64000 * H_{sb}^2 T_p^{1.5} m_b^{0.75} D^{-0.25} (\sin 2\alpha_b)^{0.6} \quad (\text{m}^3/\text{yr})$$

or

$$Q_k = 7.3H_{sb}^2 T_p^{1.5} m_b^{0.75} D^{-0.25} (\sin 2\alpha_b)^{0.6} \quad (\text{m}^3/\text{hr})$$

where  $Q_k$ , denotes  $Q$  calculated with the Kamphuis expression (Kamphuis, 2010).

These equations were derived from small scale tests but were found to be valid (without further calibration) for field results. It is important to note that these equations were found to over-predict transport on gravel beaches because they do not include a critical shear stress (Kamphuis, 2010). The grain analysis included in Chapter 5 will be used to verify that the grain sizes occurring along the Swartvlei coastline are well below the minimum grain size for gravel, as described by the ASTM method.

As already stated, the CERC formula has been criticised for over predicting  $Q$ , particularly at high wave energy conditions (Kamphuis, 2010). In South Africa, and in particular the south coast, historical wave data sets have shown that the wave climate is relatively high in energy (CSIR, 1983). This adds to the justification for using the Kamphuis formula to calculate the bulk longshore transport in this relatively high energy zone.

#### 4.3 ON-SITE INVESTIGATION

First an application for the project was submitted for approval to SANParks. This procedure involved the completion of a research application form, which SANParks had to approve, for entry into the Wilderness National Park. After the acceptance of the project by SANParks, a preliminary site visit was scheduled. The date for this site visit was scheduled for December 2012, and the planning in relation to the study timeline can be seen in Appendix 2. The site visit was classified as a data collection visit, with the co-operation and help provided by SANPark guides and officials.

The onsite investigation was focused on the data needed as prescribed by the methodology of the numerical modelling and desktop study, respectively. Rainfall, catchment and flow data from SANParks records, together with local climate information, was studied to correlate patterns that could indicate certain events at certain times of the year. The data collected was used in the process of gathering information on certain events taking place in and around the Swartvlei estuary mouth. The available data included rainfall, current measurements, bed measurements (sparse estuary profile surveys) and climate data (wind and waves).

The aim of this site visit was to collect all available data in an attempt to simulate the metocean conditions present, by generating a MIKE 21 SW numerical model and then preliminarily estimate the sediment budget scenario at the Swartvlei estuary mouth.

During the site visit the following equipment was used:

1. Kayak
2. Trimble GPS surveying equipment
3. Digital Camera
4. Eco-sounder (Lowrance X4-Pro)

With the use of a digital camera, the surrounding area was documented to identify all the possible sediment contributors. The documenting of these contributors started at the Swartvlei estuary mouth, moving west along Swartvlei beach towards Gericke Point. Refer to Figure 46 for the study area layout. Documentation from the estuary mouth, west towards Gericke point, started at low tide and by the change of the tide, towards high tide, documentation of the section from the Swartvlei estuary mouth eastward towards Myoli beach was started. It was important to identify the sediment contribution, if any, around Gericke Point into the embayment. The aim of this photographic investigation was to identify the following:

- Geological characteristics of the section along the Swartvlei coastline with specific emphasis on:
  - Gericke Point and the sandstone bluffs present on the lee side
  - The dune system along the coastline
- Transition of sandstone bluffs to dune system immediately east of Gericke Point, in front of the Gericke Point parking area
- Dune systems and beach characteristics present on the soft coastline, west of the estuary mouth and east of Gericke point
- Estuary mouth conditions
- Present scenario along the beaches immediately east of the estuary mouth, on the Myoli Beach side

A photo report is attached in Appendix 6.

With reference to dune stability research done by Barwell (2011), the dunes along the Swartvlei coastline were investigated regarding their possible contribution towards the longshore transport along the Swartvlei coastline.

The following criteria were used to analyse the dune stability:

A Preliminary Analysis of the Sediment Budget Across the Swartvlei Estuary Mouth

1. The situation of the dunes in the embayment. This is with regard to the wave incidence angle, and whether the dune section under investigation is sheltered or on an open coastline.
2. The dominant wind in the area.
3. The height of the fore-dune.
4. The pressure due to human activity.
5. The vulnerability to erosion.
6. Whether the coastline is in dynamic equilibrium, accreting, rocky or eroding.

These criteria will not be directly answered in this study, but used as an analysis tool for dune stability along the coastline.

Focus was placed on the type of material present i.e. whether it was a sandy or rocky shoreline. The collection of historical and current aerial photographs will also play a role in establishing the effects of the dominant processes along the Swartvlei coastline and specifically the estuary mouth. Through a preliminary analysis of the available aerial photographs, with regard to accretion, eroding areas and visibly dominant estuarine and marine processes, a basic theoretical estimate of the sediment transport regime present along the Swartvlei coastline can already be applied towards formation of a hypothesis, set out in Chapter 7.

After the photographic investigation of the Swartvlei coastline, as well as the estuary mouth itself, the beach area was measured by means of a Trimble GPS system, to establish beach and dune profiles along the Swartvlei coastline. Specifications of this device are attached in Appendix 3. These profiles were measured by means of walking along the beach, beginning at low tide and taking spot measurements. The profiles started at the water line and extended in a north to south orientation, from the water line towards the crest of the dune. The results of the Swartvlei coastline survey will be presented in Chapter 5. Furthermore, samples of the sand in different regions were gathered to inspect the grain characteristics. These findings are discussed in Chapter 5.1.2.

## 5. DATA COLLECTION

### 5.1 ON SITE INVESTIGATION

As described in the methodology, the site visit required the collection of data on the following parameters for the initiation of a preliminary analysis of the sediment budget across the Swartvlei estuary mouth. The data gathered included:

1. Beach profile data for input into numerical wave model
2. Grain size information
3. On-site and up to date vertical and satellite imagery

#### 5.1.1 Beach Survey

Using a Trimble GPS satellite surveyor, the dune and beach profiles were measured by means of walking the profile of the beach and taking spot measurements. The data used was post-processed with assistance from a survey specialist lecturing at the University of Stellenbosch. As a result of the lack of available benchmarks in the immediate Sedgefield area, the levels are dependent on the accuracy of the Trimble device. Referring to the technical specifications set out by registered Trimble surveying technicians, the accuracy of the device is in the order of 10-30 cm post processing. This is dependent on logging time and the number of satellites involved. For this study a minimum of ten individual measurements were taken per spot measurement, with a minimum of eight to ten satellites detected at all times. Both these parameters were well above the acceptable ranges for accurate data capturing. For the post-processing, the nearest available benchmark was a Trignet base station located at George Airport. The details of the base station are as follows:

*Table 5: Benchmark details*

Station	Station Code	Latitude (S)	Longitude (E)	Height (m)	Sensor Type
GEOA	GEOA	34° 00' 07.92707"	22° 23' 00.09972"	228.889	TRIMBLE NETR5

Fourteen beach profiles in total were taken, which included profile measurements of the sand berm in front of the estuary mouth and the estuary mouth banks (Figure 49).

A Preliminary Analysis of the Sediment Budget Across the Swartvlei Estuary Mouth



Figure 49: Beach profiles locations and pathways

The orange lines indicated in Figure 49, illustrate the actual start and end points, together with the survey lines of the Trimble beach profile survey after processing.



Figure 50: Operation of Trimble GPS

Using data obtained from research done by the South African Navy Hydrographic Office (SANHO), the following tabled tidal levels were used to calibrate the measured GPS data.

*Table 6: Water levels relative to MSL (SANHO, 2013)*

<b>CD/LAT (m)</b>	<b>MLWS (m)</b>	<b>MSL (m)</b>	<b>MLWN (m)</b>	<b>ML (m)</b>	<b>MHWN (m)</b>	<b>MHWS (m)</b>	<b>HAT (m)</b>
-0.788	-0.558	0	0.032	0.272	0.532	1.122	1.422

From published SANHO data, the values of the lowest astronomical tide (LAT) and highest astronomical tide (HAT) are computed from 19 years of predictions. The mean levels are computed from predictions of a recent year when the moon's average maximum declination was 23.5°. The definitions of the abbreviations are given in the definitions list in the beginning of this report.

Presented in Figure 51 is a summary of the GPS beach survey conducted, followed by a short description of the immediate area combined with on-site photographic imagery of significance. The individual beach profiles are presented in Appendix 7.





*Figure 52: Left (western) bank of the estuary*

The presence of transported vegetation, as seen in Figure 52, along this profile and in the area suggests that this section is occasionally flooded.

East of the estuary mouth, the profiled areas again start steepening and shortening. From the photographic survey and also a report by the CSIR (1983), there is a presence of dune rock on the eastern, right side, of the estuary mouth (see Figure 53). Sediment build-up is visible, as the presence of dune rock is preventing any further migration of the estuary mouth and it, in turn, possibly collects sediment from the longshore transport. Moving further east, to profiles 7 through 10, the beach profiles are distinctly shorter and steeper than the beach profiles west of the estuary mouth (see Figure 54). This is an important observation towards the hypothesis of this study.

A Preliminary Analysis of the Sediment Budget Across the Swartvlei Estuary Mouth



*Figure 53: Dune rock formation on the eastern bank of the estuary*



*Figure 54: Steep and narrow beach profile, east of estuary mouth*

## **5.1.2 Sand Grain analysis**

### **5.1.2.1 Introduction**

As described in the literature study, longshore sediment transport is one of the dominant processes along a sandy coastline. Waves approaching the shoreline at an oblique angle generate an alongshore current. The breaking action of the waves causes sediment to be suspended, which can then be transported by this current. Fine particles can be suspended from the seabed more readily than coarse ones, leading to higher transport rates for finer sediment under the same wave breaking conditions. This effect of particle size on longshore transport rate has long been recognised and incorporated into the equations that coastal engineers use to calculate longshore transport rates (Soltau, 2009).

As a result of the lack of available data that describes the sediment and grain sizes on the south coast of South Africa and especially the Swartvlei estuary, a basic geotechnical investigation into the surface grain sizes present was conducted in order to provide a preliminary estimate of the basic sand characteristics of the embayment.

### **5.1.2.2 Size classification**

Two descriptive grain size classification scales are commonly used. These are the ASTM or Unified Soils classification and the Wentworth classification. A classification graph is presented in Figure 55. The main difference between the two is that the Wentworth system has a greater number of classification bands. It is important to note that the same term is used to refer to quite different grain sizes in the two systems. Sand described as 'coarse' could therefore have a typical size of 2.0 to 4.75 mm (Unified Soils) or 0.5 to 1.0 mm (Wentworth). It is thus important to state which system is being referred to when describing particle size. In this study, grain sizes will generally be described in numerical units. The ASTM method was used in this study, where descriptive terms are applied.

A Preliminary Analysis of the Sediment Budget Across the Swartvlei Estuary Mouth

<b>Table III-1-2 Sediment Particle Sizes</b>						
<b>ASTM (Unified) Classification<sup>1</sup></b>	<b>U.S. Std. Sieve<sup>2</sup></b>	<b>Size in mm</b>	<b>Phi Size</b>	<b>Wentworth Classification<sup>3</sup></b>		
Boulder	12 in. (300 mm)	4096.	-12.0	Boulder		
		1024.	-10.0			
Cobble	3 in. (75 mm)	256.	-8.0	Large Cobble		
		128.	-7.0	Small Cobble		
		107.64	-6.75			
		90.51	-6.5			
		76.11	-6.25			
Coarse Gravel	3/4 in. (19 mm)	64.00	-6.0	Very Large Pebble		
		53.82	-5.75			
		45.26	-5.5			
		38.05	-5.25	Large Pebble		
		32.00	-5.0			
		26.91	-4.75			
		22.63	-4.5			
Fine Gravel	4 (4.75 mm)	19.03	-4.25	Medium Pebble		
		16.00	-4.0			
		13.45	-3.75	Small Pebble		
		11.31	-3.5			
		9.51	-3.25			
		8.00	-3.0			
Coarse Sand	10 (2.0 mm)	7.36	-2.75	Granule		
		6.73	-2.5			
		5.66	-2.25	Very Coarse Sand		
		4.76	-2.0			
		4.00	-1.75			
		3.36	-1.5			
		2.83	-1.25			
		2.38	-1.0			
Medium Sand	40 (0.425 mm)	2.00	-0.75	Coarse Sand		
		1.68	0.0			
		1.41	0.25	Medium Sand		
		1.19	0.5			
		1.00	0.75			
		0.84	1.0			
		0.71	1.25			
		0.59	1.5			
		0.50	1.75			
		0.420	2.0			
Fine Sand	200 (0.075 mm)	0.354	2.25	Fine Sand		
		0.297	2.5			
		0.250	3.0	Very Fine Sand		
		0.210	3.25			
		0.177	3.5			
		0.149	3.75			
		0.125	4.0			
		0.105	4.25			
		0.088	4.5			
		0.074	4.75			
Fine-grained Soil:	400	0.0625	5.0	Coarse Silt		
		0.0526	5.25			
		0.0442	5.5			
		0.0372	5.75			
		0.0312	6.0			
Clay if $PI \geq 4$ and plot of $PI$ vs. $LL$ is on or above "A" line and the presence of organic matter does not influence $LL$ .		0.0156	6.25	Medium Silt		
		0.0078	6.5	Fine Silt		
		0.0039	6.75	Very Fine Silt		
		0.00195	7.0	Coarse Clay		
		0.00098	7.25	Medium Clay		
		0.00049	7.5	Fine Clay		
		Silt if $PI < 4$ and plot of $PI$ vs. $LL$ is below "A" line and the presence of organic matter does not influence $LL$ .		0.00024	7.75	Colloids
				0.00012	8.0	
				0.000061	8.25	
		(PI = plasticity limit; LL = liquid limit)				

<sup>1</sup> ASTM Standard D 2487-92. This is the ASTM version of the Unified Soil Classification System. Both systems are similar (from ASTM (1994)).  
<sup>2</sup> Note that British Standard, French, and German DIN mesh sizes and classifications are different.  
<sup>3</sup> Wentworth sizes (in mm) cited in Krumbein and Sloss (1963).

Figure 55: Wentworth and ASTM classification table (CEM, 2006)

### 5.1.2.3 On-site sampling points

Four locations were selected as sampling points for this study. The first location, called Gericke Point, was selected because of its position in the bay, lee of the headland and located close to the sand bluffs. The next sample was taken at the estuary mouth itself. The purpose was to compare the properties of the sediment found on the beaches around the estuary mouth to the sediment inside the mouth. The third sample was taken on a sand spit in front of Myoli beach. Refer to Figure 56 for the sampling locations.

A fourth sample was taken inside the estuary at the old railway bridge, as a control. This sample was taken with the intention of comparing sediment found at the estuary mouth to sediment deep inside the estuary.

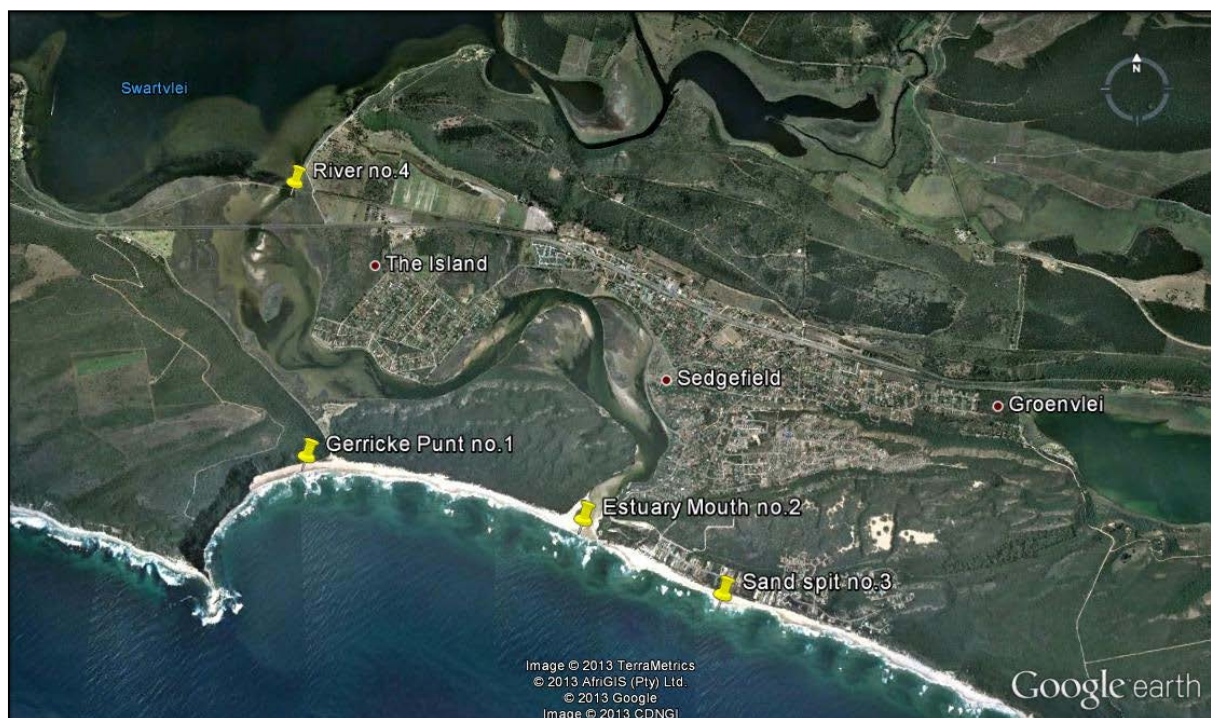


Figure 56: Locations of sediment sampling points (Google)

This sampling campaign was initiated to gather basic information on the pertinent geotechnical characteristics present in this area. As a result of the lack of published and available data on sand grain characteristics in this area, the data collected was used as basic input for the Kamphuis formula for bulk longshore transport (Kamphuis, 2010).

These samples are only surface samples and indicative of the geotechnical characteristics of the area. As a result of the lack of reliable sources available describing the geotechnical characteristics of this area, it is recommended that further in-depth geotechnical studies be performed along the Swartvlei coastline.

### 3.4.4 Results of Geotechnical Sieve grading

The sieve grading tests were performed by Geo-Technical Laboratories in Somerset-West.

The method that the laboratories used to grade the sand was the ASTM method and the results are as follows:

Table 7: Sieve analysis

Grain Size Distribution(%)								
Sample Name	Clay < 0.002	Silt 0.002-0.05	Fine Sand 0.05-0.15	Med Sand 0.15-0.425	Coarse Sand 0.425-4.75	Gravel > 4.75	D50 ( mm)	D80 (mm)
Gericke Punt	0	1	15	71	13	0	0.23	0.34
Estuary Mouth	0	1	1	58	37	3	0.37	0.54
Sand spit	0	0	9	67	24	0	0.38	0.43
River	0	0	14	67	19	0	0.24	0.40

Sediment from Gericke Point has a higher percentage of medium grained sediment in relation to the other locations along the shoreline. This is also seen as an indication of the grain characteristics of the sandy cliffs at Gericke Point. It is estimated that the finer sediment from Gericke Point is mixed with the coarser sediment originating from the historical coastal dunes systems along the Swartvlei beach, and sediment at the mouth area, resulting in the sediment found at the sand spit to the east (right) of the estuary mouth. The estuary mouth has the highest percentage of coarse materials with a corresponding  $D_{50}$  of 0.37 mm.

Understanding these sediment characteristics is essential when estimating a preliminary sediment budget around the Swartvlei estuary mouth. The Kamphuis longshore sediment transport equation discussed in section 4.2.1, requires a  $D_{50}$  or median grain size for calculating the sediment transport. To obtain these key parameters, typical sand grain distribution graphs were created to graphically estimate the  $D_{50}$  grain size (See Figures 57-60). The grain size parameters for use in the Kamphuis equation are presented in Table 7.

As already stated, due to a lack of reliable academic and published information, this campaign was undertaken to provide basic information on sand grain characteristics in the area. For the parameters of the Kamphuis formula for bulk longshore transport, an average  $D_{50}$  will be taken along the coastline. From the above results, it is seen that the grain sizes of the sediment found along the coastline are classified well below the inaccuracy ranges for grain sizes as stipulated by (Kamphuis, 2010).

Additional sampling in the form of vibrocoreing, seabed CPT (Cone Penetration Test) and deep sampling in the surf zone is recommended for more knowledge of the characteristics of the sediment scenario along the Swartvlei coastline as well as in the surf zone. The grading curves presented were used to obtain indicative values. It is recognised that more sieve sizes are

A Preliminary Analysis of the Sediment Budget Across the Swartvlei Estuary Mouth

required in order to establish the  $D_{50}$  with better accuracy. These test were however conducted to obtained indicative values and were executed by a professional institute thus insuring the greatest accuracy possible with the available data.

The graphical illustration of the grain distribution for each location is as follows:

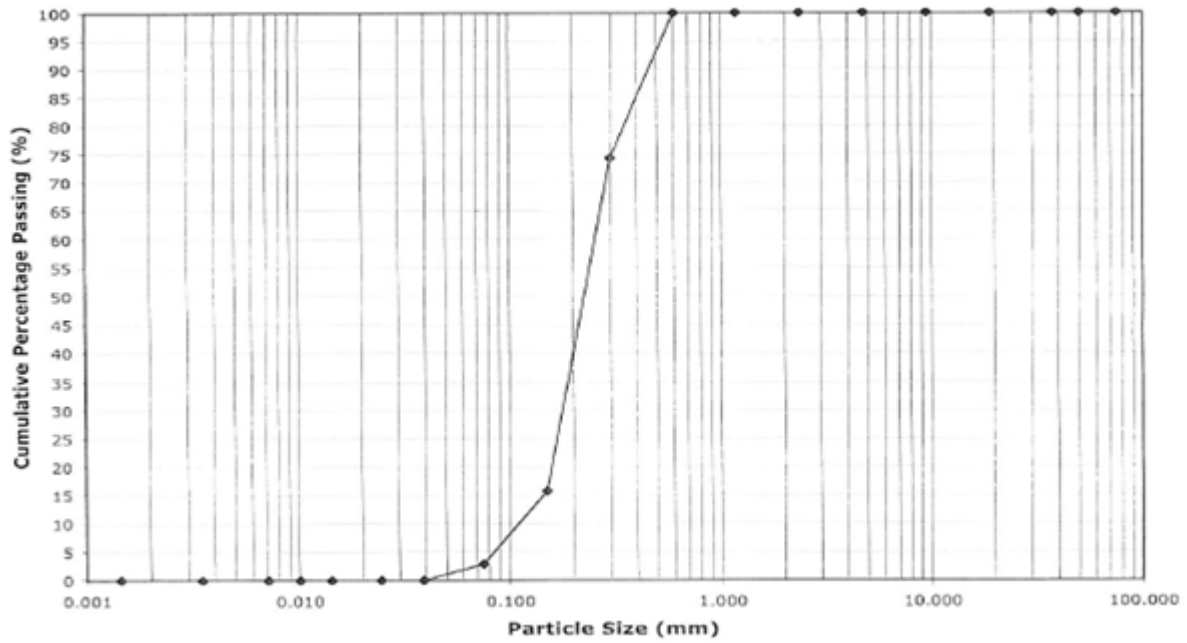


Figure 57: Grain size distribution: Gericke Point

A Preliminary Analysis of the Sediment Budget Across the Swartvlei Estuary Mouth

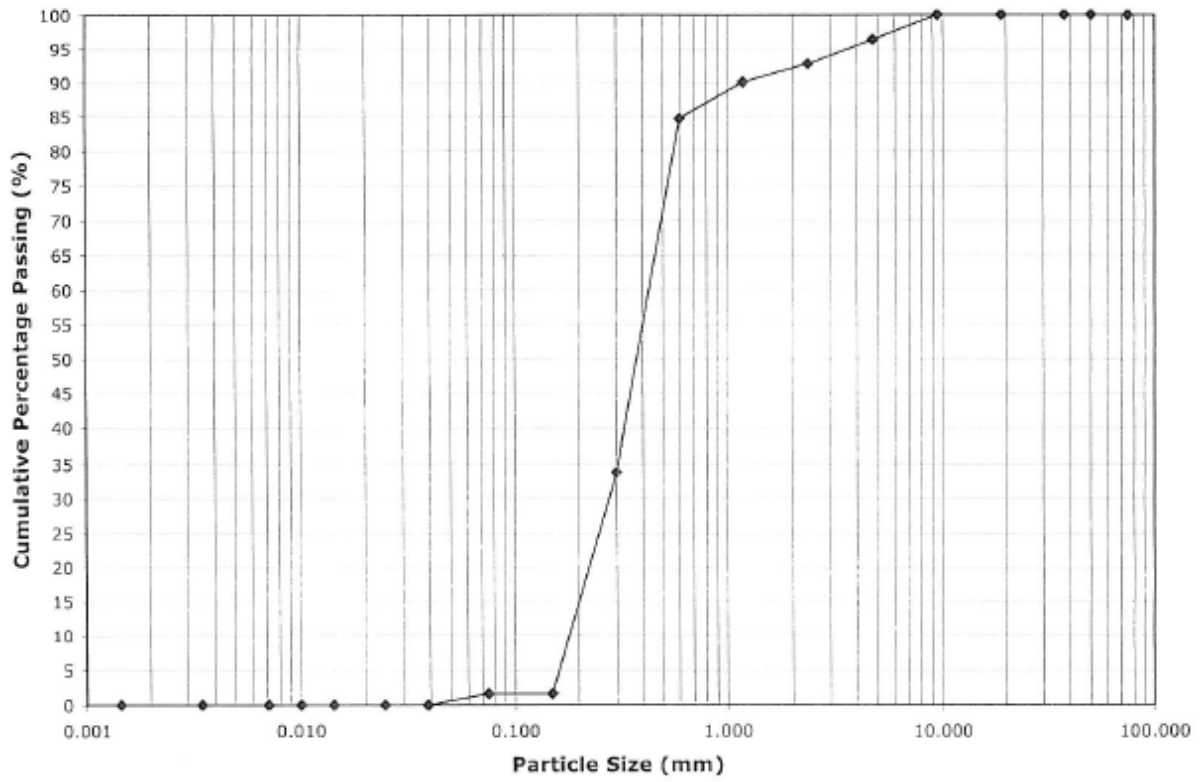


Figure 58: Grain size distribution: Estuary Mouth

A Preliminary Analysis of the Sediment Budget Across the Swartvlei Estuary Mouth

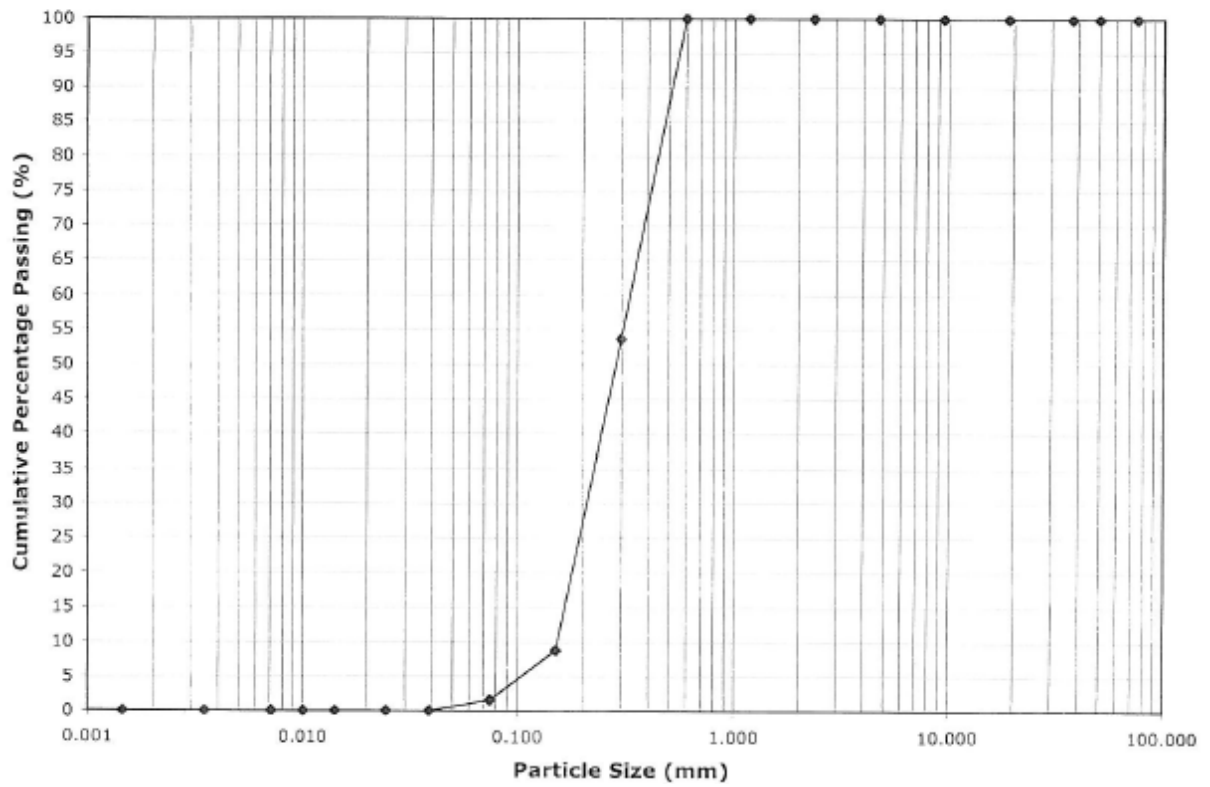


Figure 59: Grain size distribution: Sand Spit

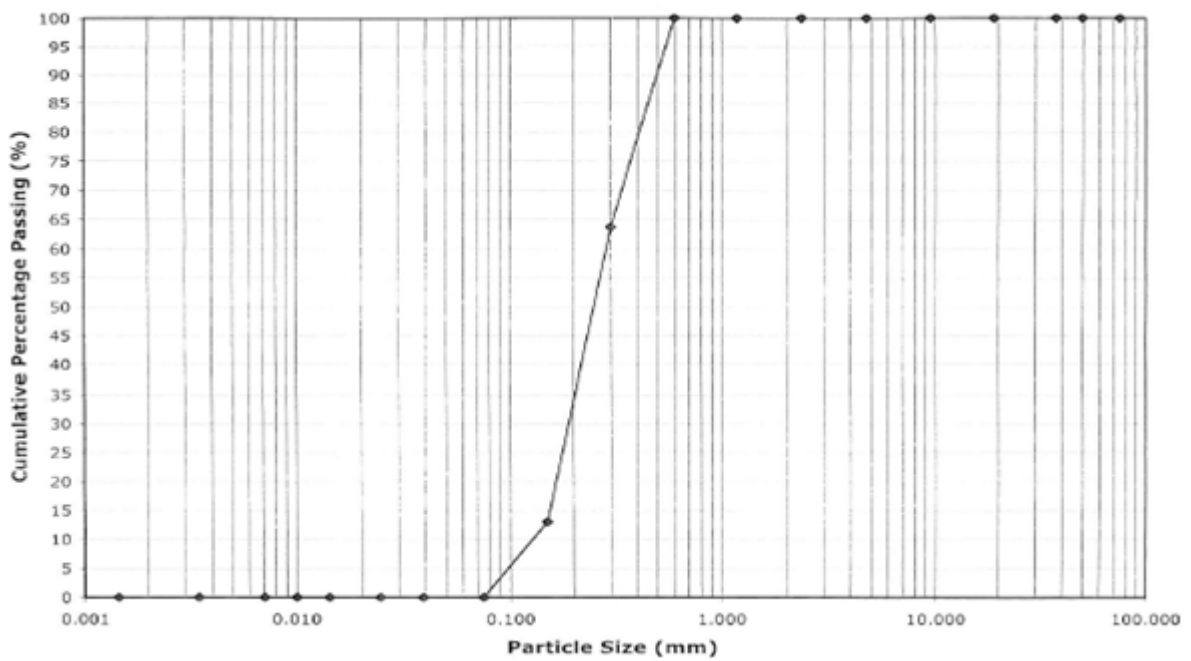


Figure 60: Grain size distribution: River

## 5.2 ESTUARY PROFILE DATA

By studying the fundamentals of a sediment budget defined by the literature presented in this study, the estuary mouth has been identified as a vital component of the Swartvlei estuary mouth sediment budget. Analysis thereof forms part of the desktop study, as described in Chapter 4.

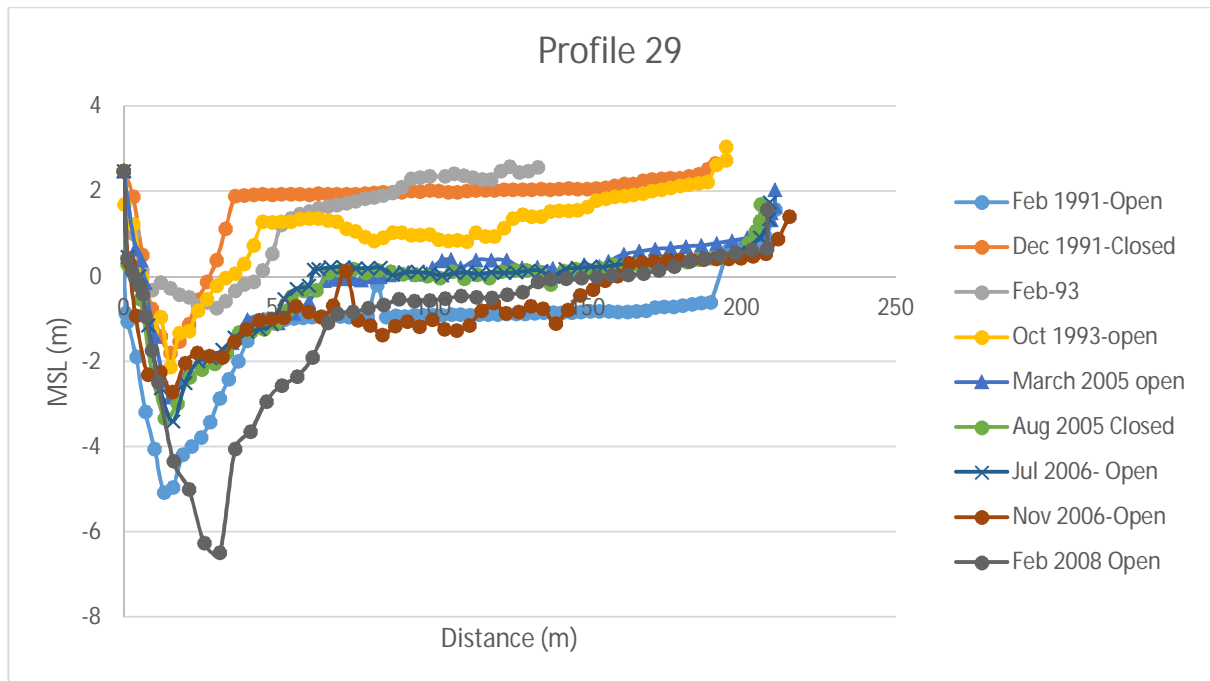
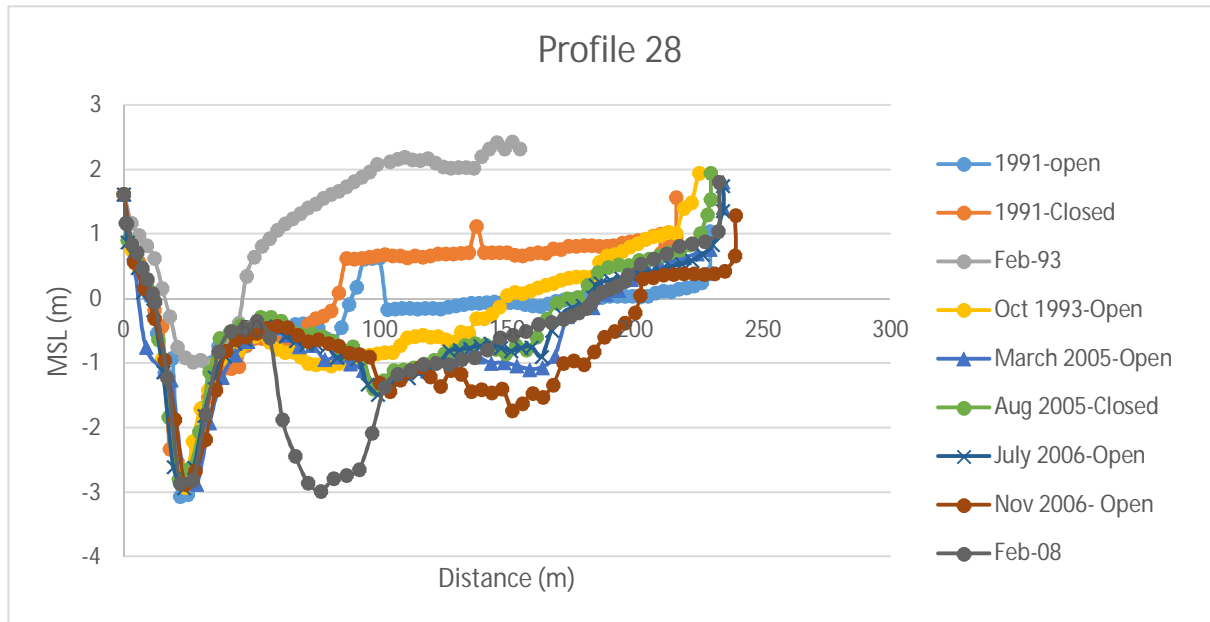
Using historical data obtained from the SANPark records, 10 historical estuarine cross section profiles were constructed. The locations of the 10 sections are illustrated in Figure 61.



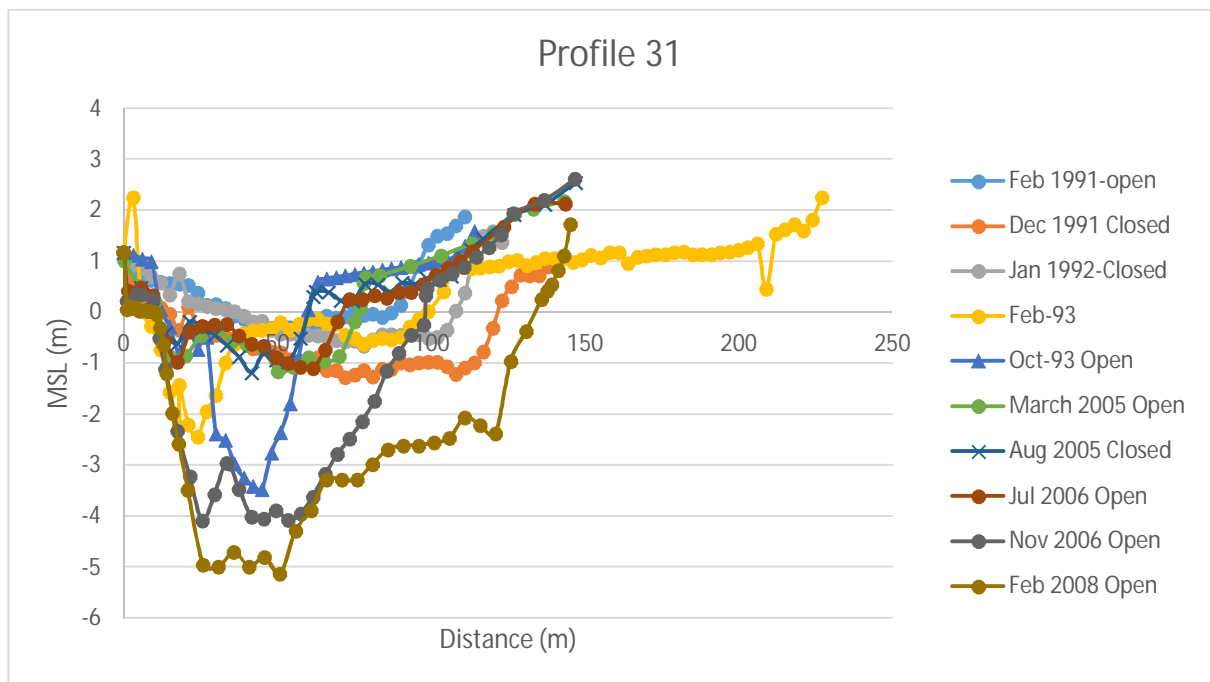
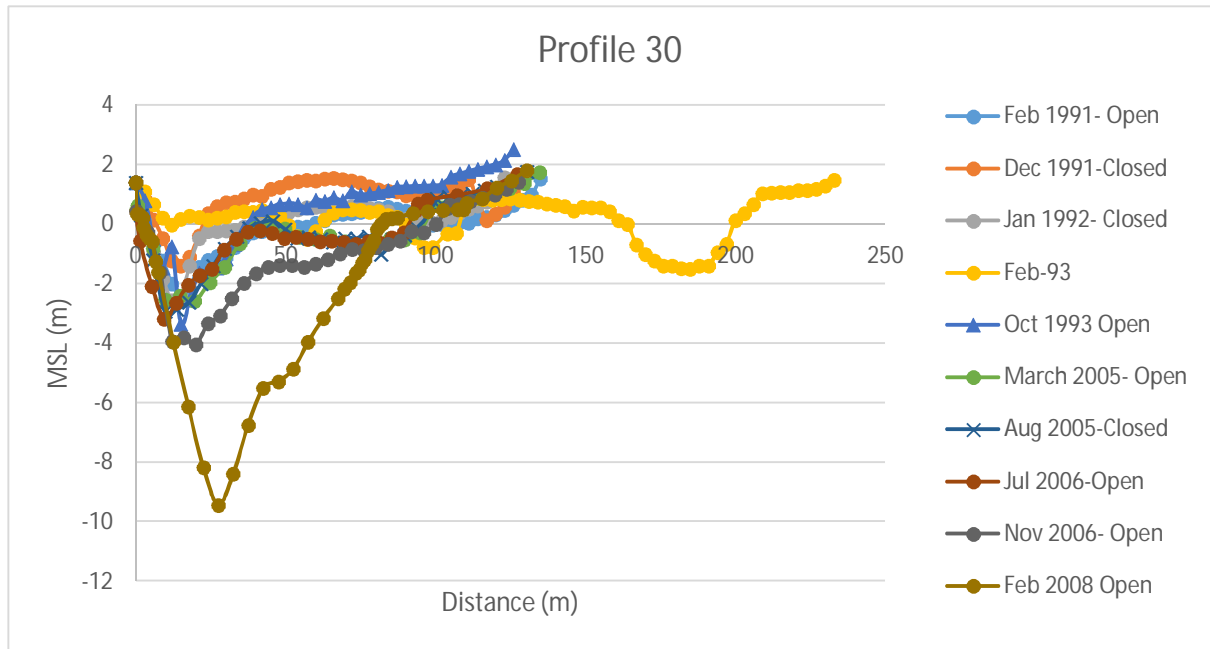
*Figure 61: Locations of historical river profiles*

For each profile a graphical comparison between successive years was constructed using the historical recorded data from SANParks (SANParks, 2012). This comparison was done to identify significant events, trends and occurrences in the estuary mouth. These findings will be used in the construction of a hypothesis, set out in Chapter 7. It is necessary to refer to relevant literature set out in the literature study to understand the fundamentals of the flood regime and mouth dynamics occurring at the Swartvlei estuary. The Swartvlei estuary open mouth conditions are dependent on the floods generated by the delayed effects of the winter

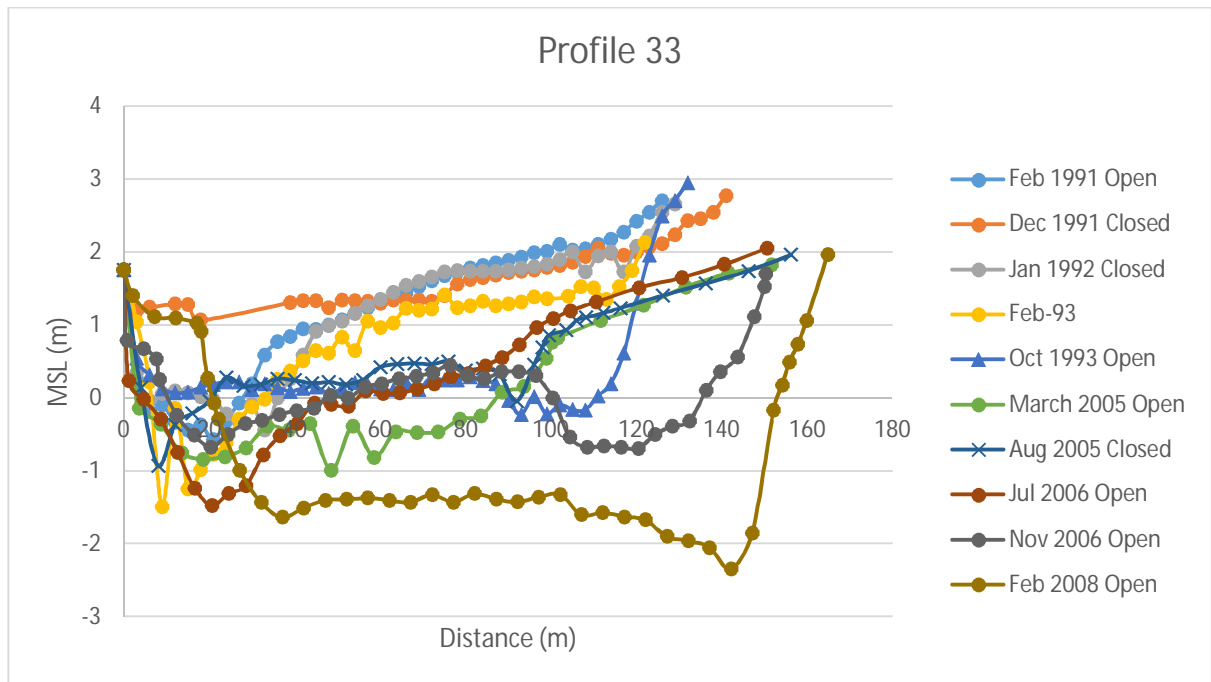
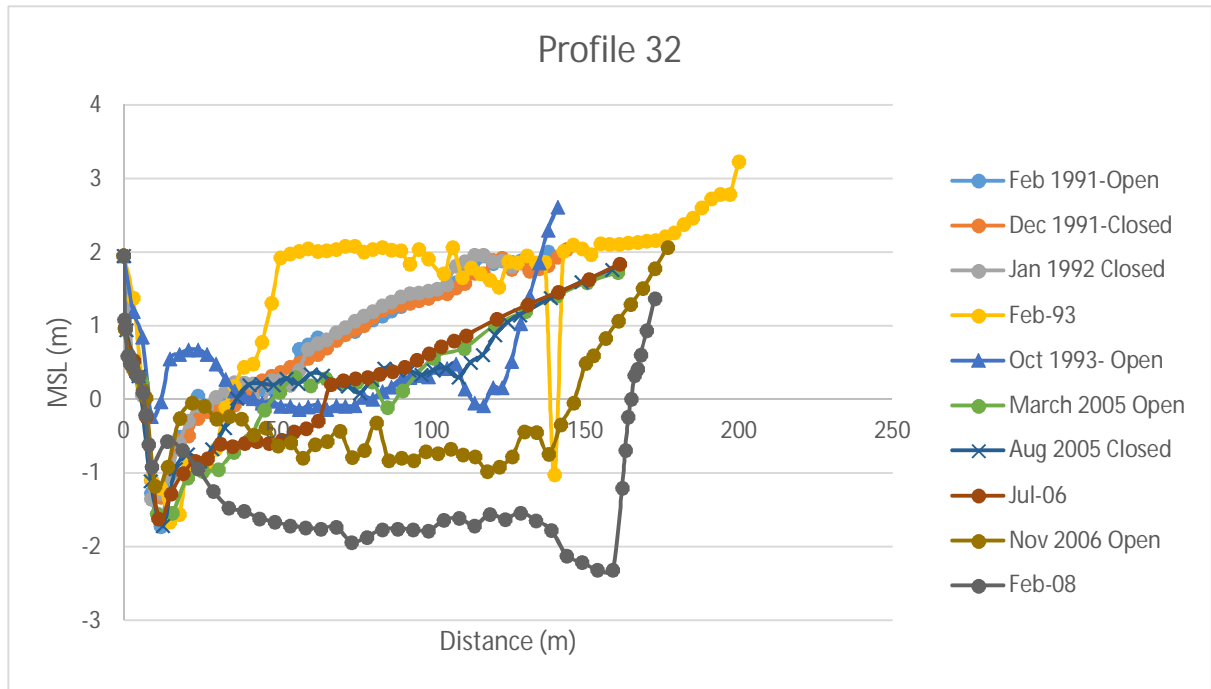
A Preliminary Analysis of the Sediment Budget Across the Swartvlei Estuary Mouth



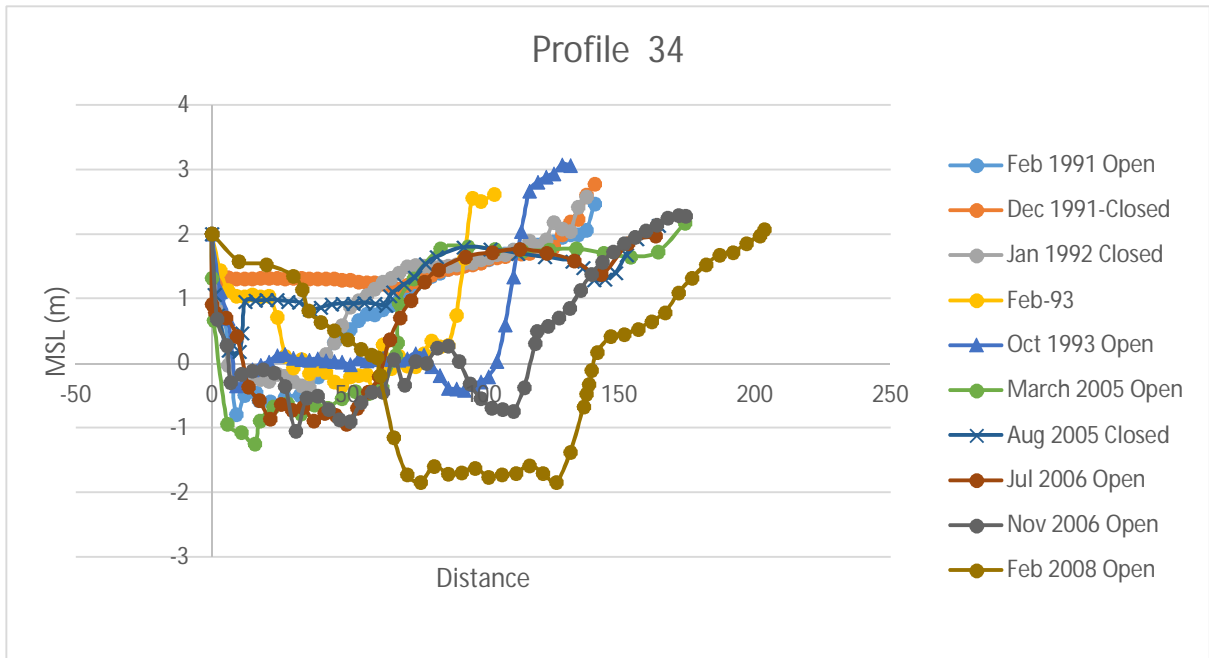
A Preliminary Analysis of the Sediment Budget Across the Swartvlei Estuary Mouth



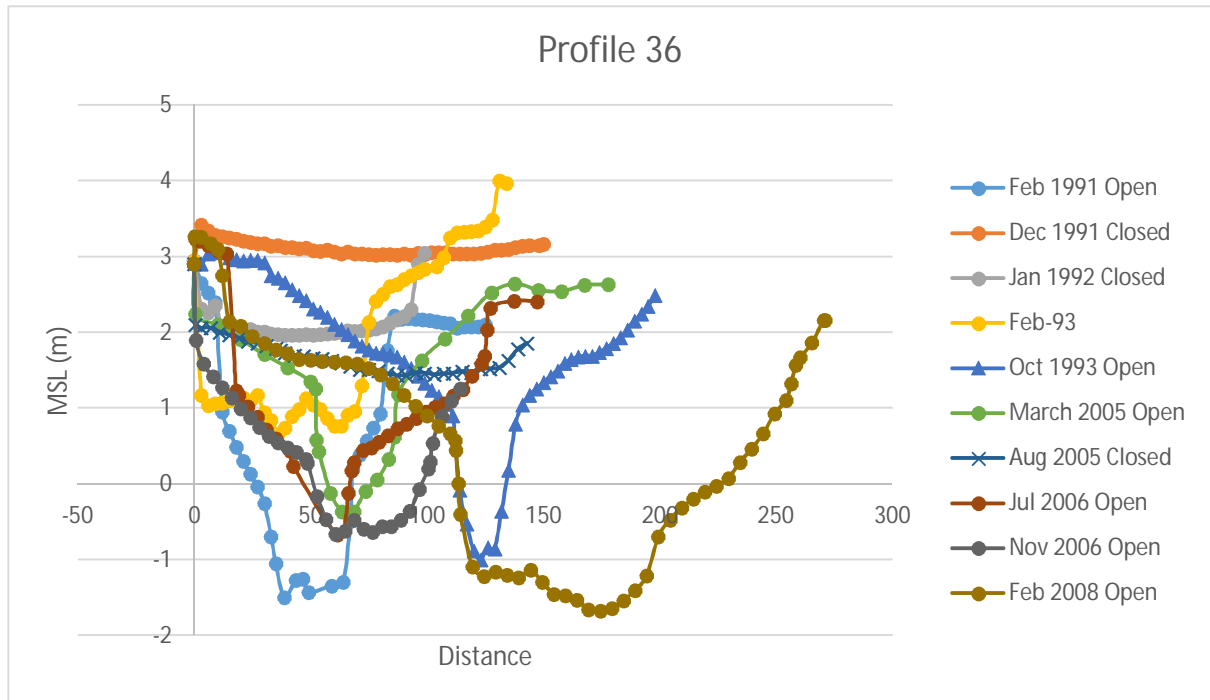
A Preliminary Analysis of the Sediment Budget Across the Swartvlei Estuary Mouth



A Preliminary Analysis of the Sediment Budget Across the Swartvlei Estuary Mouth



## A Preliminary Analysis of the Sediment Budget Across the Swartvlei Estuary Mouth



Of special interest are the sections from profile 30 to profile 36. These profiles describe the estuary characteristics inside the defined sediment budget boundaries. Through the investigation of these profiles, it was found that the estuary has been deepening towards the west and filling up towards the east, a possible effect of channel migration. From the profiles above, the effects of the severe 2007 floods can be seen. These floods dramatically changed the course and bathymetry of the estuary mouth. As a possible result of the channel migration observed from the profiles presented above, a deeper channel has been formed along the west bank of the estuary. This is an important observation toward the formation of the hypothesis set out in Chapter 7, with significant relevance towards dune slumping and erosion along the western estuary bank.

## 6. NUMERICAL MODELLING

### 6.1 AVAILABLE DATA

#### 6.1.1 Hind cast data

The historical input data that was used was hindcast data from NOAA/NECP Wavewatch III. The modelling position is located at 35.00 S, 22.50 E and is approximately 100 km offshore from Swartvlei Bay. In Figure 62, the location is shown from which the hindcast data used in this study was predicted by NCEP (National Centres for Environmental Prediction). NCEP data is derived from a numerical forecasting model which simulates climates, winds, waves and environments. It is thus not a physical buoy in the water, but a numerical prediction model. The offshore waves were predicted at the NCEP location and then modelled into the Swartvlei bay area with the use of MIKE 21 SW.



Figure 62: Location of NCEP hind cast modelling (Google)

A ten year historical record was provided, that included the following historical data (NCEP, 2011):

- Significant wave height
- Peak wave period
- Direction of peak wave period

## A Preliminary Analysis of the Sediment Budget Across the Swartvlei Estuary Mouth

- Wind magnitude
- Wind direction

For the calculation to represent actual conditions as closely as possible, the year 2009 was selected from the NCEP hindcast data. This selection was based on the fact that 2009, compared to the other years, was homogeneous in wave climates, but also consisted of slightly elevated peaks and lows that would contribute to possible significant bulk longshore transport events. These peaks and lows in the 2009 wave climate data were not the most extreme values, but average as compared to the total hindcast data set. This would result in the simulation of processes that were more frequent, rather than freak events. Figure 63 shows the  $T_p$  and  $H_s$  recorded data for 2009.

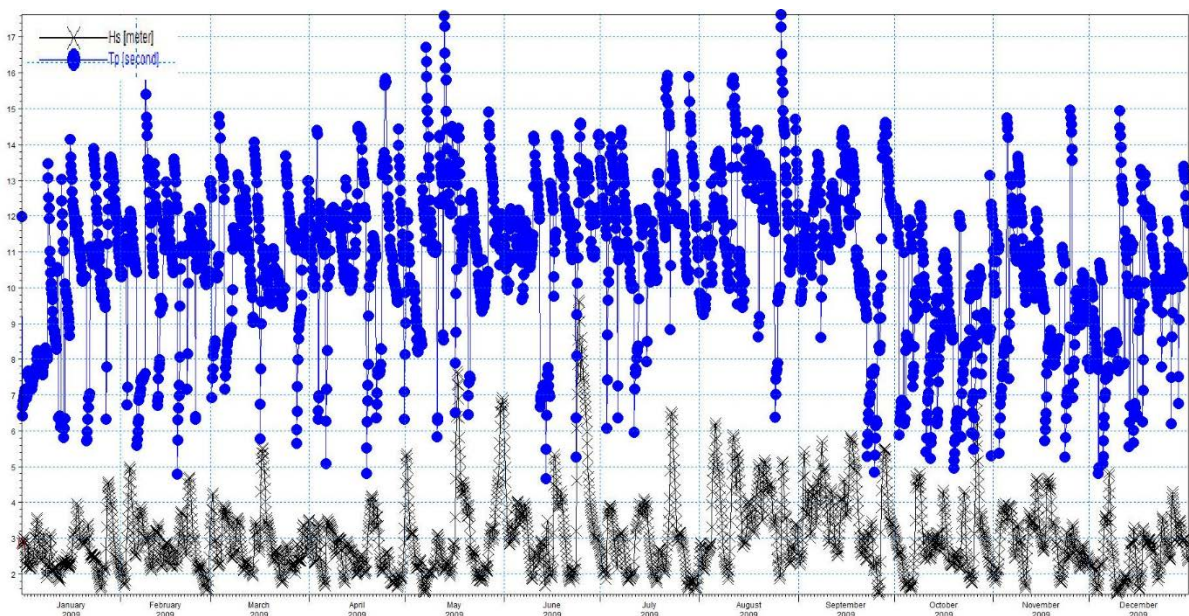


Figure 63:  $H_s$  versus  $T_p$  for 2009

The hindcast data was reduced to represent only 2009 and this data was used to derive input parameters for the MIKE 21 SW numerical model. Figure 64 to Figure 65 illustrate variations of the significant wave height ( $H_s$ ) over varying periods.

A Preliminary Analysis of the Sediment Budget Across the Swartvlei Estuary Mouth

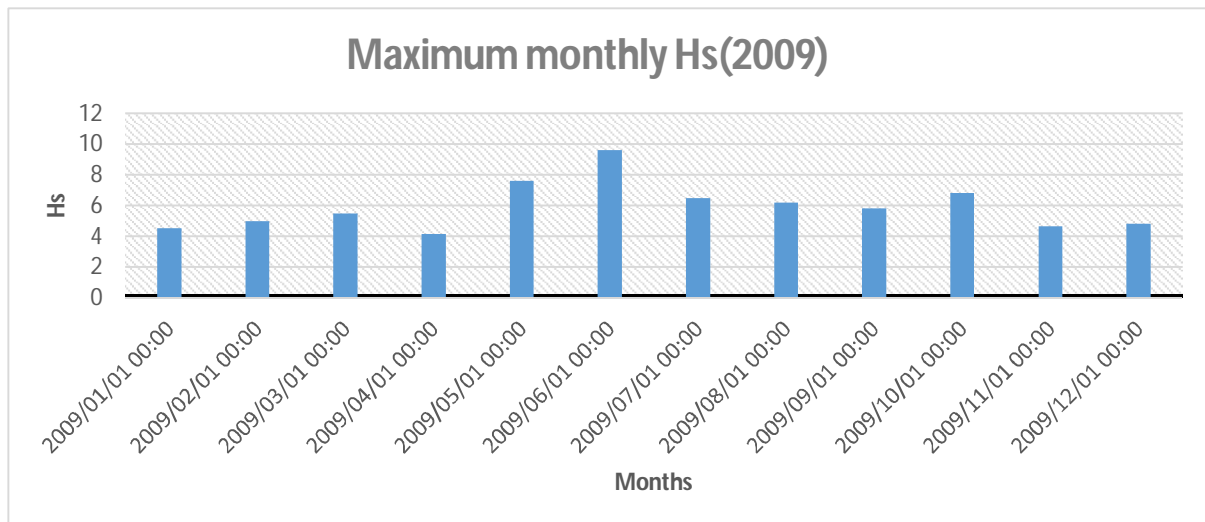


Figure 64: Maximum monthly Hs for 2009

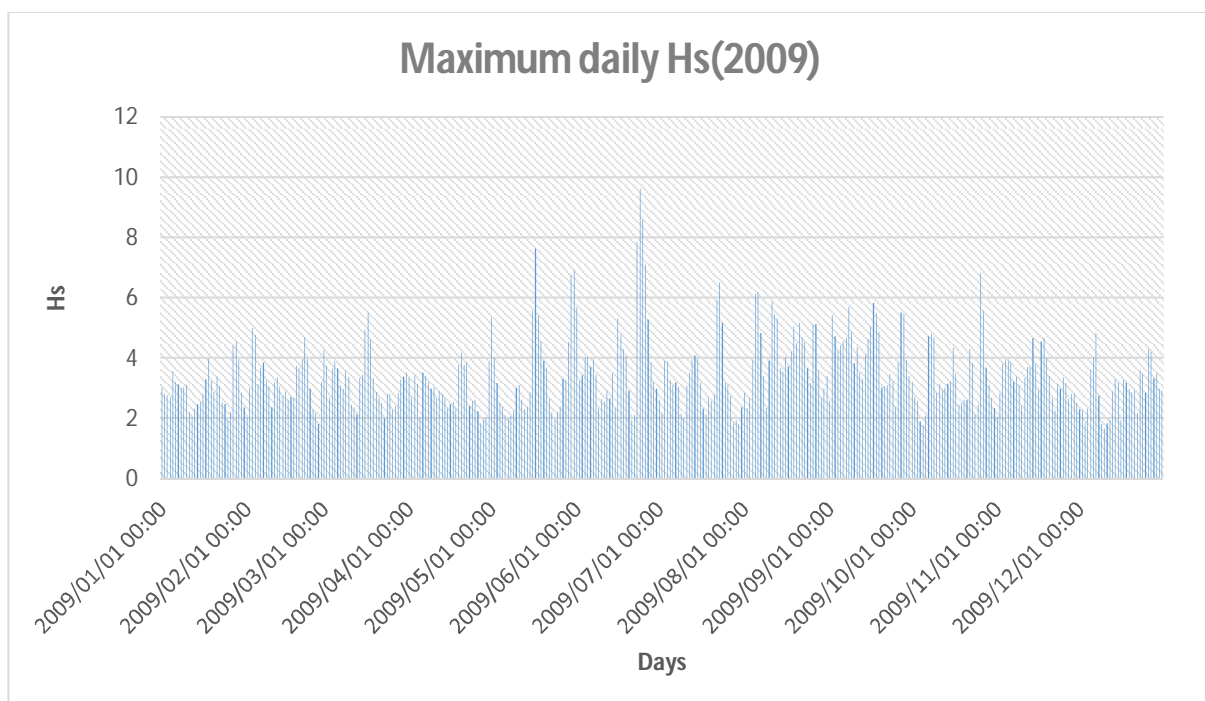


Figure 65: Maximum daily Hs for 2009

The historical data for 2009 was binned in an attempt to understand the wave climate and the typical events that will enter the bay under certain conditions. The data “binning” was done according to the following procedure:

1. Waves were binned according to the following wave criteria:

*Table 8: Wave height bins*

<b>Wave Height bins</b>
0-1
1-1.5
1.5-2
2-2.5
2.5-3
3-3.5
3.5-4
4-4.5
4.5-5
5-5.5
> 5.5

2. Wave period bins were categorized as follows:

*Table 9: Wave period bins*

<b>Wave period bins</b>
0-2
2-4
4-6
6-8
8-10
10-12
>12

## A Preliminary Analysis of the Sediment Budget Across the Swartvlei Estuary Mouth

The results of linking the wave period bins to the significant wave height bins are illustrated in Table 10.

*Table 10: Number of occurrences when comparing significant wave height (in meters) with accompanying peak periods (in seconds) for 2009*

$T_p / H_s$	0-2	2-4	4-6	6-8	8-10	10-12	>12
0-1	0	0	0	0	0	0	0
1-1.5	0	0	0	2	5	1	0
1.5-2	0	0	4	29	84	155	60
2-2.5	0	0	23	64	171	286	145
2.5-3	0	0	24	84	107	255	180
3-3.5	0	0	1	105	61	149	136
3.5-4	0	0	0	47	36	117	101
4-4.5	0	0	0	8	16	64	72
4.5-5	0	0	0	1	19	41	52
5-5.5	0	0	0	0	8	20	37
> 5.5	0	0	0	0	6	22	55

Table 10.

Table 10 illustrates that for every significant wave height bin there is an associated period bin. This results in a table that describes the number of times per year (2009) that a wave height between 1 m-1.5 m, for instance, is accompanied by a period of 6 s-8 s.

To better illustrate this table of wave height versus wave period occurrences, Table 11 was formulated to describe the percentage of occurrence of each case.

*Table 11: Percentage occurrence of wave height with its corresponding period for 2009*

$H_s / T_p$	0-2	2-4	4-6	6-8	8-10	10-12	> 12
0-1	0.00	0.00	0.00	0.00	0.00	0.00	0.00
1-1.5	0.00	0.00	0.00	0.07	0.18	0.04	0.00
1.5-2	0.00	0.00	0.14	1.02	2.94	5.43	2.10
2-2.5	0.00	0.00	0.81	2.24	5.99	10.02	5.08
2.5-3	0.00	0.00	0.84	2.94	3.75	8.94	6.31
3-3.5	0.00	0.00	0.04	3.68	2.14	5.22	4.77
3.5-4	0.00	0.00	0.00	1.65	1.26	4.10	3.54
4-4.5	0.00	0.00	0.00	0.28	0.56	2.24	2.52
4.5-5	0.00	0.00	0.00	0.04	0.67	1.44	1.82
5-5.5	0.00	0.00	0.00	0.00	0.28	0.70	1.30
> 5.5	0.00	0.00	0.00	0.00	0.21	0.77	1.93

Table 11 illustrates through a method of percentage occurrence that certain wave and period combinations were more prominent during the year. From this table it is also seen that 2009 showed a predominance towards the '8' – '>12' second periods and the 1.5 - 3.5 m wave heights.

### 3. Binning of this wave and period combination with average directions.

To estimate the wave climate entering the bay area at Swartvlei, an understanding of not only the significant wave data and the accompanying wave periods are required, but a description of the direction of the incident wave angles is also crucial in driving the sediment transport in the bay. The data set used for the wave height and peak period comparison illustrated in Table 10 and Table 11 was further statistically analysed in order to obtain a wave direction for each combination of wave height versus peak period bin. An average direction was then calculated from the sample of occurrences for each wave height versus peak period bin to formulate a preliminary understanding of these incident wave heights with their corresponding peak periods and direction. The data follows in Table 12.

*Table 12: Average incident wave directions (in degrees) for significant wave heights and wave periods*

$T_p / H_s$	0-2	2-4	4-6	6-8	8-10	10-12	> 12
0-1	0	0	0	0	0	0	0
1-1.5	0	0	0	110.555	155.978	223.03	0
1.5-2	0	0	0	144.45	179.57	214.39	218.6
2-2.5	0	0	200	131.14	182.86	210.6	216.24
2.5-3	0	0	118.9	140	174.8	203.4	211.5
3-3.5	0	0	98.71	132.95	167	209.5	215.6
3.5-4	0	0	0	115.3	168.5	212.2	215.5
4-4.5	0	0	0	110	156.19	216.1	212.81
4.5-5	0	0	0	93.9	190.24	210	214.9
5-5.5	0	0	0	0	221.8	213.8	218.9
> 5.5	0	0	0	0	218.7	219.2	216.1

Table 12 was formulated to describe the average incident wave directions from the historical data obtained from the offshore buoy. The angles are given in degrees and follow a Cartesian coordinate system as illustrated in Figure 66:

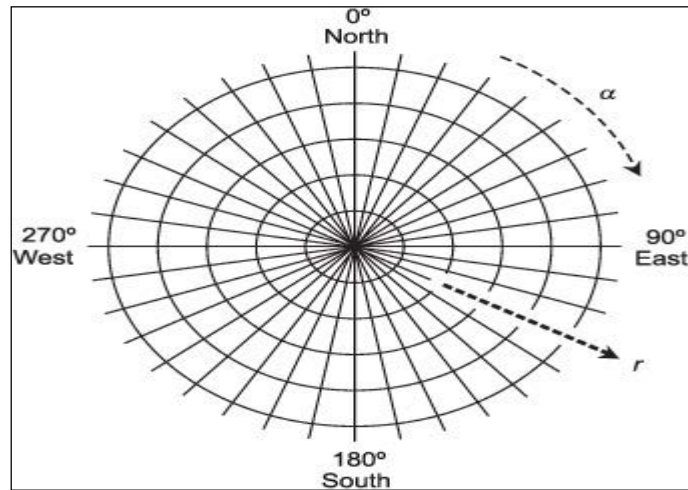


Figure 66: Relevant Cartesian coordinate system

## 6.2 MODEL SET-UP

### 6.2.1 Study area

The study area selected for the MIKE 21 SW model was the greater bay area around the Swartvlei coastline. The MIKE 21 SW model was set up with the outer boundary incorporating the NCEP location. The sensitivity of the triangular mesh generated gradually increased towards the area within the Swartvlei coastline bay area. This meant that the offshore waves would be modelled from the NCEP location into the nested grid or area which was defined as the Swartvlei bay area (see Figure 67) and then modelled within the bay.

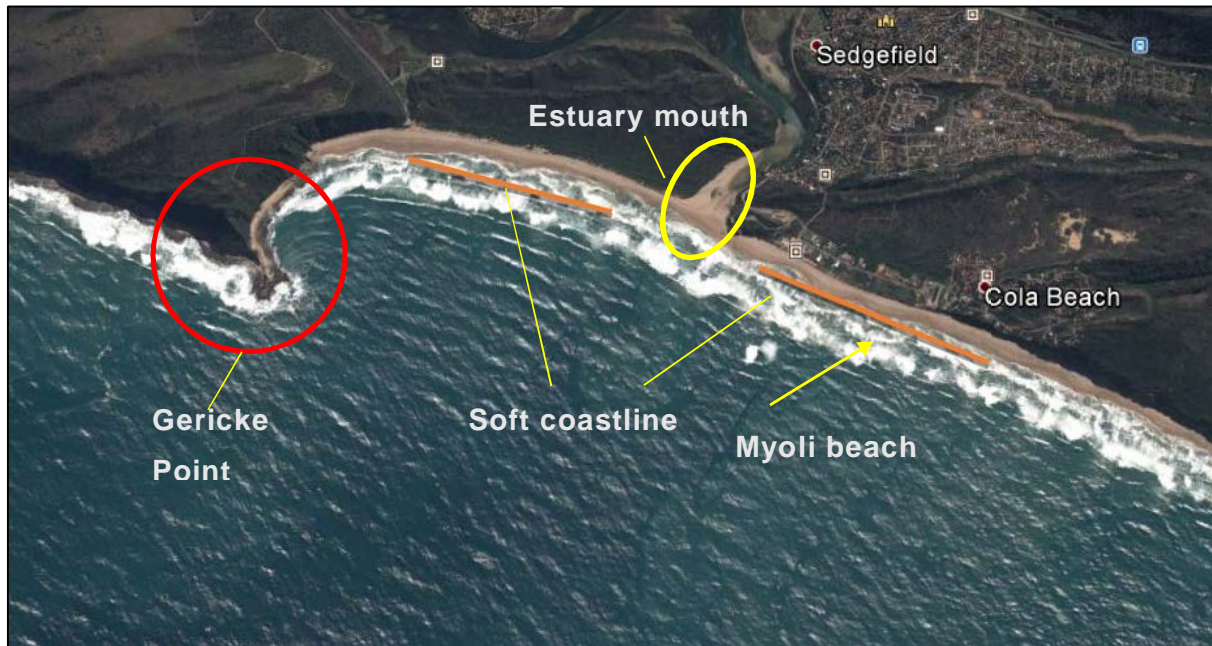


Figure 67: Study area

### **Bathymetry and Mesh**

Bathymetry data required for the numerical wave model for the Swartvlei coastline and bay area is sparse, especially in the inshore regions. The bathymetry data used for the numerical model is a digitized version of the SANHO (South African Navy Hydrographic Office) 123 chart.

The final bathymetry of the Sedgefield bay area was modelled as follows:

1. A total model boundary (referring to the entire model area) was created in MIKE 21 SW and given code values (see Figure 68). These codes 1, 2, 3 and 4 would indicate certain properties of the boundaries. These properties are explained further on in this section under 'Model input parameter and assumptions'. The large numbering in Figure 68, shows the different areas with regards to mesh sensitivity.

A Preliminary Analysis of the Sediment Budget Across the Swartvlei Estuary Mouth

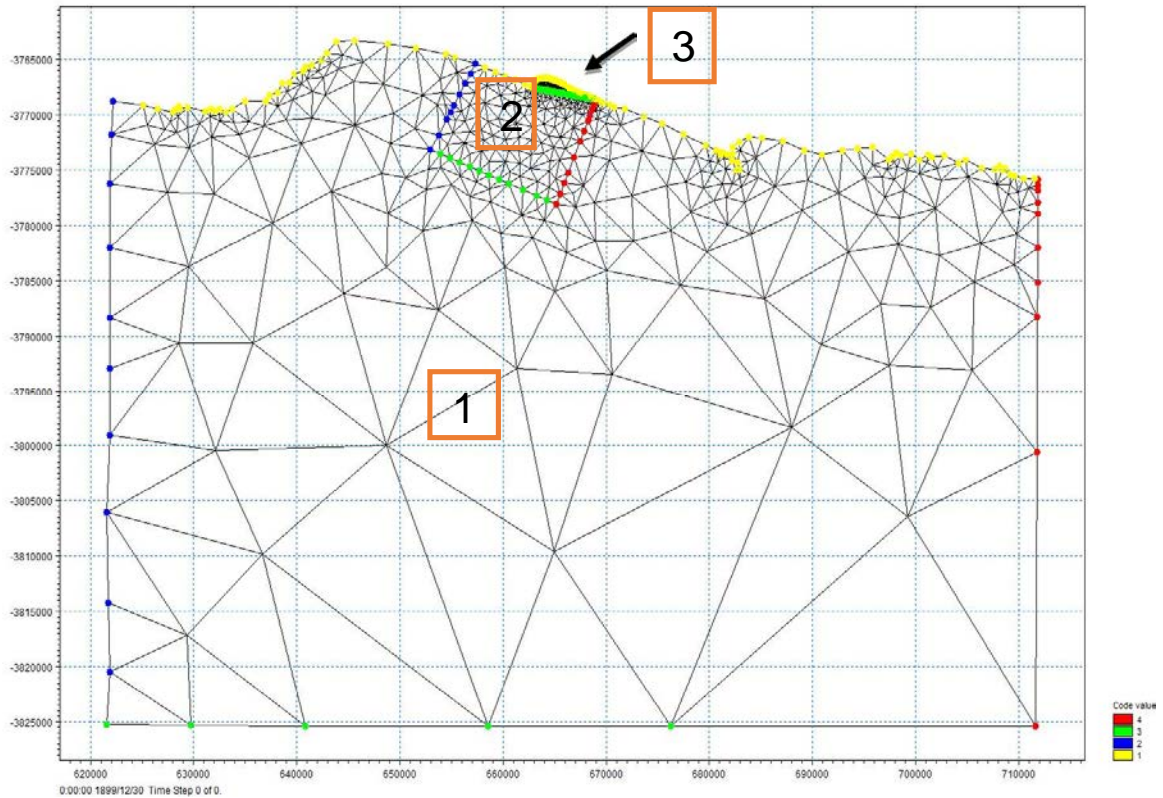


Figure 68: Model boundaries and mesh with numbered areas with finer mesh indicated

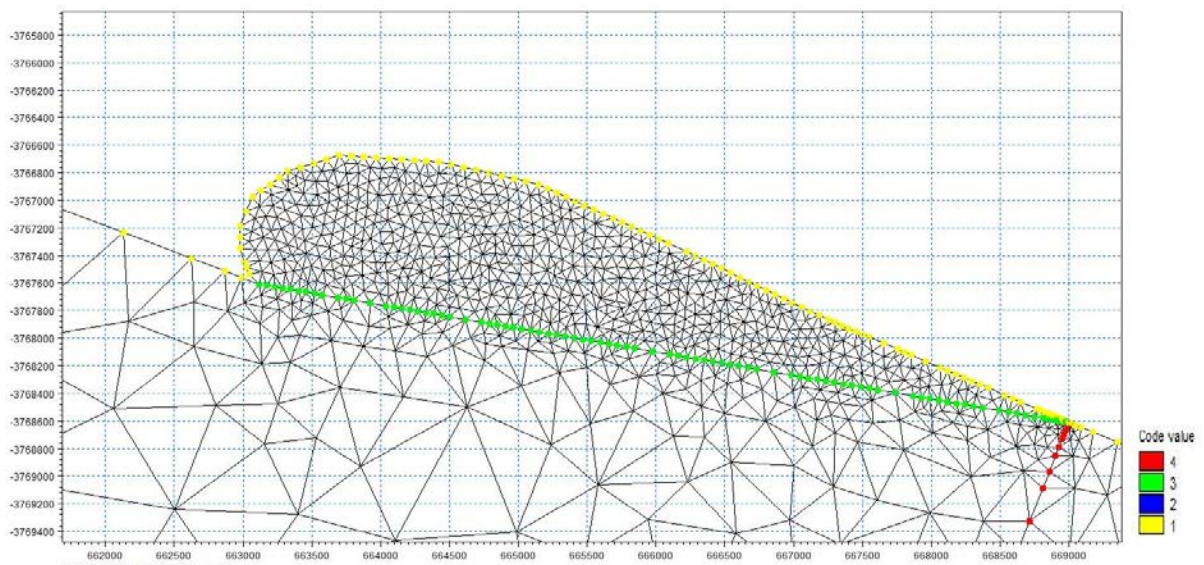


Figure 69: Mesh set-up for Swartvlei bay

2. A triangular mesh was used to best describe the modelled area. The triangular mesh model used for this study is illustrated in Figure 68, with a close up in Figure 69. As seen in Figure 68, a coarse outer mesh (area 1) was selected to model the incident wave climates approaching area 2. Inside area 2, the triangular mesh was sensitized and once more in area 3, which represents the Swartvlei bay area. The mesh size inside the bay

A Preliminary Analysis of the Sediment Budget Across the Swartvlei Estuary Mouth

area, was modelled as finely as computationally possible in an attempt to simulate the wave condition alongshore that drives the longshore transport.

- From here, the SANHO digital bathymetric scatter data was combined with the surveyed beach profile data and imposed onto the triangular mesh to create a digital bathymetric chart for the model area. This is illustrated in Figure 70 and Figure 71.

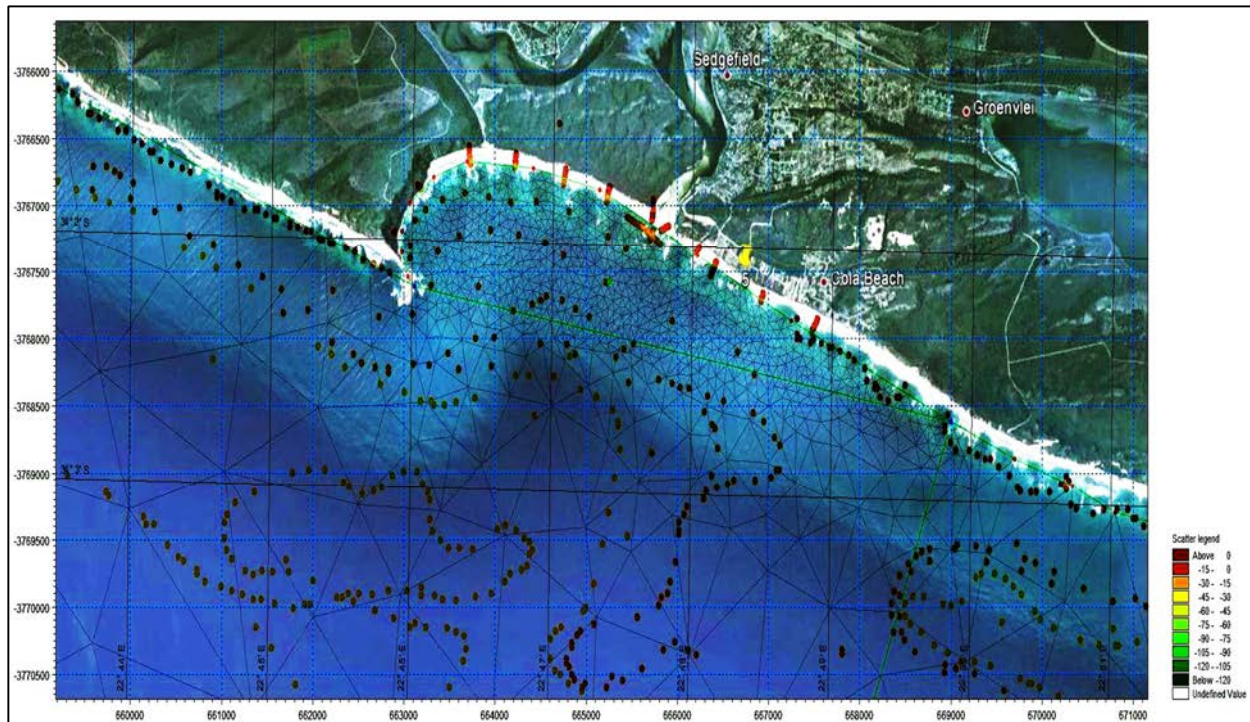


Figure 70: MIKE bathymetric scatter data in bay area

A Preliminary Analysis of the Sediment Budget Across the Swartvlei Estuary Mouth

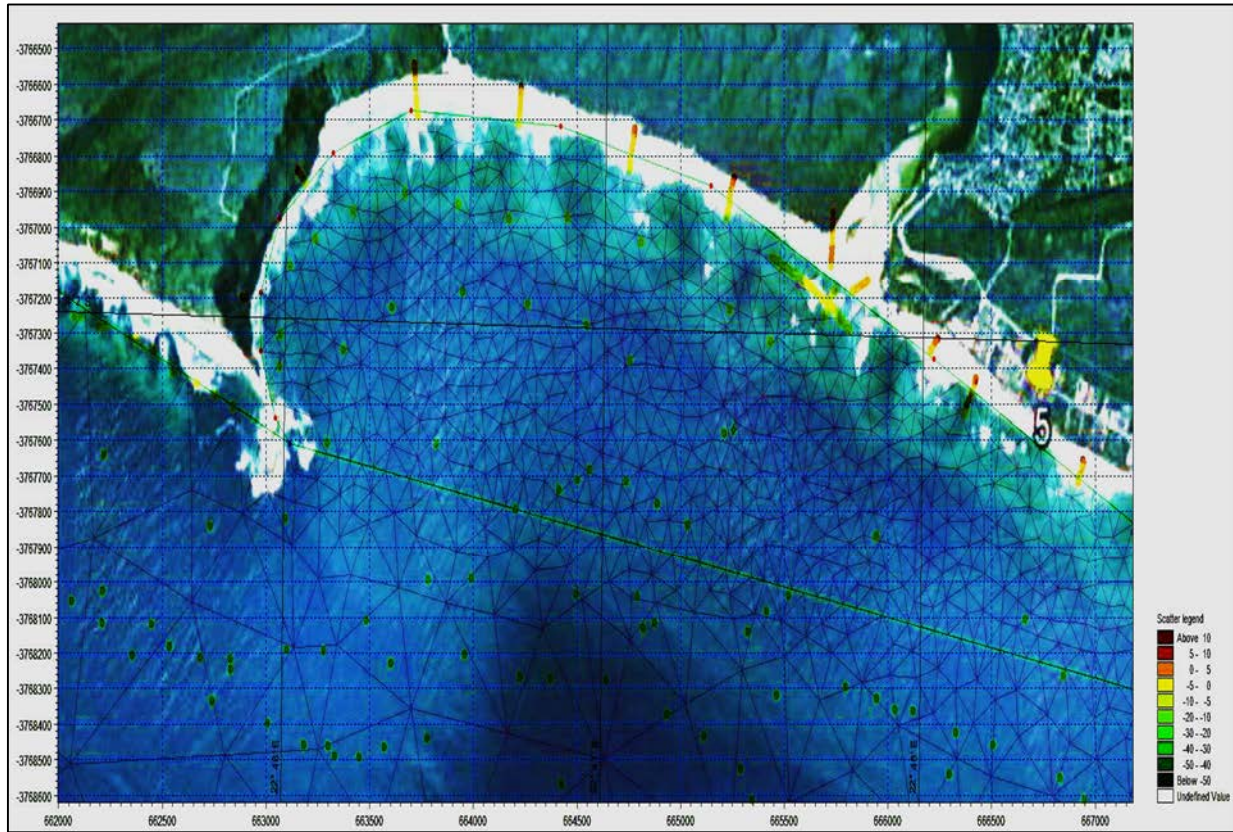


Figure 71: MIKE bathymetric scatter data with a more sensitive depth scale

A Preliminary Analysis of the Sediment Budget Across the Swartvlei Estuary Mouth

- The triangular mesh and the bathymetric scatter data were interpolated to merge the two data sets into one bathymetric chart of the area. Figure 72 illustrates the interpolated bathymetric chart.

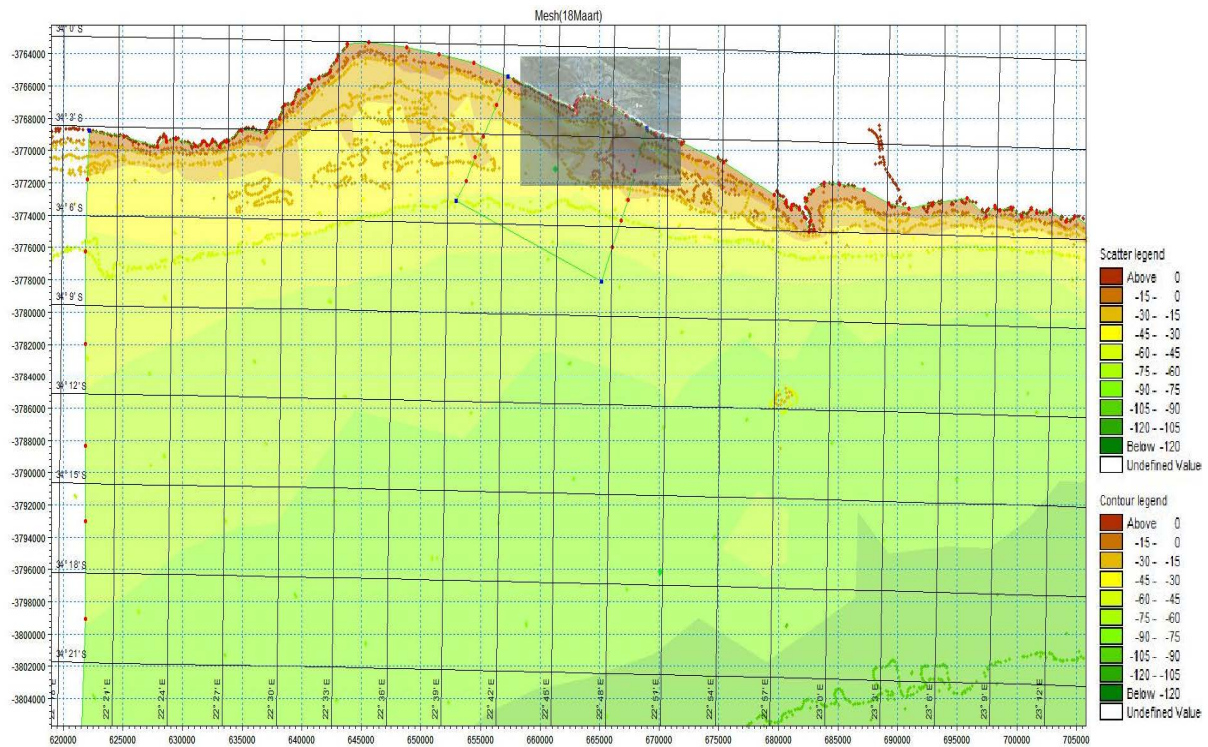


Figure 72: Interpolated bathymetric chart

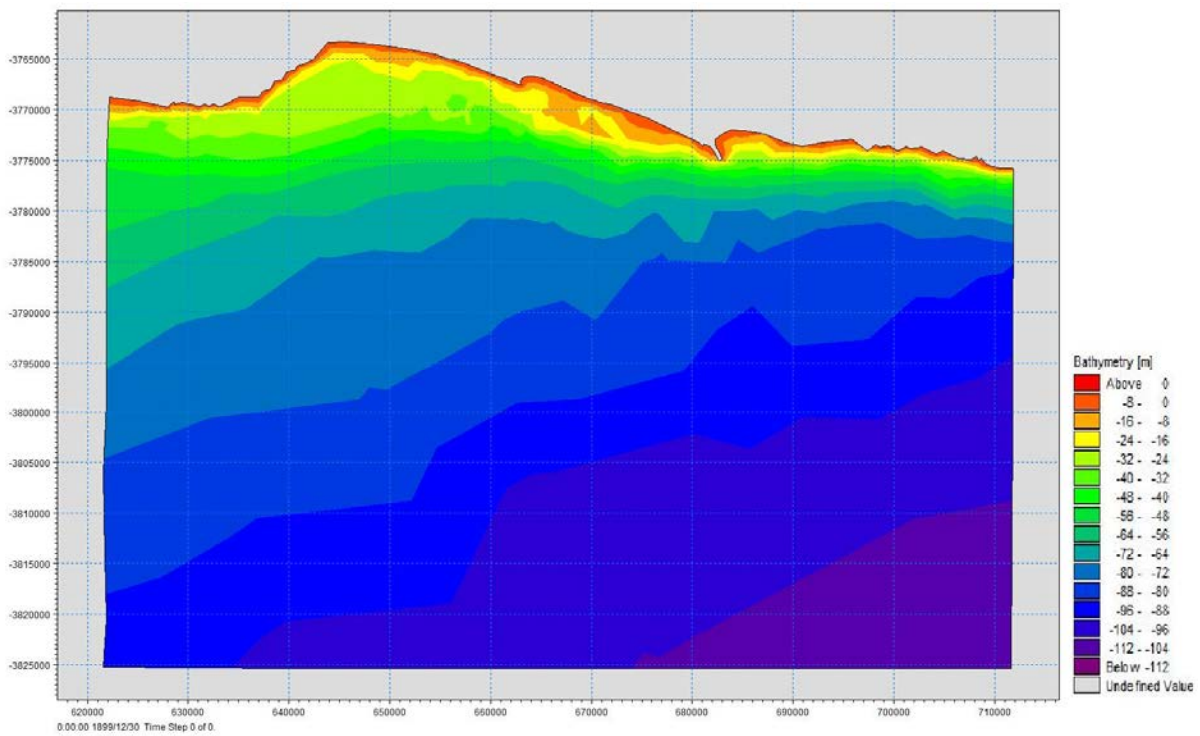
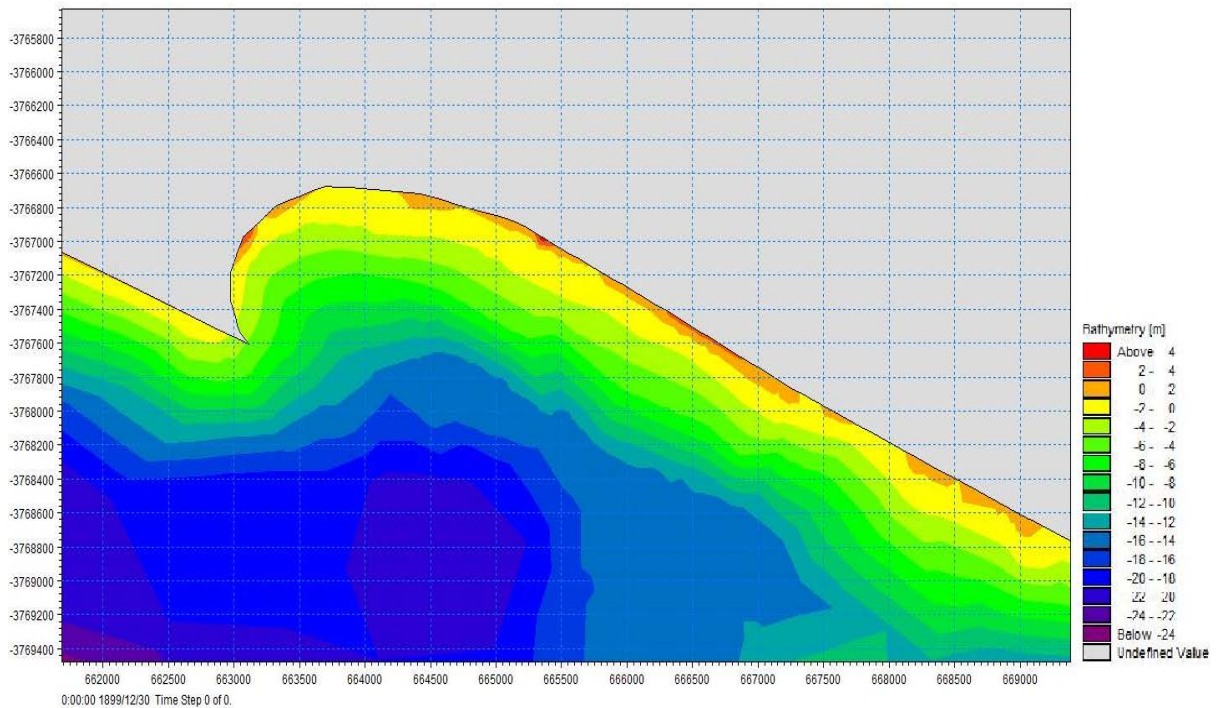


Figure 73: Bathymetric chart of total model area

## A Preliminary Analysis of the Sediment Budget Across the Swartvlei Estuary Mouth



*Figure 74: Close up bathymetric chart of Sedgefield Bay*

The final bathymetric chart, obtained from the MIKE 21 package, is shown in Figure 73 with a close up view in Figure 74. These data sets were used as the basis for the numerical MIKE 21 Spectral Wave model.

For calibration of the data, the bathymetric output was compared to the published SANHO 123 bathymetric chart for this area. Although the available data on near shore bathymetry for input in the numerical model was sparse, the comparison of the actual vs modelled data e.g. the 10 m contour in Figure 75 (published SANHO chart) with the 10 m contour obtained from the MIKE 21 output data (Figure 74), seemed to fit with reasonable accuracy.

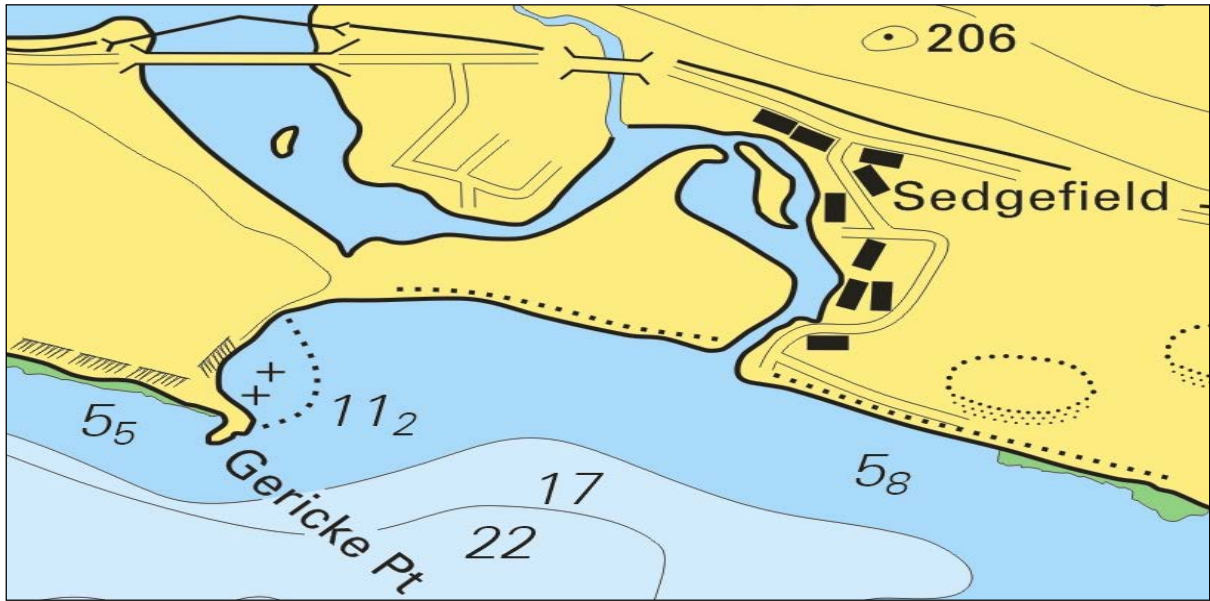


Figure 75: SANHO 123 bathymetric chart

### Model input parameters

Following the generation of the bathymetric chart, the MIKE 21 SW numerical model was set up. The MIKE 21 SW interface is centred on three main components namely:

1. Domain
2. Time
3. Spectral Wave analysis

Each of these modelling areas are essential to the numerical model. It is important to clearly define the parameters used in order to understand the results of the output file.

### Domain

The domain and mesh used in this model are the same as described for the bathymetry area described earlier in this section.

To ensure accurate modelling of the area, the map projection was modelled in UTM-34. The mesh file was created as a mesh extension and loaded in that format into the MIKE 21 SW interface (see Figure 76).

A Preliminary Analysis of the Sediment Budget Across the Swartvlei Estuary Mouth

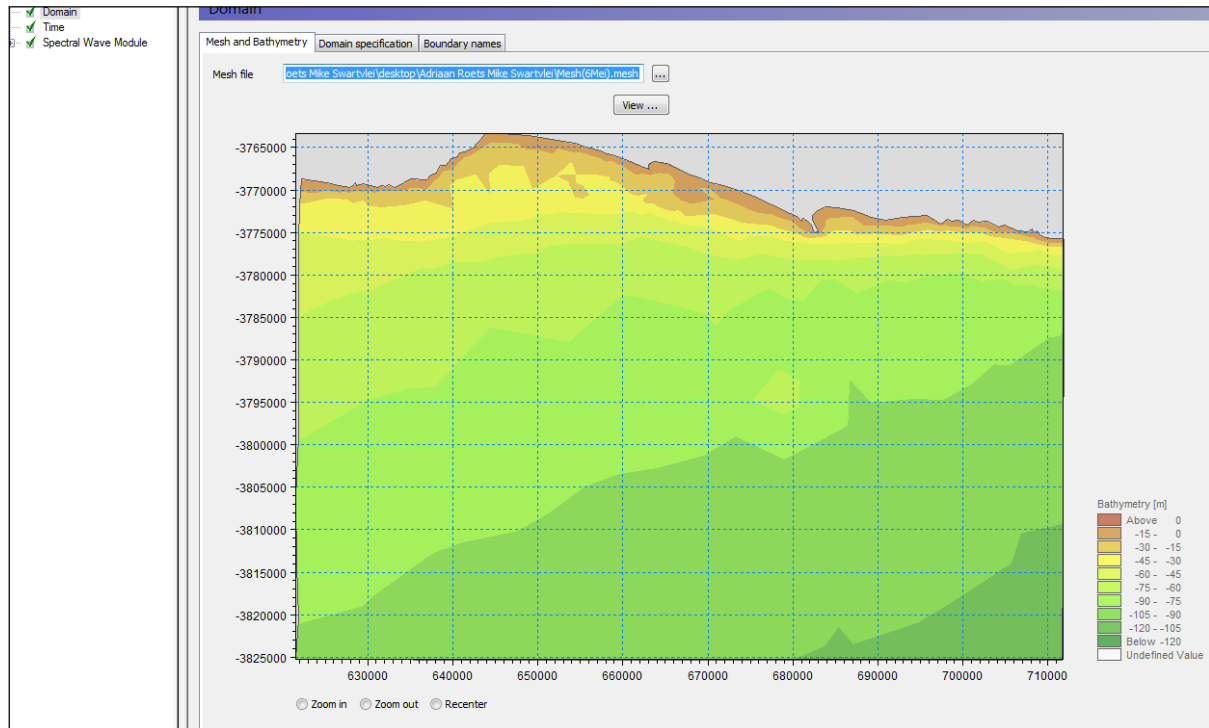


Figure 76: Insertion of domain bathymetry file

**Time**

For the MIKE 21 SW model to run successfully, the NCEP hindcast data had to be calibrated with the model time steps. The NCEP data was recorded for one year (2009) beginning on 2009/01/01 at 02h00 AM and ended on 2009/12/31 11h00 PM. This data set was recorded every three hours, which meant that the number of steps for the numerical model would be 2919 at 10 800 second intervals (every three hours), thus simulating the hindcast data time steps. These simulation parameters are illustrated in Figure 77.

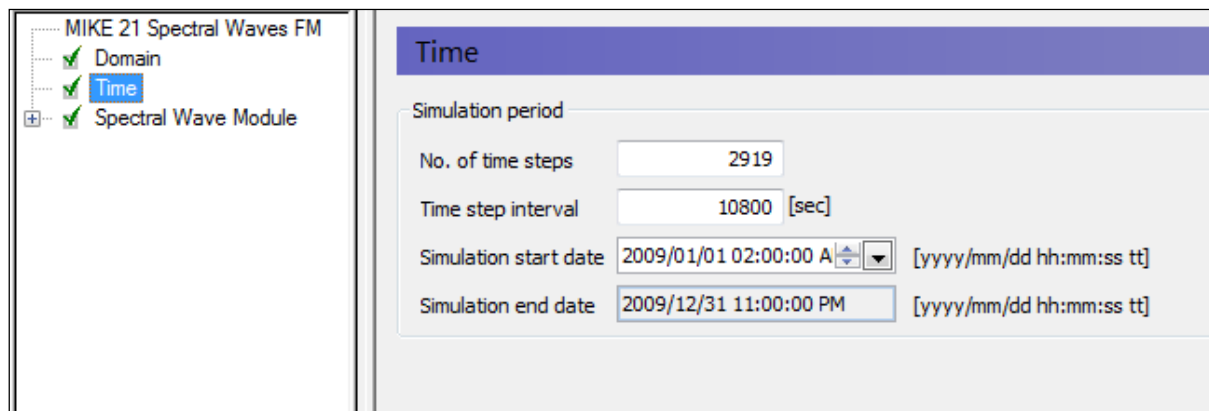


Figure 77: Model time definition

The simulation always starts with time step number zero and this simulation start date is the time step corresponding to time step zero of the NCEP hind cast data. The simulation end

date is presented as reference and is automatically calculated by MIKE according to the input values.

### ***Spectral wave parameters***

This section of the MIKE 21 SW model is sub-divided into the following categories:

- Basic equations
- Spectral discretization
- Solution technique
- Water level conditions
- Current conditions
- Wind forcing
- Ice coverage
- Diffraction
- Energy transfer
- Wave breaking
- Bottom friction
- White capping
- Structures
- Initial conditions

#### *Basic equations*

The spectral wave module includes two different formulations:

1. Directional decoupled parametric formulation
2. Fully spectral formulation

The directional decoupled parametric formulation is based on a parameterisation of the wave action conservation equation. Following Holthuijsen *et al.* (1989) the parameterisation is made in the frequency domain by introducing the initial and first moment of the wave action spectrum as dependent variables (DHI, 2011).

The fully spectral formulation is based on the wave action conservation equation as described in Komen (1994) and Young (1999), where the directional frequency wave action spectrum is the dependent variable (DHI, 2011).

For the simulation of the defined domain, a fully spectral formulation was selected for a more in-depth and defined simulation.

The basic equations parameter also includes a time formulation which is divided into two options:

1. Quasi-stationary
2. In-stationary

In the quasi-stationary option, the time is removed as an independent variable and a steady state solution is calculated at each time step. The quasi-stationary formulations are less demanding on the computational aspects, but for this study the in-stationary formulations were used (DHI, 2011).

The integration through time is based on a fractional step approach. First, a propagation step is performed, calculating an approximate solution at the new time level by solving the basic conservation equations without the source function. Secondly, a source function step is performed, calculating the new solution from the estimated solution, taking into account only the effect of the source functions (DHI, 2011).

#### *Spectral discretisation*

The dependent variable in the spectral mode is the directional-frequency wave action spectrum at each node point. The discrete frequencies and directions used to resolve the wave action spectrum are defined in this section (DHI, 2011).

For the frequency distribution there are two types, namely: logarithmic and equidistant distributions. It is recommended by DHI to always use the logarithmic distribution, which is given by:

$$f_n = f_0 c^n, n=1, 2 \dots$$

where  $f_n$  is the frequency,  $f_0$  the minimum frequency and  $c$  the frequency factor.

For this numerical model of Swartvlei, a logarithmic frequency was selected with parameters as follows:

- Number of frequencies = 25
- Minimum frequency = 0.055 hz

- Frequency factor 1.1

These were all standard values recommended by the MIKE software package. For the directional discretisation a 360 degree rose was selected because of the varying wind, waves and swell. Furthermore, the number of direction bins was defined as 16, this incorporated all possible directions. It is, however, recommended that the direction bins should be refined, but for this study with the lack of bathymetrical data available it was deemed unnecessary to model on a more sensitive interval for the directional bins in relation to the coarse bathymetric data. No separation was selected for the separation between wind, sea and swell waves.

#### *Solution technique*

The discretisation in geographical and spectral space is performed using a cell-centred finite volume method. In the geographical domain an unstructured mesh is used. The special domain is discretised by the subdivision of the continuum into non-overlapping elements. The convective fluxes are calculated using a first order up-winding scheme (DHI, 2011).

For the calculation required for the Swartvlei half-heart bay numerical model, a low order fast algorithm was selected with standard values for 'maximum number of levels in transport calculation', 'number of steps in source calculation', 'minimum time step' and 'maximum time step'.

#### *Water level selection*

A constant still-water level was applied over the entire domain. This level was taken as equal to the mean sea level.

#### *Current conditions*

No current data could be obtained for the preliminary numerical analysis of the Swartvlei bay area, thus no current variation was selected for this section.

#### *Wind forcing*

Using the historical NCEP data, the wind forcing was specified as wind speed and direction. The format of the NCEP data was further defined as varying in time but constant in domain. It should be noted that that using this offshore NCEP data set would result in an estimate of wind forcing close to the shoreline.

For MIKE to accept this format, a data file was loaded containing wind speed (m/s) and direction (in degrees from true North). This file was in a time series (.dfs0) format. It was also important to ensure that the input data file covered the complete simulation period. The time

step of the input data file does not, however, have to be the same as the time step of the spectral wave simulation. The difference in time step was overcome by linear interpolation.

#### *Ice coverage*

Ice cover is not applicable to the intended study area.

#### *Diffraction*

A limitation of the MIKE 21 SW model is that it does not permit coherent wave fields in the computational domain and subsequently cannot correctly model diffraction. However, directional spreading was applied in the wave direction data set that would result in energy transfer behind the headland, resulting in an elementary representation of the diffraction phenomena. The directions would not be as reliable as the results from a Boussinesq type model. By applying directional spreading, wave energy would be applied behind the headland and accuracy would improve moving along the headland bay.

#### *Energy transfer*

The non-linear energy transfer among wave components of the directional-frequency spectrum plays a crucial role for the temporal and spatial evolution of a wave field (DHI, 2011).

Quadruplet-wave interaction was selected for this scenario and is described by the DHI manual on spectral wave analysis as follows:

The quadruplet-wave interaction controls

- The shape-stabilisation of the high frequency part of the spectrum
- The downshift of energy to lower frequencies
- Frequency-dependent redistribution of directional distribution functions

The quadruplet-wave interaction in the spectral wave model is described by the accepted approximate, Discrete Interaction Approximate (DIA) (DHI, 2011).

#### *Wave breaking*

Depth induced wave breaking is the process by which waves dissipate energy when the waves are too high to be supported by the water depth i.e. reach a limit of wave height/depth ratio.

The formulation used in the spectral wave model is based on the formulation of Battjes and Janssen (1978). This model has been used successfully in the past in fully spectral models as well as in parameterised versions (DHI, 2011).

The model selected for this section was Specified Gamma and the Gamma data format was specified as 'constant' with a value of 0.8.

To ensure that these recommended values were site specific, *equation II-4-5* and *Figure II-4-2* from CEM (2006) were used to assess the site specific range of the gamma value ( $\gamma_b$ ). The equation used was:

$$\gamma_b = b - a * \frac{H_b}{gT^2}$$

Applying the site condition parameters, a breaking index range of 0.752–0.789 was calculated. Applying the same parameters to *Figure II-4-2*, CEM (2006), results in a breaking index range of 0.78-0.85 as a function of the breaking wave height, specific gravity and the wave period.

The alpha value controls the rate of dissipation and is a proportional factor of the wave breaking source function. A default value of 1 was selected for this model.

#### *Bottom friction*

As the waves propagate into shallow water, the orbital wave velocities penetrate the water depth and the source function due to wave-bottom interaction becomes important. The dissipation source function used in the spectral wave module is based on the quadratic friction law and linear wave kinematic theory. The dissipation coefficient proportionally depends on the hydrodynamic and sediment conditions as described in (DHI, 2011).

Nikuradse roughness was selected and assigned a constant value of 0.04 m. This is the corresponding value to use when using offshore data.

#### *White Capping*

White capping is primarily controlled by the steepness of the waves. The breaking wave dissipation source function is described in detail in Komen *et al.* (1994) and includes two free parameters-  $C_{dis}$  and  $\Delta_{dis}$  (DHI, 2011).

White capping was included in this model and values for  $C_{dis}$  and  $\Delta_{dis}$  were assumed as 4.5 and 0.5 respectively. These values were again specified by the MIKE software and user's manual.

#### *Structures*

No structures are present in the model area.

#### *Initial conditions*

For this model a zero spectra was selected and wave action was set to zero at all node points.

#### *Boundary conditions*

As previously discussed in 'boundary conditions', certain boundary codes were assigned to the model. The set-up editor scans the mesh file for these boundary codes and displays the recognised codes with their default names. Referring to Figure 65, the colour boundary conditions are indicated; yellow indicates land, blue and red indicate closed boundaries and green indicates open boundaries.

By selecting the wave parameters (Version 1) on the green boundary, a parametric representation of the spectral distribution was used and the following parameters were supplied to the model:

- Significant wave height,  $H_{m0}$ (m)
- Spectral peak period,  $T_p$ (s)
- Mean wave direction, MWD (deg)

The above mentioned parameters were all obtained from the available NCEP hindcast data and standard values for auxiliary inputs as defined by (DHI, 2011).

## 7. HYPOTHESIS

From the literature presented in Chapter 2 and the application of this literature to the Swartvlei bay itself in Chapter 3, it is seen that Swartvlei fits the criteria for a typical headland bay. Using this theory, the hypothesis will attempt to describe the present scenario with specific emphasis on the present bulk sediment regime at the estuary mouth. This will be done as accurately as possible with the available data.

Headland bays similar to that of the Swartvlei coastline are expected to be sensitive to changes in wave climates and wind directions. These wave climates, accompanied by their incident angles, are the main drivers of sediment inside the bay. By following the fundamental principles set out by Hsu (2010) on spiral shaped bays and Hsu & Evans (1989) on the methods of parabolic bay shaped equations and applying them in mathematical models, as presented in Chapter 3, a basic understanding can be formed on the ideal or planform shape of the Swartvlei coastline. Using literature presented by Mather, (2008), Figure 78 represents the theoretical scenario for headland bay beaches with soft coastlines. Assuming only a theoretical approach in the initial definition of a typical headland whereby, it also warranted the defining of the theoretical planform by means of an auxiliary mathematical approach. The mathematical approach, as described in section 3.9, verified the theoretical shape of the Swartvlei bay. The green equilibrium shoreline profile as illustrated in Figure 78, is the theoretical shape, based on bay shape and orientation literature, of a typical headland bay.

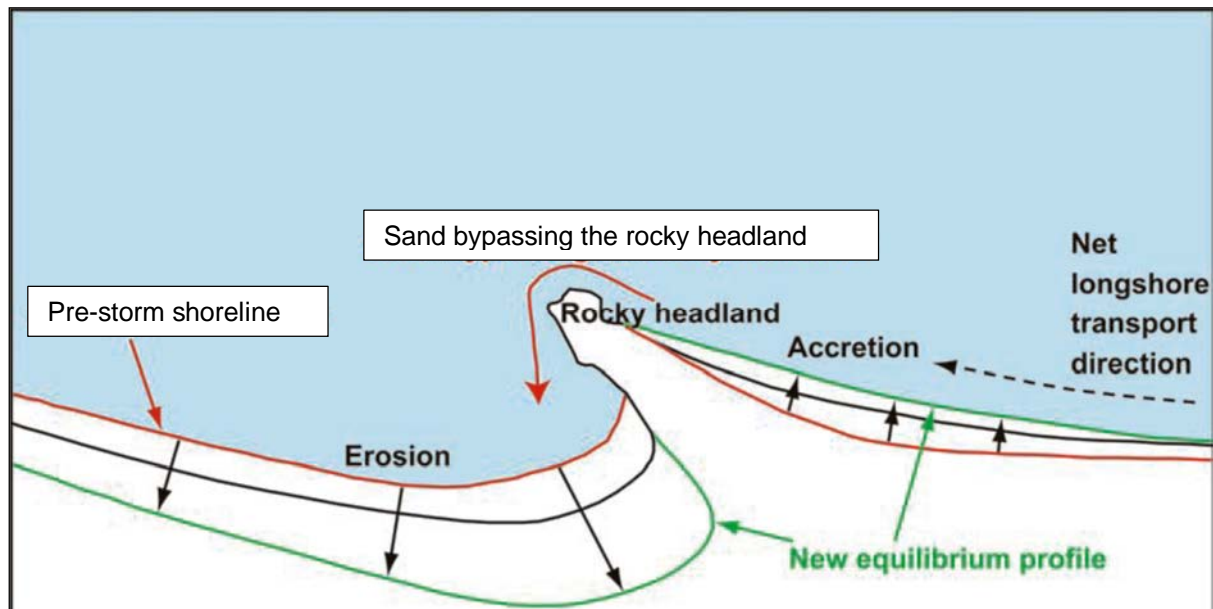
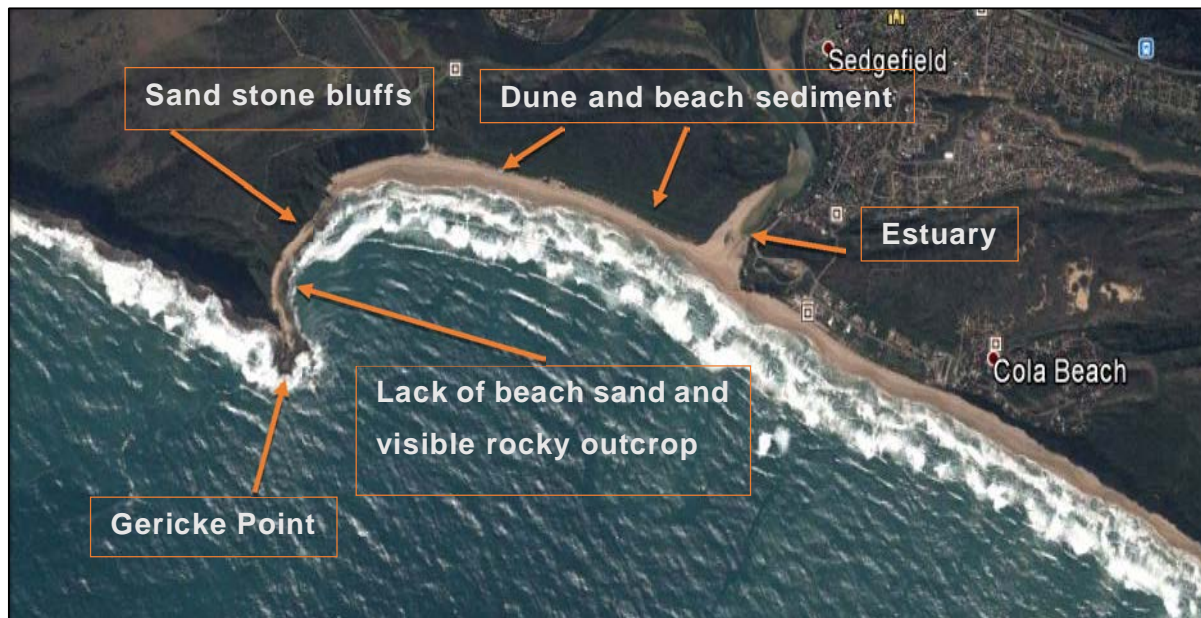


Figure 78: Hypothetical equilibrium shoreline profile (Green) of a typical headland bay coastline under soft sediment conditions (Mather, 2008)

From the available NCEP data, combined with VOS data, the dominant offshore incident wave direction for the Swartvlei bay area is south-westerly (NCEP, 2011). Combining this with a predominantly south westerly wind direction (CSIR, 1983), a basic understanding of the dominant metocean conditions can be formed. Refer to section 3.4 for a full description of the climate conditions present at Swartvlei.



*Figure 79: Orientation map for the Swartvlei bay*

Starting at Gericke Point, the western boundary of the Swartvlei bay area, this headland is acting as a permanent immovable barrier to the main longshore transport. For this study the main and dominant longshore transport regime is from west to east, driven by the dominant wave and wind climates. This estimate is based on the available wave and wind data (NCEP, 2011; CSIR, 1983). The headland creates a sheltered bay in its lee and as the waves approach from a south westerly direction, they diffract around Gericke Point and enter the sheltered bay at a lower wave height than the waves on the open, unsheltered coastline. The result is a return current generated by a difference in wave set-up.

However, due to the lack of visible accretion observed from historical imagery, there is no evidence to suggest that this return current is dominant and that it is depositing sediment in the lee of the headland. Although sediment is possibly entering this sheltered region from around Gericke Point, the protruding rocky shoreline is hard and provides a steep slope which result in the conclusion that sediment is not actively settling in sufficient quantities in the lee of the headland for significant beach accretion to occur. The visible lack of beach sediment in Figure 79, and the imagery of the rocky shoreline present in the sheltered bay (Figure 80), originating from the on-site survey, support this conclusion.

The assumption of dominant west to east longshore transport scenario is supported by the above mentioned estimations. These observations and estimates are based purely on available data and further in-depth studies are recommended to support these estimations.



*Figure 80: Rocky shoreline immediately east of Gericke Point*

As already illustrated in Figure 80, the shoreline near Gericke Point is predominantly rocky and, as a result of this, the beach profile has reached a premature state of equilibrium. In comparing the calculated equilibrium planform of Swartvlei Bay originating from the PBSE and the relevant literature by Hsu & Evans (1989) and Mather (2008), with the current actual coastline, presented in Figure 81, it is evident that the coastline area is not behaving according to the theoretical scenario expected from a soft coastline in the lee of a headland. The natural erosion set to take place behind the headland has been counteracted to an extent by the presence of rocky outcrops rather than the soft sand as set out in the ideal theoretical scenario.

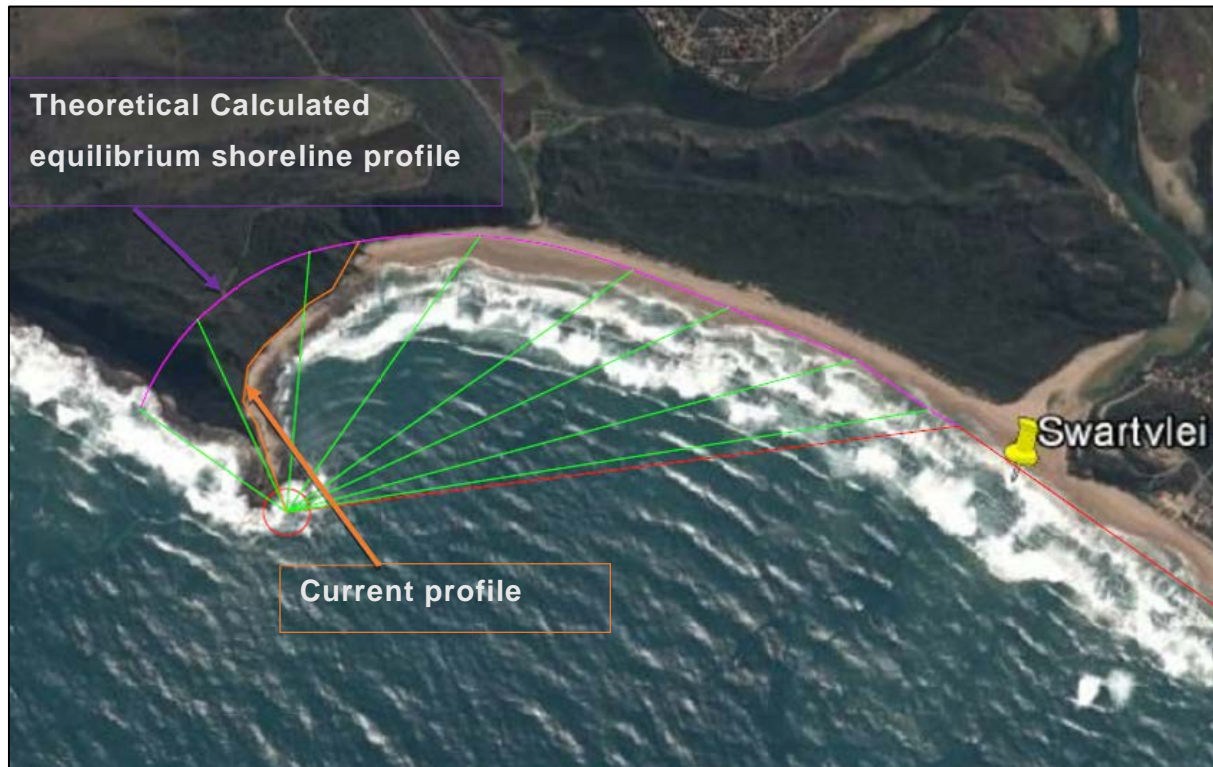


Figure 81: Current beach profile compared with a mathematical PBSE of Gericke Point

The theoretical equilibrium shoreline scenario illustrated in Figure 81, would be applicable in this case if the headland consisted of erodible material. However, the rocky shoreline on the inside of Gericke Point is preventing further retreat of the beach profile, resulting in a narrow beach fronted by a rocky shoreline.

The impenetrable rocky shore has created a hard flat surface for wave run-up to reach the sandy cliffs at the back of the narrow beach. The cliffs are slowly being undermined and thus slumping is occurring. See Figure 82 and refer to the relevant literature on dune slumping and erosion presented in Chapter 2.

*Slumping* is a term used to describe the phenomenon where the toe or foundation of a dune or cliff is eroded away and, as a result of this, the dune face collapses in order to re-stabilise itself.



*Figure 82: Erosion of sand cliffs at Gericke Point*

Moving east along the Swartvlei beach, away from Gericke Point and past the parking area onto the straight beach, the sandstone bluffs give way to more gently sloped beaches with steep dunes at the back. The tapering of the sand stone bluff into dunes is illustrated in Figure 83.



*Figure 83: Tapering of the cliffs into steep dunes*

These steep dunes are fronted by notably more gently sloped beaches with beach widths varying from 150 m to 200 m during low water, as observed and measured during the on-site investigation. This section of soft coastline is identified as a major sand source for the sediment budget defined at the estuary mouth area. From the available historical Google imagery (Figure 79 and Figure 81), it is seen that sediment is settling in this area east of Gericke Point. From a first inspection it is estimated that the bulk longshore transport regime will start to assume the dominant west to east direction, as well as gradually increase from this area onwards towards the east. It is estimated that the majority of longshore sediment transport destined for the budget boundaries at the estuary mouth, comes from the dunes and beach sections along the Swartvlei beach coastline. These sections acting as a sediment source for the longshore transport regime along the coastline are kept in dynamic equilibrium by the following identified sediment supplying processes:

- Slumping of the sandstone bluffs in the lee of Gericke Point, which feeds the dominant west to east longshore sediment transport regime.
- Aeolian transport from west to east over the headland and along the Swartvlei coastline
- Cross shore transport from incident wave climates in the sheltered bay
- Longshore transport around Gericke point by the predominant eastward transport along the southern coastline of South Africa.
- Historical sediment sources



*Figure 84: Swartvlei Estuary in 1936, showing two historical sediment sources (CSIR, 1983)*

As seen in Figure 84, two dominant historical sediment source zones were present along the Swartvlei coastline. With the ingress of vegetation and human developments, these areas have either been overgrown or developed as property. However, these areas are still adjudged to supplement beach sediment by means of slumping and the retreat of vegetation caused by marine processes and aeolian influences. The eastern historical sediment source has been developed into residential areas. This development within the coastal processes set back area has led to the restriction of sediment contributions towards the eastern beaches.

The stretch of coastline from Gericke Point towards the estuary mouth is illustrated in Figure 85.



*Figure 85: Dunes and beach profile leading up to the estuary mouth*

Moving east along the Swartvlei coastline (see Figure 79) the Swartvlei estuary mouth is located. Investigation into the estuary channel data set out in Chapter 5 shows that there is a distinct migration of a deeper channel towards the western side of the estuary mouth. This most probably is an effect of storm floods initiating channel migration.



*Figure 86: Deep channel near west bank of estuary*

Although this deeper channel is not directly connected to the marine environment, it is deep enough and close enough to the west bank that the dunes on the western edge of the estuary are bound to be affected by the marine and estuarine processes occurring in this area (See Figure 86). These processes include but are not limited to the following:

- Water level variation due to spring tides
- Wave action during open mouth conditions
- Influences by floods on water level and velocity

The evidence presented, gathered from the available data, has led to the assumption that the western bank of the estuary is a major contributor of sediment, from an estuarine point of view, towards the sediment budget at the estuary mouth. For this study, slumping and erosion from seasonal floods and tidal pulses, as previously defined in the literature, has been identified as the main catalyst for the contributions from this western sandbank.

As previously stated, the channel on the western edge of the estuary is the main platform leading to dune slumping and erosion defined for this area. From Figure 87, dune slumping has been identified along the western edge of the estuary.

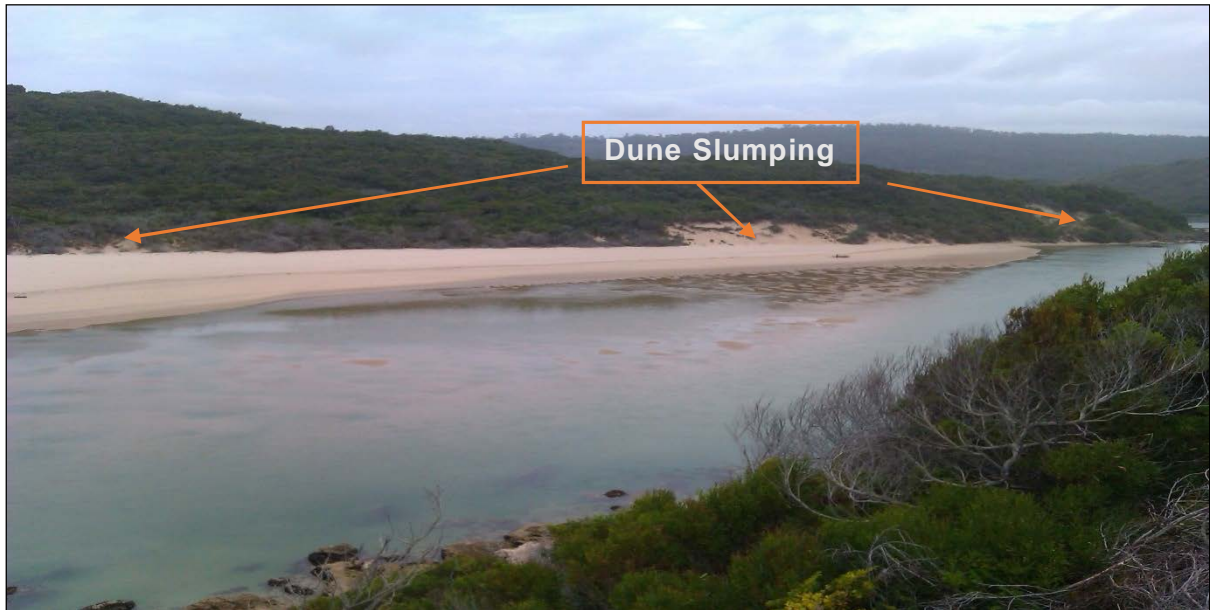


*Figure 87: Western bank of estuary with slumping present*

An historical approach was followed in an attempt to estimate the contribution from the dunes on the side of the estuary and more specifically the contribution of the dune slumping and erosion occurring along the western bank of the estuary.

Historical imagery, obtained from Google Earth, was used to define the vegetation line in and around the estuary mouth. The available historical imagery depicted years 2003, 2004, 2006, 2010 and 2013. The result of the vegetation line migration, as well as the area identified for possible dune slumping contributions along the western edge of the estuary, is illustrated in the Figure 88.



*Figure 88: Historical vegetation lines with defined area for contribution from the estuary*

Although this approach is elementary and is influenced by technical issues such as the inaccuracy of Google historical representations and the influence of tides on imagery, it indicates a distinct chronological pattern in vegetation migration. It was found from historical imagery that the vegetation is relatively constant in years 2003 to 2006, with an average estimated yearly retreat of 1 m - 2 m. This range was calculated from studying available historical imagery.

From 2006 towards 2010 and 2013 there is a distinct retreat of the vegetation line. This is partly due to estuarine and marine processes, but also due to the major floods that occurred in 2007. The flood washed away significant amounts of peripheral estuary vegetation, subsequently transporting vast amounts of sediment out to sea.

From a contour map (Attached in Appendix 4) published by the Chief Directorate of Surveys and Mapping for the Government of South Africa, the heights of the vegetated dunes on the western bank vary from 16 m (at the northern end of the sandbank) to 4 m (at the estuary mouth).

Combining the topographic surface into a volumetric AutoCAD simulation and applying the historical vegetation line migration of 1 m -2 m, an estimated contribution of 30-40 m<sup>3</sup>/yr. per meter was calculated for dune slumping and erosion along this defined western sand bank. For calculation purposes the effects surrounding the 2007 severe flooding period will not be considered. The influence of sediment pulses resulting from seasonal floods over this sand bank and in the main estuary channel itself will, however, be factored in for the estimation of the preliminary sediment budget.

Furthermore, referring to Chapter 3.6, where the Swartvlei estuary mouth is defined as being dominated by marine sediments; Figure 89 is used to present evidence that the area of the sand bank situated at the mouth of the estuary is absorbing sediment and dominated by marine processes. From the available historical imagery it is seen that the sand bank is protruding into the estuary itself.

The lack of flushing or scouring potential, as a result of agricultural and residential abstractions combined with the dominant wave and wind climates and other marine processes results in a sediment absorbing characteristic by the estuary mouth. With reference to Figure 51, the summary of the beach profile survey, there is a distinct indication that the beach profiles east of the estuary are shorter and steeper than the profiles west of the estuary, with clear indications of erosion. The beach sections west of the estuary mouth are characterized by a rocky outcrop which inhibits mouth migration. The rocky outcrop descends into sand dunes and finally into large sand bluffs further west. As the survey profiles illustrate narrow, steep beach profiles with an almost non-existent hummock dune zone, wave run up and sediment retention by the estuary tend to limit the visible accretion along these beaches. Combining this observation with the available evidence presented throughout this section, along with the sand grain analysis, the consensus is that the estuary mouth is acting as a sink towards the transported marine sediment. Although this is possibly not a natural aspect of the estuary itself, this sediment absorption characteristic has feasibly been induced by human interference in combination with the dominant marine processes. However, human management of the estuary mouth, combined with significant flooding e.g. the 2007 floods and the seasonal run-off, regulate the estuary mouth to ensure frequent open mouth occurrences and flushing needed to redistribute accumulated sediment.

## A Preliminary Analysis of the Sediment Budget Across the Swartvlei Estuary Mouth

The geotechnical scenario presented in this study is subject to the data available supplemented with a basic grain analysis of sediment in the area (see Chapter 5). Further in-depth geotechnical studies are recommended to provide a better understanding surrounding the geotechnical characteristics present at the estuary mouth.



*Figure 89: Historical mouth imagery and sand bank growth*

To the east, as previously mentioned the estuary mouth is bordered by a dune rock formation preventing the migration of the estuary mouth in an easterly direction. The geotechnical characteristics of this rock formation has been verified by studies done by CSIR (1983).

## A Preliminary Analysis of the Sediment Budget Across the Swartvlei Estuary Mouth

rainfalls that initiate a rise in water levels and result in the scouring of a channel through the on-shore sand berm. This results in open mouth conditions, mainly during the spring and early summer months.

Using Table 4 in Chapter 3.8, the mouth conditions are illustrated according to published SANParks data (EWISA, 2003). Combining this data with the surveyed data from SANParks (2012), for river profiles close to the estuary mouth (see Figure 61), a hypothesis can be formed around typical trends of the channels and mouth dynamics.

The profiles presented below were statistically analysed in Microsoft Excel and are plotted from east to west. The starting point or axis origin is a fixed survey position on the east bank of the estuary obtained from SANPark records. The profiles are illustrated in a downstream direction and levels are relative to MSL and SANParks measuring techniques. Refer to Figure 61 for the graphical location of each profile.

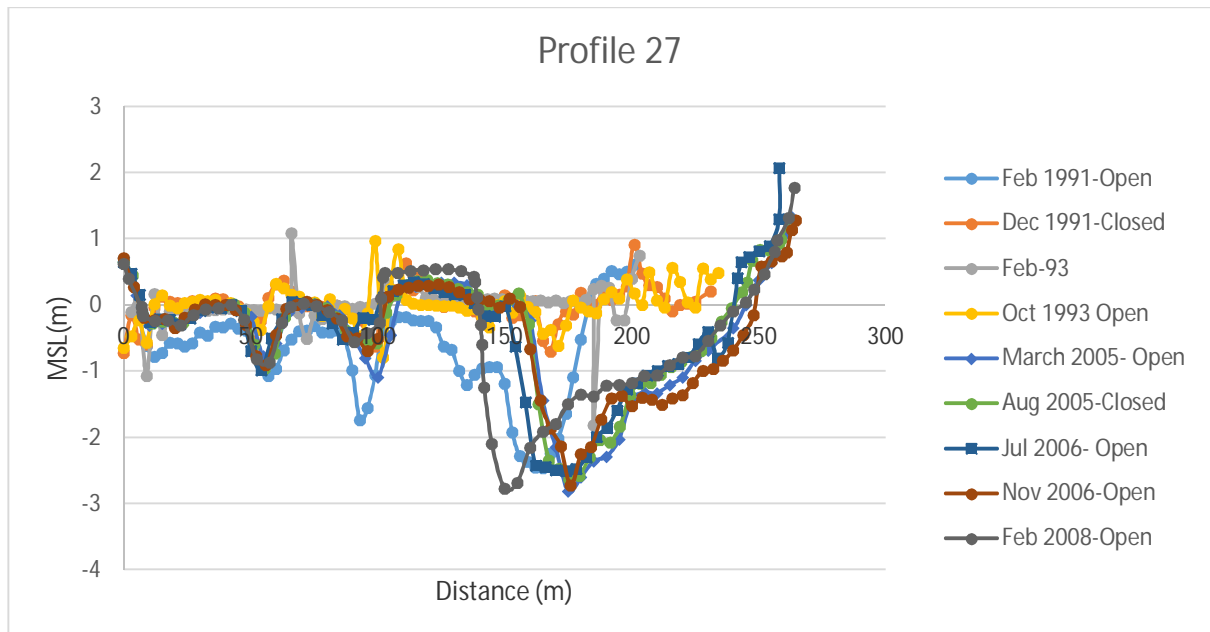




*Figure 90: Dune rock present on the eastern bank of the estuary mouth*

Combining the vegetation line migration illustrated in Figure 88 with the visible dramatic erosion of the beach sections along the eastern side of the estuary, it is estimated that the eastern beaches are retreating more dramatically than the beaches west of the estuary. The beach sections to the west, although vegetated, have minimal impact from human development as regards the historical sediment sources available (see Figure 84). The eastern beaches, however, have been developed and stabilised for property development and as a result a limited supply of sediment is available. Continuing with the dominant west to east longshore transport regime along the Swartvlei coastline, it is expected that the longshore sediment transport regime on the eastern side of the estuary mouth should increase in comparison to that of the upstream, or the western side of the estuary. From on-site investigations and available historical imagery, it is seen that erosion has had major effects on beaches downstream, or east of the estuary mouth (see Figure 45). Also noteworthy is the absence of a dune buffer zone here, in comparison with the coastline upstream, or west of the estuary mouth (see Figure 43). Figure 54 illustrates the absence of this dune buffer zone on the beaches east of the estuary mouth.

This leads to the conclusion that although sediment is entering the estuary mouth area along the longshore current, originating from Gericke point and the soft coastline to the west, it is not exiting in sufficient quantities from the estuary mouth to supplement the sediment demand of the beaches east of the mouth. Again, this can be ascribed to the dominance of marine processes relative to the natural estuarine processes at the estuary, resulting in predominant periodical absorption of sediment by the estuary mouth until a major flood or human estuary mouth management intervenes.

The various possible contributors of sediment towards the preliminary budget boundaries (Figure 91) from Gericke Point to the west, and moving in an easterly direction towards the estuary mouth, are as follows:

- Longshore transport consisting of contributors such as
  - Slumping and erosion of sandstone bluffs in the lee of Gericke Point
  - Accumulated beach sand from dunes and beach material along the Swartvlei coastline (in the section east of Gericke point and west of the estuary mouth)
  - Possible aeolian contributions
- Contributions from the estuary
  - Dune slumping and erosion, flooding, marine processes.

The basic processes that act as catalysts for these identified contributions towards the area are discussed in detail in the literature study. It is estimated that the longshore sediment transport regime will tend to increase from its origin, in the lee of Gericke Point, towards the estuary mouth, until it stabilises along the straight coastline of the half-heart bay.

The initial sediment budget boundaries were defined as follows in Figure 91:



Figure 91: Initial definition of sediment budget boundary



Figure 92: Illustration of theoretical sediment contributors along the Swartvlei coastline

Represented in Figure 92 are the dominant theoretical pathways, the magnitudes of the sediment contributors, as well as the sediment transport regime, obtained from available data and literature. The symbols mean the following:

- T1- Erosion of sandstone bluffs in the lee of Gericke Point
- T2- Dominant west to east longshore sediment transport regime. The transport is expected to originate in the lee of Gericke Point and gradually increase until it stabilises along the coastline
- T3- Dune and beach sediment contributing towards the longshore transport
- T4- Contributions from the western banks of the estuary
- T5- Minor contribution from the estuary
- T6- Aeolian transport along the beach above the high water line.

Referring to Figure 92, it is estimated that as a result of the diffraction of waves around the point, a small amount of sediment travels in a reverse direction. As previously discussed, this sediment is driven by a current in the reverse direction induced by a difference in wave-set up and, alternatively, a less dominant south-easterly wave climate. The effect is, however, not significant due to the lack of visible accretion on a predominantly rocky, steep coastline in the lee of Gericke Point. Moving from west to east along the Swartvlei beach coastline, away from the headland, the bulk longshore sediment transport regime is hypothesised to increase away from Gericke Point and the sheltered waters around it. This is due to the fact that dominant south westerly waves are entering the unprotected coastline east of Gericke point at an oblique angle and generating an alongshore current. This observation has been verified by an historical Google imagery representation of wave angles entering the Swartvlei bay, combined with the data sets presented, from NCEP and CSIR. The results of the historical incident wave angle comparison are attached in Appendix 9.

The dunes to the west of the Swartvlei estuary mouth along the coastline, in the regions between the Gericke Point parking area and the western side of the estuary, are considered to be the main contributors towards the longshore sediment budget. Dune slumping and erosion in and around the estuary mouth will need to be quantified by estimating the amount of retreat per year along the defined section specified in Figure 88 (circled in orange), as this has been identified as the main contributor coming from the estuary. Aeolian transport in and around the budget boundaries will be estimated and presented as part of the sediment budget.

Through the incorporation of all the available data and the literature presented, it is now possible to preliminarily refine a sediment contribution scenario to represent the theoretical

sediment budget at the Swartvlei estuary mouth. Presented in Figure 93 is the preliminary sediment budget scenario as described through this hypothesis.



*Figure 93: Preliminary sediment budget across the Swartvlei estuary mouth*

Figure 93 describes the hypothesised sediment budget scenario present at the Swartvlei estuary mouth. The contributors are as follows:

- S1- Estuary supply
- S2- Dominant west to east longshore transport, through the western boundary
- S3- Dominant west to east longshore transport, through the eastern boundary
- S4- Dune slumping and erosion along the western sandbank in the estuary
- S5- Onshore and offshore tidal and marine influences
- S6- Aeolian transport from west to east, through the western boundary
- S7- Aeolian transport from east to west, through the eastern boundary

As a result of the dynamic processes occurring at the Swartvlei estuary mouth, described in Chapter 3, the net effect of the scenario described in Figure 93 is the tendency towards the periodical seasonal closure of the estuary mouth due to marine sediment deposits in the mouth area. As a result of low lying property development along the estuary banks (which requires the artificial breaching of the mouth), civil structures (railway bridge) and water abstraction

from the catchment areas, the natural balance between the processes controlling the mouth dynamics has been significantly influenced. Seasonal water level elevations resulting from the delayed effect of winter rainfall and occasional floods, combined with the artificially opening of the mouth when the sand bar level and estuary water level are optimum, results in a scour channel that flushes away the raised sand bar level until the estuary is once again able to achieve and maintain open mouth conditions. The process then repeats itself until it reaches a closed mouth condition and management is once again needed. The estuary, left to itself, would possibly be able to achieve an open mouth condition, but the raised water levels required for this would cause flood damage to the residential developments on the shores of the Swartvlei estuary. Refer to Figure 36 for an example of an artificial mouth opening.

An estimated sediment budget scenario has been formed in this hypothesis by means of incorporating available data obtained from historical data and theoretical assumptions based on literature. By means of a MIKE 21 SW numerical model, the Kamphuis formula for bulk longshore transport, Kamphuis (2010), and available data, an attempt will be made to replicate this theoretical hypothesis with actual bulk quantities.

However, to fully understand and accurately predict a sediment budget around the Swartvlei estuary mouth, additional in-depth studies are recommended. The results of this research paper will thus be only a preliminary attempt to estimate and predict the general sediment transport parameters and characteristics in and around the Swartvlei estuary mouth.

## 8. RESULTS

### 8.1 MIKE 21 SW OUTPUT

As previously stated, the MIKE 21 SW numerical model applied for the estimation of the wave climate in the Swartvlei bay area is based on the available NCEP hind cast data and SANHO bathymetric charts.

Using the MIKE 21 generated bathymetric chart, the contours for the 2 m, 4 m, 6 m and 8 m depths were interpolated, using bathymetric scatter data in an attempt to simulate the near shore bathymetry. As discussed in Chapter 6, the scatter data used as input for bathymetric generation was a digitised SANHO bathymetric chart. As a result of the lack of bathymetric data available for the near shore area, the simulated values are to be considered as only approximates and detailed numerical studies are recommended. The colour pins indicating the different depth contours are represented in Figure 94:

- 2 m – Blue
- 4 m – Yellow
- 6 m – Turquoise
- 8 m – Green

Figure 94 indicates the nine defined sediment transport profiles along the coastline.

A Preliminary Analysis of the Sediment Budget Across the Swartvlei Estuary Mouth



Figure 94: Illustration of MIKE 21 SW output locations, the orange numbered transport profiles comprising the individual output points which are also indicated

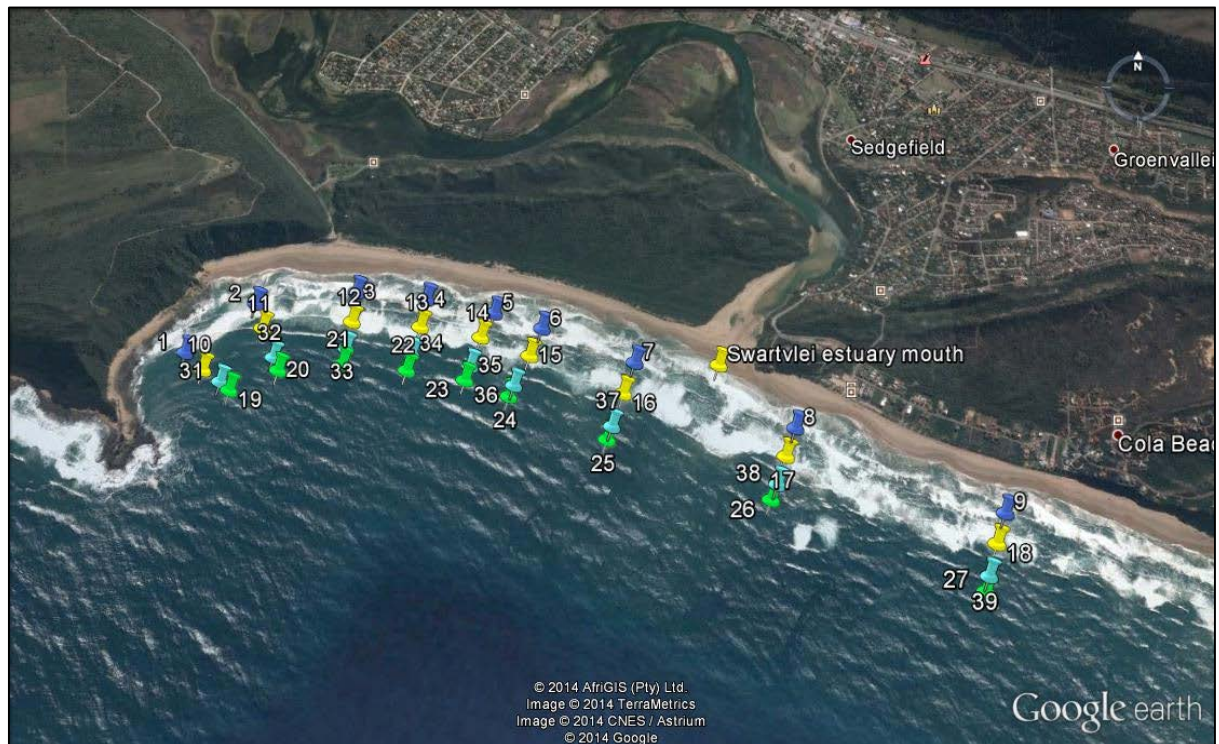


Figure 95: Individual MIKE 21 SW output points

Following the methodology set out in Chapter 4, a MIKE 21 SW numerical simulation of the wave height, wave direction and peak wave period at each point was completed. These points were selected to represent the near shore area, as well as the surf zone.

From the numerical model with input parameters as discussed in Chapter 6, results were obtained for each of the individual points, numbered 1-39, indicated in Figure 95. The coordinates of the output locations are attached in Appendix 10. Referring to the numerical model set-up, also described in Chapter 6, the offshore wave climate was simulated from the NCEP location into the Swartvlei bay area. From there, with a fine triangular mesh, the incident waves were simulated into the bay with the interpolated bathymetry from the available SANHO data. Upon completion of the numerical model, information on the wave climate for each individual output point (Figure 95) became available and the percentage of the year that each point represents a breaking wave at that depth was derived.

As a result of the sparse data available for in-depth near shore numerical wave modelling, the MIKE 21 SW output data was used as part of a statistical UNIBEST-type approach. The statistical approach was used to quantify the bulk longshore transport at breaking condition for the various individual points which, combined with the percentage occurrence of breaking at that point resulted in a total transport per year across the defined profiles as depicted in Figure 94.

The statistical approach was applied along each of the nine profiles, as illustrated in Figure 94. For each MIKE 21 SW output point along these profiles, the wave height, wave direction and peak wave period were analysed for the entire data set of 2009. Each output point corresponds to a certain depth e.g. 2 m, 4 m, 6 m and 8 m. Using a conservative approach, based on literature from CEM (2008), the theoretical breaking height of waves at that point was calculated using the formula below:

$$H_b = 0.6 * D_b$$

where,

$H_b$  = Wave height at breaking

$D_b$  = Depth at breaking

*Table 13: Theoretical height of breaking wave to corresponding depths*

$D_b$ (m)	$H_b$ (m)
2	1.2
4	2.4
6	3.6
8	4.8

The theoretical breaking wave heights for the corresponding depth values were used to create minimum criteria for wave breaking and, in turn, for sediment transport. At each point the wave height data set was used to sample for wave height conditions above the theoretical breaking wave height, to obtain the number of breaking waves and their attributes. If an incoming wave was thus larger than the minimum theoretical breaking wave height calculated for that point (Table 13), sediment transport would occur from that point towards the shore.

A cumulative approach was applied along each of the nine profiles (refer Figure 94 for profile definition). Corresponding with the nine hour interval for every interim data capture from the MIKE 21 SW model, the number of steps would be 973 at each point. Applying a cumulative wave analysis to the data set would result in 100% of waves breaking when the shoreline (0 m depth) was reached. Each point was then analysed to obtain the number of occurrences of a breaking wave encountered at that point. If an occurrence is encountered, it would indicate a breaking wave and thus transport from that point towards the shore.

To avoid double counting consecutive landward sections a cumulative approach was used to calculate the number of breaking wave occurrences for each section individually in relation to the entire profile, thus resulting in a 100% occurrence at the shoreline (0 m). A section was defined between two consecutive contour points along the profile. By means of this approach each section was weighted in relation to the profile sample. The advantage of this approach would be that for each defined output point there would be an analysed occurrence for breaking waves. A summary of the breaking wave occurrence for each individual point would be accompanied by an average wave direction and a corresponding peak period for this wave breaking sample.

For input into the Kamphuis equation, the breaking wave at each point, and thus for each section between consecutive contour points along a profile, was estimated to be at the

theoretical breaking wave height at that depth; see Table 13 for theoretical breaking wave heights. The number of wave breaking occurrences for each point would thus be calculated, and the breaking wave height at that depth, and across the subsequent landward section until the next output point (contour) along the individual profile, was defined as the theoretical breaking wave height. This approach would add weight to the significantly larger wave sets that result in more sediment transport, rather than an averaging approach that would give equal weight to all breaking waves encountered at that point.

The Kamphuis formula for bulk longshore transport (Kamphuis (2010)), could now be applied for each section and the sum of all these sectional transports would result in the sediment transport across a defined profile. The result of this approach was the preliminary estimation of the sediment transport regime along the Swartvlei coastline, with input from individual wave data at breaking along the defined profiles.

The limitations and conservative nature of this cumulative process are evident but, due to the lack of available data for in-depth numerical modelling, this approach was deemed the most accurate and effective method to apply for a preliminary estimation of the sediment transport regime along the Swartvlei coastline. It is thus recommended that an additional numerical study, coupled with an extensive bathymetric survey, be performed for more in-depth results.

## 8.2 Kamphuis longshore sediment transport calculations

For the calculation of the bulk longshore sediment transport rates along the Swartvlei coastline, a MIKE 21 SW model was combined with the Kamphuis formula for bulk longshore sediment transport (Kamphuis, 2010).

Referring to the literature study and Chapter 4.2, respectively, the Kamphuis formula used to calculate the yearly transport ( $Q_k$ ) in m<sup>3</sup>/year was as follows:

$$Q_k = 64000 * H_{sb}^2 T_p^{1.5} m_b^{0.75} D^{-0.25} (\sin 2\alpha_b)^{0.6} \quad (\text{m}^3/\text{yr.})$$

The significant breaking wave height and corresponding wave period were obtained for each of the individual MIKE 21 SW output locations. Using the data represented in Chapter 5.1, the beach slopes ( $m_b$ ) were estimated using the closest beach profile from the conducted survey, whereby the elevations of the two surveyed points closest to the waterline together with the depth of the appropriate, MIKE 21 SW, simulation point was divided by the total distance between the points. The two land based survey point were taken on the extremities of the shore profile, one point in the water as far as the equipment would safely allow for, and one point on the landward edge of the beach before the dune system began. Figure 96 illustrates the typical slope of the wide beaches west of the estuary mouth.



*Figure 96: Gentler beach slopes east of Gericke Point*

The slopes were found to be fairly steep lee of Gericke Point and east of the estuary mouth in comparison to the more gentle coastline west of the estuary mouth. All relevant input parameters for the Kamphuis equation are attached in Appendix 8, where a detailed bulk transport calculation breakdown for each profile is illustrated.

For the approximation of the relative median grain size, the results from the investigation by Geo-Technical laboratories in Somerset West were used.

Using the MIKE 21 SW output, the wave incidence angle at breaking was obtained for each point. For each of the MIKE 21 SW output locations, the orientation of that point relative to the coast, or shore normal orientation, was calculated using a Cartesian coordinate system with North as  $0^\circ$ . The wave incidence angle at breaking ( $\alpha_b$ ) is defined as the difference between the shore normal orientation and the wave incidence angle obtained from the MIKE numerical model.

A graphical illustration of various historical incident wave climates within Swartvlei bay are attached in Appendix 9.

By incorporating all the required parameters into the Kamphuis formula, an estimated bulk sediment transport regime along the Swartvlei coastline could be calculated. These yearly values were then weighted by the occurrence of waves breaking at that point throughout the year, according to the defined cumulative approach along each of the nine profiles. The results are tabulated in Table 14.

A Preliminary Analysis of the Sediment Budget Across the Swartvlei Estuary Mouth

Table 14: Bulk sediment transport rates for the nine profiles (Figure 94) along the area studied estimated using Kamphuis (2010)

Line	Point	Depth at breaking ( $D_b$ )	Wave height @breaking( $H_b$ ) @ $0.6^{\circ}Db$	Occurence of wave breaking between next landward point	Weight ito year	$T_p$ (s)	Alpha (Degrees)	mb	D50 (mm)	Q (m <sup>3</sup> /yr)	Q (weighted value)	Total year(m <sup>3</sup> /year)
1	1	2	1.2	355	0.365	11.1018	0.632	0.016	0.23	22461.78	8195.20	105253.25
	10	4	2.4	550	0.565	12.1328	0.879	0.016	0.23	125147.49	70741.13	
	31	6	3.6	68	0.070	12.93528	1.216	0.016	0.23	376564.08	26316.91	
	19	8	4.8	0	0							
				973	1							
2	2	2	1.2	367	0.377	11.217	0.954	0.014	0.23	26420.86	9965.52	110554.85
	11	4	2.4	534	0.549	12.3778	0.987	0.014	0.23	125062.85	68636.76	
	32	6	3.6	72	0.074	13.05768	1.764	0.014	0.23	431803.47	31952.57	
	20	8	4.8	0	0							
				973	1							
3	3	2	1.2	347	0.357	12.08688	1.098	0.012	0.23	28636.32	10212.54	140749.78
	12	4	2.4	535	0.550	12.7436	1.701	0.012	0.23	161253.26	88664.43	
	33	6	3.6	91	0.094	12.88928	2.348	0.012	0.23	447716.87	41872.80	
	21	8	4.8	0	0							
				973	1							
4	4	2	1.2	300	0.308	13.918	0.268	0.012	0.23	15197.59	4685.79	172670.77
	13	4	2.4	589	0.605	12.76569	2.480	0.012	0.23	202621.44	122655.73	
	34	6	3.6	84	0.086	12.88977	3.065	0.012	0.23	525063.77	45329.25	
	22	8	4.8	0	0							
				973	1							
5	5	2	1.2	303	0.311	11.1387	1.065	0.012	0.23	24879.54	7747.69	186807.75
	14	4	2.4	581	0.597	12.21621	2.864	0.012	0.23	206750.37	123455.25	
	35	6	3.6	88	0.090	12.8063	3.921	0.012	0.23	602328.84	54475.78	
	23	8	4.8	1	0.001	12.9324	3.993	0.012	0.23	1098537.42	1129.02	
				973	1							
6	6	2	1.2	273	0.281	11.08606	1.027	0.012	0.3	22616.18	6345.55	188212.12
	15	4	2.4	600	0.617	11.97978	2.863	0.012	0.3	187854.54	115840.42	
	36	6	3.6	96	0.099	12.7147	4.715	0.012	0.3	622308.49	61399.40	
	24	8	4.8	4	0.004	12.91721	4.663	0.012	0.3	1125459.84	4626.76	
				973	1							
7	7	2	1.2	224	0.230	11.1308	0.974	0.012	0.3	22044.93	5075.09	202808.89
	16	4	2.4	645	0.663	11.9714	2.784	0.012	0.3	184534.73	122327.75	
	37	6	3.6	96	0.099	12.7091	4.891	0.012	0.3	635600.11	62710.80	
	25	8	4.8	8	0.008	12.95	7.915	0.012	0.3	1544059.68	12695.25	
				973	1							
8	8	2	1.2	197	0.202	11.08488	0.879	0.012	0.3	20604.58	4171.74	212115.14
	17	4	2.4	612	0.629	11.8151	2.306	0.012	0.3	161637.72	101667.30	
	38	6	3.6	157	0.161	12.5411	4.461	0.012	0.3	589853.09	95176.71	
	26	8	4.8	7	0.007	13.12827	7.632	0.012	0.3	1542814.78	11099.39	
				973	1							
9	9	2	1.2	177	0.182	11.65948	0.894	0.012	0.3	22450.46	4084.00	226479.00
	18	4	2.4	616	0.633	11.82787	2.411	0.012	0.3	166273.47	105266.66	
	39	6	3.6	173	0.178	12.47147	4.608	0.012	0.3	596340.58	106029.72	
	27	8	4.8	7	0.007	13.12827	7.631	0.012	0.3	1542708.21	11098.62	
				973	1							

As a result of the lack of available data for accurate numerical modelling, the limitations of this conservative statistical analysis of the MIKE 21 SW numerical model output, combined with the sensitivity of the Kamphuis formula for bulk longshore transport is not ideal. It must be recommended that an in-depth numerical study combined with extensive near shore bathymetrical surveys be conducted to verify these preliminary results.

However, given the accuracy and quality of the measured data presented in this study, the approach taken is seen to fit the hypothesis set out by this study in Chapter 7.

By graphically comparing the results from the calculations to the theoretically expected scenario presented in the hypothesis, Figure 93, a preliminary dominant sediment budget regime along the Swartvlei coastline is reproduced with the calculated quantities. Figure 97 illustrates the concept of how the calculated quantities originate small in the sheltered waters in the lee of Gericke Point and then gradually increase towards a stable transport along the coastline. The orange arrows indicate the transport regime and magnitude only; not the region in which it occurs.

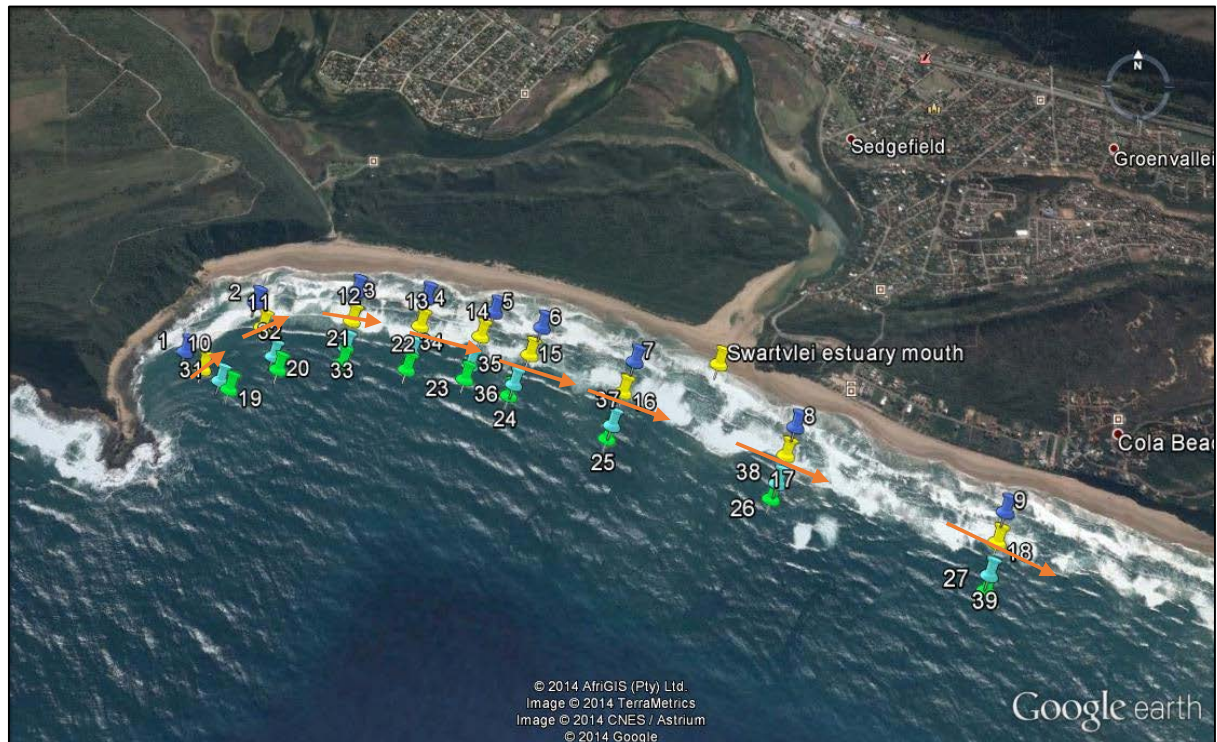


Figure 97: Calculated sediment transport vectors (orange)

By graphically illustrating the results from Table 14: Bulk sediment transport rates for the nine profiles (Figure 94) along the area studied in Figure 97, it is evident that the transport rates and directions follow the trend hypothesised for longshore transport along this type of coastline and area.

Using these results and estimating the sediment contributions from the estuary itself, a preliminary sediment budget can be formulated to represent the study area.

### 8.3 SWARTVLEI ESTUARY MOUTH SEDIMENT BUDGET

Using the data presented in this study with reference to the literature study, specific characteristics and processes of Swartvlei, the desktop study and analysis of the data collected during the site visit, a preliminary representation of the Swartvlei estuary mouth sediment budget was constructed. The main contributors are illustrated in Figure 98.



*Figure 98: Net sediment budget across the Swartvlei estuary mouth*

The contributors are as follows:

- S1- Estuary supply and sediment pulses resulting from floods
- S2- Net Dominant west to east longshore transport, through the western boundary
- S3- Net Dominant west to east longshore transport, through the eastern boundary
- S4- Dune slumping and erosion along western sandbank
- S5- Onshore and offshore tidal and marine influences
- S6- Aeolian transport from west to east, through the western boundary
- S7- Aeolian transport from east to west, through the eastern boundary

The dominant longshore sediment transport regime originates in the sheltered bay, in the lee of Gericke Point. In the lee of the headland the sandstone bluffs act as the main sediment source for the longshore transport regime occurring along the immediate sheltered coastline. However, various elements has been identified as influencing sediment transport in this area, as discussed in Chapter 3, and result in sediment not settling in sufficient quantities to initiate visible beach accretion along the immediate sheltered coastline. It has been identified that sediment from the coastline in the lee of the headland is transported with the dominant west to east longshore current and feeds into the dominant west to east bulk longshore sediment transport regime.

The sediment transport magnitudes increase along the soft coastline in an easterly direction moving away from Gericke Point and are estimated to stabilise along the parabolic shape of the coastline. The main longshore transport from west to east (defined as S2 in Figure 98) enters the sediment budget and exits the sediment budget on the eastern side (defined as S3 in Figure 98) of the estuary mouth to supplement the beaches to the east.

For this study the contribution from the estuary mouth was focused on calculating the dune slumping and erosion quantities occurring along the western bank of the estuary mouth. The quantities were calculated using slopes derived from a contour map (Attached in Appendix 4), as well as the on-site topographical survey. Combining the topographic surface data with the estimated cross sectional retreat, a volumetric scenario was simulated to obtain the contribution due to slumping and erosion along the sand bank and dune system.

This budget was defined in terms of  $\text{m}^3/\text{year}$  and marine sediments were observed to be dominant. The dominant contributors towards the sediment budget were assigned first. Although a MIKE 21 SW numerical model and the Kamphuis bulk longshore transport formula were used in estimating the preliminary longshore sediment transport rates, it was technically problematic to derive accurate input for the smaller and more detailed contributors without an additional numerical model representing the sediment transport scenario along the Swartvlei coastline. Further data collection in the fields of bathymetry and estuarine flow rates is also recommended to refine the contributions from the various sources. The calculated ranges for Figure 98 are illustrated in Table 15.

Table 15: Preliminary sediment budget across the Swartvlei estuary mouth

ID	Description	Range (m <sup>3</sup> /year)
S1	Estuary supply and sediment pulses resulting from floods and tides	2 000-4 000
S2	Longshore transport from west to east, through the western boundary	180 000- 200 000
S3	Longshore transport from west to east, through the eastern boundary	200 000- 230 000
S4	Dune slumping and erosion along the western sandbank	20 000-25 000
S5	Onshore and offshore tidal and marine influences	4 000-6 000
S6	Aeolian transport from west to east, through the western boundary	7 000-9 000
S7	Aeolian transport from east to west, through the eastern boundary	7 000-9 000

The longshore transport ranges were calculated using the output values from the MIKE 21 SW numerical model and combining them with the Kamphuis formula for bulk longshore transport. The dominant contribution from the estuary itself was focused on the quantification of the dune slumping and erosion occurring per year along the western bank of the estuary.

Aeolian transport was calculated using the NCEP wind and magnitude data. Using the CEM (2006) an empirical relationship was used to apply the offshore data to an overland data set and an estimated Aeolian transport rate of 60 m<sup>3</sup>/yr. per meter of cross sectional beach was calculated. With beach widths ranging between 120 m and 150 m, the range of transport across the boundaries is represented in Table 15.

To balance the sediment budget it was estimated that estuarine sediment pulses arising from tidal variation and suspended sediment in the estuary water column would fluctuate and interact with the pertinent marine process. The range of these smaller, less dominant effects are indicated in Table 15.

From the calculated results it is seen that on average the Swartvlei estuary mouth has a tendency towards the absorption of sediment, resulting in a net gain within the budget. This could be feasibly induced by the artificial management of the mouth which result in less flushing potential which would relate to longer open mouth conditions. If the estuary is left to

its natural cycles and processes, the longer open mouth conditions could possibly lead to greater redistribution of sediment within the budget, possibly resulting in a naturally balanced sediment budget.

The results presented were focused on describing the preliminary Swartvlei estuary budget under typical conditions. Further in-depth studying is recommended to quantify these various contributors on a more refined scale. These further investigations should take into account the long term budget scenario with special emphasis on the contributions from major river floods.

## 9. CONCLUSIONS AND RECOMMENDATIONS

Extensive research and studies have been performed in an attempt to define the processes within headland bay beaches. The reality, however, is that these areas are very dynamic and very sensitive to variation in the wind and wave climates, as well as currents.

The objective of this study was to estimate a preliminary sediment budget across the Swartvlei estuary mouth. This was achieved by assessing the various contributions from:

- Dominant longshore transport regime consisting of contributors such as
  - Slumping and erosion of the sandy bluff in the lee of the headland, Gericke Point.
  - Accumulated beach sand from dunes and beach material along the Swartvlei coastline
  - Aeolian transport resulting from dominant wind directions.
- Estuary contributions such as
  - Slumping and erosion of dunes and the low crested sand bank on the western side of the estuary.
  - Estuarine sediment pulses resulting from tidal variations as well as suspended sediment in the estuary water column

This assessment was done by numerically simulating the Swartvlei coastline and bay area. NCEP hindcast data combined with measured data from various available sources (on-site surveys, SANPark records, published records etc.) was used as a foundation for the numerical MIKE 21 SW model.

By combining the simulated numerical data with the Kamphuis formula for bulk longshore transport, sediment contribution ranges in  $m^3/yr$  were calculated for the various dominant contributors. A statistical approach was used to cumulatively define the bulk longshore transport regime along the Swartvlei coastline. Using the point specific MIKE 21 SW breaking wave output data, a refined preliminary understanding of the pertinent metocean conditions occurring along the coastline could be achieved and evaluated. The limitations of the sparse bathymetrical data, combined with the nature of the Kamphuis formula for bulk longshore transport, would possibly lead to a estimation as a range rather than precise quantities.

However, with the accuracy and quality of data presented throughout this study, the results obtained from the calculation process fit the general trend set out in the hypothesis.

Through these calculations and historical- and on-site imagery the following conclusions were made:

1. In the lee of the headland, Gericke Point, bluff erosion and subsequent slumping has been identified as the main contributor of sediment in this region. However, due to factors such as the rocky geology of the immediate coastline and steep bathymetry, sediment is not settling in sufficient quantities to initiate significant beach accretion in this region. The majority of sediment present in this area has been estimated to supplement the dominant west to east longshore transport regime. The end result is the erosion of the coastline in this area to solid bedrock and subsequently a premature static equilibrium beach profile is reached.
2. The dunes and wide, flat sloped foreshore along the western beaches of the Swartvlei coastline were identified as the main contributors towards the longshore transport from west to east across the estuary mouth, resulting in 180 000- 200 000 m<sup>3</sup>/year entering the sediment budget as net longshore transport and 200 000- 230 000 m<sup>3</sup>/year exiting the budget as net longshore transport towards beaches east of the estuary mouth.
3. From evidence presented in Chapter 7, it was estimated that the Swartvlei estuary mouth area is marine sediment dominated. This is due to a lack of flushing potential induced by human interference, run-off abstraction and the dominant marine processes. Furthermore, conclusions from the on-site investigation reveal a significant retreat of the beaches east of the estuary mouth relative to the western beaches. This means that the sediment transported into the budget area is absorbed and does not transfer in adequate quantities across the opposite boundary towards the east. Insufficient sediment transport as a result of the lack of flushing potential from the estuary, the lack of an active primary dune system and the dominant longshore transport regime, combine and result in the erosion of these eastern beaches. Verification of this estimate consisted of on-site photography of the erosion occurring along these beach regions and available aerial imagery of the mouth area. The dune and beach survey also showed that these beaches (on the Myoli beach side) were very narrow with steep dunes at the back, making them very susceptible to wave run-up and metocean processes leading to erosion
4. By defining a large sediment budget area, minor estuarine and marine influences were absorbed in the budget area before crossing the opposite boundary. This meant that although they were contributing sediment, they were not influencing the sediment budget as defined in this study. Dune slumping and erosion along the western bank

## A Preliminary Analysis of the Sediment Budget Across the Swartvlei Estuary Mouth

of the estuary, due to the migration of deep channels, were identified as the main estuary contributors and an estimated range of 20 000–25 000 m<sup>3</sup>/year towards the sediment budget was calculated.

5. Aeolian transport was estimated. NCEP wind direction and magnitude data was used as input and refactored to overland values. Transport in the main west - east direction was calculated to be in the order of 60 m<sup>3</sup> per meter of beach width per year. With an average beach boundary width of 150 meters an estimated range of 7 000 m<sup>3</sup>-9 000m<sup>3</sup> per year was defined.

The hypothesis presented during this study was based on the literature review and data collections and was verified and justified by the various calculations, quantities and observations presented. The limitations due to the lack of available data, however, are clear and duly noted. It is therefore recommended that further in-depth studies be performed in future, in an attempt to replicate the sediment transport scenario and more specifically the sediment budget across the Swartvlei estuary mouth, on a more refined scale. These studies should include:

- Additional numerical modelling of the Swartvlei coastline
- Additional numerical sediment transport models of the Swartvlei coastline

Future surveys and environmental data gathering should include:

- Bathymetric surveys of the Swartvlei coastline, including the surf zone, by means of a jet ski or equivalent craft mounted with a single beam echo sounder.
- Wave and current measurements over a 24 month period
- Sediment sampling processes consisting of vibrocoring to a depth of at least 5 m (measured downward from the sea floor )

Currently the eastern beaches away from the estuary mouth towards Myoli beach are eroding due to a lack of sediment supply. This is estimated to be a result of sediment being trapped and absorbed into the estuary mouth area and not exiting in sufficient quantities to feed the beaches to the east sufficiently for significant beach accretion. Along these eastern beaches there are numerous residential developments, situated on the primary dunes within the recommended coastal processes setback area. These residential developments, and the subsequent stabilisation of the historical dunes system, results in significant pressure on the natural dune forming processes and subsequently a lack and even an absence of a stable buffer dune system. Combining the lack of sediment trapping capacity of this buffer dune

system, which would result in dune formation, with the sediment absorbing effects of the estuary mouth, will lead to continued erosion along these eastern beaches.

It is recommended that strict setback lines along the estuary banks and coastal dune areas be enforced. A long term dune vegetation rehabilitation programme is recommended, to be implemented along the eastern dune slope with designated pathways leading down to the beaches. No developments should take place within these littoral and inland dune systems. Stricter monitoring of agricultural and domestic water abstraction from the river catchments should be implemented.

Following on the conclusions presented and based on the proposed additional investigations, it is additionally recommended that a more research-orientated management strategy should be implemented and applied towards the long-term maintenance of the estuary mouth. This management strategy should ideally be based on:

1. Community input gathered through public meetings
2. In-depth numerical models of the wave climate and sediment transport scenarios present
3. Additional consultation by accredited institutes which particular knowledge and experience with the Swartvlei system
4. Input from environmental agencies

By applying these recommendations the natural wonder of the Swartvlei estuary and its surrounds can be successfully managed for generations to come.

## REFERENCES

- ABP Marine and Environmental Research, 2008. *Sediment budget analysis*. [Online] Available at: [http://www.estuary-guide.net/pdfs/sediment\\_budget\\_analysis.pdf](http://www.estuary-guide.net/pdfs/sediment_budget_analysis.pdf)
- Anderson, J., 2004. *The role of sand bar dynamics in the water quality of Moore River Estuary: an intermittently open estuary in South West Australia.*, Perth: University of Western Australia.
- Bagnold, R. A., 1941. *The Physics of Blown Sand and Desert Dunes*. London, UK: Methuen.
- Barwell, L., 2011. *Integrity assessment procedure for buffer dune systems on the Cape south coast, South Africa*, Stellenbosch: Stellenbosch University.
- Beck, J., 2005. *Sediment transport dynamics in South African estuaries*. MEng Thesis, Stellenbosch: University of Stellenbosch.
- Birch, G. F. & Du Plessis, A., 1977. *Offshore and onshore geological and geophysical investigations in the Wilderness lake regions*, Cape Town: University of Cape Town.
- Birkemeier, W., 1985. *Field Data on Seaward Limit of Profile Change, Research Hydraulic Engr., U.S. Army WES, Coastal Engineering Research Center, Field Research Facility, Duck, N.C. 27949*
- Britannica, 2000. Sandbar [Online] Available at: <http://www.britannica.com/EBchecked/topic/522050/sandbar>
- CSIR, 1983. *Estuaries of the Cape: Swartvlei*, Stellenbosch: National Research Institute for Oceanology.
- City of Cape Town Municipality, 2008. *Zandvlei: Factors concerning water level management*, Cape Town: City of Cape Town Municipality.
- Dean, R. G., 1977. *Equilibrium Beach Profiles: U.S. Atlantic and Gulf Coasts*, Department of Civil Engineering. Newark: University of Delaware.
- Detle, H. & Uliczka, K., 1987. *Prototype Investigation on Time-Dependent Dune Recession and Beach Erosion*. Proceedings: Coastal Sediments '87, New Orleans, 1430-1444.
- Deyr, K., 1997. *Estuaries: A physical introduction*, New York:
- DHI, 2011. *MIKE 21 SW Manual, Spectral Wave FM Module, and Users Guide*: Danish Hydraulic Institute 2011.
- Dronkers, J., 2005. *Dynamics of Coastal Systems*, Singapore: World Scientific Publishing

Republic of South Africa, Department of Water Affairs and Forestry, (DWAFF), 2009.

*Resource Directed Measures: Reserve Determination studies for selected surface water, groundwater, estuaries and wetlands in the Outeniqua catchment: Ecological Water Requirements Study.* Pretoria: Department of Water Affairs and Forestry.

Elgar, S., Gallagher, E. & Guza, R. T., 2001. *Nearshore sandbar migration.* *Journal of Geophysical Research*, Vol. 106, No. C6, Pages 11,623-11,627, June 15, 2001.

EWISA, 2003. *Swartvlei estuaries.* [Online] Available at: [www.ewisa.co.za](http://www.ewisa.co.za) [Accessed 31 January 2013].

Falques, A., Coco, G. & Huntly, D. A., 2000. *A mechanism for the generation of wave driven rhythmic pattern.*

FEMA, 2007. *Guidelines and specifications for flood Hazard Mapping Partners*, US: US department of Homeland security.

Fijen, A. & Kapp, J., 1995. *Swartvlei lake catchment, Diep-, Klein-, Wolwe, Hoëkraal and Katara Rivers, water management strategy*, Pretoria: Department of Water Affairs and Forestry.

Fijen, A. & Kapp, J., 1995. *The water management strategy for Wilderness, Swartvlei and Groenvlei lake catchment*, Pretoria: Department of Water Affairs and Forestry.

Froneman, P. W., 2004. Food web dynamics in a temperate temporarily open/closed estuary. *Estuarine, Coastal and Shelf Science*, 59:87-95.

Griffiths, S. P., 2001. Factors Influencing Fish Composition in an Australian Intermittently Open Estuary. Is Stability Salinity-Dependent? *Estuarine, Coastal and Shelf Science*, 52:732-752.

Hallermeier, R., 1978. *Uses for a Calculated Limit Depth to Beach Erosion.* *Proceedings of the 16<sup>th</sup> International Conference on Coastal Engineering*, Hamburg, ASCE, pp. 1493-1512.

Hodgkin, E. P. & Clark, R., 1988. *The estuaries of the Wilson, Irwin and Parry Inlets*, Perth: Environmental Protection Authority of Western Australia.

Hodgkin, E. P. & Clark, R., 1990. *An inventory of Estuaries of the shire of Albany*, Perth: Environmental Protection Authority of Western Australia.

Hoefel, F. & Elgar, S., 2003. *Wave-induced sediment transport and sandbar migration.* *Woods Hole Oceanographic Institution, Wood Hole, MA, USA*

Holthuijsen, D., Booij, N. & Herbers, T., 1989. *A prediction model for stationary, short crested waves in shallow water with ambient currents.* *Coastal Engineering*, 13, 23-54.

- Howard, W. & Allanson, B., 1979. *The ecology of Swartvlei: Research for planning and future management*, Pretoria: Water Research Commission.
- Hsu, J., 2010. Static bay beach concept for scientists and engineers. A review: *Coastal Engineering*, 56(2), 79-91.
- Hsu, J. & Evans, C., 1989. *Parabolic bay shapes and applications*. *Proceedings of the Institution of Engineers, London*, Part 2, 87: 557-570.
- James, N. & H. T., 2008. *A preliminary survey of the estuaries on the south coast of South Africa, Cape St Blaize, Mossel Bay–Robberg Peninsula, Plettenberg Bay, with particular reference to the fish fauna*. *Transactions of the Royal Society of South Africa* 63(2)
- Kamphuis, W., 2010. *Introduction to coastal engineering and management*. Singapore: World Scientific.
- Kluger, J. W., 1975. *Hydrographic survey of Sedgefield*. Pretoria: Council for Scientific and Industrial Research.
- Kok, H. & Whitfield, A., 1986. *The influence of open and closed mouth phases on the marine fish fauna of the Swartvlei estuary*. *South African Journal of Zoology* 21
- Komar, P., 1998. *Beach Processes and Sedimentation 2nd Ed*. New Jersey: Prentice-Hall.
- Komen, G., 1994. *Dynamics and modelling of ocean waves*. UK: Cambridge University Press.
- Kriebel, D. & Dean, R., 1993. Convolution Method for Time-Dependent Beach-Profile Response. *Journal of Waterway, Port, Coastal and Ocean Engineering*, American Society of Civil Engineers, 119(2): 204-227.
- Larson, M. & Kraus, N. C., 1989. *SBEACH: Numerical Model for Simulating Storm-induced Beach Change; Report 1: Empirical Foundation and Model Development*, Vicksburg, MS: U.S. Army Engineer Waterways Experiment Station.
- Lausman, R., Klein, A. & Stive, M., 2010. *Uncertainty in the application of the Parabolic Bay Shape Equation: Part 1*. *Coastal Engineering*. [Online] Available at: <http://dx.doi.org/10.1016/j.coastaleng.2009.09.009> Accessed 24 February 2013.
- Lausman, R., Klein, A. & Stive, M., 2010. *Uncertainty in the application of the parabolic bay shape equation: Part 2*. [Online] Available at: <http://linkinghub.elsevier.com/retrieve/pii/S0378383909001392>.
- Longuet-Higgins, M.S., 1970. Longshore current generated by oblique incident sea waves, 2. *Journal of Geophysical research*, 75(33). Corvallis, Oregon: Oregon State University.

- Malan, P., 2012. *The impact of climate change effects on the planform of a headland-bay beach on the southern coast of South Africa*, Stellenbosch: University of Stellenbosch.
- Marshall, J., 1993. *Physical Processes of Wilson Inlet*, MEng Thesis, Perth: University of Western Australia.
- Martin, A. R. H., 1962. Evidence relating to the quaternary history of the Wilderness lakes, *Transactions of the Geological Society*. 65; 19-42.
- Mather, A., 2008. *Living with coastal erosion in KwaZulu-Natal, a short term best practice guide*, Pietermaritzburg: KwaZulu-Natal Department of Agriculture and Environmental Affairs.
- Moreno, L. & Kraus, N., 1999. *Equilibrium shape of headland-bay beaches for engineering design in Coastal Sediments. Proceeding for Coastal Sediments 1999*.
- Mynhart, M., 2012. *Karatara River weir*: Technical Report, Tuiniqua Consulting Engineers.
- National Centres for Environmental protection (NCEP), U. g., 2011. *National Centers for Environmental Prediction (NCEP)*. [Online]  
Available at: [www.ncep.noaa.gov](http://www.ncep.noaa.gov) Accessed 2 January 2013.
- Pattiaratchi, C., Masselink, G. & Ranasinghe, R., 1999. A Morphodynamic Model to Simulate the Seasonal Closure of Tidal Inlets. *Coastal Engineering*, **34**: pp. 1-35.
- Pethick, J., 1992. *Strategic planning and coastal defence. 27th River and Coastal Engineers Conference, MAFF, London*, pp. 3.1.1-3.1.7.
- Plant, N. G., Ruessink, B. G. & Wijnberg, K. M., 2001. *Morphologic properties derived from a simple cross-shore sediment transport model. Journal of geophysical research. Pt. C: Oceans*, 106 (C1). pp. 945-958. ISSN 2169-9275
- Potter, I. C. & Hyndes, G. A., 1999. Characteristics of ichthyofaunas of southwestern Australian estuaries, including comparisons with holarctic estuaries and estuaries elsewhere in temperate Australia: A review, *Australian Journal of Ecology*.
- Ranasinghe, R. & P. C., 1999. *The seasonal closure of tidal inlets: Wilson Inlet- a case study. Coastal Engineering (37) pp 37-56*.
- Republic of South Africa, South African Navy Hydrographic Office (SANHO), 2013. *SANHO Tides 2013*. Pretoria: The South African Navy Hydrographic Office.
- South African National parks (SANParks), W. b., 2012. *Estuary profile data, Wilderness: SANParks*.

Schoonees, J.S., 2001. Longshore Sediment Transport: Applied Wave Power Approach, Field data Analysis and Evaluation of the formulae. PhD thesis, University of Stellenbosch: Stellenbosch.

Schoonees, J.S., 2012. Presentation on *longshore transport*, MEng Course Notes. Stellenbosch: Stellenbosch University.

Schoonees, J.S. & Theron, A., 1994. Accuracy and application of the SPM longshore transport formula. *International Conference on Coastal Engineering*, 3(1), pp. 2595-2609.

Schoonees, J.S. & Theron, A., 1996. *Improvement of the most accurate longshore transport formula*. International Conference on Coastal Engineering, 3(1), p. 3652-3665.

Schumann, E., 2003. *Towards the management of marine sedimentation in South African Estuaries with special reference to the Eastern Cape*.

Schwartz, M., 2005. *Encyclopaedia of Coastal Science*, Dordrecht: Springer.

Silvester, R. & Ho, S., 1980. *Use of crenulated shaped bays to stabilize coasts*. American Society of Civil Engineers (ASCE) 17<sup>th</sup> International Conference on Coastal Engineering, Sydney, Australia: 1306-1319.

Silvester, R., Tsuchiya, Y. & Shibano, Y., 1972. *Zeta bays, pocket beaches and headland control*. American Society of Civil Engineers (ASCE), Vancouver, Canada: 1347-1365.

Sloss, C. R., Hesp, P. & Shepherd, M., 2012. Coastal dunes: Aeolian transport. *Nature Education Knowledge*, 3(10): 21.

Soltau, C., 2009. *The cross-shore distribution of grain size in the longshore transport zone*, MEng Thesis. Department Of Civil Engineering, Stellenbosch: Stellenbosch University.

Swart, D., 1974. *Offshore sediment transport and equilibrium beach profiles*. 131 Ed., Delft: Delft Hydraulics Laboratory.

Theron, A K, Schoonees, J S, Huizinga, P and Phelp, D T(2003). *Beach Diamond Mining Design at the Rocky Namaqualand Coast*. Proceedings, 4<sup>th</sup> Coastal Structures Conference, ASCE, Portland, Oregon, 2003.

Theron, A K, 2004. *Sediment Transport Regime in the area of the East London Harbour Entrance*. MEng Thesis, Stellenbosch: Stellenbosch University.

Todd, D., 1995. *Wilson Inlet Hydrodynamic Study: Part 2. Effectiveness of bar opening*, Perth: Port and Harbour Consultants.

Townend, I. & Whitehead, P., 2003. A preliminary net sediment budget for the Humber Estuary. *The Science of the Environment*, pp. 314-316, 755-767.

U.S. Army Corps of Engineers, 2006, *Coastal Engineering Manual (CEM)*, Engineer Manual 1110-2-1100, (6 volumes). Washington, D.C: U.S. Army Corps of Engineers.

Whitfield, A., 1986. *Ichthyoplankton interchange in the mouth region of a Southern African estuary. Marine Ecology Progress Series, Vol. 54: 25-33, 1989.*

Whitfield, A., 2000. *Available scientific information on individual South African Estuarine Systems*. Unpublished Water Research Commission report.

Whitfield, A., Allanson, B. & Heinecken, T., 1983. *Estuaries of the Cape, Part II: Synopses of available information on individual systems. Report No. 22: Swartvlei (CMS11).*

Yasso, W., 1965. Plan Geometry of Headland-Bay Beaches. *Journal of Geology*, pp. 702-714.

Young, I., 1999. *Wind Generated Ocean waves*, Vol. 2. Amsterdam: Elsevier 1999.

Yu, J., 2000. *Formation of sand bars under surface waves. Journal of Fluid Mechanics*, 416; 315:348.

## **APPENDIX 1: AVERAGE YEARLY RAINFALL FOR THE SEDFIELD REGION (2002-2010)**

A Preliminary Analysis of the Sediment Budget Across the Swartvlei Estuary Mouth

**SEDFIELD - SUMMARY OF YEARLY RAINFALL**

YEAR RAIN	MONTH												Total Yr to date	Average Monthly Rainfall	Hist. total yr to date mm	% Hist avg
	jan	feb	mrch	apr	may	jun	jul	aug	sept	oct	nov	dec				
	2002	74	12	23	45	31	50	82	54	102	11	33				
2003	32	49	280	46	103	55	28	28	17	68	13	60	779	65	779	90%
2004	78	83	133	70	44	48	40	58	105	82	44	271	1056	88	1056	122%
2005	50	52	92	60	61	46	23	23	60	28	108	71	674	56	674	77%
2006	77	69	95	101	171	68	101	362	46	114	35	52	1291	108	1291	147%
2007	139	61	125	38	130	12	113	39	25	76	362	144	1264	105	1264	144%
2008	95	61	62	33	9	109	16	86	41	90	107	25	734	61	734	84%
2009	18	75	15	64	17	64	78	26	76	82	61	75	651	54	651	74%
2010	66	74	34	63	34	102	87	40	18	89	84	174	865	72	865	98%
Hist avg for mth	70	60	95	58	67	62	63	80	54	71	94	105	879		879	mm. Hist. avg yr to date

## **APPENDIX 2: GANTT CHART**

## **APPENDIX 3: TRIMBLE GPS TECHNICAL INFORMATION**



### TRIMBLE R7

The Trimble R7 RTK GPS receiver puts you on track for the future of GPS surveying. The Trimble R7 features Trimble's new R-Track technology, which includes the capability of tracking the new civil signal, L2C. The combination of R-Track and all the features and functionality of the 5700 RTK GPS receiver allows you to maximize your return on investment by purchasing a system that is ready for the future.

### HIGH-ACCURACY ANTENNA OPTIONS

#### LIGHTWEIGHT, HIGH-ACCURACY ZEPHYR GPS ANTENNA

Zephyr™ technology for extremely low multipath, outstanding low elevation tracking, and sub-millimeter phasecenter accuracy. Geodetic performance in a compact form.



#### STEALTH TECHNOLOGY

The Trimble Zephyr Geodetic™ antenna uses the patented Trimble Stealth™ ground plane. This revolutionary design literally burns up multipath energy using technology similar to that used by Stealth aircraft to hide from radar.

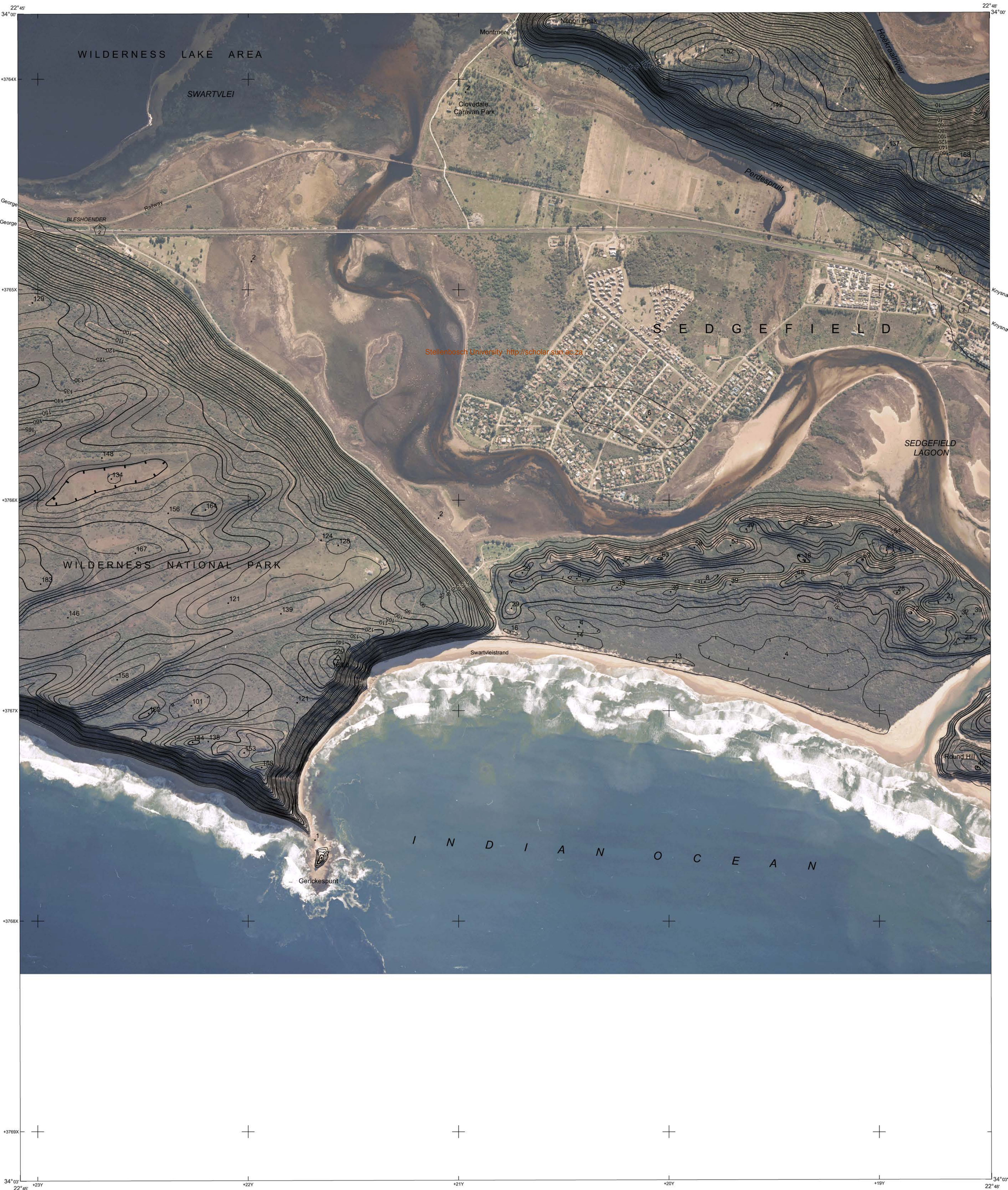
The Zephyr and Zephyr Geodetic antennas have broken new ground in survey GPS antenna technology. For additional information, see the Trimble white paper, "Advancements in GPS Antenna Technology: The New Trimble Zephyr Antennas," available on [www.trimble.com](http://www.trimble.com).

#### HIGH-ACCURACY ZEPHYR GEODETTIC ANTENNA

The Trimble Zephyr Geodetic antenna has demonstrated performance to meet the highest Geodetic standards in extensive tests. Submillimeter phase center repeatability, better low elevation tracking and significantly reduced ground-bounce multipath with the new Trimble Stealth ground plane technology all add up to the best accuracy ever from a portable antenna.



## **APPENDIX 4: CONTOUR PLAN OF THE ESTUARY REGION**



Published by the Chief Directorate: Surveys and Mapping, Private Bag X10, Mowbray.  
 Gepubliseer deur die Hoof Direktooraat: Opmetings en Kartering, Private Sak X10, Mowbray  
 Photography 498/616  
 Fotografie 498/616  
 © State Copyright 2008 Staatsouteursreg

Gauss Conform Projection, Central Meridian 23° East  
 Contour Interval 5 Meters  
 Grid Interval 1 000 Meters  
 Hartebeesthoek 94 Datum  
 WGS84 Ellipsoid

1:10 000



Gauss Konforme Projeksie, Middelmeridiaan 23° Oos  
 Kontourtussenruimte 5 Meter  
 Ruittussenruimte 1 000 Meter  
 Hartebeesthoek 94 Datum  
 WGS84 Ellipsoid

3422 BB 1 THIRD EDITION DERDE UITGAWE 2006

INDEX TO SHEETS INDEKS VAN VELLE

3422DC25	3422DD21	3422DD22
3422BA5	3422BB1	3422BB2
3422BA10	3422BB6	3422BB7

Whilst every effort is made to ensure the accuracy of this map, users noting errors and omissions are requested to notify the Chief Directorate: Surveys and Mapping.  
 Alle pogings moontlik word aangewend om die akkuraatheid van hierdie kaart te verseker. Gebruikers word versoek om die Hoofdirektooraat: Opmetings en Kartering, te verwittig van enige foute of weglatings.

ALSO AVAILABLE IN COLOUR BUT IN DIGITAL FORMAT ONLY

## **APPENDIX 5: MIKE 21 SW DESCRIPTION**

## **APPENDIX 6: PHOTO REPORT**



*Figure 1: Estuary mouth channels*



*Figure 2: Estuary mouth looking inwards from sea*



*Figure 3: Estuary mouth looking seaward*



*Figure 4: Sandbar in front of estuary, facing west*



*Figure 5: Looking west towards Gericke point*



*Figure 6: Surveying dunes west of estuary mouth*



*Figure 7: Presence of buffer dune system with higher back dunes present*



*Figure 8: Sand stone cliffs at Gericke point*



*Figure 9: Slumping section in sand stone cliffs*



*Figure 10: Gericke point with rocky shoreline*



*Figure 11: Rocky shoreline at Gericke point*



*Figure 12: Coastline east of the estuary mouth*



*Figure 13: Steep dunes with no buffer zone on section east of estuary mouth*



*Figure 14: Tidal currents at railway bridge*

## APPENDIX 7: BEACH SURVEY

During the site visit to Sedgefield in December 2012, the profiles shown on the following pages were obtained by means of a Trimble handheld GPS device. With the use of software specifically designed to convert Trimble data to XYZ co-ordinates with an accuracy of +/-10–30 cm, the following profiles were obtained:

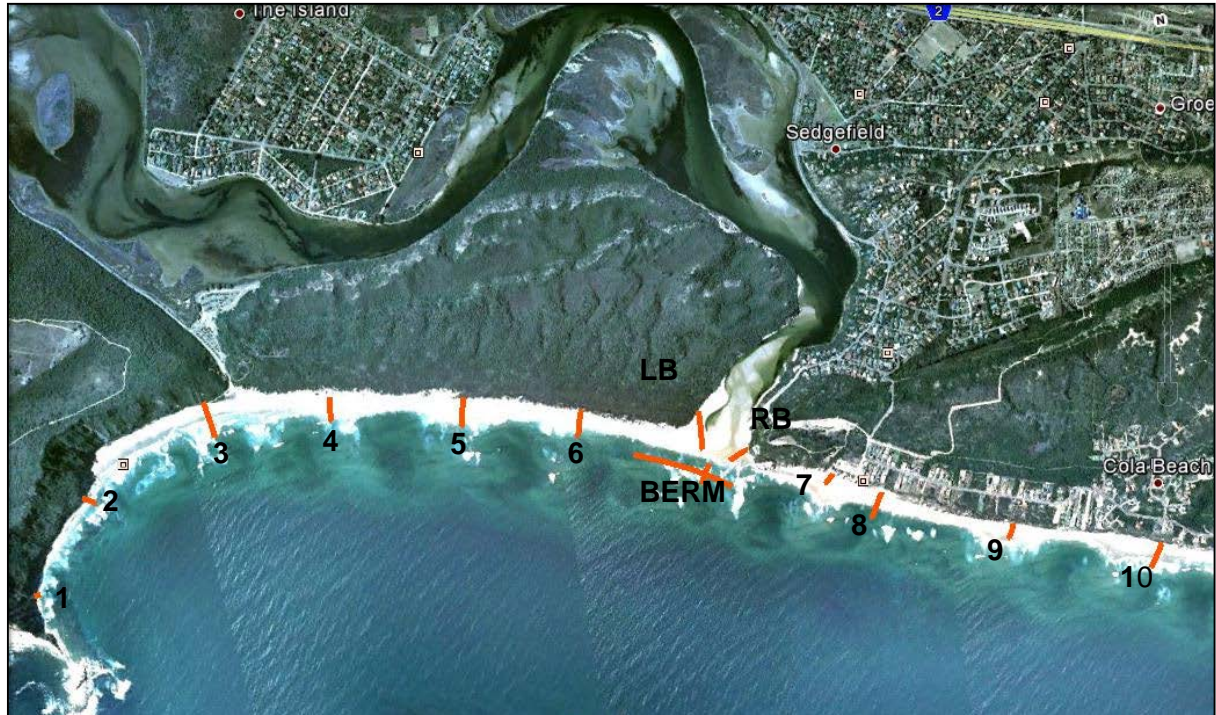


*Figure 99: Trimble profiles*

Illustrated in Figure 99 are the fourteen profiles that were measured during the site visit. These include the berm in front of the estuary mouth and the left and right banks of the estuary, here expressed as LB and RB, respectively. These profiles were labelled facing the estuary from the sea side.

All profiles were measured from the sea towards land. The longitudinal berm profile was measured from left to right.

## 7.1 PROFILE ONE

The figure below illustrates the position of profile one.

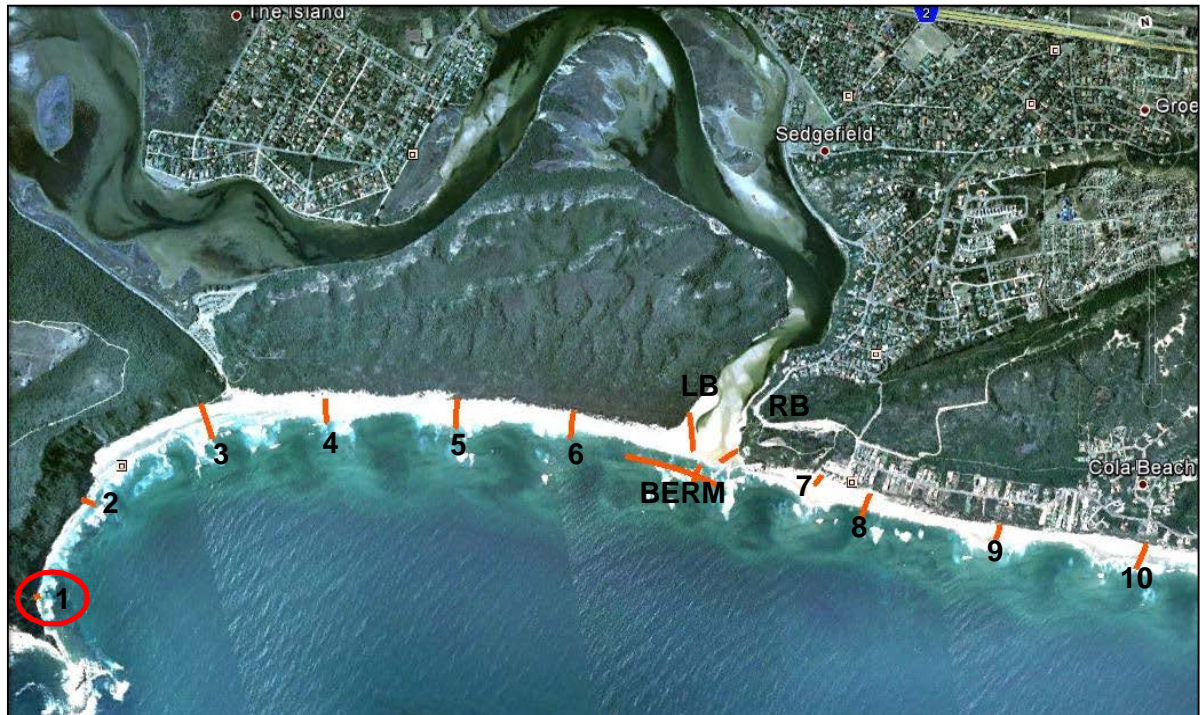


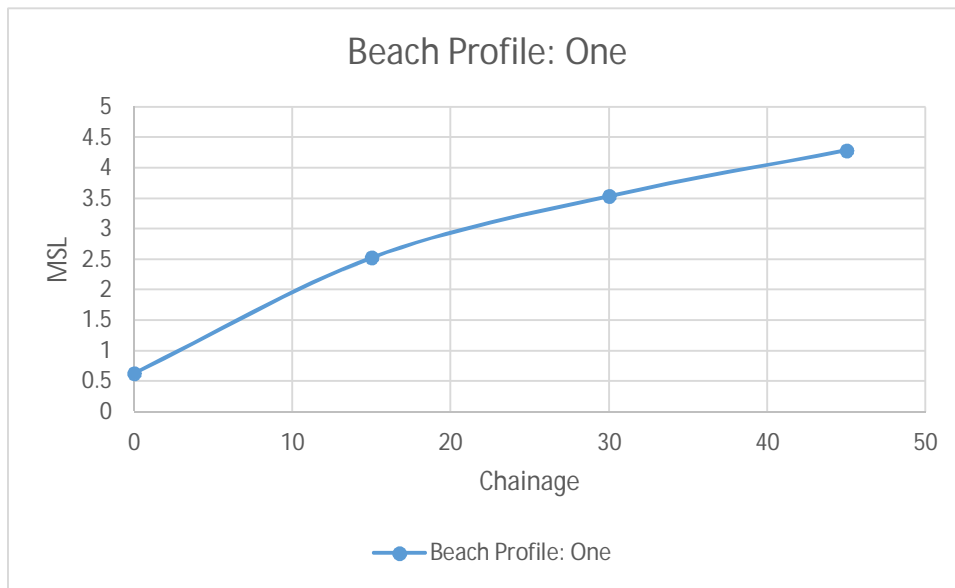
Figure 100: Location of position one

Table 16 summarises the data obtained from on-site measurements. Five measurements were taken at the profile at 15 m intervals.

Table 16: Profile one

Point Name	Height above MSL in m	Chainage
129	0.636	0
130	2.53	15
131	3.541	30
132	4.293	45

## A Preliminary Analysis of the Sediment Budget Across the Swartvlei Estuary Mouth



*Figure 101: Profile one*

From Figure 101 it is concluded that the on-shore beach slope close to Gericke Point is more sloping, relative to the beach profiles towards the estuary. This contributes to the theory that the sheer sandstone cliffs are depositing sediment onto the narrow beach which is then immediately eroded away into the longshore sediment transport regime along the Swartvlei coastline.

The geological characteristics of the cliffs at the back of the beach are the main reason for the short and relatively steep nature of the beach slopes in the vicinity of profile one, depicted in Figures 102 and 103.

A Preliminary Analysis of the Sediment Budget Across the Swartvlei Estuary Mouth



*Figure 102: Profile one with sheer sandstone cliffs*

A Preliminary Analysis of the Sediment Budget Across the Swartvlei Estuary Mouth



*Figure 103: Beach near profile one*



*Figure 104: Erosion of the sandstone cliffs near profile one*

From Figure 104 it can be seen that erosion is a constant threat to the fragile sandstone cliffs at the back of the beach profiles at Gericke Point.

## 7.2 PROFILE TWO

The location of profile two is shown in Figure 105.

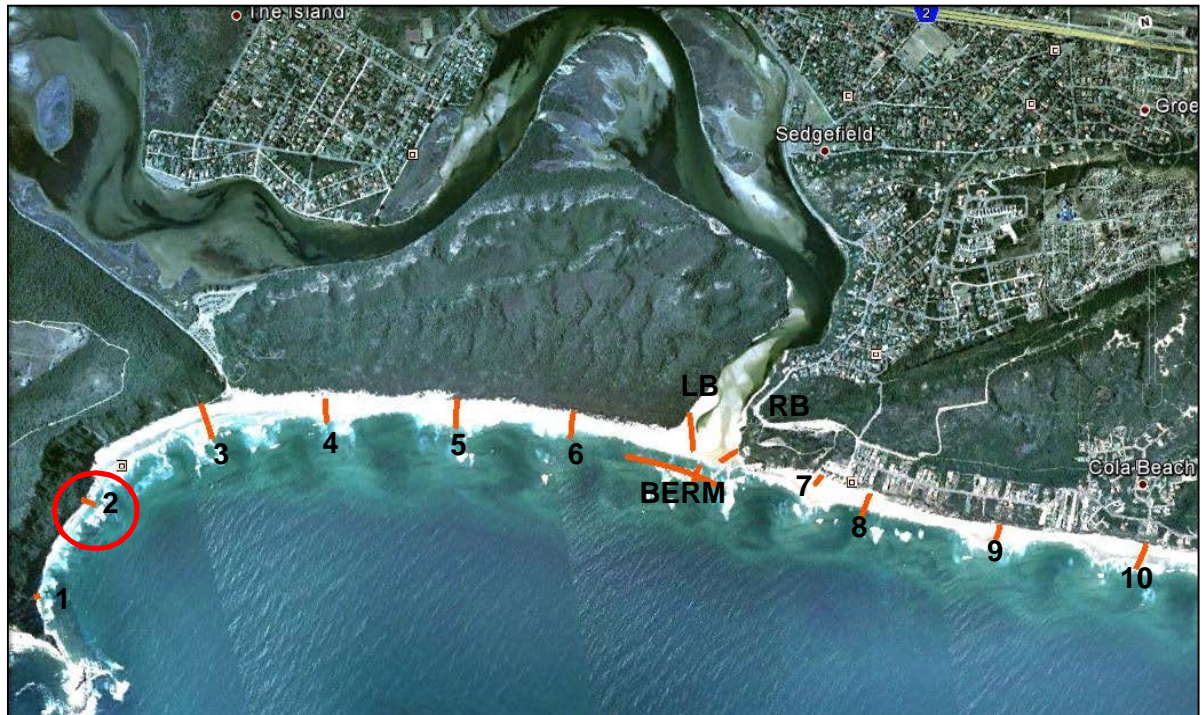
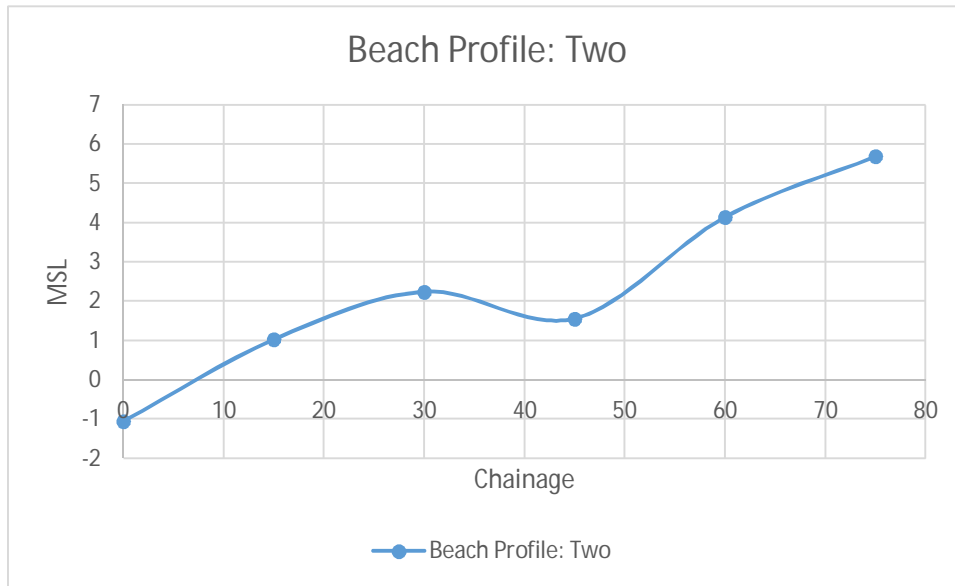


Figure 105: Location of profile two

Table 17: Profile two

Point Name	Height above MSL in m	Chainage
133	-1.055	0
134	1.03	15
135	2.248	30
136	1.565	45
137	4.151	60
138	5.693	75

A Preliminary Analysis of the Sediment Budget Across the Swartvlei Estuary Mouth



*Figure 106: Profile two*

Profile two shows a steady incline in the slope from the sea towards the back of the beach. It is also evident from the site photo, Figure 106 that this steady rise in beach slope could be the result of sediment deposits by longshore transport arising from the steep sandstone cliffs at the back of the beach.



*Figure 107: Profile two*

### **7.3 PROFILE THREE**

From Figure 108 the location of profile three can be seen in comparison to the Swartvlei coastline. It is located closest to the Gericke Point parking area.

A Preliminary Analysis of the Sediment Budget Across the Swartvlei Estuary Mouth

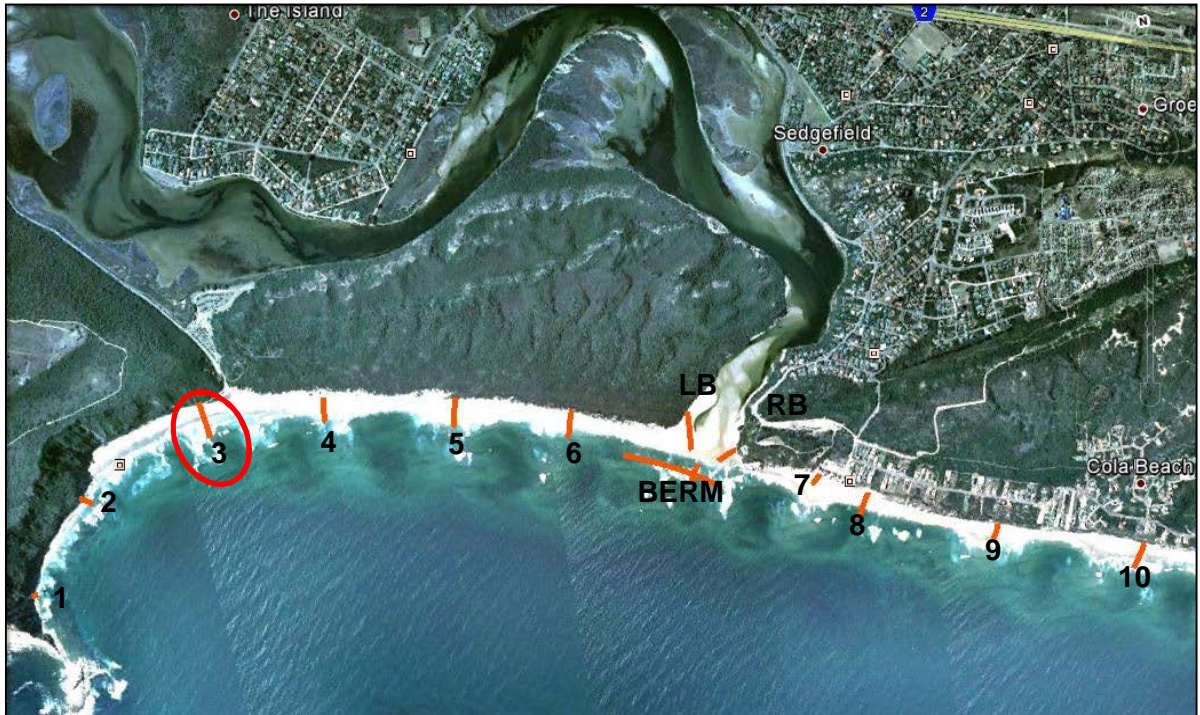
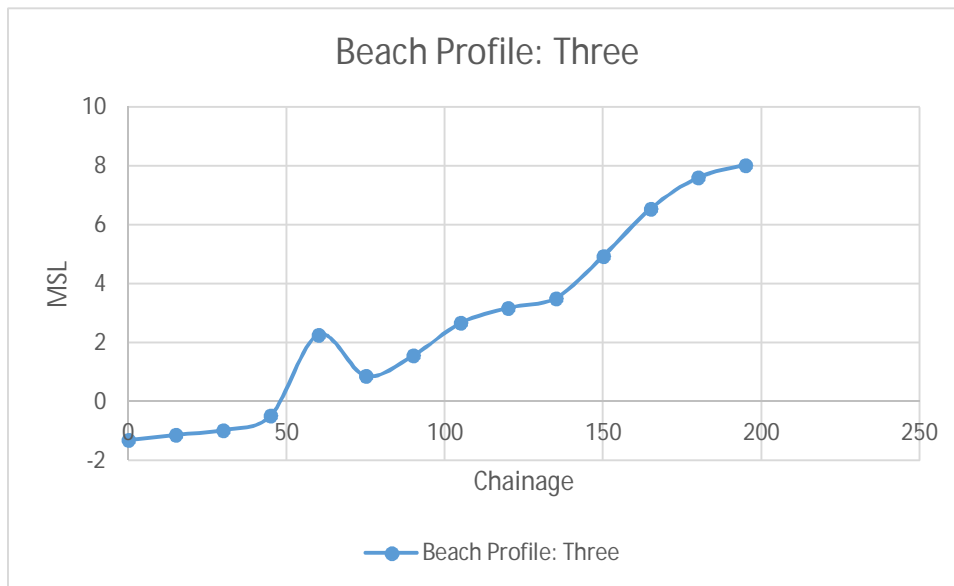


Figure 108: Position of profile three

Table 18: Profile three

Point Name	Height above MSL in m	Chainage
100	-1.309	0
101	-1.135	15
102	-0.964	30
103	-0.471	45
104	2.276	60
105	0.872	75
106	1.562	90
107	2.67	105
108	3.18	120
109	3.513	135
110	4.939	150
111	6.55	165
112	7.613	180
113	8.038	195

## A Preliminary Analysis of the Sediment Budget Across the Swartvlei Estuary Mouth



*Figure 109: Profile three*

A much gentler slope is present at profile three. It is evident from the on-site photographs that there are sandstone cliffs present, but it is estimated that the sediment transported via longshore transport from profiles one and two is supplementing profile three. A beach width of 200 m was measured with the GPS and a steady rise in elevation of almost 10 m from start to finish is present.



*Figure 110: Profile three: On site photo*

It can be seen from Figure 110 that the slope at profile three is gentler than those of the previous two profiles towards Gericke Point.

#### **7.4 PROFILE FOUR**

From Figure 111 the location of profile four can be seen in comparison to the Swartvlei coastline. It is located just right of the Gericke Point parking area.

A Preliminary Analysis of the Sediment Budget Across the Swartvlei Estuary Mouth

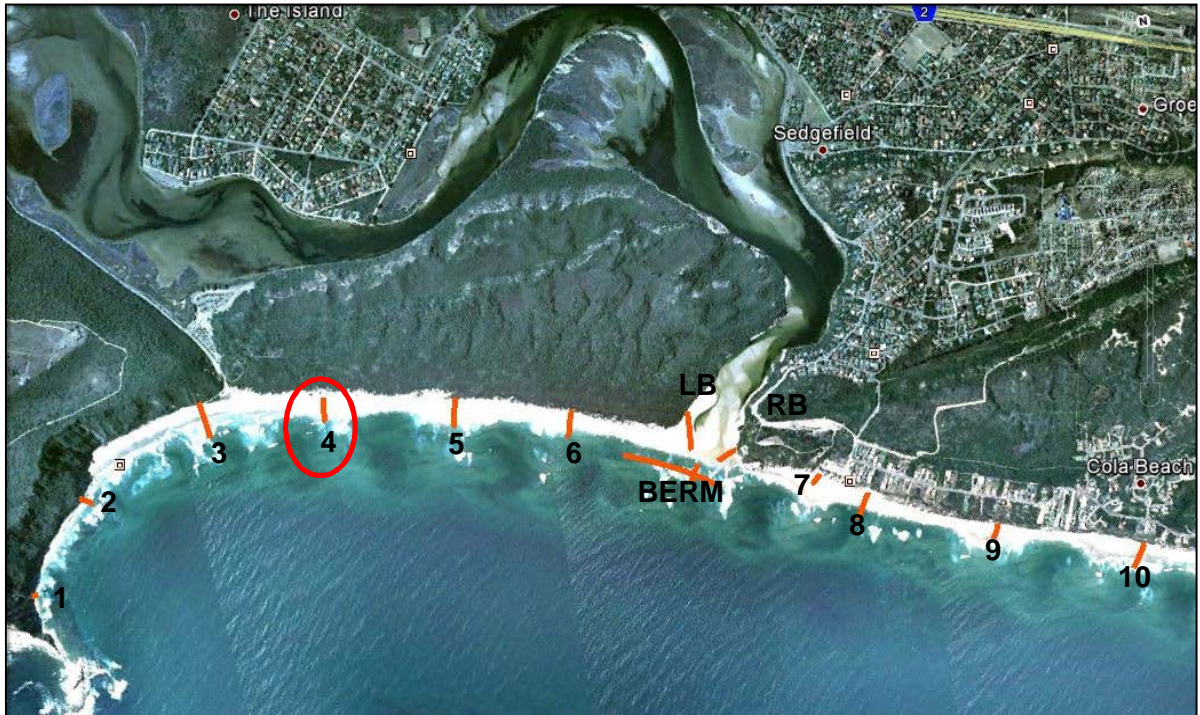


Figure 111: Position of profile four

Table 19: Position four

Point Name	Height above MSL in m	Chainage
114	-0.797	0
115	-0.836	15
116	-0.403	30
117	0.35	45
118	1.036	60
119	1.702	75
120	1.667	90
121	1.914	105
122	2.632	120
123	3.518	135
124	4.3	150
125	5.137	165
126	6.227	180
127	7.075	195
128	7.466	210

## A Preliminary Analysis of the Sediment Budget Across the Swartvlei Estuary Mouth

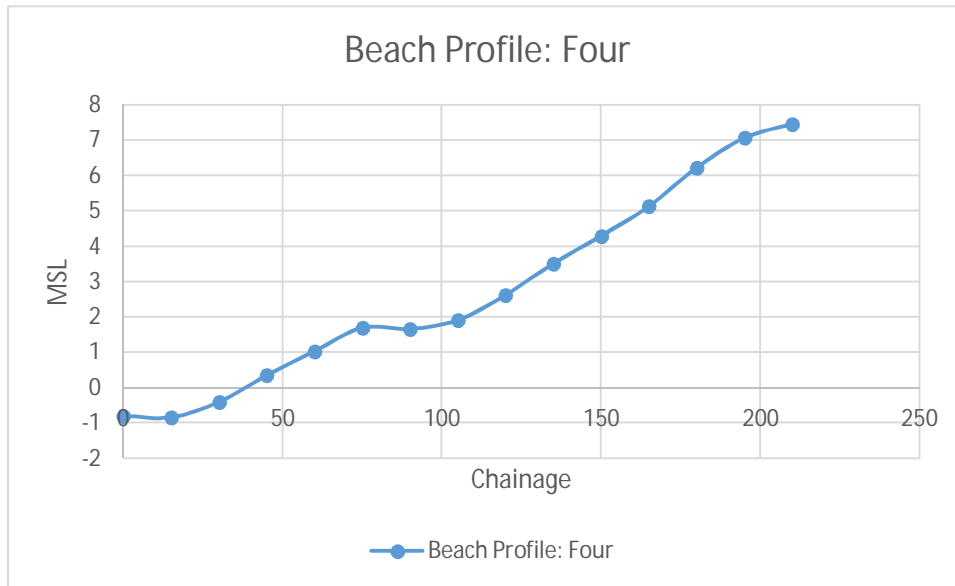


Figure 112: Profile four

The slope continues to decrease as the profiles move away from the sheer sandstone cliffs. Profile four is measured over 210 m and displays a rise in elevation of 8.3 m.

## 7.5 PROFILE FIVE

From Figure 113 the location of profile five can be seen in comparison with the Swartvlei coastline. It is located in the region between the Gericke Point parking area and the Swartvlei estuary mouth.

A Preliminary Analysis of the Sediment Budget Across the Swartvlei Estuary Mouth

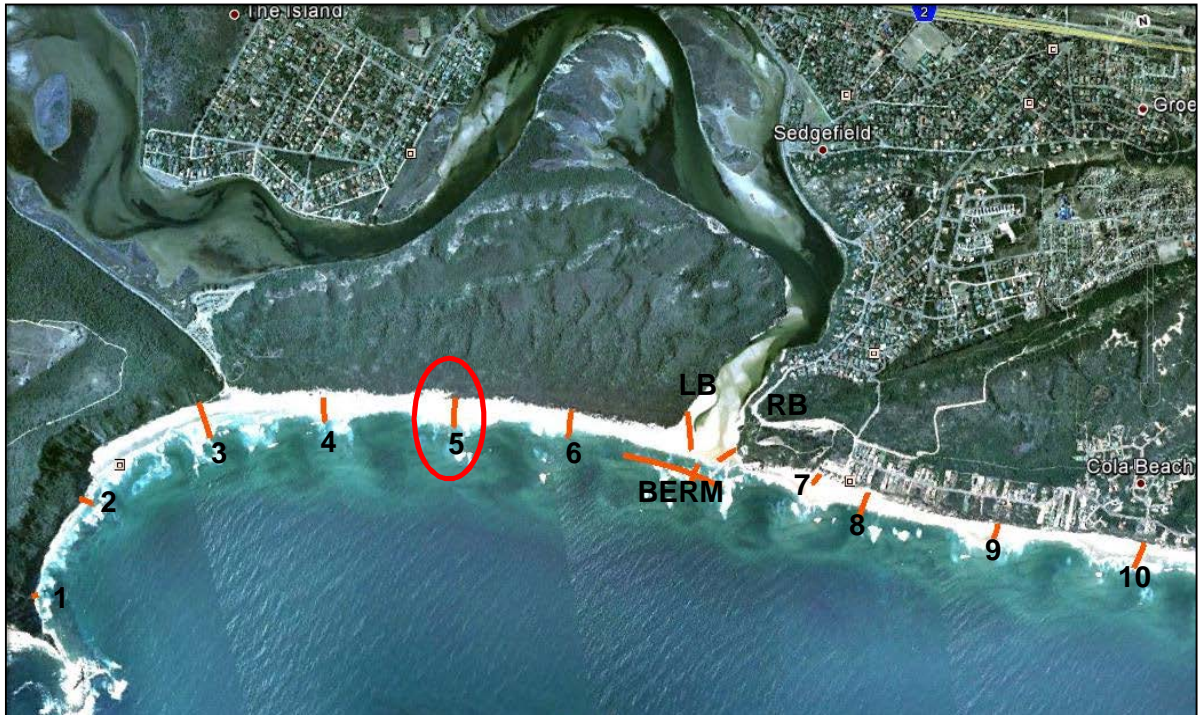


Figure 113: Location of profile five

Table 20: Profile five

Point Name	Height above MSL in m	Chainage
139	-1.126	0
140	-0.768	15
141	-0.508	30
142	-0.194	45
143	0.508	60
144	1.715	75
145	2.836	90
146	3.844	105
147	4.836	120
148	5.362	135
149	5.833	150
150	6.891	165
151	7.914	180

A Preliminary Analysis of the Sediment Budget Across the Swartvlei Estuary Mouth

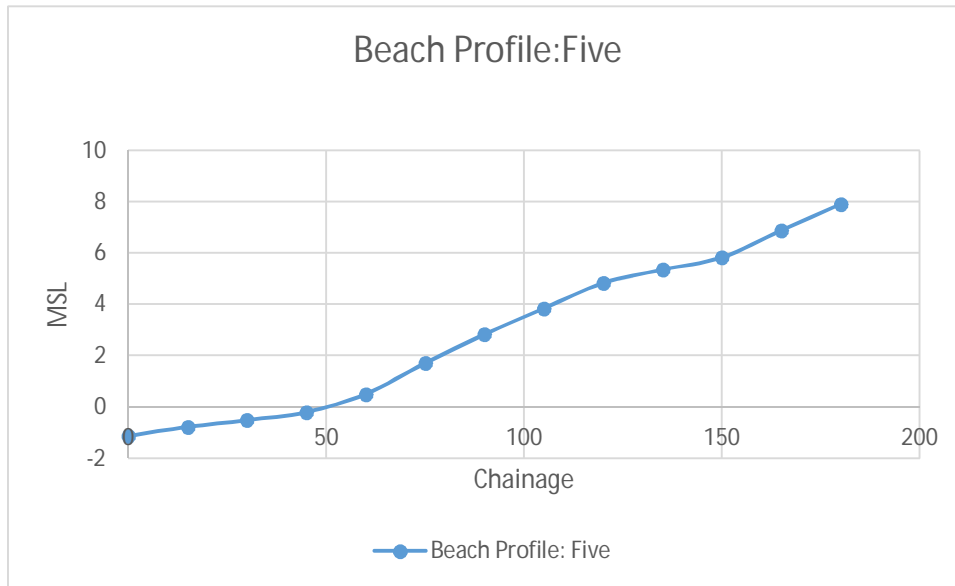


Figure 114: Profile Five

It is evident from Figures 114 and 115 that the slope is similar to that of profiles three and four. This is a result of the beach slope stabilising over the stretch from the Gericke Point parking area towards profile number five.



Figure 115: On site photo of profile five

## 7.6 PROFILE SIX

From Figure 116 the location of profile six can be seen. It is located in the region between the Gericke Point parking area and the Swartvlei estuary mouth.

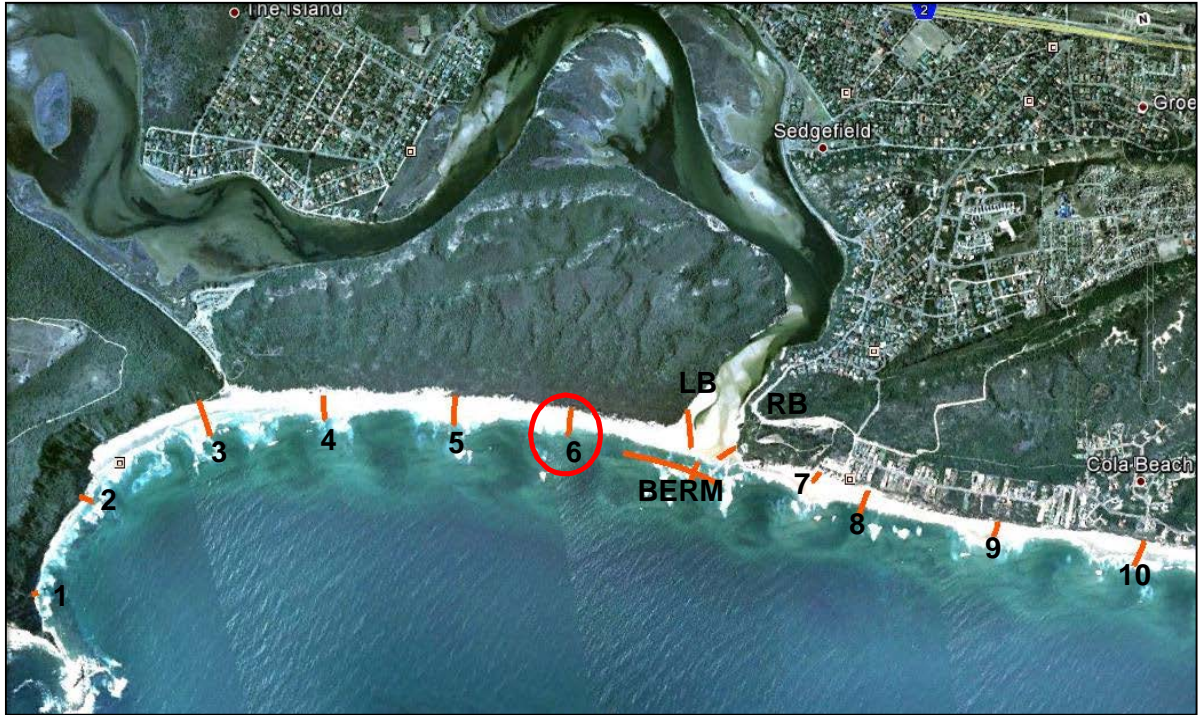


Figure 116: Position of profile six

Table 21: Profile six

Point Name	Height above MSL in m	Chainage
16	-1.302	0
17	-0.392	15
18	-0.064	30
19	0.704	45
20	1.563	60
21	1.923	75
22	2.625	90
23	3.628	105
24	5.885	120
25	8.492	135
26	11.595	150
27	12.433	165

A Preliminary Analysis of the Sediment Budget Across the Swartvlei Estuary Mouth

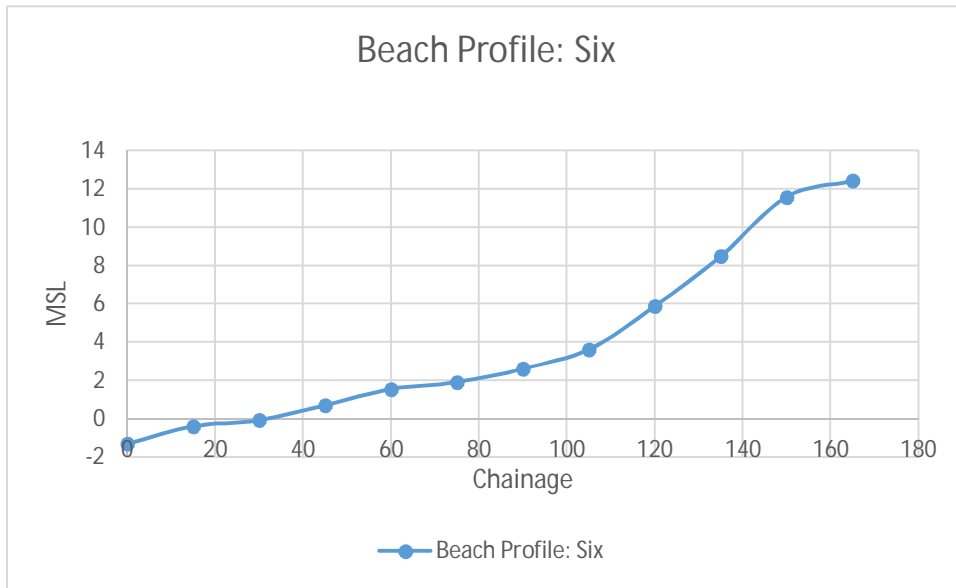


Figure 117: Profile six



Figure 118: On-site profile photo of profile six

A Preliminary Analysis of the Sediment Budget Across the Swartvlei Estuary Mouth

From data gathered at profile six, it is estimated that profile six fits into the trend of the gentle slopes as seen in profiles three to five.

### 7.7 PROFILE - LEFT BANK OF THE RIVER

From Figure 119 the location of the left bank of the river can be seen in comparison to the Swartvlei coastline.

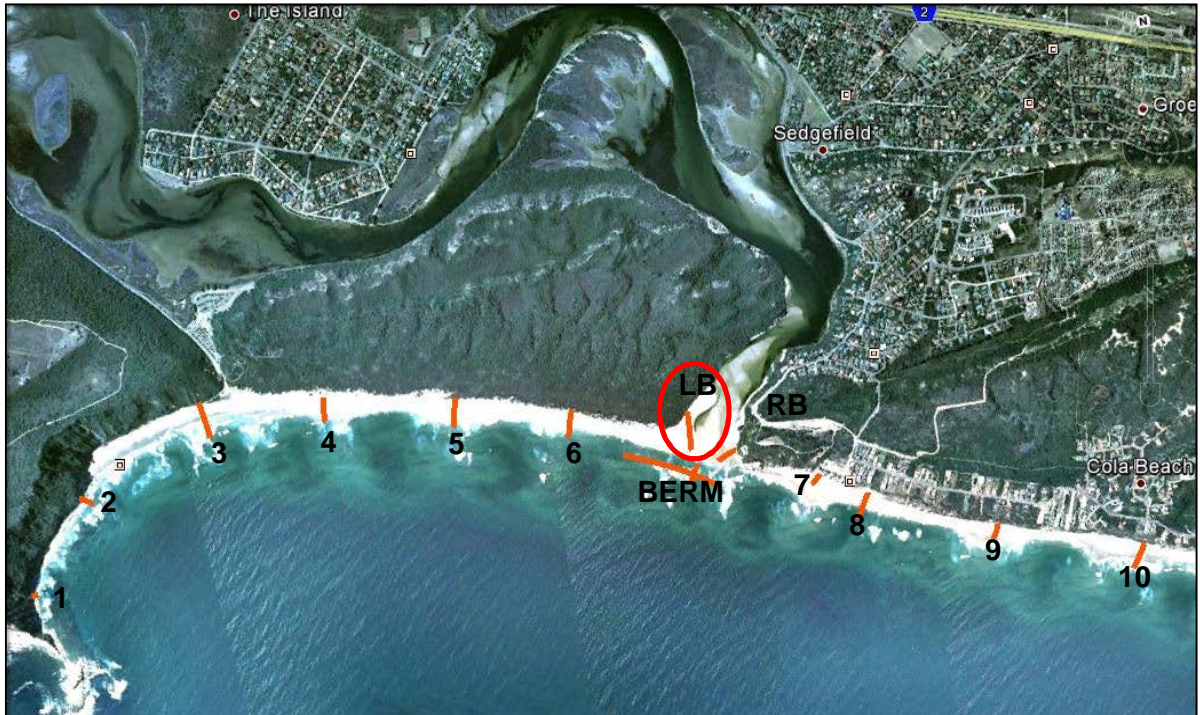


Figure 119: Position of profile LB

A Preliminary Analysis of the Sediment Budget Across the Swartvlei Estuary Mouth

Table 22: Profile LB

Point Name	Height above MSL in m	Chainage
1	-0.487	0
2	0.484	15
3	1.459	30
4	1.479	45
5	1.825	60
6	2.381	75
7	2.555	90
8	2.505	105
9	2.55	120
10	2.587	135
11	2.872	150
12	2.454	165
13	2.024	180
14	2.314	195
15	3.344	210

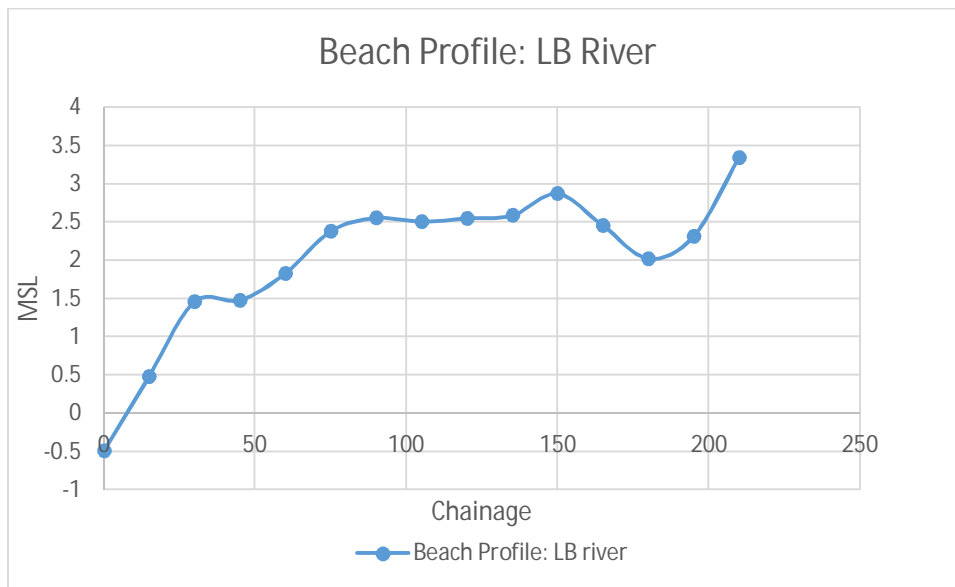


Figure 120: Illustration of profile LB

A Preliminary Analysis of the Sediment Budget Across the Swartvlei Estuary Mouth



*Figure 121: On-site photo of profile LB*



*Figure 122: On-site photo of profile LB and profile pathway in red*

From the figures presented and the surveyed data it can be seen that the left bank of the river has a relatively flat profile. It is separated from the inshore berm by a channel and evidence of partial submersion of the river bank can be seen in Figure 122.

## **7.8 PROFILE BERM-LONG PROFILE**

From Figure 123 the location of the sand berm can be seen.

A Preliminary Analysis of the Sediment Budget Across the Swartvlei Estuary Mouth

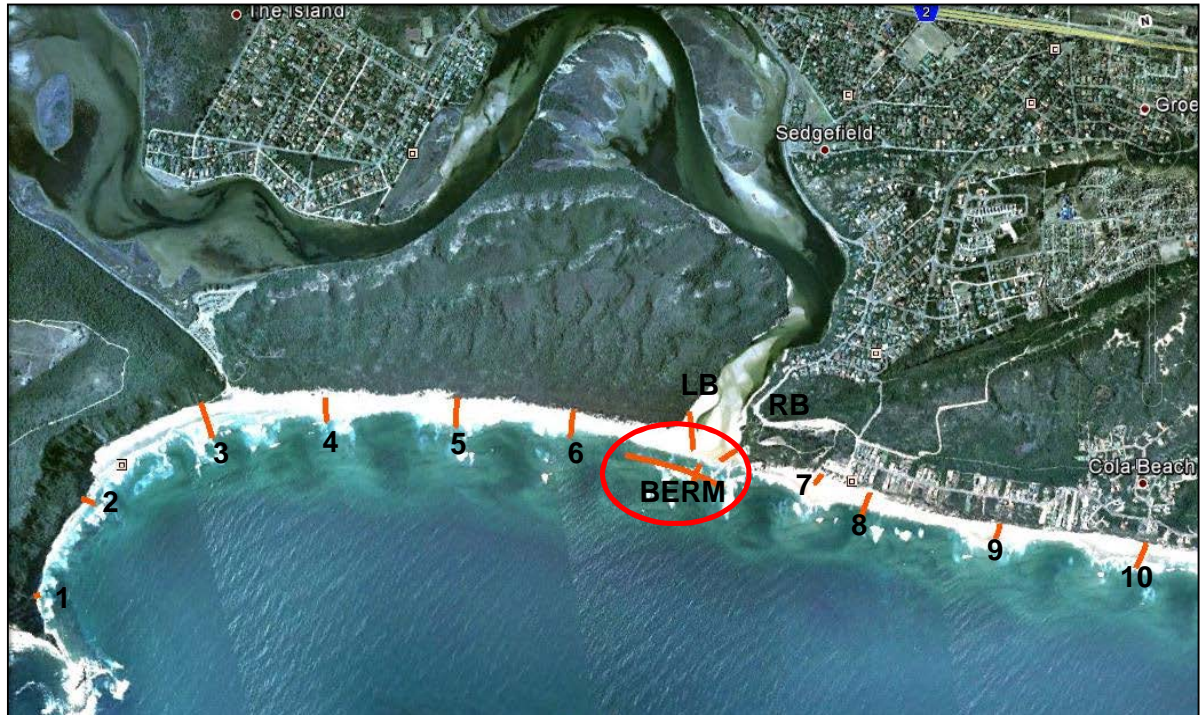


Figure 123: Location of Berm longitudinal profile

## A Preliminary Analysis of the Sediment Budget Across the Swartvlei Estuary Mouth

Table 23: Longitudinal profile of berm

Point Name	Height above MSL in m	Chainage
99	-0.769	0
98	-0.885	15
97	-0.781	30
96	-0.693	45
95	-0.569	60
94	-0.455	75
93	-0.327	90
92	-0.396	105
91	-0.43	120
90	-0.458	135
89	-0.479	150
88	-0.508	165
87	-0.437	180
86	-0.519	195
85	-0.801	210
84	-0.483	225
83	-0.47	240
82	-0.466	255
81	-0.486	270
80	-0.465	285
79	-0.411	300
78	-0.377	315
77	-0.334	330
76	-0.285	345
75	-0.254	360
74	-0.23	375
73	-0.236	390
72	-0.212	405
71	-0.167	420
70	-0.173	435
69	-0.169	450
68	-0.146	465
67	-0.134	480
66	-0.147	495
65	-0.162	510
64	-0.138	525
63	-0.176	540
62	-0.194	555
61	-0.201	570
60	-0.24	585
59	-0.269	600
58	-0.333	615
57	-0.366	630
56	-0.429	645
55	-0.389	660
54	-0.404	675
53	-0.469	690
52	-0.477	705
51	-0.535	720
50	-0.669	735
49	-0.697	750
48	-0.748	765
47	-0.864	780

A Preliminary Analysis of the Sediment Budget Across the Swartvlei Estuary Mouth

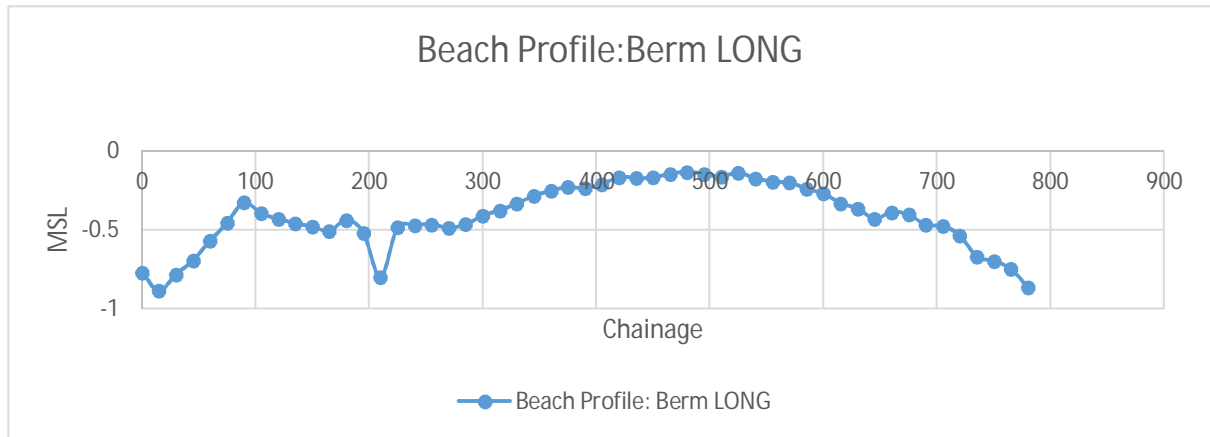


Figure 124: Illustration of Longitudinal profile of sand berm

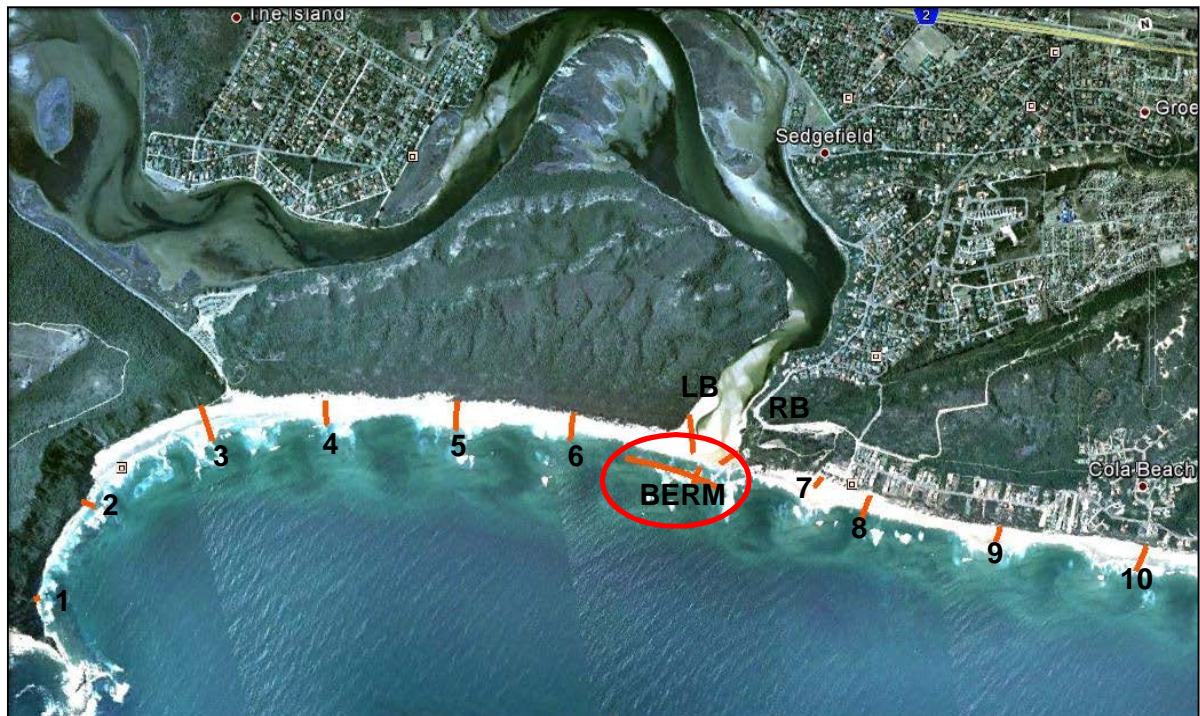


Figure 125: On-site photo of longitudinal profile of the sand berm

It is evident that the sand berm has a relatively flat profile and during high tides this berm is completely flooded. This sand berm is kept in balance by the sediment coming from the river and the wave action from the sea.

## 7.9 PROFILE BERM - CROSS PROFILE

From Figure 126 the location of the sand berm can be seen in comparison with the Swartvlei coastline.



*Figure 126: Location of cross profile of the sand berm*

Table 24: Cross Profile of sand berm

Point Name	Height above MSL in m	Chainage
45	-1.849	0
44	-1.725	15
43	-1.622	30
42	-1.486	45
41	-1.375	60
40	-1.353	75
39	-1.241	90
38	-1.215	105
37	-1.183	120
36	-1.135	135
35	-1.172	150
34	-1.135	165
33	-1.147	180
32	-1.131	195
31	-1.157	210
30	-1.15	225
29	-1.209	240
28	-0.991	255

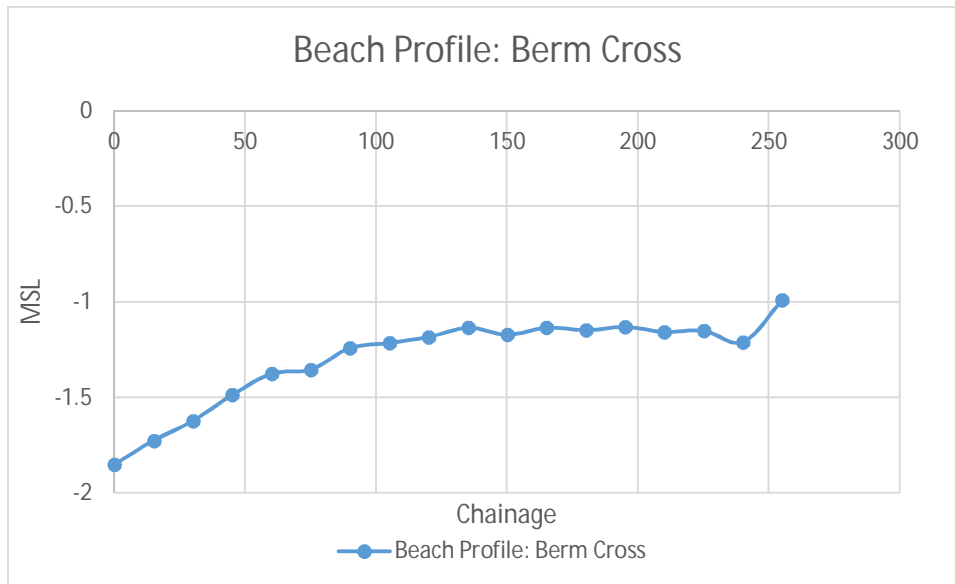


Figure 127: Cross profile of sand berm



*Figure 128: On-Site photo of sand berm cross profile*

From the data illustrated above, it is seen that this is a very flat sand berm in terms of surface slope. The relative XYZ data was measured during a low tide.

#### **7.10 PROFILE RIVER-RIGHT BANK**

From Figure 129 the location of the right bank of the estuary can be seen.

A Preliminary Analysis of the Sediment Budget Across the Swartvlei Estuary Mouth

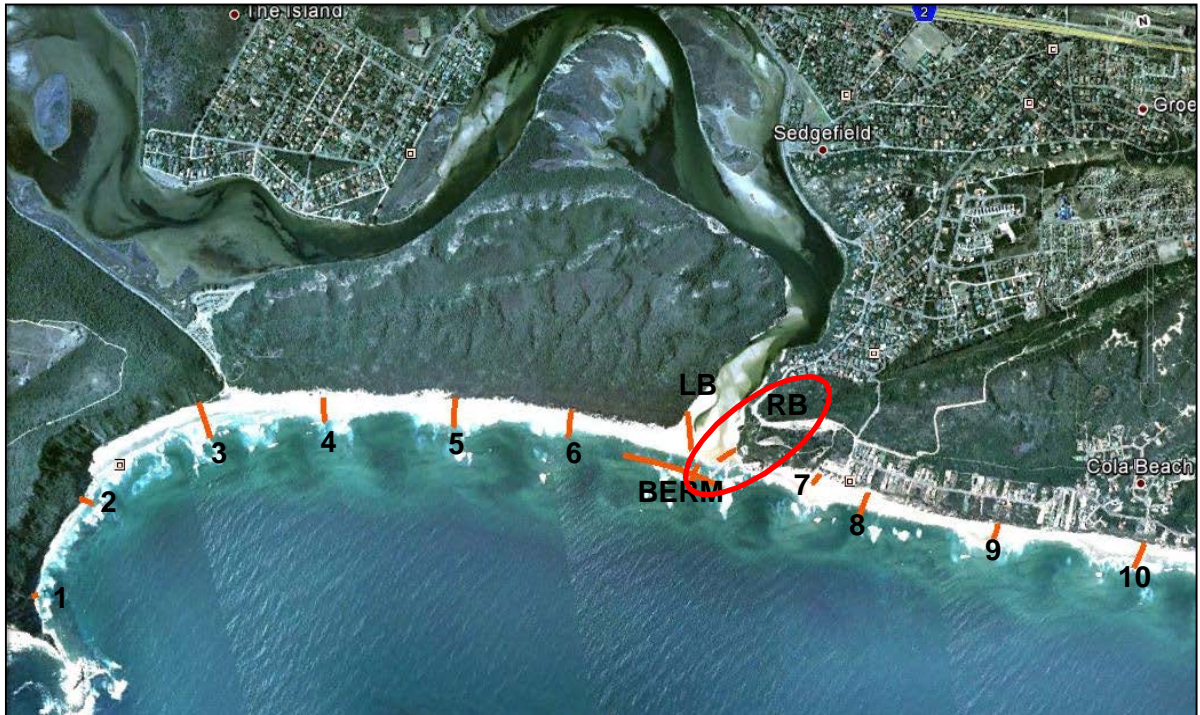


Figure 129: Location of profile RB

Table 25: River right bank profile

Point Name	Height above MSL in m	Chainage
171	0.518	0
172	1.613	15
173	2.198	30
174	2.268	45
175	2.374	60
176	2.26	75
177	2.045	90
178	2.064	105
179	2.997	120

A Preliminary Analysis of the Sediment Budget Across the Swartvlei Estuary Mouth

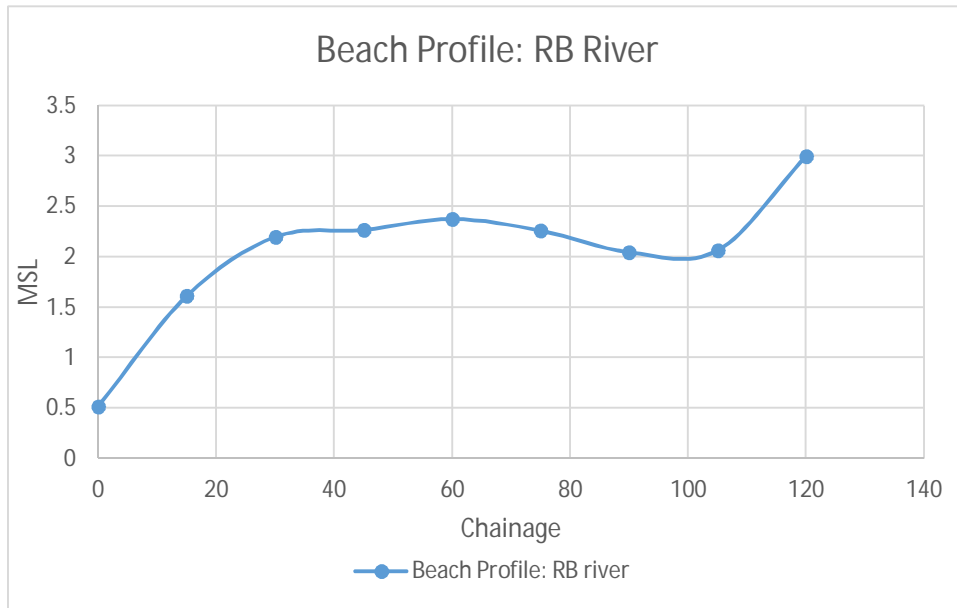


Figure 130: Profile of right bank of the river



Figure 131: On-site photo of the right bank of Swartvlei estuary

### 7.11 PROFILE SEVEN

From Figure 132 the location of profile seven can be seen.

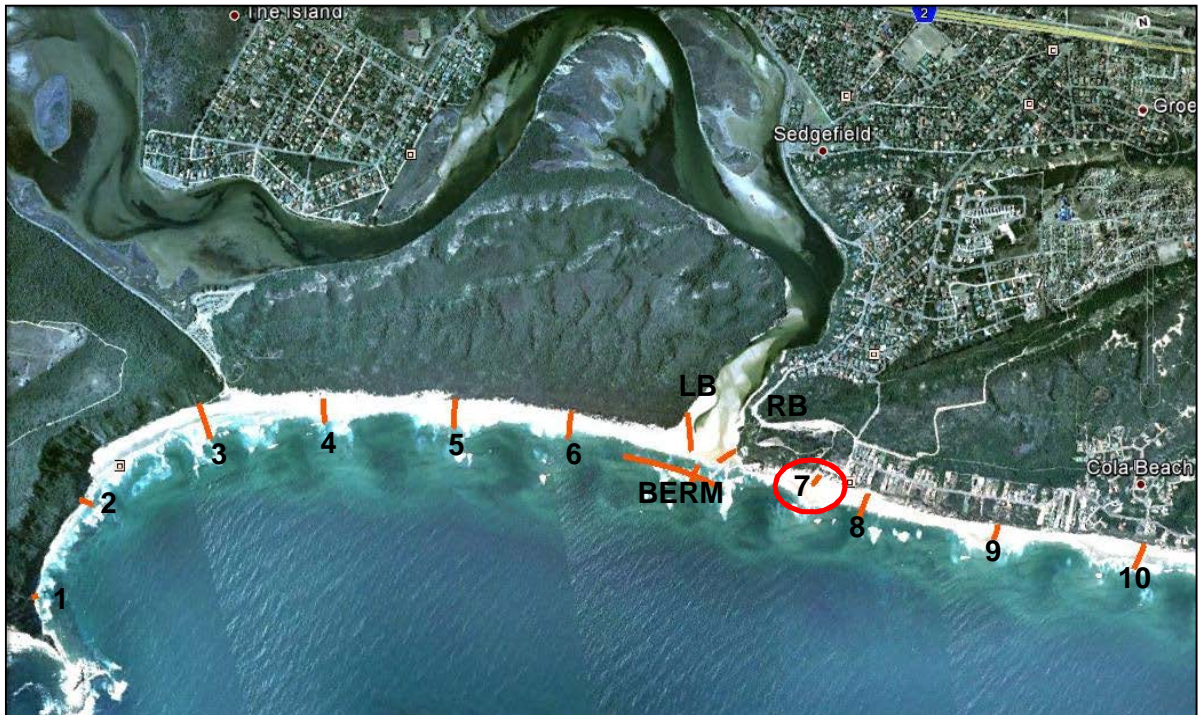


Figure 132: Location of profile seven

Table 26: Profile seven data

Point Name	Height above MSL in m	Chainage
190	0.872	0
191	1.753	15
192	3.019	30
193	3.951	45
194	5.852	60
195	8.582	75
196	13.978	90

A Preliminary Analysis of the Sediment Budget Across the Swartvlei Estuary Mouth

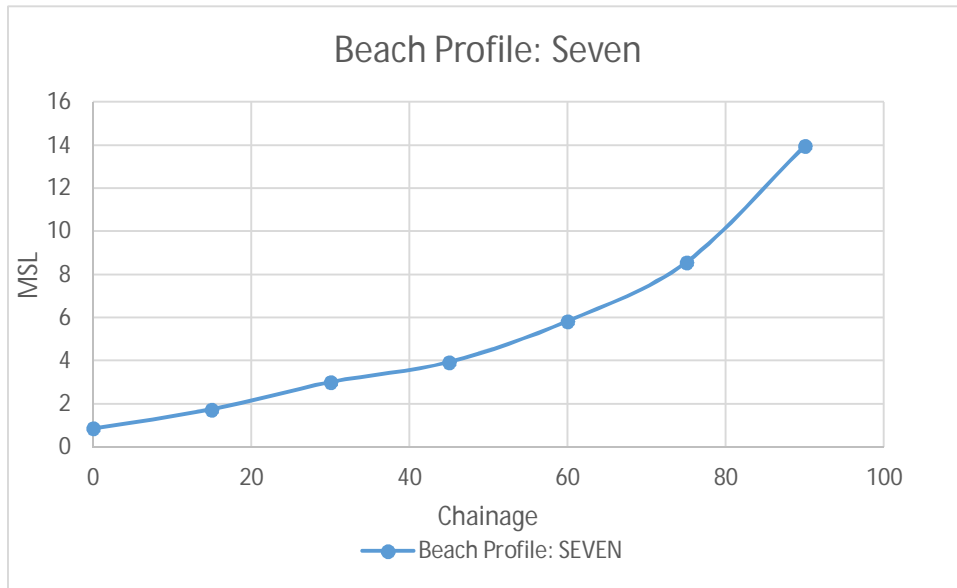


Figure 133: Illustration of profile seven



Figure 134: On-site photo of profile seven

The measurements of this profile were taken during an incoming, or pushing, tide and the rising water level can be seen in Figure 134. The following on-site photographs also show that the marine processes have access to the public property at the back of the beach section, making erosion a problem on this particular profile section.



*Figure 135: Erosion at profile seven*

## **7.12 PROFILE EIGHT**

From Figure 136 the location of profile eight can be seen. It is important to note the similarities that profile eight shares with profile seven, in order to understand the erosion and wave run-up problems these areas have.

A Preliminary Analysis of the Sediment Budget Across the Swartvlei Estuary Mouth

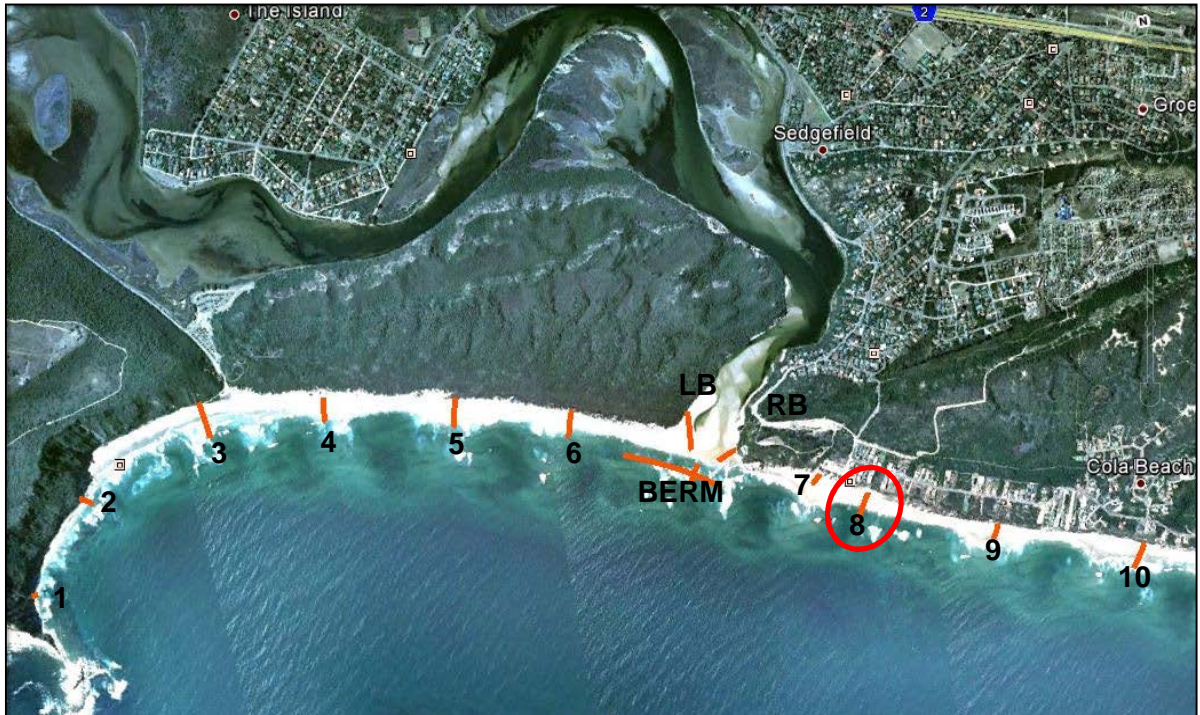
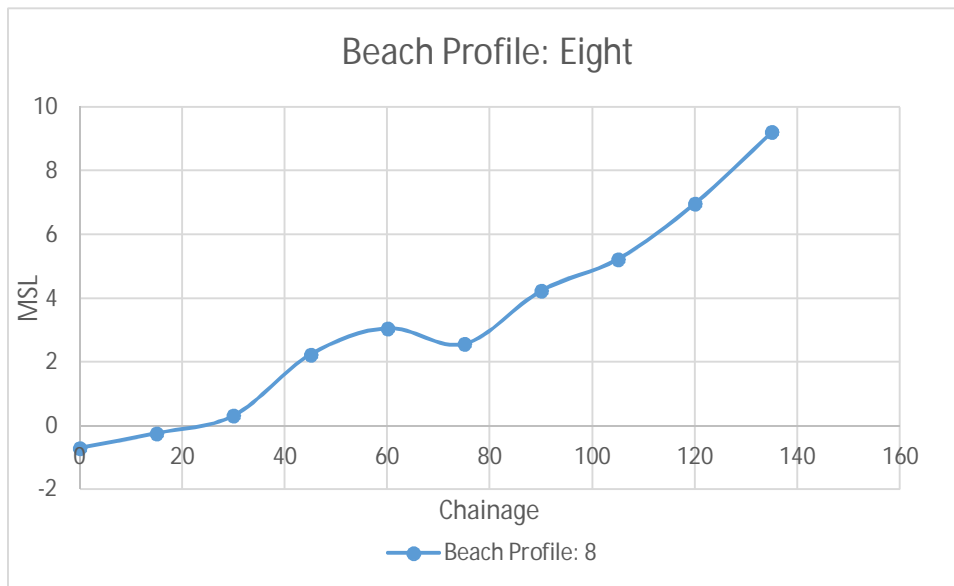


Figure 136: Location of profile 8

Table 27: Profile eight data

Point Name	Height above MSL in m	Chainage
180	-0.693	0
181	-0.234	15
182	0.319	30
183	2.241	45
184	3.065	60
185	2.569	75
186	4.239	90
187	5.235	105
188	6.982	120
189	9.216	135

## A Preliminary Analysis of the Sediment Budget Across the Swartvlei Estuary Mouth



*Figure 137: Survey of profile 8*

From the gathered data it is evident that profiles seven and eight have relatively short beach sections with steep beach dune profiles at the back. As a result of this sudden main back dune and the lack of dune buffer zones in this area, erosion is clearly affecting the man-made structures around these areas.

### 7.13 PROFILE NINE

From Figure 138 the location of profile nine can be seen in comparison to the Swartvlei coastline.

A Preliminary Analysis of the Sediment Budget Across the Swartvlei Estuary Mouth

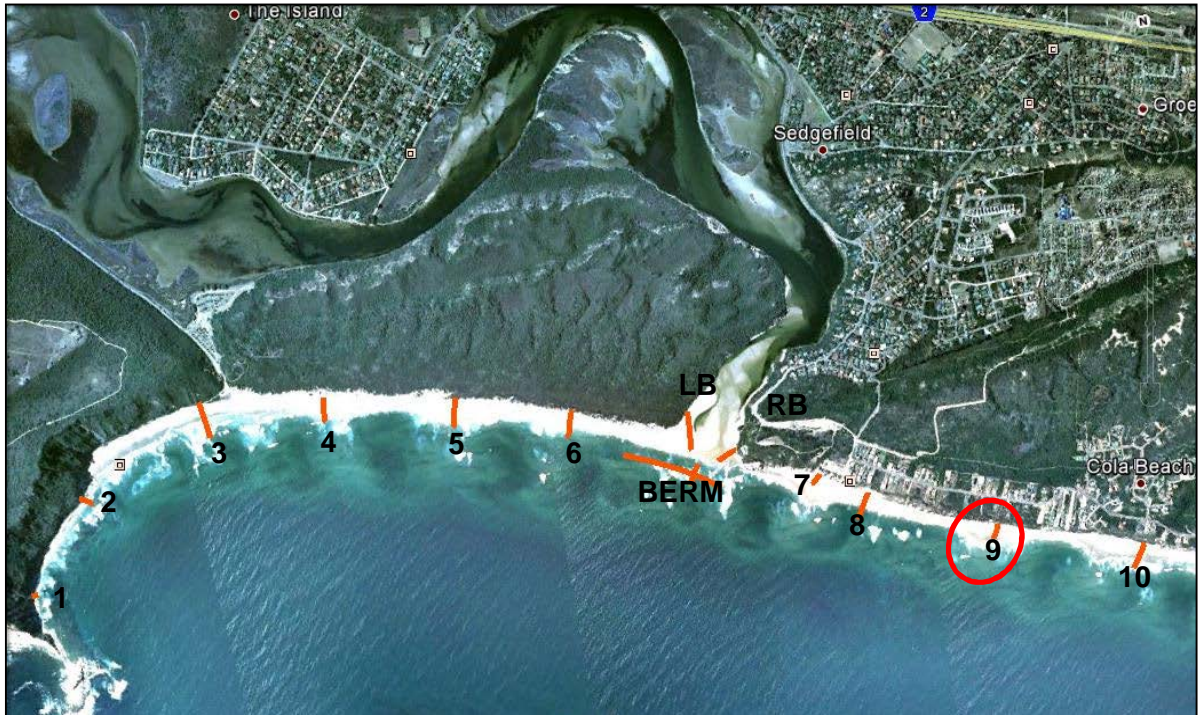


Figure 138: Location of profile nine

Table 28: Profile nine data

Point Name	Height above MSL in m	Chainage
162	1.159	0
163	2.457	15
164	2.035	30
165	3.175	45
166	6.66	60
167	7.427	75
168	9.357	90
169	10.003	105
170	12.314	120

A Preliminary Analysis of the Sediment Budget Across the Swartvlei Estuary Mouth

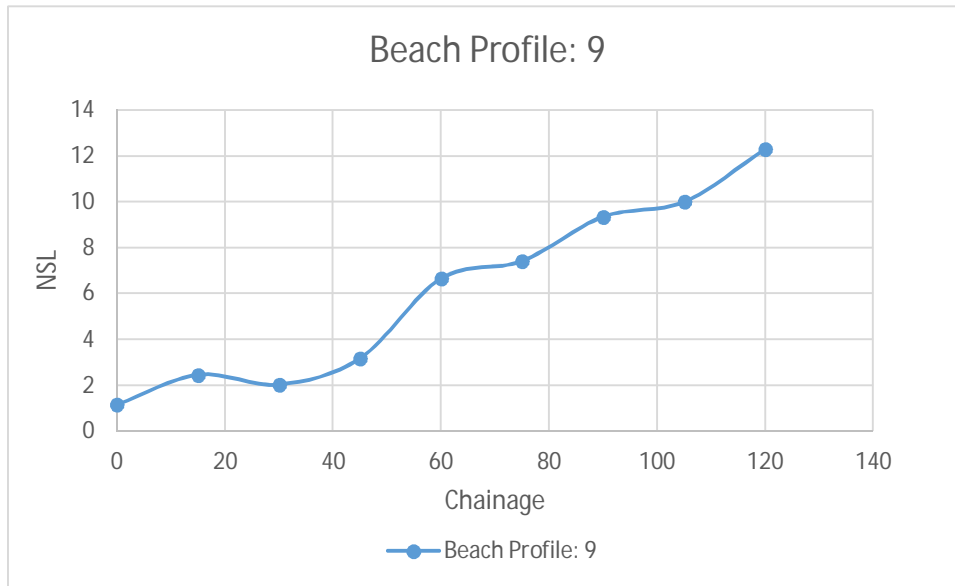


Figure 139: Illustration of profile nine



Figure 140: On-site photo of profile nine

From the above photo a slight build-up of sediment can be seen protecting the back dune. The beaches are still relatively narrow, with steep dunes at the back, thus allowing waves to access the main dunes at the back quite frequently during storm periods.

### 7.14 PROFILE TEN

From Figure 141 the location of profile ten can be seen.

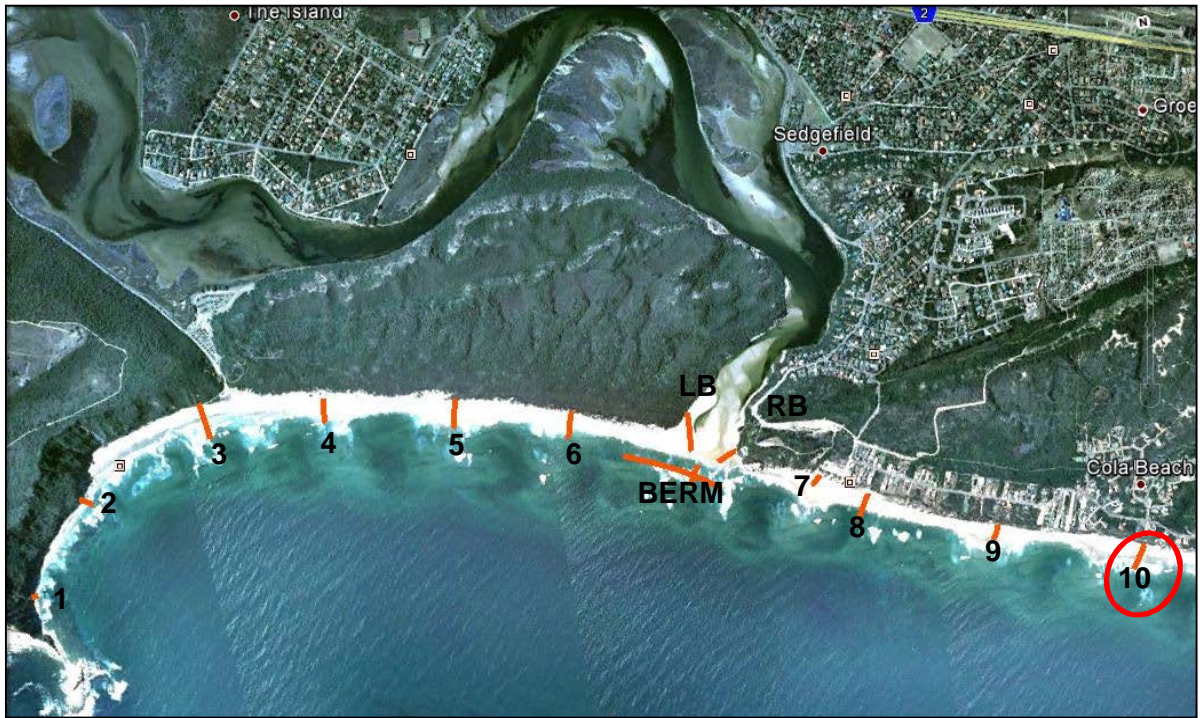


Figure 141: Location of profile 10

Table 29: Profile ten data

Point Name	Height above MSL in m	Chainage
152	-0.622	0
153	0.077	15
154	2.498	30
155	2.983	45
156	2.113	60
157	2.605	75
158	2.959	90
159	4.736	105
160	5.172	120
161	6.41	135

A Preliminary Analysis of the Sediment Budget Across the Swartvlei Estuary Mouth

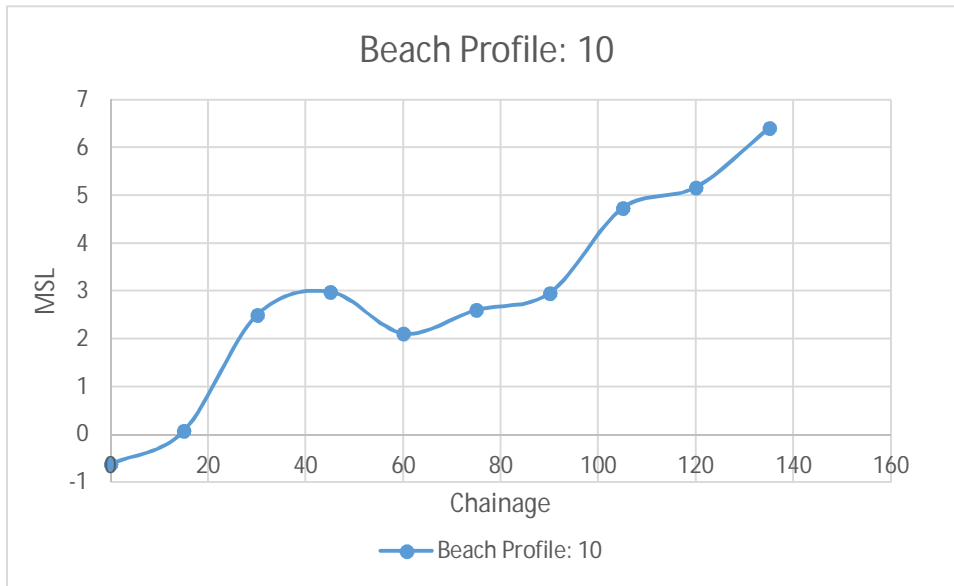


Figure 142: Illustration of profile ten

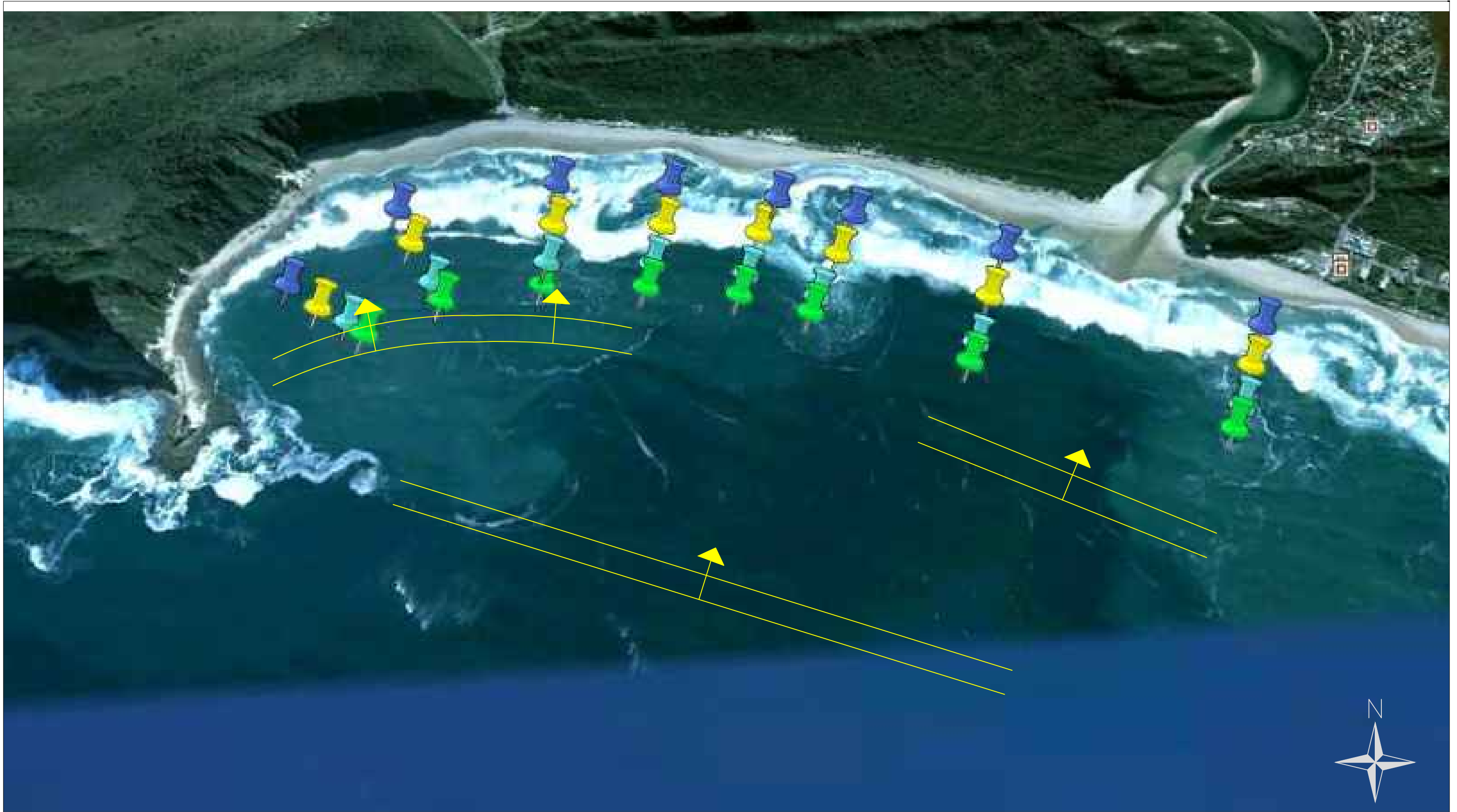
## **APPENDIX 8: KAMPHUIS BULK SEDIMENT TRANSPORT CALCULATION**

Db 2 4 6 8  
 Hb 1.2 2.4 3.6 4.8

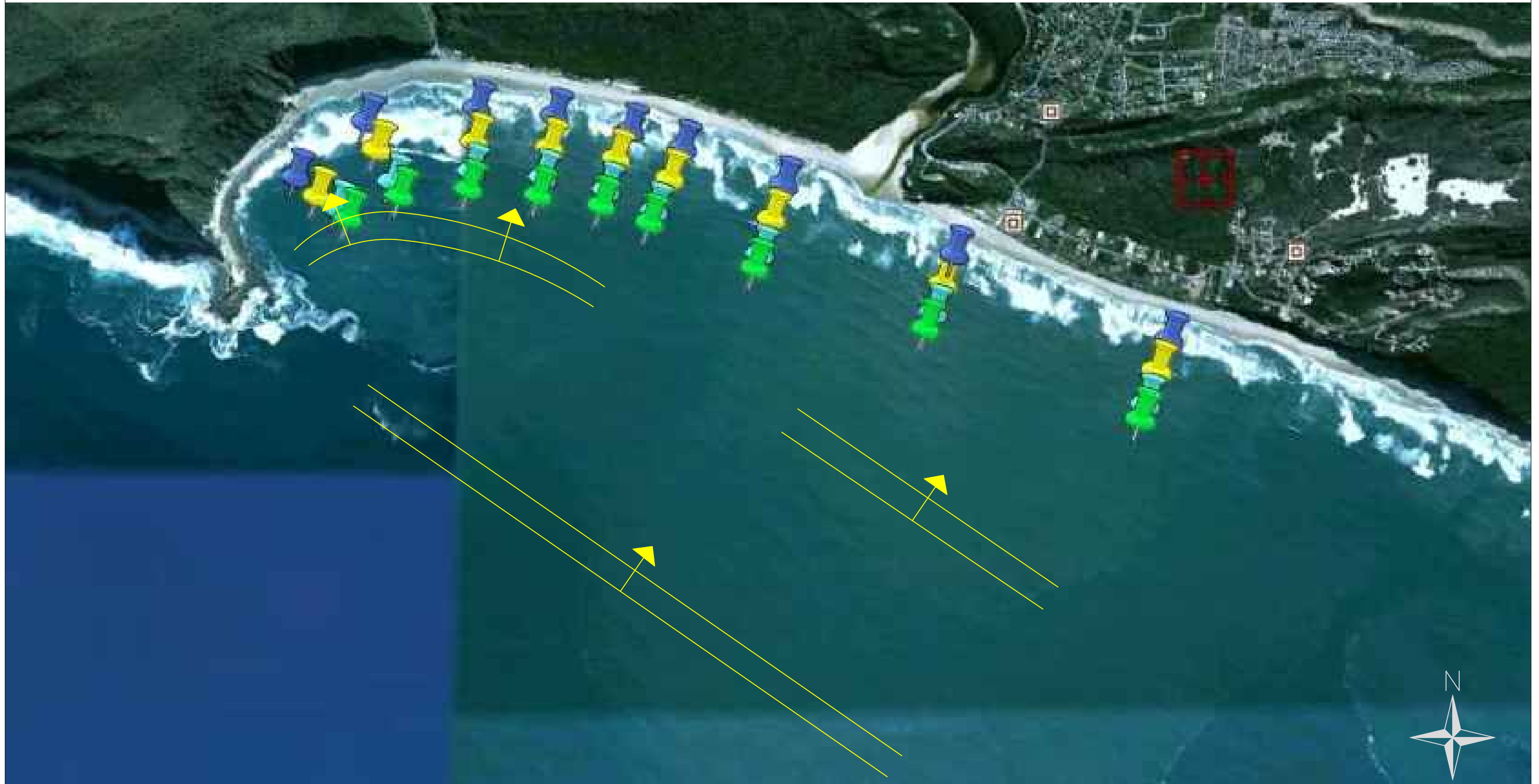
Comulative approach

Line	Point	Depth at breaking(D <sub>b</sub> )	Wave heigh@breaking(H <sub>b</sub> ) @ 0.6*Db	Avg Hb	Occurance of wave breaking between next landward point	Weight ito year	Tp	Mean Wave dir (Degrees)	Shore Normal (Degrees)	Alpha (Degrees)	Rad	mb	D50	Q	Q (weighted value)	Total year( m3/year)
1	1	2	1.2	0.714	355	0.364850976	11.1018	150.632	150	0.632	0.01103	0.016	0.23	22461.7775	8195.201452	105253.247
	10	4	2.4	1.452	550	0.565262076	12.1328	150.879	150	0.879416	0.015349	0.016	0.23	125147.4926	70741.1315	
	31	6	3.6	2.636	68	0.069886948	12.93528	151.216	150	1.216494	0.021232	0.016	0.23	376564.0797	26316.9141	
	19	8	4.8	Not breaking	0	0										
					973	1										
2	2	2	1.2	0.725	367	0.377183967	11.217	168.954	168	0.954	0.01665	0.014	0.23	26420.85658	9965.5235	110554.848
	11	4	2.4	1.468	534	0.548818088	12.3778	168.987	168	0.98743	0.017234	0.014	0.23	125062.8519	68636.75529	
	32	6	3.6	2.613	72	0.073997945	13.05768	169.764	168	1.7644	0.030795	0.014	0.23	431803.4706	31952.56926	
	20	8	4.8	Not breaking	0	0										
					973	1										
3	3	2	1.2	0.755	347	0.356628983	12.08688	180.098	179	1.09761	0.019157	0.012	0.23	28636.32304	10212.54275	140749.777
	12	4	2.4	1.526	535	0.549845838	12.7436	180.701	179	1.701	0.029688	0.012	0.23	161253.2593	88664.4334	
	33	6	3.6	2.624	91	0.09352518	12.88928	181.348	179	2.3484521	0.040988	0.012	0.23	447716.8741	41872.80118	
	21	8	4.8	Not breaking	0	0										
					973	1										
4	4	2	1.2	0.761	300	0.308324769	13.918	187.268	187	0.2683	0.004683	0.012	0.23	15197.58924	4685.793187	172670.773
	13	4	2.4	1.533	589	0.605344296	12.76569	189.480	187	2.47974	0.04328	0.012	0.23	202621.4419	122655.7341	
	34	6	3.6	2.637	84	0.086330935	12.88977	190.065	187	3.065	0.053494	0.012	0.23	525063.7663	45329.24601	
	22	8	4.8	Not breaking	0	0										
					973	1										
5	5	2	1.2	0.897	303	0.311408016	11.1387	191.065	190	1.065	0.018588	0.012	0.23	24879.54089	7747.688479	186807.748
	14	4	2.4	1.573	581	0.597122302	12.21621	192.864	190	2.8639	0.049984	0.012	0.23	206750.3653	123455.2541	
	35	6	3.6	2.686	88	0.090441932	12.8063	193.921	190	3.92086	0.068432	0.012	0.23	602328.8441	54475.78446	
	23	8	4.8	3.574	1	0.001027749	12.9324	193.993	190	3.993	0.069691	0.012	0.23	1098537.422	1129.020989	
					973	1										
6	6	2	1.2	0.950	273	0.28057554	11.08606	195.027	194	1.0269	0.017923	0.012	0.3	22616.18311	6345.547779	188212.124
	15	4	2.4	1.628	600	0.616649538	11.97978	196.863	194	2.86341	0.049976	0.012	0.3	187854.5413	115840.416	
	36	6	3.6	2.706	96	0.098663926	12.7147	198.715	194	4.715	0.082292	0.012	0.3	622308.4882	61399.39863	
	24	8	4.8	3.557	4	0.004110997	12.91721	198.663	194	4.6633	0.08139	0.012	0.3	1125459.838	4626.761926	
					973	1										
7	7	2	1.2	1.025	224	0.230215827	11.1308	196.974	196	0.9741548	0.017002	0.012	0.3	22044.9257	5075.090808	202808.891
	16	4	2.4	1.638	645	0.662898253	11.9714	198.784	196	2.7841815	0.048593	0.012	0.3	184534.7274	122327.7484	
	37	6	3.6	2.748	96	0.098663926	12.7091	200.891	196	4.8911	0.085366	0.012	0.3	635600.1128	62710.80249	
	25	8	4.8	3.692	8	0.008221994	12.95	203.915	196	7.915	0.138143	0.012	0.3	1544059.682	12695.24918	
					973	1										
8	8	2	1.2	1.048	197	0.202466598	11.08488	199.879	199	0.8794	0.015349	0.012	0.3	20604.58168	4171.739559	212115.136
	17	4	2.4	1.710	612	0.628982528	11.8151	201.306	199	2.3060	0.040247	0.012	0.3	161637.723	101667.3037	
	38	6	3.6	2.753	157	0.161356629	12.5411	203.461	199	4.4610	0.077859	0.012	0.3	589853.0873	95176.70577	
	26	8	4.8	3.798	7	0.007194245	13.12827	206.632	199	7.6319	0.133202	0.012	0.3	1542814.779	11099.3869	
					973	1										
9	9	2	1.2	1.086	177	0.181911614	11.65948	199.894	199	0.8942	0.015606	0.012	0.3	22450.4558	4083.998641	226478.999
	18	4	2.4	1.785	616	0.633093525	11.82787	201.411	199	2.4110	0.04208	0.012	0.3	166273.4693	105266.6569	
	39	6	3.6	2.790	173	0.177800617	12.47147	203.608	199	4.6080	0.080425	0.012	0.3	596340.5806	106029.723	
	27	8	4.8	3.796	7	0.007194245	13.12827	206.631	199	7.6310	0.133186	0.012	0.3	1542708.208	11098.6202	
					973	1										

## **APPENDIX 9: LAYOUT OF INCIDENT WAVE ANGLE**



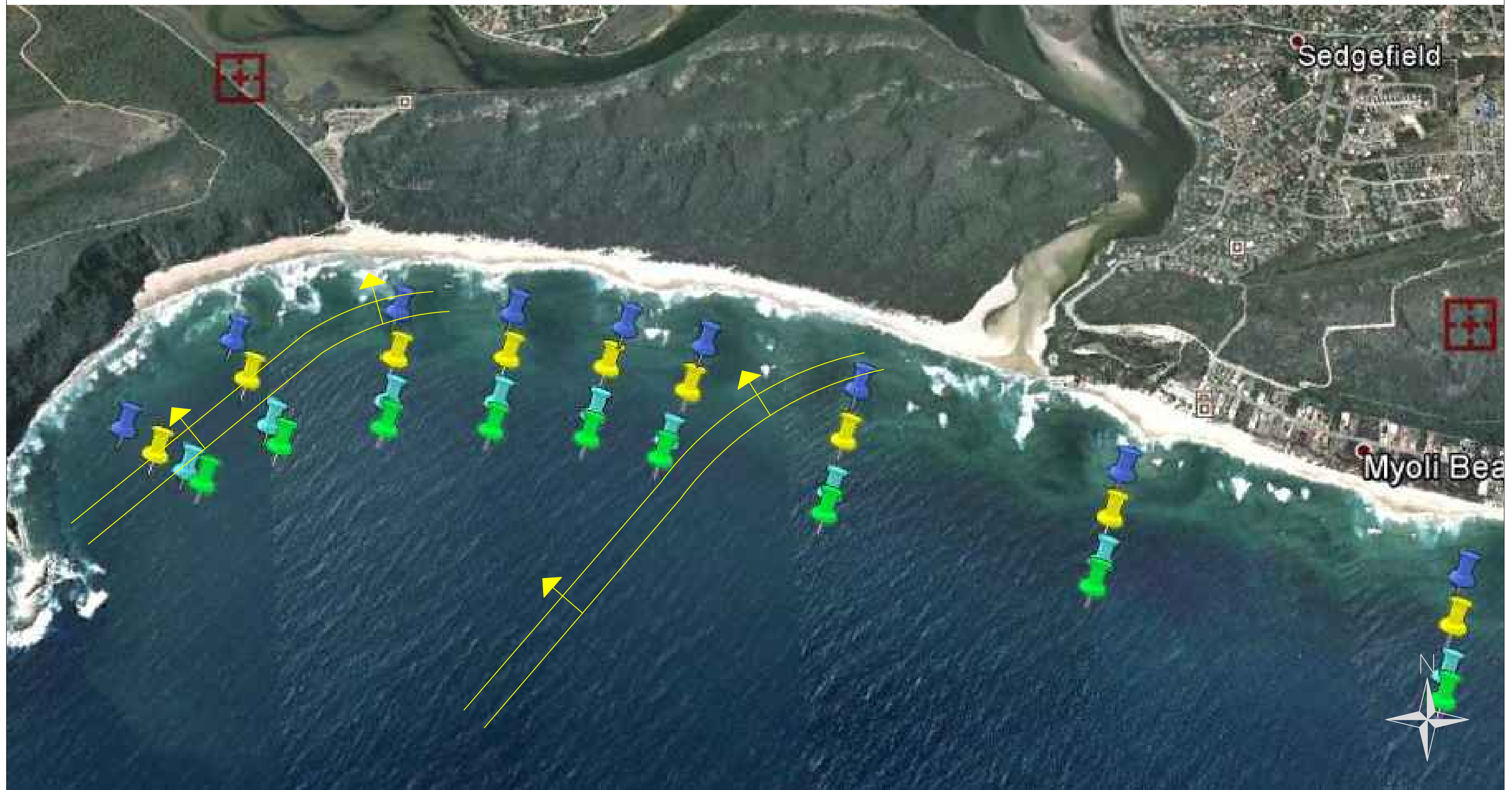
Project	A PRELIMINARY ANALYSIS OF THE SEDIMENT BUDGET ACCROSS THE SWARTVLEI ESTUARY MOUTH--A.ROETS
Description	HISTORICAL AERIAL IMAGERY WAVE ANGLE ANALYSIS
Scenario	SCENARIO #1: 2003
Date	2014



Project	A PRELIMINARY ANALYSIS OF THE SEDIMENT BUDGET ACCROSS THE SWARTVLEI ESTUARY MOUTH-A.ROETS
Description	HISTORICAL AERIAL IMAGERY WAVE ANGLE ANALYSIS
Scenario	SCENARIO #2: 2004
Date	2014



Project	A PRELIMINARY ANALYSIS OF THE SEDIMENT BUDGET ACCROSS THE SWARTVLEI ESTUARY MOUTH-A.ROETS
Description	HISTORICAL AERIAL IMAGERY WAVE ANGLE ANALYSIS
Scenario	SCENARIO #3: 2006
Date	2014



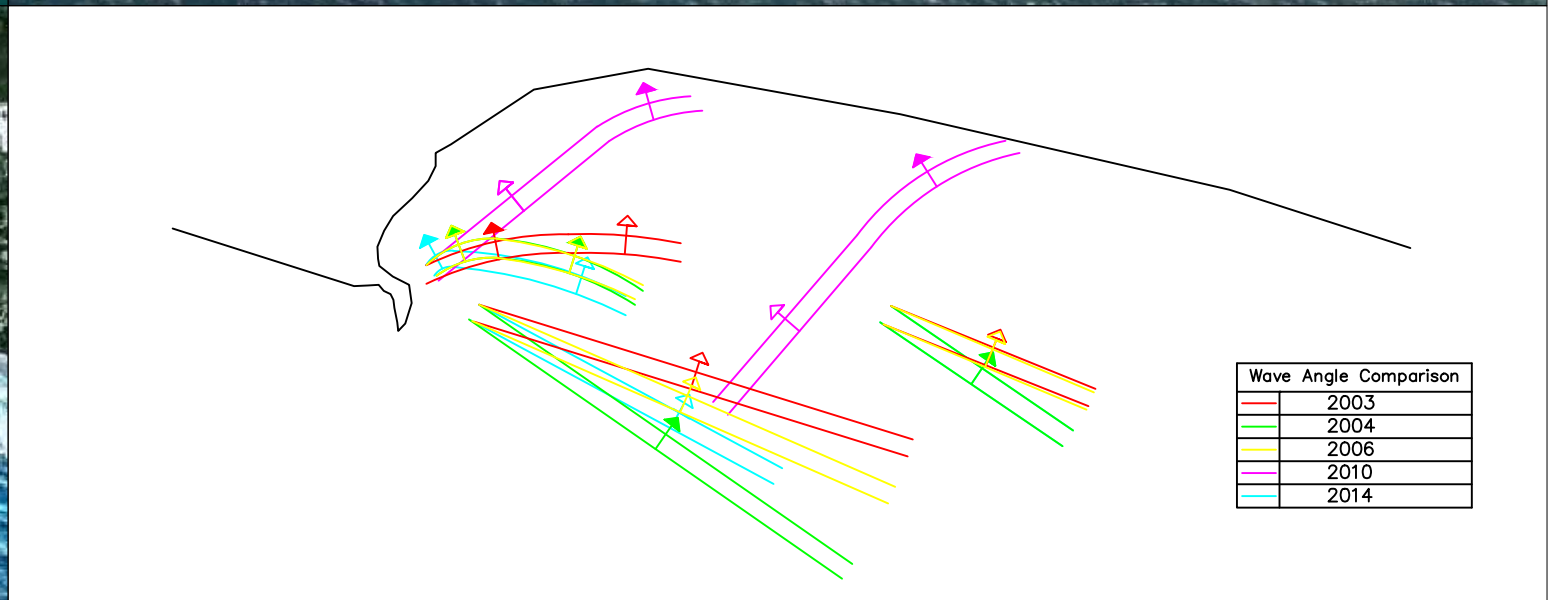
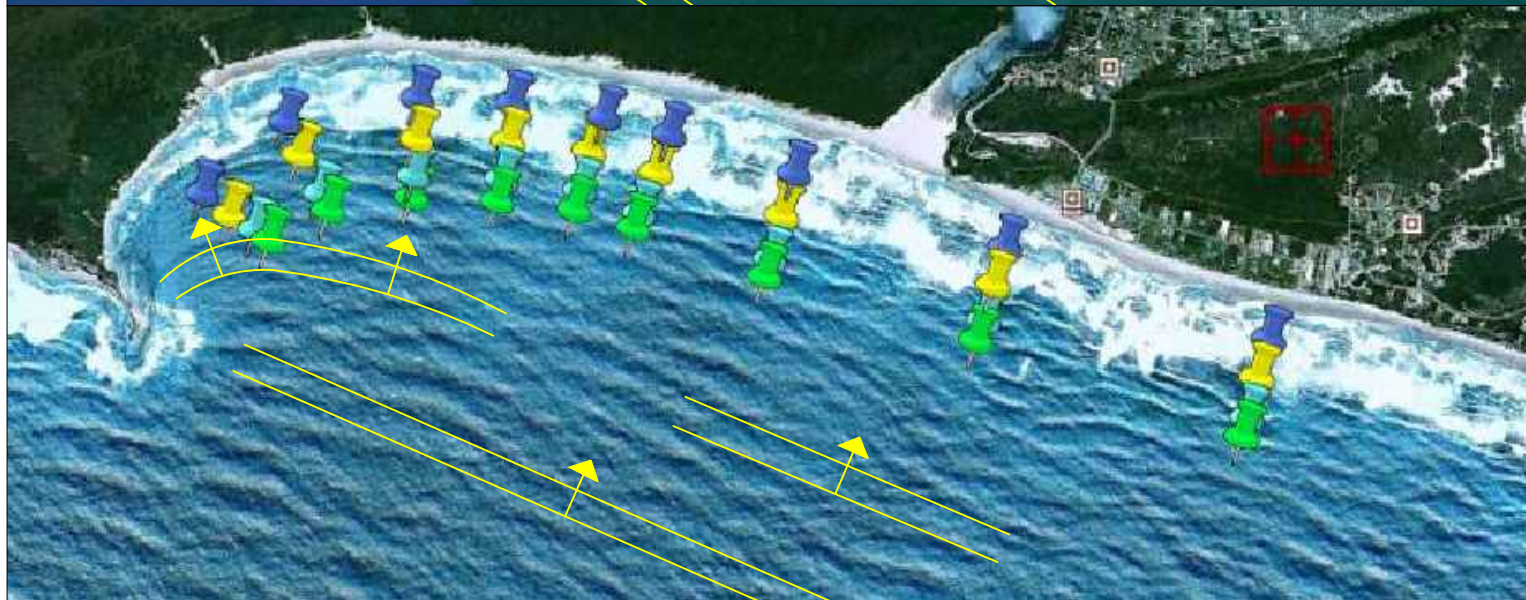
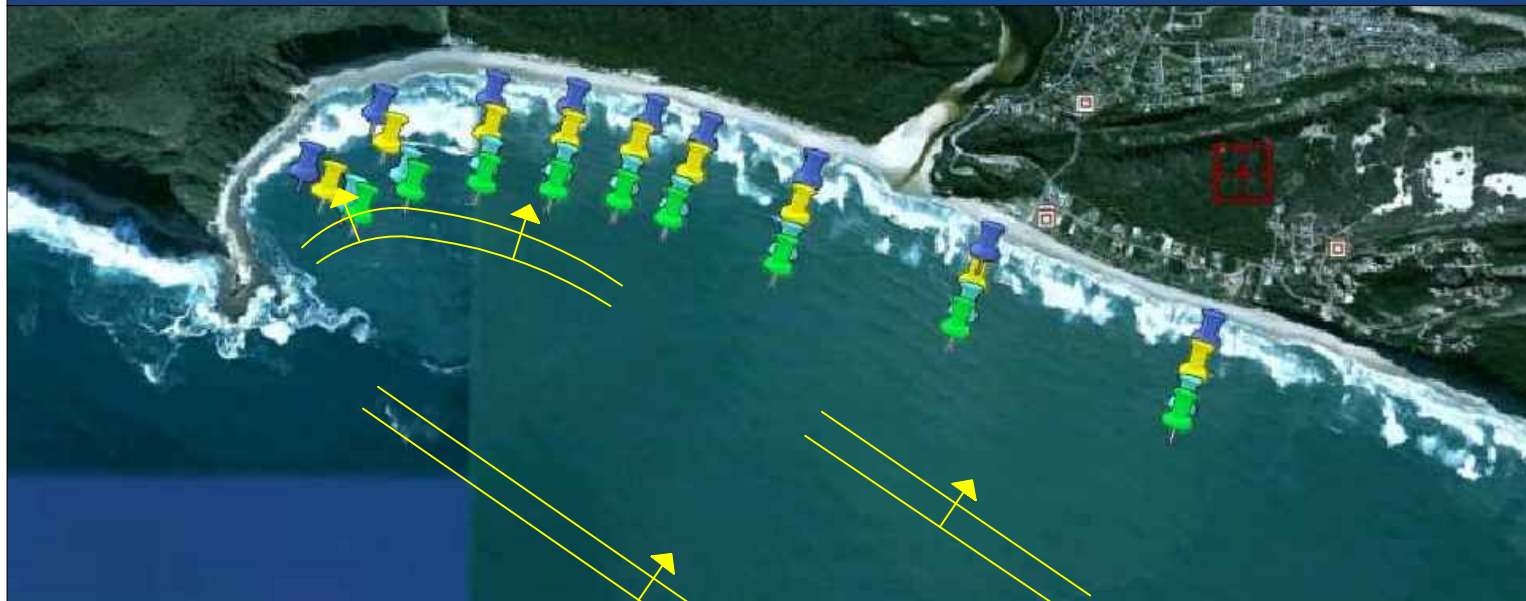
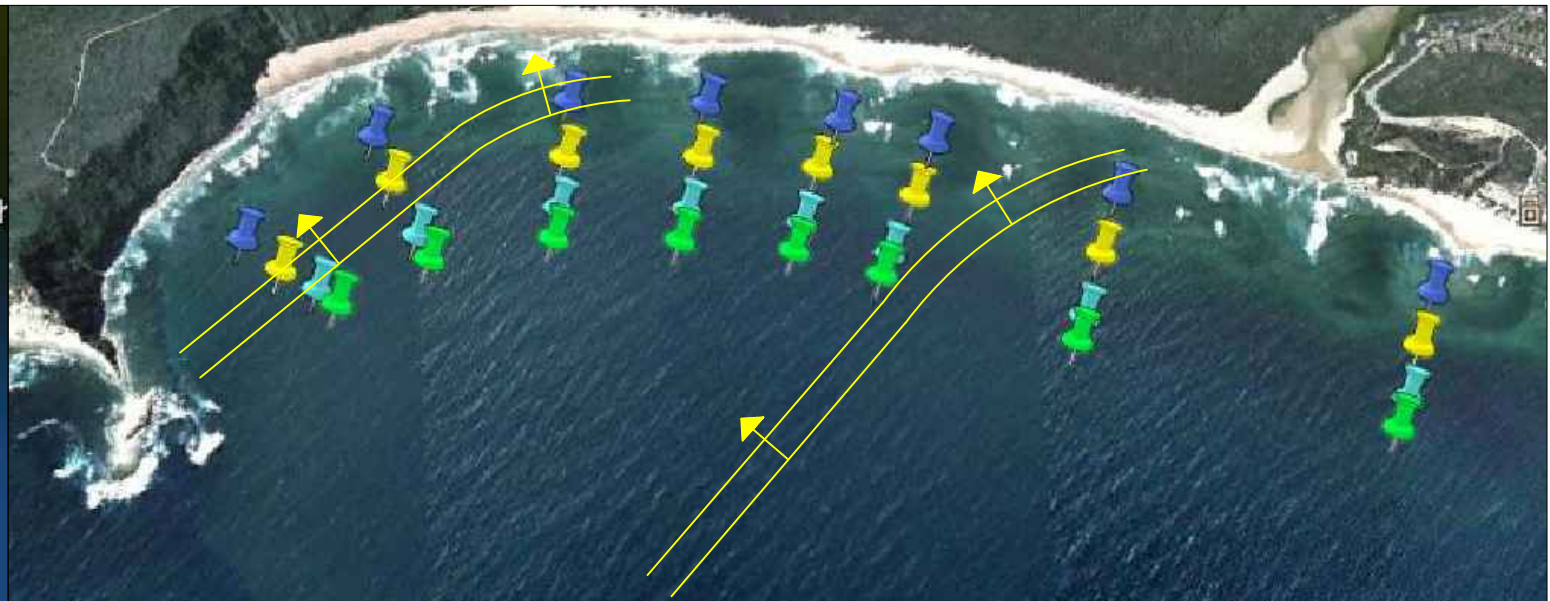
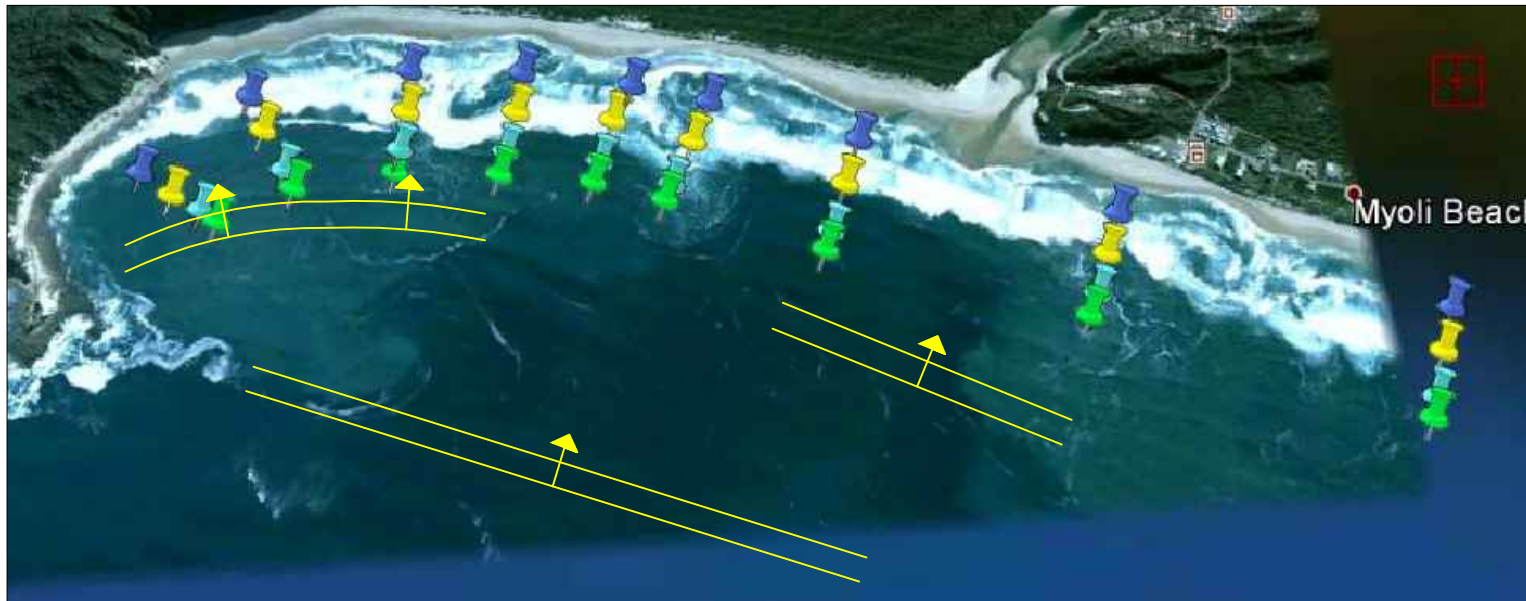
Project	A PRELIMINARY ANALYSIS OF THE SEDIMENT BUDGET ACCROSS THE SWARTVLEI ESTUARY MOUTH-A.ROETS
Description	HISTORICAL AERIAL IMAGERY WAVE ANGLE ANALYSIS
Scenario	SCENARIO #4: 2010
Date	2014



Cola Beach



Project	A PRELIMINARY ANALYSIS OF THE SEDIMENT BUDGET ACCROSS THE SWARTVLEI ESTUARY MOUTH-A.ROETS
Description	HISTORICAL AERIAL IMAGERY WAVE ANGLE ANALYSIS
Scenario	SCENARIO #5: 2014
Date	2014



Project	A PRELIMINARY ANALYSIS OF THE SEDIMENT BUDGET ACCROSS THE SWARTVLEI ESTUARY MOUTH-A.ROETS
Description	HISTORICAL AERIAL IMAGERY WAVE ANGLE ANALYSIS
Scenario	SCENARIO #: OVERVIEW
Date	2014

## **APPENDIX 10: MIKE OUTPUT LOCATIONS**

<u>ID</u>	<u>X</u>	<u>Y</u>
1	663187	6232800
2	663490	6233051
3	663972	6233106
4	664316	6233065
5	664649	6232990
6	664881	6232908
7	665323	6232730
8	666058	6232405
9	666961	6232007
10	663285	6232714
11	663539	6232924
12	663966	6232953
13	664297	6232923
14	664590	6232867
15	664826	6232771
16	665268	6232579
17	666005	6232274
18	666904	6231875
19	663424	6232612
20	663640	6232709
21	663940	6232737
22	664247	6232703
23	664524	6232652
24	664733	6232571
25	665190	6232360
26	665923	6232077
27	666823	6231672
28	662730	6232160
29	663092.7	6232183
30	663297.6	6232396
31	663374	6232653
32	663608.6	6232773
33	663949.7	6232816
34	664264.1	6232783
35	664545.5	6232722
36	664754.7	6232623
37	665212	6232421
38	665942.3	13767869
39	666846	6231735